FUNCTIONAL CHARACTERIZATION OF AUGMENTER OF LIVER REGENERATION (ALR) IN ZEBRAFISH LIVER DEVELOPMENT

LI YAN

(B. Sc. Yunnan University)

A THESIS SUBMITTED

FOR THE DEGREE OF DOCTOR OF PHILOSOPHY

DEPARTMENT OF BIOLOGICAL SCIENCES

NATIONAL UNIVERSITY OF SINGAPORE

2012

DECLARATION

I hereby declare that this thesis is my original work and it has been written by me in its entirety. I have duly acknowledged all the sources of information which have been used in the thesis.

This thesis has also not been submitted for any degree in any university previously.

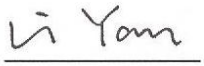

Li Yan

28 June 2012

ACKNOWLEDGEMENT

First of all, my deepest and most sincere gratitude goes to my dear supervisor, Associate Professor Ge Ruowen. I would like to thank her for all the guidance, continuous support and encouragement, which were the motivation throughout my PhD study. Her vision and advices are of great value to me and have helped me improve a lot.

I would like to thank my Qualifying Exam committee: Associate Professor Hong Yunhan, Associate Professor Liou Yih-Cherng and Associate Professor Christoph Winkler for the valuable suggestions on my project. The gratitude also goes to Dr Thomas Lisowsky who is an expert of Erv1/Alr proteins and provides helpful suggestions on my project.

I would like to thank my mentor Dr Muhammad Farooq for teaching me the basic zebrafish work. Dr Farooq started this project by showing the expression and possible function of *alr* in zebrafish liver development. Fig 3.6B (2^{nd} and 3^{rd} rows), Fig 3.10A&B, Fig 3.11B were contributed by Dr Farooq. I thank the following undergraduate students Lan Tian, Chanchal Chandramouli and Ng Wan Ting, for their involvement in this study. Fig 3.11C was contributed by Lan Tian. Fig 3.34B and Fig 3.35 were contributed by Chanchal Chandramouli. Fig 3.45 and Fig 3.49B were contributed by Ng Wan Ting. I also thank Mr Balan and Qinghua for their help in maintaining the zebrafish.

My sincere thanks also go to all the members in my laboratory, both past and present, for their kindness, assistance and friendship: Dr Xiang Wei, Dr Zhang Yong, Dr Ke Zhiyuan, Dr Fan Huapeng, Dr Soheila Sharghi Namini, Nilesh Kumar Mahajan, Jia Jinghui, Chen Mo, Saran Kumar, Nithya Rao Velliyuir Nott, Shruthi Venugopal, Zhou Yalu, *etc*.

I thank National University of Singapore for offering me the research scholarship to carry out this study.

Finally, I thank my parents and sister for their care and support in my life. I thank my dear husband Mr Cheng Dongqiang who shared the best and worst moments of my doctoral journey. Their strong support, understanding and love motivate me to complete my PhD study.

TABLE OF CONTENTS

SUMMARY

Augmenter of Liver Regeneration (ALR) is a sulfhydryl oxidase carrying out fundamental functions by facilitating protein disulfide bond formation. In mammals, it also functions as a hepatotrophic growth factor that specifically stimulates hepatocyte proliferation and promotes liver regeneration after liver damage or partial hepatectomy. Whether ALR also plays a role during vertebrate hepatogenesis is unknown.

In this work, we investigated the function of *alr* in liver organogenesis in zebrafish model. We showed that *alr* is expressed in liver throughout hepatogenesis. Knockdown of *alr* through morpholino antisense oligonucleotides leads to suppression of liver outgrowth while overexpression of *alr* promotes liver growth. The small-liver phenotype in *alr* morphants results from a reduction of hepatocyte proliferation without affecting apoptosis. When expressed in cultured cells, zebrafish Alr is localized in mitochondria as well as the cytosol but not in the nucleus or secreted outside of the cell. Similar to mammalian ALR, zebrafish Alr is a FAD-linked sulfhydryl oxidase that exists as homodimer and mutation of the conserved cysteine in the CxxC motif abolishes its enzymatic activity. Interestingly, overexpression of either wild-type Alr or enzymatic-inactive Alr^{C131S} mutant can promote liver growth and rescue the liver growth defect of *alr* morphants. Nevertheless, alr^{C131S} is less efficacious in both functions. These results suggest that *alr* promotes zebrafish liver outgrowth using mechanisms that are dependent as well

as independent of its sulfhydryl oxidase activity. This is the first demonstration of a developmental role of *alr* in vertebrates.

The ubiquitous and transient knockdown by microinjection of morpholinos into one-cell stage embryos limits its usefulness in studying temporal and tissue-specific gene function, especially during late developmental and adult stages. To overcome these limitations, a novel controlled knockdown method in stable transgenic zebrafish was developed. By combining a tissue-specific promoter controlled LexPR inducible gene expression system with the artificial miRNA knockdown system, temporal and spatial control of stable gene knockdown can be achieved. Specifically, the artificial miRNA using the *mir-30e* backbone was embedded in intron 2 of a partial actin gene followed by EGFP, so that the artificial miRNA and ΔActin-EGFP can be simultaneously expressed under the dual control of the mifepristone-inducible operator-promoter LexPR and the liver-specific promoter *lfabp*. Using *alr* gene as an example, stable and inducible transgenic knockdown of *alr* in liver suggested that this gene is also involved in larval and juvenile stage liver growth and expression of *alr* in those stages is essential for fish survival. Our stable transgenic knockdown system provides the first example of temporally- and spatially-controlled loss-of-function study in zebrafish.

LIST OF PUBLICATIONS RELATED TO THIS STUDY

Yan Li, Muhammad Farooq, Donglai Sheng, Chanchal Chandramouli, Tian Lan, Nilesh K. Mahajan, R. Manjunatha Kini, Yunhan Hong, Thomas Lisowsky, **Ruowen Ge**. (2012) Augmenter of Liver Regeneration (*alr*) Promotes Liver Outgrowth during Zebrafish Hepatogenesis. PLoS ONE 7(1): e30835.

LIST OF FIGURES

LIST OF TABLES

LIST OF ABBREVIATIONS

Ac	maize Activator transposase
AD	activation domain
AP-1	activator protein-1
BMP	bone morphogenetic protein
C/EBP	CCAAT/enhancer binding protein
CDS	coding sequence
CMV	Cauliflower mosaic virus
COX	cytochrome c oxidase
cp	ceruloplasmin
Dars	aspartyl-tRNA synthetase
DBD	DNA binding domain
DIG	digoxygenin
dpf	days post fertilization
Ds	maize Dissociation transposable elements
dsRBD	double-stranded RNA binding domain
dsRed	red fluorescent protein variant
DTT	dithiothreitol
Eefla1l1	eukaryotic translation elongation factor 1 α 1 like 1
EGF	epidermal growth factor
EGFP	enhanced green florescent protein
EGFR	epidermal growth factor receptor
elaA/B	elastase A/B
ER	endoplasmic reticulum
ERV1/2	essential for respiration and viability 1 /2
ESC	embryonic stem cells
FAD	flavin adenine dinucleotide
FGF	fibroblast growth factor
FoxA1/2/3	forkhead box protein a1/2/3
FPLC	fast performance liquid chromatography
GATA	GATA-binding factor
gfer	growth factor Erv1-like
Gfm1/2	G elongation factor mitochondrial 1/2
GFP	green fluorescent protein
GSH	reduced glutathione
hdac	histone deacetylase
HGF	hepatocyte growth factor
hhex	hematopoietically-expressed homeobox protein
hpf	hours post fertilization
HPO	hepatopoietin
HSS	hepatic stimulator substance

IL-6	interleukin-6
IMS	mitochondrial intermembrane space
JAB1	Jun activation domain-binding protein 1
JNK	c-Jun amino-terminal kinase
LBD	ligand binding domain
lfabp	liver fatty acid-binding protein
MAPK	mitogen-activated protein kinase
Mia40	mitochondrial intermembrane space import and assembly protein 40
miRNA	microRNA
MO	morpholino antisense oligonucleotide
MS	mass spectrometry
NFκB	nuclear factor κ B
ORF	open reading frame
PCNA	proliferating cell nuclear antigen
p-H3	phosphor-histone 3
pre-miRNA	precursor microRNA
pri-miRNA	primary microRNA
prox1	prospero-related homeobox 1
QSOX	quiescinsulfhydryl oxidases
RISC	RNA-induced silencing complex
RNAi	RNA interference
rps18	ribosomal protein S18
sePb	selenoprotein Pb
shRNA	short hairpin RNA
siRNA	small interfering RNA
STAT3	signal transducer and activator of transcription 3
STM	septum transversum mesenchyme
TALEN	transcription activator-like effector nuclease
TE	transposable element
TGFβ	transforming growth factor β
TIM	translocase in the inner membrane
TNFa	tumor necrosis factor α
TOM	translocase in the outer membrane of mitochondria
TUNEL	terminal deoxynucleotidyl transferase-mediated dUTP nick-end labelling
UTR	untranslated region
VDAC	voltage dependent anion channel protein
WISH	whole-mount in situ hybridization
ZFL	zebrafish liver cell
ZFN	zinc-finger nuclease

CHAPTER 1. INTRODUCTION

1.1 Zebrafish as a model organism in vertebrate developmental biology

The zebrafish, *Danio rerio*, is a tropical fresh water fish that belongs to the Cyprinidae family and Cypriniformes order. Zebrafish has become an important vertebrate model organism in recent years. Use of the zebrafish model organism has contributed to advances in the fields of developmental biology, oncology, genetics, regenerative medicine, neurobiology, toxicology, *etc*.

Zebrafish is advantageous as a model organism to study embryonic development for several reasons: they can breed large numbers of offspring frequently; they are small in size and easy to maintain; they develop rapidly and externally, most of the internal organs will form within 5 days post fertilization; the embryos are optically clear for easy microscopic observation; development of pigmentation which starts from the second day can be inhibited by simply incubating embryos under 1-phenyl-2-thiourea (PTU) without affecting embryonic development; homologs of many zebrafish genes have been shown to play conserved roles in humans, making zebrafish a suitable model organism for the study of vertebrate development; the embryos receive sufficient oxygen from water through diffusion, so cardiovascular defective embryos are viable throughout embryogenesis and develop relatively normally (Stainier, 2001). Zebrafish is different from mammals; its liver is not responsible for embryonic hematopoiesis. This makes liver developmental study in zebrafish especially advantageous, as liver organogenesis could be studied independently from the defects

caused by hematopoietic deficiencies (Field et al., 2003).

Study of gene function during zebrafish development can be carried out by either gain-of-function or loss-of-function approaches. For gain-of-function approaches, transgenic technique has become a fundamental tool. Transgenic fish can be established to overexpress the gene of interest in a tissue-specific manner under a proper promoter. Temporal control of the expression could be achieved using inducible gene expression systems. Another commonly used gain-of-function approach is by injecting the *in vitro* synthesized mRNA into one-cell stage embryos to overexpress the gene of interest. This method allows rapid determination of the effect of overexpression. However, the injected mRNAs generally have short lifespans, so only transient and ubiquitous overexpression can be achieved.

Traditional loss-of-function approaches include morpholino antisense oligonucleotides (MOs)-mediated gene knockdown, dominant-negative approaches and large-scale forward genetic screening for novel genes involved in embryogenesis. Forward genetic screening has been well established in zebrafish, facilitated by their large number of offsprings and small body size. Large pools of random mutations affecting various developmental or disease processes are now available by chemical mutagens such as N-ethyl-N-nitrosourea (ENU), ionizing irradiation, and retrovirus- or transposon-mediated insertional mutagenesis (reviewed by Patton and Zon, 2001). The desired phenotypes can be screened by large-scale whole-mount in situ hybridization or through using transgenic zebrafish lines expressing fluorescent

protein in cell types of interest. For chemical- or radiation-induced mutations, identifying the mutated site by positional cloning is labor-intensive and expensive. Insertional mutagenesis using retrovirus or transposon allows for rapid cloning of the mutation (Amsterdam et al., 1999).

MOs have been widely used for studying gene function and have made significant advances, because of its effectiveness and convenience. MOs are able to induce phenotypes similar to that of mutants (Nasevicius and Ekker, 2000). MOs are synthetic oligonucleotides about 25 morpholino bases in length. They are similar to DNA or RNA oligonucleotides except that they have a morpholine ring instead of a ribose ring (Eisen and Smith, 2008). MOs can undergo base pairing and offers advantages over conventional oligonucleotides because of their resistance to nucleases. They can target genes for inactivation or modification by blocking mRNA translation or interfering pre-mRNA splicing. The effectiveness of knockdown can be examined at protein level for translation-blocking MOs and at mRNA level for splicing-inhibiting MOs.

New technologies aimed for targeted gene inactivation are being developed, although gene knockout by homologous recombination is not available in zebrafish. One of the successful examples is through zinc-finger nuclease (ZFN). ZFN is a chimeric fusion between the cleavage domain of the restriction enzyme FokI and the Cys_2His_2 zinc-finger protein. The zinc-finger protein can be engineered to recognize different DNA sequences. Heterodimerization of two ZFNs bound to DNA in precise

orientation will lead to a double-strand break in the DNA and repair of the double-strand break may introduce mutations. The ZFN technique has been successfully adopted in zebrafish, with high frequencies of mutation created in the founder fish (Doyon et al., 2008; Meng et al., 2008). Recently, Miller *et al*. demonstrate that transcription activator-like effector nuclease (TALEN) can also be used for introducing targeted mutations in zebrafish at comparable rate as ZFN (Wood et al., 2011). TALEN is similar as ZFN, except that the zinc-finger protein part is replaced by an engineered array of transcription activator-like effector repeats. With each transcription activator-like effector repeat binds to one base pair of DNA, TALEN can be designed to target wider range of sequences than ZFN. These two techniques will be proven powerful and useful in the future with the growing availability of ZFN and TALEN engineering platforms.

1.2 Vertebrate liver development

1.2.1 Organization of liver

The liver, an internal organ derived from the endoderm, plays essential functions in metabolism, detoxification, and homeostasis. Liver metabolizes lipid, protein and carbohydrate; detoxify toxic substances and metabolic byproducts. It has exocrine property by producing bile, as well as endocrine properties by releasing serum factors including albumin. The liver contains several differentiated cell types, with the hepatocytes composing 80% of the liver and being the major functional cells. Other

cell types in mammals include cholangiocytes (bile duct cells), endothelial cells, sinusoid endothelial cells, Kuffer cells (liver macrophages), pit cells (liver natural killer cells) and hepatic stellate cells (reviewed by Si-Tayeb et al., 2010). Kuffer cells, hepatic stellate cells and pit cells have not been identified or studied in zebrafish.

The organizations of fish liver and mammalian liver are considerably different, illustrated in Fig. 1.1 (adapted from Lorent et al., 2004). In mammals, hepatocytes organize into bi-layered plates that are lined by sinusoidal capillaries which radiate from a central vein, forming the basic architectural unit - the liver lobule. A portal tract is located at each of the corners of the hexagonal liver lobules, containing a portal vein, hepatic artery and bile duct (Si-Tayeb et al., 2010). While in fish, hepatocytes surround small biliary ducts and are arranged like tubules. The hepatic arteries, portal veins and large bile ducts seem randomly distributed, rather than arranged in portal tracts like in mammals (Hinton and Couch, 1998; Lorent et al., 2004). It is not well understood how the different cell types are generated and arranged precisely into the functionally important three-dimensional architecture. But the early liver morphogenesis process and the genetic control of the liver organogenesis has been extensively studied in different model organisms.

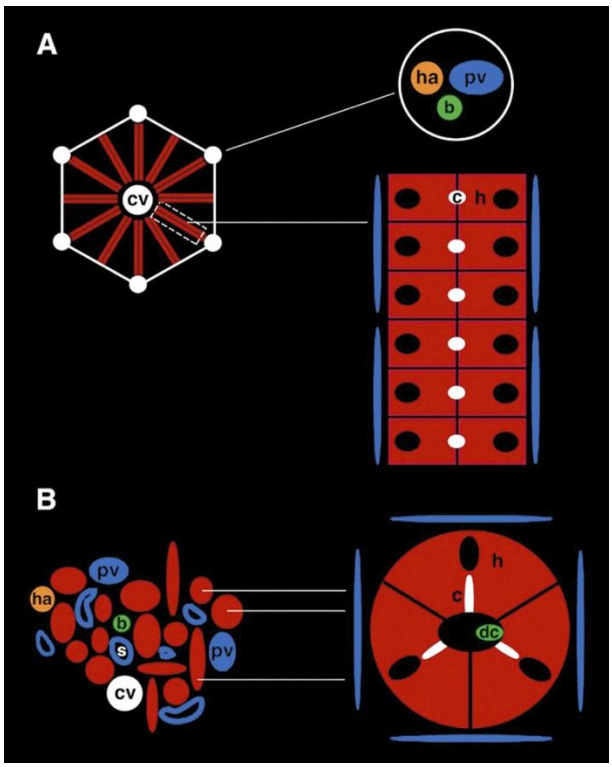

Fig. 1.1 Mammalian and teleost liver architecture. (Adapted from Lorent et al., 2004)

A, schematic illustration of the mammalian liver lobule. White circles at each of the corners of the hexagonal liver lobules represent the portal tracts. The enlarged portal tract is shown at the top right. Longitudinal section of the dash line circled region of the lobule is enlarged and shown at the bottom right. B, schematic illustration of the teleost tubular liver. The left part shows the random distribution of hepatic arteries, portal veins and large bile ducts within hepatocytes and sinusoids network. The right part is a schematic of the liver tubule (ductal cells anatomized with three hepatocyte canaliculi). The liver tubules can be observed in longitudinal, transverse and oblique sections. cv, central vein; h, hepatocytes; ha, hepatic artery; pv, portal vein; b, bile ducts; c, canaliculi located between nearby hepatocytes; s, sinusoid; dc, ductal cells.

1.2.2 Liver morphogenesis in mammals

The liver morphogenesis process in mouse embryo was illustrated in Fig. 1.2 (Si-Tayeb et al., 2010). At around 2-4 somites stage in the mouse embryos, the anterior endoderm has become competent to give rise to different foregut derivatives. Regions of the anterior endoderm, which is adjacent to the developing heart and lateral plate mesoderm generating the septum transversum mesenchyme (STM), will

adopt a hepatic fate after receiving inductive signal from the nearby cardiac mesoderm and STM (reviewed by Duncan, 2003). The specified liver progenitor cells - hepatoblasts will then proliferate and invade the surrounding STM, forming the liver bud. After migrating into the septum transversum, the hepatoblasts will differentiate into cholangiocytes and hepatocytes.

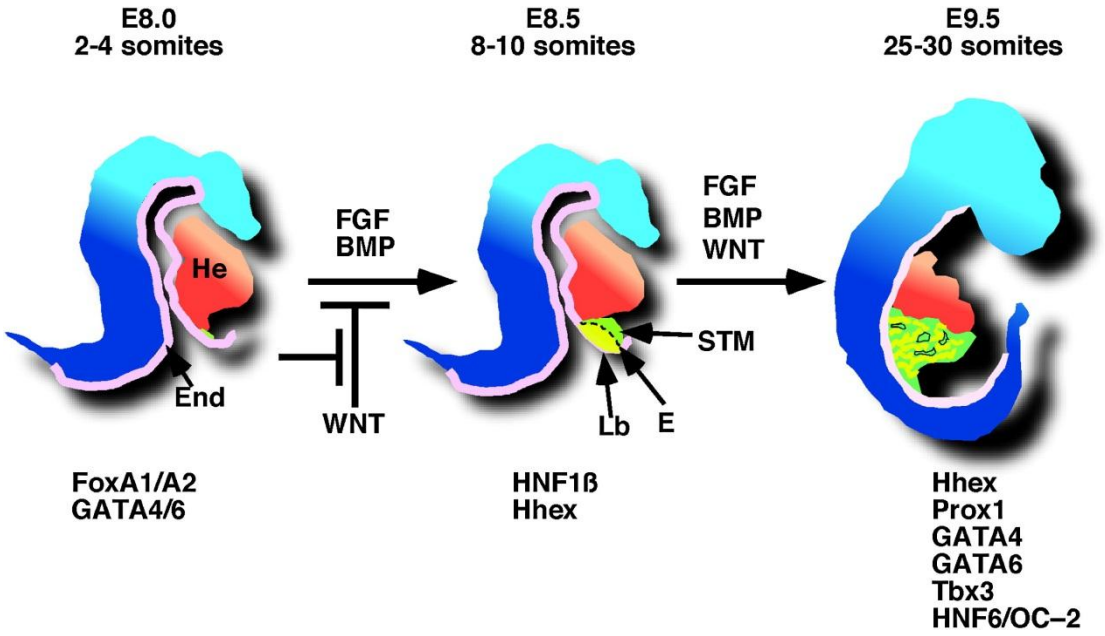

Fig. 1.2 Early liver organogenesis in mouse embryo. (Adapted from Si-Tayeb et al., 2010)
The early liver morphogenesis in mice was illustrated. Signaling molecules and transcription factors controlling this process was indicated. End, foregut endoderm (pink); He, heart (red); Lb, liver bud (yellow); STM, septum transversum mesenchyme (green); E, vascular endothelial cells (black).

1.2.3 Liver morphogenesis in zebrafish

In zebrafish, endoderm cells which is a sparse layer of cells during early somitegenesis, move medially and form a solid rod at the midline by 20 hpf (Fig. 1.3A), which can be tracked by the expression of several marker genes, e.g. the *forkhead box A1* (*foxA1*) and *foxA3* (Ober et al., 2003). Some of these cells receive

adequate Wnt signaling from lateral plate mesoderm (Ober et al., 2006), Bmp and Fgf signals from the surrounding endoderm or mesoderm tissue (Shin et al., 2007), and become specified to the liver progenitor cells – the hepatoblasts. This specification is indicated by the localized expression of *hematopoietically expressed homeobox* (*hhex*) and *prospero-related homeobox 1* (*prox1*) from 22 hpf onwards (Field et al., 2003). Around 24 to 28 hpf, an aggregation of the these cells at the ventral left side of the intestinal rod aligning with the first somite marks the initiation of liver budding (Fig. 1.3B). During the budding phase, the bipotential hepatoblast starts to differentiate into either the liver parenchymal cell – hepatocyte, or the bile duct cell – cholangiocyte. The differentiated hepatocytes can be identified by a range of specific markers. The earliest to be observed is *ceruloplasmin* (*cp*) detected in liver from 32 hpf (Korzh et al., 2001). In addition, *selenoprotein Pb* (*sePb*), *transferrin* and *liver fatty acid-binding protein* (*lfabp*) (Mudumana et al., 2004) are also hepatocyte makers that can be detected later. By about 50 hpf, the formation of the hepatic duct between the liver and the intestinal bulb primordium marks the completion of the budding phase. Following that is the growth phase when the liver increases rapidly in size by proliferation of hepatocytes and other liver cells (Field et al., 2003). The liver also becomes vascularized during this phase around 3 dpf and presumably starts its physiological function shortly thereafter.

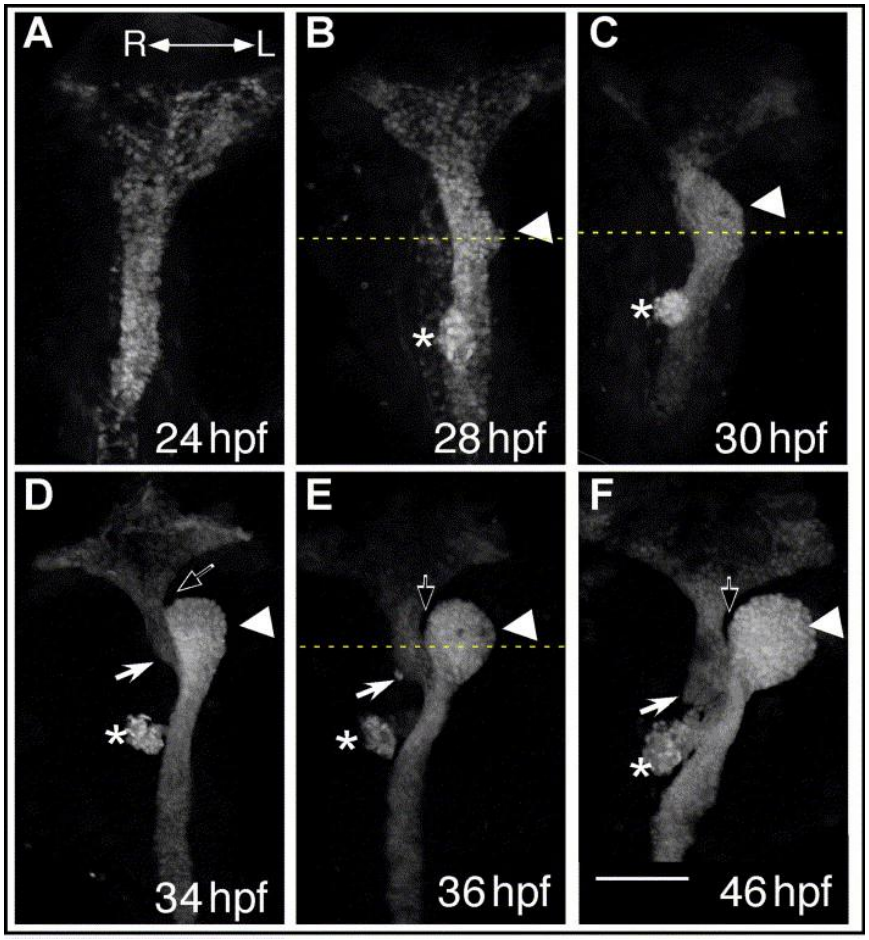

Fig. 1.3 Zebrafish early liver morphogenesis. (Adapted from Field et al., 2003)
(A–F) Two-dimensional projections of confocal stacks showing ventral views of the gutGFP line, anterior to the top. Scale bar, 100 μm. (A, B) The liver (arrowhead) starts budding from the intestinal rod between 24 and 28 hpf. (C) At 30 hpf, the liver forms a smooth thickening on the anterior and left side of the intestinal bulb. (D) A furrow (open arrow) begins to form between the medial anterior edge of the liver and the adjacent esophagus and continues to expand posteriorly (E, F) to separate the liver from the intestinal bulb. The pancreas (asterisk) and endodermal lining of the swim bladder (arrow) can also be seen developing from the intestinal bulb over time.

1.2.4 Signaling pathways controlling liver organogenesis

Studies in mouse embryos have revealed the dynamic and complex signaling networks controlling liver organogenesis, using various methods including mouse embryo culture, intervention by inhibitors, conditional gene knockout, *etc*. What's more, many of the pathways have been demonstrated conserved during zebrafish liver

organogenesis, establishing zebrafish as a suitable model for studying liver development.

The role of cardiac mesoderm for the hepatic cell fate induction from foregut endoderm was initially recognized in the mouse embryo tissue explant and co-culture study (Gualdi et al., 1996; Houssaint, 1980). The inductive role was later found to be contributed by fibroblast growth factors (FGF) (Gualdi et al., 1996; Jung et al., 1999). Another adjacent tissue of the liver bud - transversum mesenchyme is also required for liver specification by producing the transcription factor GATA4 (Watt et al., 2007) which in turn promotes the morphogen BMP4 expression (Rossi et al., 2001). The requirement of signaling molecules FGF and BMP as well as transcription factor GATA in inducing liver competency has been demonstrated to be conserved in other species including zebrafish (reviewed by Si-Tayeb et al., 2010). Other signals including TGFβ (Wandzioch and Zaret, 2009), WNT (McLin et al., 2007; Ober et al., 2006), and FOXA1/2 (Lee et al., 2005) are also required for liver specification in multiple model organisms. The Hhex and Prox1 transcription factors are expressed in hepatoblasts, with Hhex controlling the initiation and budding stage of liver organogenesis (Bort et al., 2006) and Prox1 required for outgrowth of liver bud and migration into septum transversum messenchyme (Sosa-Pineda et al., 2000)

In addition to the knowledge obtained in mouse, liver development study has been greatly advanced with the using of other model organisms such as zebrafish, facilitated by large-scale forward genetic screening and morpholino knockdown of

genes. Fig. 1.4 (modified from Chu and Sadler, 2009) provides an overview of the genes that are involved in zebrafish liver development.

Except for the conserved genes discussed above, many additional genes have been identified in zebrafish regulating budding or growth of liver. For example, mutation of the *myosin phosphatase targeting subunit 1* (*mypt1*) gene causes mis-positioning of Bmp2a-producing lateral plate mesoderm cells, leads to reduction of hepatoblast proliferation and eventual abortion of hepatoblasts by apoptosis (Huang et al., 2008). Knockdown of *neuron navigator 3* (*nav3*) leads to significant reduction of liver size, by impeding the outward movement of hepatoblast from the gut endoderm during liver budding stage (Klein et al., 2011). Sorting nexin 7 (Snx7) is a liver-enriched anti-apoptotic protein required for the survival of hepatoblasts (Xu et al., 2012). Knockdown of *snx7* activates the FLICE-like inhibitory protein (c-FLIP)/caspase 8 pathway and induces liver apoptosis.

Genes required for expansion growth of liver include *liver-enriched gene 1* (*leg1*) (Chang et al., 2011; Cheng et al., 2006), the RNA binding gene *nil per os* (*npo*) (Mayer and Fishman, 2003), *digestive-organ expansion factor* (*def*) (Chen et al., 2005b), *ubiquitin-like protein containing PHD and ring finger domains-1* (*uhrf1*) (Sadler et al., 2007), *translocase of outer mitochondrial membrane 22* (*tomm22*) (Curado et al., 2010), *matrix metalloproteinase 23b* (*mmp23b*) (Qi et al., 2010) and *core promoter element binding protein* (*copeb*) (Zhao et al., 2010). Mutation of *def* leads to arrest of liver expansion growth, through up-regulating Δ113p53 which

triggers arrest of cell cycle (Chen et al., 2005b). Morpholino knockdown of *mmp23b* results in reduced hepatocyte proliferation during liver outgrowth stage; *mmp23b* functions in liver growth through the tumor necrosis factor (TNF) signaling pathway (Qi et al., 2010), *progranulin A* (*grnA*) (Li et al., 2010). Morpholino knockdown of *copeb* blocks hepatocyte proliferation and expansion growth of the liver as a result of upregulation of the cell cycle inhibitor *cdkn1a*. Several epigenetic regulators are also required for liver development, such as *histone deacetylase (hdac) 1/3* (Farooq et al., 2008; Noël et al., 2008), *DNA methyltransferase* (*dnmt*) *1/2* (Chu and Sadler, 2009; Rai et al., 2007), *topoisomerase IIα* (*top2a*) (Dovey et al., 2009). The *hdac1* is required for both liver specification and hepatoblast differentiation (Noël et al., 2008). The *hdac3* is required for hepatic outgrowth, by repressing the expression of Tgfβ family member *growth differentiation factor 11* (*gdf11)* (Farooq et al., 2008).

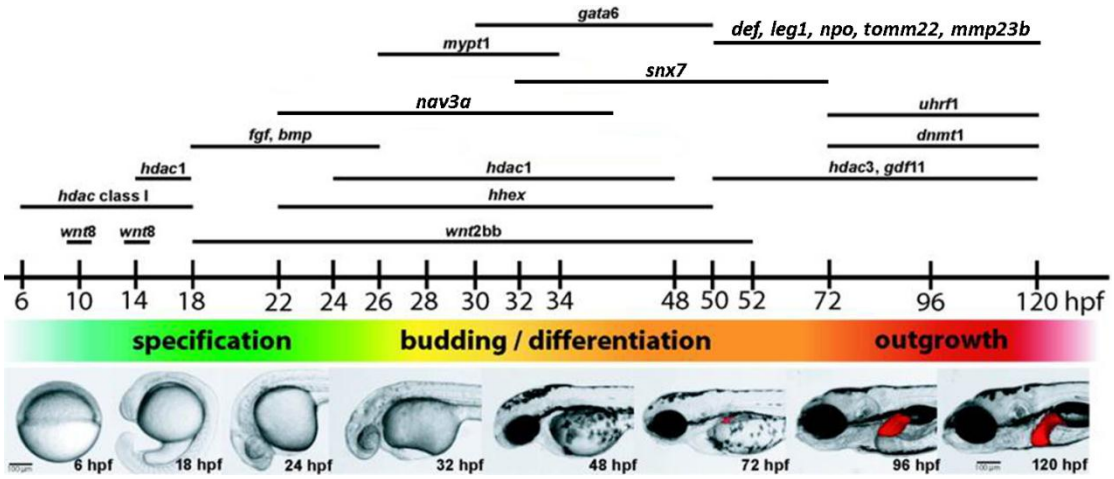

Fig. 1.4 Overview of genes involved in zebrafish liver development. (Modified from Chu and Sadler, 2009)
The genes and the corresponding embryonic stages they are involved in were indicated. Live images of *Tg(lfabp10: dsRed)* embryos from different stages were shown. Red color indicates the red fluorescent protein expressed under the liver-specific promoter *lfabp10*.

1.3 Augmenter of liver regeneration (Alr)

1.3.1 Erv1/Alr protein family

Augmenter of Liver Regeneration (ALR), also known as Hepatopoietin (HPO) and growth factor ERV1-like (GFER), is a protein best known for its ability to promote liver regeneration by stimulating hepatocyte proliferation. La Brecque and Pesch first reported the existence of hepatic stimulator substance (HSS) in the liver of weanling or partially hepatectomized adult rats, but not in the quiescent liver of adult rat (LaBrecque and Pesch, 1975). ALR was subsequently purified from the crude HSS extract, with the ability of stimulating hepatocyte proliferation and supporting liver regeneration in organ specific while species nonspecific manner similar as the HSS (Reviewed by Gatzidou et al., 2006).

ALR was first cloned from rat liver as a protein of 125 amino acids, and it was found to have 50% homology with the protein sequence of yeast Essential for Respiration and Viability 1 (Erv1) (Hagiya et al., 1994). The human ALR was subsequently purified and cloned from human fetal liver (Lisowsky et al., 1995; Yang et al., 1997) and was also named hepatopoietin (HPO). The human ALR was concluded to be the ortholog of yeast Erv1 because of the protein sequence similarity and its ability to rescue the yeast Erv1 mutants (Lisowsky et al., 1995). With homologous proteins identified in more species, the mammalian ALR and the yeast Erv1 together with other homologous proteins have been named the Erv1/Alr protein family, the highly conserved Erv1/Alr domain at the C-terminus being the hallmark of the protein

family.

To date, homologous ALR proteins have been found throughout the eukaryotic kingdom from fungi to human, suggesting their roles in common and important biological processes. While the enzymatic domain at the C-terminus is conserved, the N-terminal region is highly variable among ALRs in different species, implicating potentially distinct functions of this protein in different species. Members of the Erv1/Alr protein family have even been identified in DNA virus. Senkevich *et al*. studied the vaccinia virus E10R protein (the viral Erv1/Alr homolog), and found that E10R had a central role a viral pathway of disulfide bond formation, by introducing active-site disulfide bonds in the G4L glutaredoxin, the L1R viral membrane protein and a related protein encoded by the F9L ORF (Senkevich et al., 2000). They hypothesized that Erv1/Alr family proteins might function as thiol oxidoreductases in conjugation with thioredoxins or glutaredoxins, suggesting a fundamental cellular role of proteins in this family. Erv1/Alr protein was also found and studied in plant. The *Arabidopsis thaliana* Erv1 exhibits all of the common features of the Erv1/Alr protein family, the redox-active CXXC motif, non-covalently bound FAD, and sulfhydryl oxidase activity (Levitan et al., 2004).

Yeast Erv1 is the first and best characterized member of the Erv1/Alr family. Yeast Erv1 is a sulfhydryl oxidase localized in the intermembrane space of mitochondria and is essential for yeast cell survival (Lee et al., 2000). In yeast, Erv1 is also involved in Fe/S cluster formation in proteins and Fe homeostasis (Lange et al., 2001)

1.3.2 Alr and liver regeneration

1.3.2.1 Liver regeneration

Liver as an essential organ has the ability to regenerate after various injuries, such as physical damage, viral infection and toxic injury. Liver regeneration process can restore tissue mass of liver to the original level and maintain the liver and body mass ratio. The regeneration ability of liver is amazing. Liver can regrow to its normal size even after losing 70% mass and in a relatively short duration (7-10 days for rats, and 3-6 months for human) (reviewed by Pawlowski and Jura, 2006). Liver regeneration is coordinated by many growth factors, hormones and cytokines that regulate hepatocyte proliferation and apoptosis processes, as well as with the help of non-parenchymal cells such as Kupffer cells (Pawlowski and Jura, 2006). While liver regeneration has been extensively studied in mammals for about half a century, zebrafish has just been established as a model for liver regeneration study in the past few years.

In normal adult liver, cell division is rear and most of the cells are resting in G0 phase (Michalopoulos and DeFrances, 1997; Taub, 2004). When liver damage happens, hepatocyte proliferation and DNA synthesis will start soon after liver damage and peak around 12-24 hours. The factors that have been extensively studied and proven important for liver regeneration are interleukin 6 (IL-6), tumor necrosis factor alpha (TNFα), transforming growth factor alpha (TGFα), epidermal growth factor (EGF), hepatocyte growth factor (HGF) and insulin (reviewed by Pawlowski and Jura, 2006;

Taub, 2004). Fig. 1.5 illustrates the events that trigger liver regeneration (adapted from Taub, 2004) after liver injury. Factors of the innate immune system, such as gut-derived lipopolysaccharide (LPS), C3a and C5a from the complement system, can serve as the priming signal to trigger liver regeneration. They can induce the production of IL-6 and TNFα from Kupffer cells (macrophages) in the liver, by interacting with their receptors on Kupffer cells.

IL-6, produced by Kuffer cells in the liver, is responsible for liver regeneration priming. Impaired liver regeneration was found in IL-6 knockout mice (Li et al., 2001). IL-6 binds to hepatocytes surface receptor gp130, activates the tyrosine-kinase activity of the Janus Kinases (JAKs). The activated JAK then phosphorylates and activates signal transducer and activator of transcription (STAT3), which will then enter nucleus and activate gene transcription for cell-cycle entry (Hemmann et al., 1996; Stahl et al., 1994). Activation of STAT3 also activates the mitogen-activated protein kinases (MAPKs) signal cascade (Li et al., 2002a). TNFα is another cytokine involved in liver regeneration priming. TNFα can activate stress-activated protein kinase (SAPK) and induce the expression of IL-6, nuclear factor kappa B (NFκB) and CCAAT/enhancer binding proteins (C/EBPs) (Diehl et al., 1995; Kirillova et al., 1999; Webber et al., 1998). While TNF-receptor 1 knockout mice (Yamada et al., 1997) suggests a role of TNFα in liver regeneration, it is not known why knockout of TNFα wo not affect liver regeneration (Hayashi et al., 2005).

After priming of liver regeneration, several growth factors function as mitogens to

promote hepatocyte proliferation, with hepatocyte growth factor (HGF), transforming growth factor alpha (TGFα), epidermal growth factor (EGF) being the most important mitogens. HGF, as a paracrine growth factor released by non-parenchymal cells (Kupffer and endothelial cells) (Noji et al., 1990), binds to its receptor c-Met on hepatocytes and induces multiple pathways, including promoting TGFα production in hepatocytes (reviewed by Taub, 2004). The HGF-Met signal pathway is critical for DNA synthesis during liver injury (Huh et al., 2004). Both TGFα and EGF act on EGF receptor (EGFR) to stimulate a mitogenic cascade of protein kinases (Argast et al., 2004; Gallucci et al., 2000). TNFα could also stimulate TGFα production in hepatocytes (reviewed by Pawlowski and Jura, 2006). The pancreatic hormone insulin acts as an indirect mitogen, promotes DNA synthesis and hepatocyte proliferation in damaged liver (reviewed by Pawlowski and Jura, 2006).

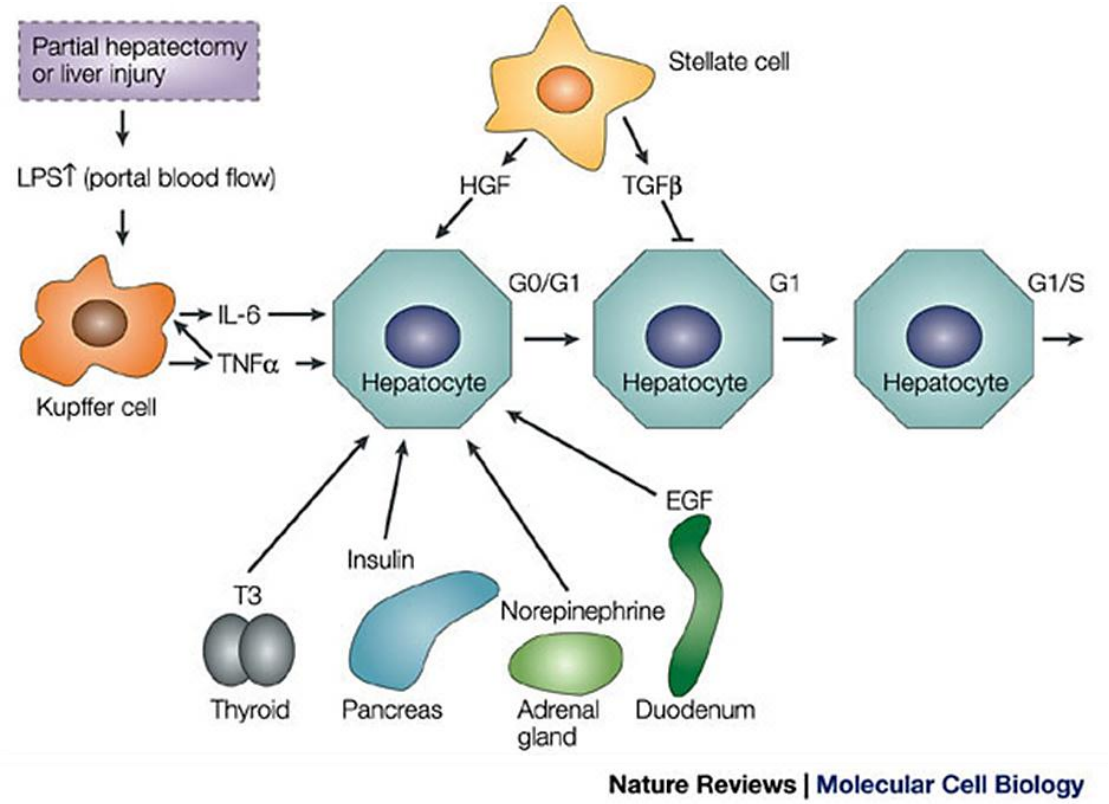

Fig. 1.5 Factors that trigger liver regeneration. (Adapted from Taub, 2004)
After liver injury, the gut-derived blood vessel LPS are upregulated, which will increase the production of TNF and IL-6 from Kupffer cells. Factors from other tissues include insulin (pancreas), EGF (duodenum or salivary gland), norepinepherine (adrenal gland), triodothronine (T3, thyroid gland) and HGF (stellate cells). Those factors cooperate to allow cell-cycle entry of hepatocytes. TGFβ signaling inhibits hepatocyte DNA synthesis. Thus, it is blocked during initial liver regeneration and restored at the end of regeneration to return hepatocytes to the quiescent state.

1.3.2.2 Role of ALR in liver regeneration

Previous studies reported the existence of hepatic stimulator substance (HSS) in the liver of weanling or partially hepatectomized adult rats (LaBrecque and Pesch, 1975), which is able to promote liver regeneration after partial hepatectomy. ALR was subsequently purified from the crude HSS extract, and had the ability of stimulating hepatocyte proliferation and supporting liver regeneration in organ specific while species nonspecific manner similar as the HSS (Francavilla et al., 1994; Hagiya et al.,

1994). ALR is believed to be predominantly and constitutively produced and stored in hepatocytes in an inactive form in the adult rat liver. Upon partial hepatectomy or other hepatic damage, ALR is activated and secreted out of hepatocytes into circulation (Gandhi et al., 1999). But it is not known how ALR is secreted into the circulation from hepatocytes during liver regeneration, as no signal peptide was found on the amino acid sequence of ALR.

The signal pathways that ALR utilize to promote hepatocyte proliferation and liver regeneration were illustrated in Fig. 1.6. Extracellularly, recombinant ALR protein stimulates phosphorylation of Mitogen-Activated Protein Kinase Kinase (MAPKK) and Mitogen-Activated Protein Kinase (MAPK) in a fast and transient manner, by binding to the ALR receptor specifically expressed on hepatocyte cell surface (Li et al., 2000; Wang et al., 1999). However, the identity of the cell surface ALR receptor is not yet known. ALR also stimulates phosphorylation of EGFR. The activation of MAPK by ALR is dependent on phosphorylation of EGFR. However, blocking EGF and EGFR binding wo not affect the mitogenic effect of ALR, indicating the stimulation of EGFR by ALR is not through EGF (Li et al., 2000). ALR is therefore called a “cytozyme”, possessing both cytokine and enzyme functions. Nevertheless, it is not clear if the cytokine activity of ALR is dependent on its enzymatic activity. Wang et al. (2006) found that the rat extracellular ALR could stimulate Kupffer cells proliferation by binding to an unknown high affinity receptor on Kupffer cells, to indirectly affect hepatocyte proliferation. Moreover, ALR could inhibit interferon-γ

production in liver Natural Killer cells and protects hepatocytes from interferon-γ inhibition of proliferation (Polimeno et al., 2000; Tanigawa et al., 2000).

Intracellularly, ALR binds to Jun Activation domain-Binding protein 1 (JAB1, a subunit of the COP9 signalosome), potentiates Activator Protein-1 (AP-1) by promoting c-Jun phosphorylation, independent of c-Jun amino-terminal kinase (JNK) and MAPK pathway (Lu et al., 2002a). This pathway of ALR is dependent on the sulfhydryl oxidase activity, possibly through oxidizing JAB1 (Chen et al., 2003). Further studies show that the short form ALR could also directly bind to COP9 signalsome (CSN) in nucleus and regulates AP-1 activity (Wang et al., 2004). ALR was also found interacting with thioredoxin and is able to oxidize it, thus affecting the subsequent redox regulation of NK-κB activity by thioredoxin (Das, 2001; Li et al., 2005).

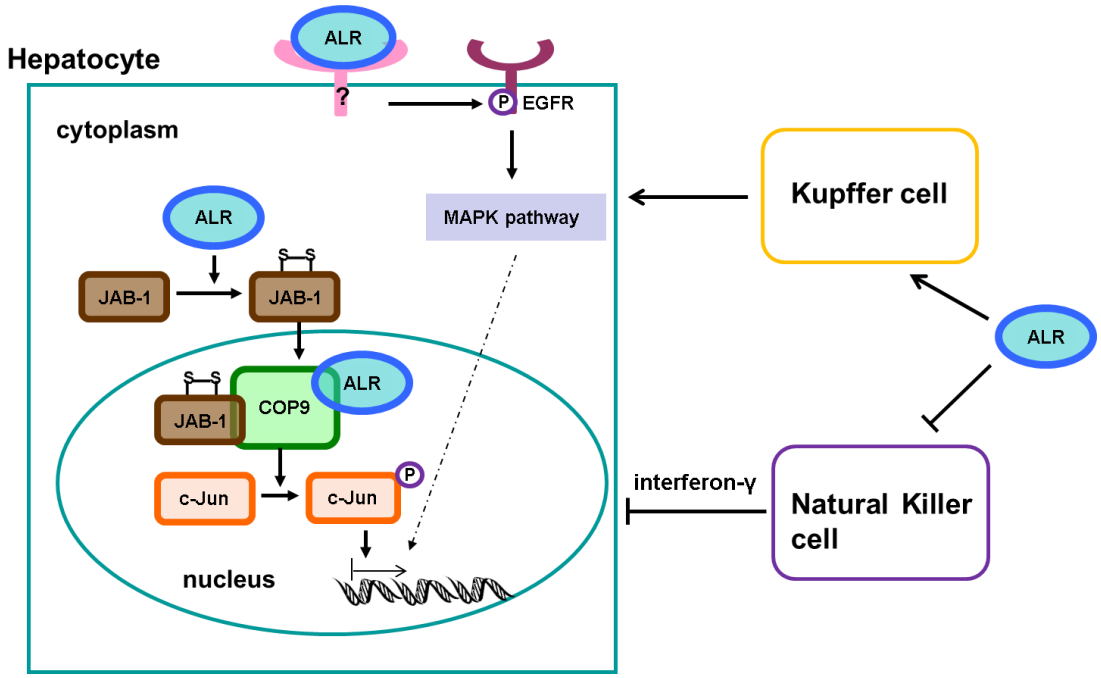

Fig. 1.6 Mechanism of ALR promoting hepatocyte proliferation and liver regeneration.

The extracellular ALR activates EGFR and MAPK pathway by binding to the unknown ALR receptor expressed on hepatocyte cell surface. Intracellular ALR binds and oxidizes JAB1 (a subunit of COP9), leading to increased c-Jun phosphorylation. Nucleus ALR can also bind COP9 directly, and regulate c-Jun phosphorylation. Extracellular ALR can protect hepatocytes by inhibiting the interferon-γ production in liver Nature Killer cells. Extracellular ALR can bind to unknown receptors on Kupffer cells and promote Kupffer cell proliferation, thus promoting liver regeneration.

1.3.3 Erv1/Alr as sulfhydryl oxidases

1.3.3.1 Flavin adenine dinucleotide (FAD)-linked sulfhydryl oxidases

Sulfhydryl oxidases are protein enzymes that catalyse the formation of disulfide bonds in proteins and small molecules substrates, using the molecular oxygen as the electron receptor: $2R\text{-}SH + O_2 \rightarrow R\text{-}S\text{-}S\text{-}R + H_2O_2$ (Thorpe et al., 2002b). So far, three families of sulfhydryl oxidases that bind FAD have been identified in eukaryotes, being the Essential for respiration and viability (Erv) family (Fass, 2008), Endoplasmic Reticulum Oxidoreductin (Ero) family (Sevier and Kaiser, 2008) and a multi-domain Quiescinsulfhydryl oxidases (QSOX) family (Coppock and Thorpe, 2006). While Erv1/Alr proteins are involved in protein folding in mitochondria intermembrane space, Ero1 proteins mediate protein folding in the endoplasmic reticulum (ER). The mammalian ALR is located primarily in mitochondria, similar as its yeast ortholog. Various subcellular localizations including the cytosol, nucleus as well as being secreted outside of the cell have been reported (Gandhi et al., 1999; Li et al., 2000; Lu et al., 2002a; Lu et al., 2002b; Wang et al., 1999; Wang et al., 2004). The diverse cellular localization is fundamental to its multiple functions in regulation of protein synthesis, cell proliferation and apoptosis, either dependent or independent

of its enzymatic activity. The QSOX enzymes, which contain a N-terminal thioredoxin domain and a C-terminal Erv1/Alr domain (Coppock et al., 1998), have also been reported with diverse cellular localizations in ER, Golgi, plasma and nuclear membrane (Amiot et al., 2004; Benayoun et al., 2001; Mairet-Coello et al., 2004; Wittke et al., 2003).

1.3.3.2 The Erv1/Alr family proteins as sulfhydryl oxidases

Several members of the Erv1/Alr protein family have been demonstrated having sulfhydryl oxidase activity, being the Erv1 from yeast (Lee et al., 2000), ALR in rat and human (Farrell and Thorpe, 2005; Lisowsky et al., 2001) and Erv1 of *Arabidopsis thaliana* (Farver et al., 2009; Levitan et al., 2004). Viral homolog of Erv1/Alr, the E10R gene product in vaccinia virus, was also identified as a sulfhydryl oxidase (Senkevich et al., 2000).

The yeast Erv1 is the best studied sulfhydryl oxidase in the Erv1/Alr proteins family. Yeast Erv1 has been well known for constituting a disulfide relay system with Mia40 (mitochondrial intermembrane space import and assembly pathway 40) in the mitochondrial intermembrane space (IMS), which promotes the oxidative folding of proteins imported into the IMS of mitochondria (Fig. 1.7). Most of the mitochondrial proteins are synthesized in the cytosol with a mitochondrial targeting sequence. They will be recognized by receptors on the outer membrane of mitochondria and get imported into the IMS through translocase in the outer membrane (TOM). The imported proteins in unfold and reduced state was then oxidized by Mia40 which

introduce disulfide bonds to them. After oxidative folding, those proteins will either be imported into mitochondrial matrix through translocase in the inner membrane (TIM) complex or remain in the IMS. Erv1 will then oxidize the reduced Mia40 to recycle it (Mesecke et al., 2005). The disulfide relay system is connected to the respiratory chain. The reduced Erv1 will subsequently pass its electrons to Cytochrome c; the reduced Cytochrome c is then oxidized by Cytochrome c oxidase and passes the electrons to oxygen (Allen et al., 2005; Bihlmaier et al., 2007).

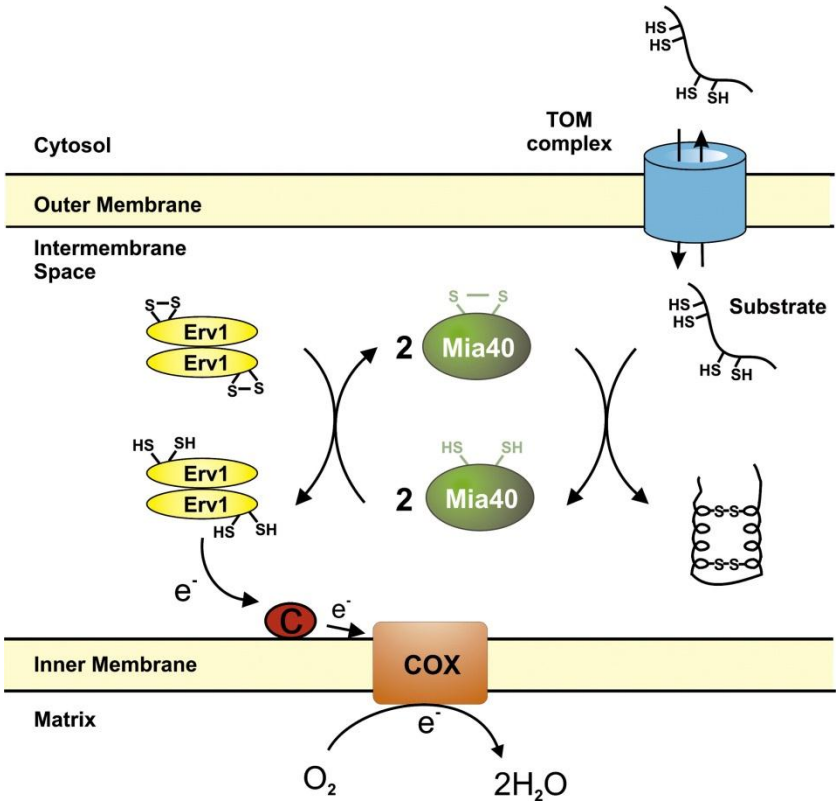

Fig. 1.7 The disulfide relay system of Erv1 and Mia40 in the intermembrane space of mitochondria. (Adapted from Hell, 2008)
Schematic illustration of the disulfide relay system in the IMS of mitochondria which promotes oxidative folding of proteins imported into mitochondria. The cytosolic nascent proteins in reduced state are imported into IMS through TOM complex and oxidized by Mia40, to undergo oxidative folding. The reduced Mia40 will then be oxidized by Erv1 to be recycled. The disulfide system is connected to the respiratory chain. The reduced Erv1 will subsequently pass its electrons to cytochrome c and finally to oxygen through Cytochrome c oxidase (COX).

In both yeast and human, the mitochondria protein Mia40 and cytochrome c have been identified as direct *in vivo* substrates of Erv1/ALR (Allen et al., 2005; Farrell and Thorpe, 2005; Mesecke et al., 2005). For the human ALR, additional substrates in the cytosol - JAB1 and thioredoxin were also reported which involves in cell proliferation regulation (Chen et al., 2003; Li et al., 2005). Whether ALR have other additional *in vivo* substrates inside mitochondria and at other subcellular locations is still a mystery.

1.3.3.3 Conserved cysteines and sulfhydryl oxidase activity

Cysteine disulfide bonds are very important for the proper function of proteins, as they mediate protein folding and stabilize the three-dimensional protein structure. In sulfhydryl oxidases, cysteine disulfide bonds have additional functions. They are involved in thiol and disulfide switches between the enzyme and substrate. The Erv1/Alr family members have several conserved and important cysteine pairs. The conserved cysteines and intramolecular disulfides in yeast Erv1, yeast Erv2, *Arabidopsis thaliana* Erv1 and human long form ALR were illustrated in Fig. 1.8 (adapted from Ang and Lu, 2009). Two highly conserved cysteine pairs in the Erv1/Alr domain are observed, being the CxxC and $Cx_{16}C$. The CxxC motif is structurally close to the isoalloxazine ring of the FAD moiety. The CxxC and FAD together constitute the catalytic active center. Apart from these two cysteine pairs, one extra cysteine pair was found either in the N-terminal region (yeast Erv1 and human ALR) or in the C-terminus (yeast Erv2 and *Arabidopsis thaliana* Erv1). It has been

hypothesized that the extra cysteine pair functions as a shuttle disulfide bond during electron transfer (Ang and Lu, 2009).

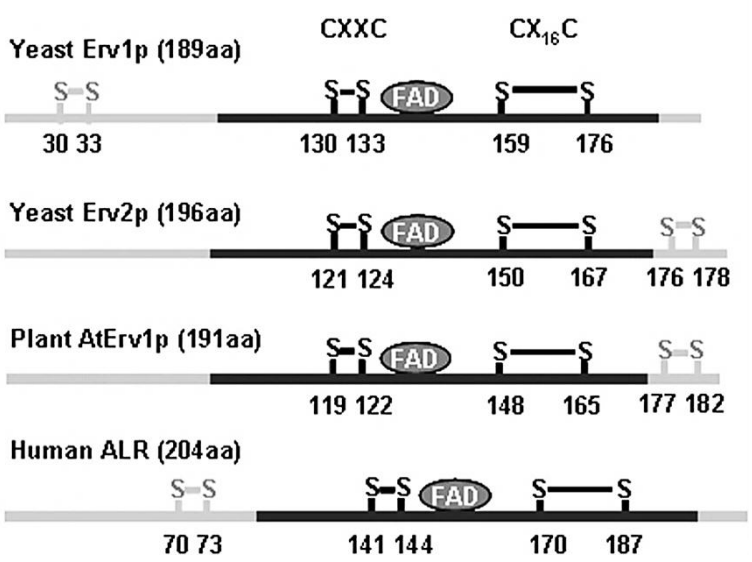

Fig. 1.8 Intramolecular disulfide bonds in Erv/ALR proteins. (Adapted from Ang and Lu, 2009)
Schematic illustration of the conserved intramolecular disulfide bonds in yeast Erv1 and Erv2, *Arabidopsis thaliana* Erv1, human long form ALR. The blank bars represent the conserved Erv1/Alr domain. The gray bars represent the rest non-conserved regions. The numbers below the bars show the position of each cysteine.

The importance of each cysteine for the sulfhydryl oxidase activity, FAD binding and dimer maintenance was reported in a serial of studies. Lee et al. (2000) reported that the Erv1/Alr domain alone of yeast Erv1 was able to bind FAD and was enzymatically active, suggesting that the N-terminal Cys_{30}-Cys_{33} is not required for the enzymatic activity. But the yeast Erv1/Alr domain alone could not form homodimers as the full length Erv1, suggesting the involvement of N-terminus in dimer formation. Lisowsky et al. (2001) first reported that both the rat and human short form ALR (lacking the N-terminal 80 amino acids compared to long form ALR) are FAD-linked sulfhydryl

oxidases. They further demonstrated that the active-site CxxC mutant could not bind FAD anymore and lost the enzymatic activity. The $Cx_{16}C$ mutation of human short form ALR was investigated by Chen et al. (2003). Mutation of $Cx_{16}C$ only had a mild effect on its enzyme activity, suggesting that the $Cx_{16}C$ is not essential for enzymatic acitivity. But contrary to Lisowsky et al. (2001), their results showed that none of the cysteine to serine mutation in either active-site CxxC or $Cx_{16}C$ motif would affect FAD binding. Daithankar et al. (2009) reported that the active-site CxxC was required for enzymatic activity, but not the N-terminal CxxC (Cys_{70}-Cys_{73}). They also found that all the CXXC sites mutants bond FAD normally. Taken together, studies from human ALR show that the sulfhydryl oxidase activity is dependent on the active-site CxxC only while not the N-terminal CxxC or the $Cx_{16}C$; mutation of any of the cysteine pairs alone is not able to disrupt FAD binding. Similar phenomenon are also proved later for yeast Erv1 in a systematic study of the roles of individual disulfide bonds (Ang and Lu, 2009).

1.3.4 Structural study of Erv1/Alr proteins

High-resolution structures of several Erv/Alr proteins from different species have been determined through X-ray crystallography, including yeast Erv2 (PDB code: 1JR8, 1JRA) (Gross et al., 2002), rat short form ALR (PDB code: 1OQC) (Wu et al., 2003), Arabidopsis thaliana Erv1 (PDB code: 2HJ3) (Vitu et al., 2006), human short form ALR (PDB code: 3MBG) (Daithankar et al., 2010) and a viral homolog pB119L from African swine fever virus (PDB code: 3GWL, unpublished).

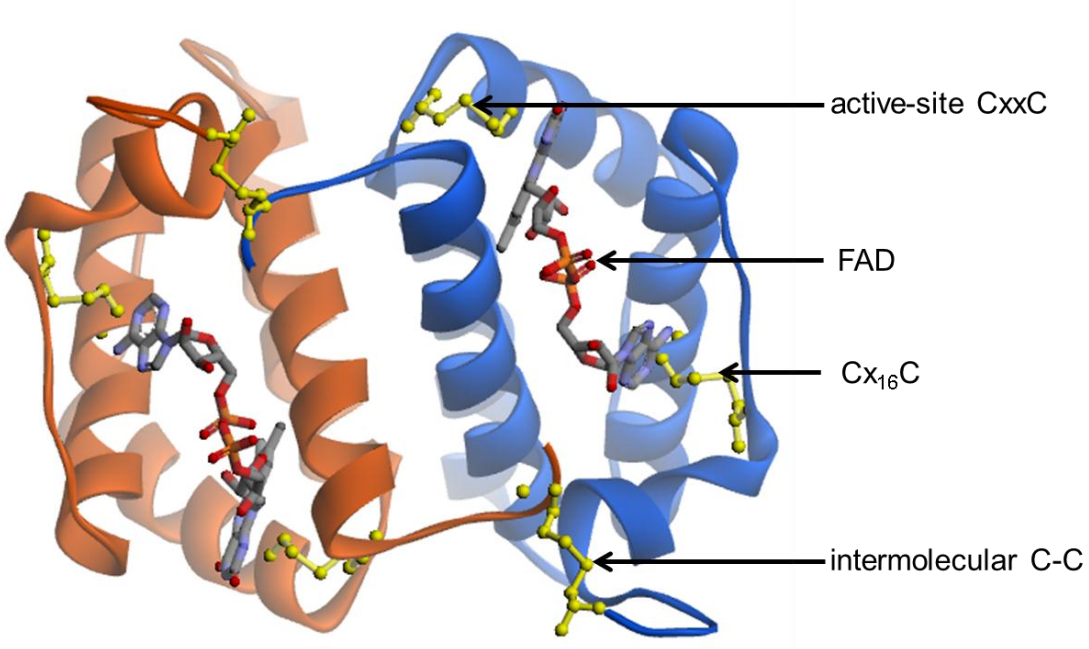

Fig. 1.9 Ribbon diagram showing the rat ALR homodimer structure. (PDB code: 1OQC)
The two subunits of the homodimer were positioned head-to-tail, represented in orange and blue colour respectively. The FAD moiety was presented in stick. The three cysteine pairs that form disulfide bonds were highlighted in yellow. Two intramolecular disulfide bonds (formed by active-site CxxC and the Cx16C respectively) and one intermolecular disulfide bonds (formed by cysteines at the N- and C-terminus) were found.

All crystal structures so far are produced from C-terminal region (around 100 a.a) of Erv1/Alr proteins, containing the Erv1/Alr domain only. The Erv1/Alr protein structures are quite conserved; they form homodimers with the two subunits positioned head-to-tail. The rat ALR protein structure (PDB code: 1OQC) (Wu et al., 2003) was presented in Fig. 1.9 as an example. The Erv1/Alr proteins typically form a cone-shaped five-helix bundle and non-covalently bind to FAD at the mouth of the helical cone. The FAD moiety is close to the active-site CxxC disulfide bond and the $Cx_{16}C$ disulfide bond within the Erv1/Alr domain, with the isoalloxazine ring of FAD closely related to active-site CxxC disulfide bond. Formation of the $Cx_{16}C$ disulfide

bond brings the short fifth helix closer to the four-helix bundle (Ang and Lu, 2009).

No disulfide bond was found between the two subunits of the yeast Erv2 homodimer. But an intermolecular disulfide bond was found between the two units of the mammalian short form ALR homodimer, involving two cysteines at the N- and C-terminal end respectively (Fig. 1.9) (Wu et al., 2003). However, the intermolecular disulfide bond is not necessary for maintaining the dimer, as mutation of these two cysteines wo not abolish dimerization. Most of the hydrophobic residues on helix 1 and 2 are located on the interface of the ALR dimer, thus the hydrophobic force is one of the major forces to stabilize homodimer interaction. Presence of salt bridges and hydrogen bonds also help maintain dimer structure (Wu et al., 2003).

As shown previously in Fig. 1.8, proteins of the Erv1/Alr family usually have three pairs of cysteines: active-site CxxC, $Cx_{16}C$ and an extra cysteine pair located in either N- or C-terminus. The $Cx_{16}C$ cysteines are probably involved in maintain the stability of Erv/ALR proteins (Ang and Lu, 2009). The extra cysteine pair which is structurally flexible is hypothesized to function as a shuttle disulfide bond for electron transfer.

Recently, the first human disease due to ALR R194H mutation has been identified as an autosomal-recessive infantile mitochondrial disorder presenting myopathy with cataract and combined respiratory-chain deficiency (Di Fonzo et al., 2009). The crystal structure of short form human ALR (sfALR) indicated that R194 is located at the subunit interface, close to the inter-subunit disulfide bridges (Daithankar et al., 2010). In vitro characterization indicated that R194H mutation affected the stability of

both the long form and short form of human ALR, leading to a significant increase in conformational flexibility (Daithankar et al., 2010).

1.4 RNA interference and its application for targeted gene knockdown

RNA interference (RNAi) is known as the process that silence gene expression by RNA molecules through post-transcriptional regulation. Well-studied natural RNAs that can mediate RNAi are microRNAs (miRNAs) and small interfering RNAs (siRNAs). While miRNAs are processed from endogenous RNA transcripts and target mRNAs from unrelated loci, siRNAs originate from exogenous long double-stranded RNAs and tend to target the loci that generate them (such as virus and transposon). Thus, it is proposed that miRNAs primarily function in gene regulation and siRNAs play important role during defence against virus and foreign DNA (reveiwed by Bartel, 2004). Based on the knowledge of miRNAs and siRNAs, RNAi has been extensively used for targeted gene knockdown and has become an important tool for elucidating gene function during the past decade. In this section, I will focus on the knowledge and knockdown strategies related to miRNA, as our following targeted gene knockdown in transgenic zebrafish is miRNA-based.

1.4.1 miRNA

miRNAs are short (~22 nucleotides) single-stranded RNAs that are produced from endogenous precursor transcripts and function as key post-transcriptional regulators. The first miRNA *lin-4* was discovered in *Caenorhabditis elegans* in 1993 (Lee et al.,

1993), which binds to multiple complementary sites in the 3' UTR of the *lin-14* gene to reduce its expression and control *C.elegans* development. Seven years later, a second miRNA *let-7* was discovered in *C.elegans* which functions similarly as *lin-4* (Reinhart et al., 2000). The *let-7* targets 3' UTR of *lin-41* and *hbl-1* to repress their expression and promote the late larval to adult transition. The identification of homologous *let-7* genes in many other species opened a new page of fast-growing and extensive study of miRNAs, leading to the discovery of thousands of miRNA genes in human genome (reviewed by Du and Zamore, 2005).

1.4.1.1 Gene structure and transcription of miRNAs

Based on the analysis of miRNA genomic locations (Rodriguez et al., 2004), their positions in the genome can be classified into three categories: exonic miRNAs in their own or other non-coding transcription units; intronic miRNAs in non-coding transcription units; intronic miRNA in protein-coding transcription units (reviewed by Du and Zamore, 2005; Kim, 2005). Intronic miRNAs usually reside in sense orientation in the pre-mRNA transcript they share (Baskerville and Bartel, 2005; Rodriguez et al., 2004). While some miRNAs form their own transcription units, a large portion of miRNAs can form clusters and are transcribed as polycistronic transcripts that contain a series of miRNA-producing hairpin structures (Du and Zamore, 2005; Kim, 2005).

It is known that the most of the primary transcripts containing miRNAs are produced by RNA polymerase II, although it is also possible that some small miRNA genes

might be transcribed by RNA polymerase III (Lee et al., 2004). Generally, miRNA genes are transcribed by RNA polymerase II into 5'-capped and poly(A)-tailed primary miRNAs (pri-miRNAs), with the length ranging from hundreds to thousands of nucleotides (Cai et al., 2004; Lee et al., 2004).

1.4.1.2 Maturation of miRNAs and mode of action

The maturation process of miRNAs is illustrated in Fig. 1.10 (adapted from Krol et al., 2010), using the process in human as an example. First, miRNA precursor pri-miRNAs are transcribed by RNA polymerase II either as independent transcripts or in the introns of co-transcripts. The pri-miRNAs are then cleaved by Drosha (RNase III family enzyme) in the nucleus, to remove the flanking regions and generate ~70 nucleotide precursor miRNAs (pre-miRNAs) with hairpin structures. For the accurate and efficient processing of pri-miRNA, Drosha needs to form complex with a double-stranded RNA binding domain (dsRBD) protein, known as DGCR8 in mammals (Gregory et al., 2004; Han et al., 2004). Some pre-miRNAs (termed "mirtrons") can bypass the Drosha-DGCR8 complex processing step, as they span the whole intron and are generated by splicing machinery (Ruby et al., 2007).

The pre-miRNAs are then specifically recognized and exported into cytoplasm by Exportin5/RanGTP (Lund et al., 2004; Yi et al., 2003). In the cytoplasm, Dicer/ dsRBD protein trans-activator RNA binding protein (TRBP) complex will cleave the pre-miRNA into ~22 bp miRNA/miRNA* duplex, (Chendrimada et al., 2005; Ketting et al., 2001). In mammals, the Argonaute 2 (AGO2) can cleave the 3' arm of certain

pre-miRNAs using its RNaseH-like endonuclease activity before Dicer processing (Diederichs and Haber, 2007). One strand of the miRNA/miRNA* duplex (either the 5’ or the 3’ arm) will be preferentially incorporated into the RNA-induced silencing complex (RISC) as the mature miRNA, while the other strand miRNA* will get degraded. For some miRNAs, both strands can become mature miRNAs.

Plant miRNA maturation process is different from that of animals, as plants lack the Drosha homolog. The RNase III enzyme Dicer-Like 1 (DCL1) is used for cleavage of pri-miRNA into pre-miRNA and pre-miRNA into the miRNA/miRNA* duplex in the nucleus. The miRNA/miRNA* duplex was then transported into cytoplasm and get methylated at 3’ end before incorporating into RISC (reviewed by Bartel, 2004; Du and Zamore, 2005).

Plant miRNAs often have perfect or near-perfect complementarity to the mRNA targets (Rhoades et al., 2002). But most animal miRNAs imperfectly bind 3’UTR of their target mRNAs, mainly involving nucleotides 2 to 8 (the seed region) from the 5’ end of miRNA (Du and Zamore, 2005). Thus, the animal miRNAs are predicted to have large number of targets.

The miRNAs can direct RISC to target mRNAs by base pairing with the target and then downregulate gene expression by posttranscriptional mechanisms: either translational repression or degradation of mRNA. It is generally believed that the miRNA will result in cleavage of mRNA target if there is sufficient complementarity; otherwise, translation repression will take place (Bartel, 2004).

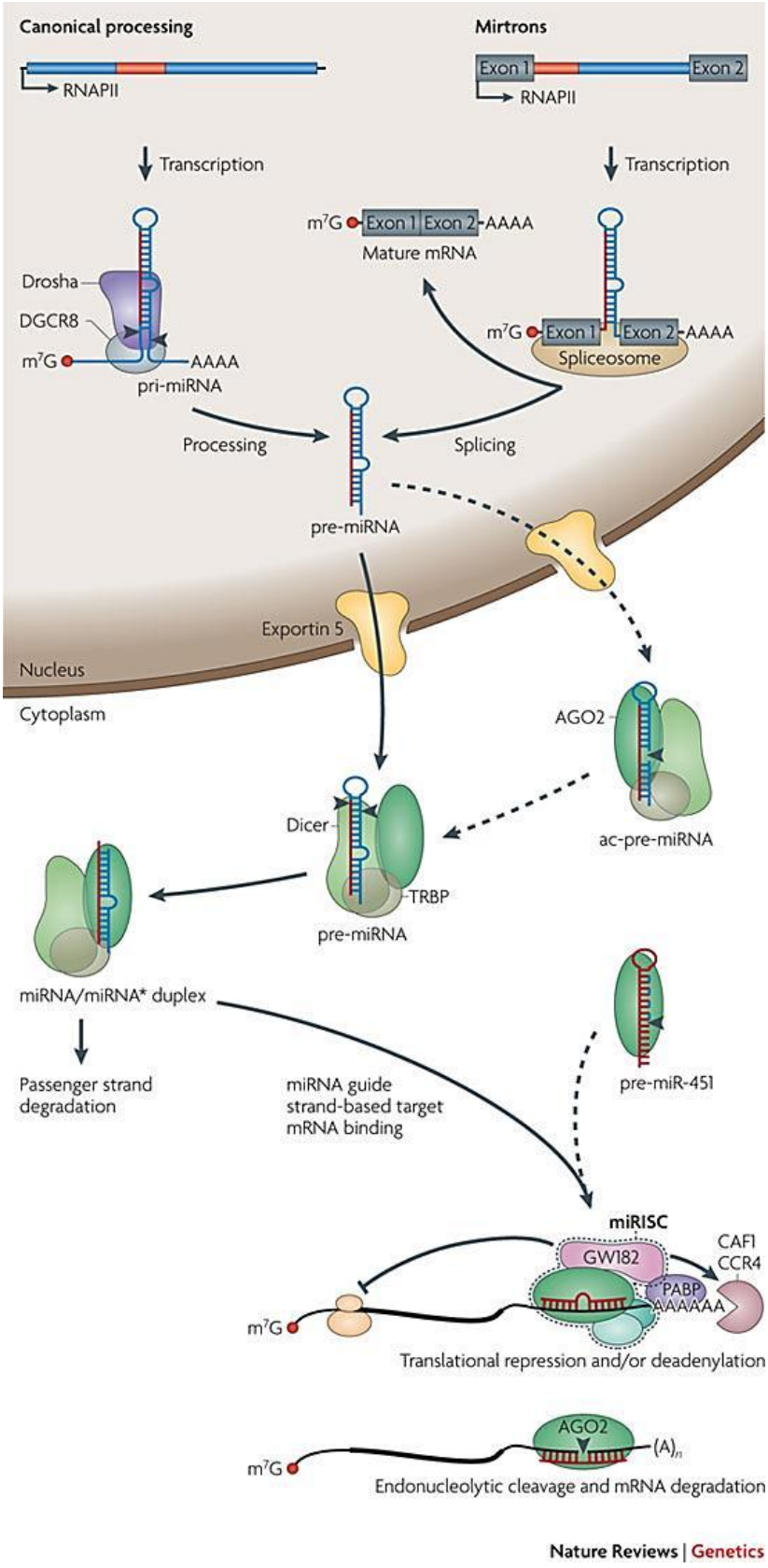

Fig. 1.10 miRNA biogenesis and mode of action in mammals. (Adapted from Krol et al., 2010)

Briefly, the maturation of miRNA involves two basic steps: Drosha-DGCR8 cleavage

of pri-miRNA into pre-miRNA hairpin in the nucleus and Dicer-TRBP processing of pre-miRNA into ~22-bp miRNA/miRNA* duplex in the cytoplasm. Argonaute 2 (AGO2) can support Dicer cleavage by cutting the 3' arm of some pre-miRNAs. Processing of pre-miR-451 requires AGO2 cleavage but not Dicer. One strand of the miRNA/miRNA* duplex will be loaded into RISC complex for post-transcriptional regulation of gene expression either by blocking translation or degradation of mRNA.

1.4.2 Targeted gene knockdown by RNA interference

RNAi-mediated gene knockdown has become an important strategy for loss-of-function study. A few types of RNAs have been experimentally used for knockdown of target genes: long double-stranded RNA (>100nt), short double-stranded RNA (also called small interfering RNA), vector-based short hairpin RNA (shRNA) and vector-based miRNA-based shRNA (also known as artificial miRNA). Once introduced into the cell, those RNAs will enter different stages of the miRNA/siRNA maturation process and eventually mediate gene knockdown through RISC complex.

Gene knockdown by RNAi was initially carried out by transfection or injection of long dsRNAs; but the problem of using long dsRNAs is that they might lead to non-specific toxicity by triggering an interferon response (reviewed by Lan et al., 2011). Later, small interfering RNA (siRNA) was used with success. The siRNAs are ~21 nt double-stranded RNAs that do not need processing and can be directly incorporated into RISC to mediate gene knockdown (Elbashir et al., 2001). But gene knockdown by transfected or injected siRNA is transient and can only last a few days, so it cannot be used to examine the gene knockdown effect for long time. To overcome this problem, vector-based RNAi was later developed for continual

expression of the RNA effector (either shRNAs or artificial miRNAs).

The first type of vector-based RNAi utilizes shRNAs. Those shRNAs, containing a stem region of sense and antisense strand and a short linker region of a few nucleotides, are usually ubiquitously expressed at high levels under RNA polymerse III promoters such as U6 and H1. The second type of vector-based RNAi uses artificial miRNAs, which are designed by replacing the stem region of endogenous miRNA precursors with sequences that target other genes of interest. The backbone of the endogenous miRNA precursor will be retained to facilitate processing of the artificial miRNA. The artificial miRNAs can be controlled by RNA polymerase II promoters, to enable tissue-specific expression (reviewed by Lan et al., 2011). Zeng et al. (2002) first showed that artificial miRNAs can be expressed using the human mir-30 precursor under an RNA polymerase II promoter (the CMV promoter). Zhou et al. (2005) further demonstrated that the EGFP reporter gene can be placed downstream of intronic artificial miRNAs, so that the artificial miRNA and reporter gene can be simutanously expressed. Chung et al. (2006) established a Pol II promoter vector that can express polycistronic artificial miRNAs based on miR-155. Large-scale miR-30-based shRNA libraries were constructed to facilitate systematically analysis of individual gene function in mouse and human (Silva et al., 2005). Recently, RNAi vectors using either Pol II or Pol III promoters as well as enabling inducible gene expression have been commercially available in mammals.

1.4.3 Targeted gene knockdown using RNA interference in zebrafish

Use of long dsRNA or siRNA in zebrafish has produced conflicting results, which blocked their further use in zebrafish. While some studies observed success of gene knockdown by dsRNA or siRNA, there are many studies reported non-specific toxicity (reviewed by Skromne and Prince, 2008). Nevertherlessly, morpholino antisense oligonucleotide has become an important tool for transient gene knockdown in zebrafish. But stable and well controlled gene knockdown tools are urgently needed for zebrafish.

So far, very few studies have reported the development of vector-based RNAi tools in zebrafish. Ying and Lin (2006) reported the successful expression of an intronic artificial miRNA that was designed to target EGFP for knockdown in zebrafish. Heritable and tissue-specific gene knockdown using vector-based artificial miRNAs was reported by Dong et al. (2009) in zebrafish. In their design, artificial miRNAs in pri-miR-30e backbone are placed in the intron of truncated *actin* gene, the 3' end of which is fused to DsRed reporter gene. The intronic artificial miRNAs and the Actin-DsRed fusion protein will be simultanously expressed, under the control of a tissue-specific Pol II promoter. Efficient knockdown of both reporter EGFP and endogenous genes have been achieved, either transiently or stably in transgenic fish. They also show that polycistronic artificial miRNAs can be expressed in a single transcript, by placing multiple copies of artificial miRNA hairpin precursor within the mir-30e flanking regions, to enhance the efficiency of gene knockdown. Their study provides a valuable tool for stable and tissue-specific knockdown in zebrafish

embryos. But this system could not be used for precise study of genes that have dynamic functions in the same tissue in different embryonic stages, as it does not allow temporal control of gene knockdown. Moreover, loss-of-function study in different physiological and pathological conditions of adult zebrafish is not feasible with this system, if the gene have early developmental roles. Recently, Leong et al. (2012) tested the possibility of using commercial mouse miRNA backbone-derived miRNA vector system in zebrafish. They showed that the mouse miRNA backbone was able to drive artificial miRNA expression in zebrafish and the transiently expressed artificial miRNA could target EGFP for knockdown which has the target sequence embedded in 3'UTR. This study suggested the possibility of using the well-developed commercial mammalian artificial miRNA expression vector in zebrafish.

1.5 Inducible gene expression in transgenic fish

1.5.1 Inducible gene expression systems

Controlling of transgene expression in zebrafish is mainly through tissue-specific promoters, to restrict the spatial expression of transgene. Temporal control of transgene expression is also possible by using heat-shock promoters. However, it would be quite useful if the expression of transgene can be regulated both spatially and temporally, to precisely analyse gene function in either embryo development or adult disease process. Tissue-specific promoters and conditional gene expression

systems have been combined in transgenic zebrafish, to turn on or off transgene expression at desired stage in a particular tissue. The conditional gene expression systems that have been adopted in zebrafish are illustrated in Fig. 1.11, including the Tet-on system, mifepristone-inducible LexPR system, GAL4/UAS system and Cre-loxP system.

In the tetracycline-inducible Tet-on system (Fig. 1.11A), the regulatory protein rtTA transactivator is a fusion of mutated Tet repressor from bacteria and the Herpes simplex virus VP16 activation domain. The response element contains a tetracycline-response element (TRE) and minimal CMV promoter controlling the expression of gene of interest. Only in the presence of the inducer doxycycline, rtTA can bind to TRE and turn on the expression of gene of interest.

Another system that also uses small chemical as inducers is the mifepristone-inducible LexPR system (Emelyanov and Parinov, 2008). In this system (Fig. 1.11B), the regulatory protein is the hybrid transactivator LexPR (Lex^{DBD}-$PR^{LBD\Delta}$-$p65^{AD}$ in detail). LexPR is engineered by fusion of the DNA binding domain (DBD) of the bacterial LexA repressor, the truncated ligand binding domain (LBD) of human progesterone receptor and the activation domain (AD) of human p65 protein (Emelyanov and Parinov, 2008). The response element of LexPR is the LexOP operator-promoter, which consists of a synthetic LexA operator fused to a minimal 35S promoter from Cauliflower Mosaic Virus. In the presence of mifepristone, it will bind to the LBD of LexPR. The transactivator LexPR will be activated and bind to the

LexA operator to turn on the target gene expression. While without mifepristone, the gene of interest will remain silence. In our study, we will also use the LexPR system to control the target gene expression, because of its effectiveness to drive gene expression.

For the Tet-on and LexPR systems, the regulatory element and the response element can be either put into one plasmid to get a single driver-effector line or kept separately in the driver line and the effector line (the binary system). Maintain a driver-effector line would be simpler, as in the binary system the driver line and the effector line need to be crossed to express the target gene. But the binary system is more flexible, because the effector line can be crossed with different driver lines to induce the target gene expression in different tissues. In our study, we choose to establish the driver-effector line rather than using the binary system, as our study will focus on liver.

For the Gal4/UAS system (Fig. 1.11C), the gene of interested will be expressed only when the driver line expressing the yeast Gal4 transactivator and the effector line containing UAS (the Gal4 targeting sequence) are crossed. Miferpristone-inducible Gal4/UAS system have been used in mice, *Xenopus* and *Drosophila*, but not in zebrafish (reviewed by Emelyanov and Parinov, 2008). In the miferpristone-inducible Gal4/UAS systems, the regulatory element is a chimeric transactivator consisting of yeast Gal4 DNA binding domain, progesterone receptor ligand binding domain and virus VP16 activation domain (or human p65 activation domain). A problem with

using the Gal4/UAS system in zebrafish is that it can be toxic and cause some developmental defect on embryos (reviewed by Huang et al., 2011; Köster and Fraser, 2001).

In the Cre-loxP system (Fig. 1.11D), the gene of interest is not expressed in the absence of Cre recombinase. Once Cre recombinase is introduced, it can remove the mCherry and the stop signal within the loxP sites, thus turn on the expression of the gene of interest under the tissue-specific promoter. The Cre recombinase can be introduced by injecting mRNA or plasmids into embryos, or by crossing the effector line with in a transgenic fish of inducible Cre expression (Huang et al., 2011). An advantage of this system over the chemical-inducible systems is that the activation of gene expression does not need continual chemical treatment which might have some side effect on fish. The disadvantage is that the activated expression could not be turned off, while expression of target gene can be turned off by withdrawing the chemical inducer in Tet-on and LexPR system.

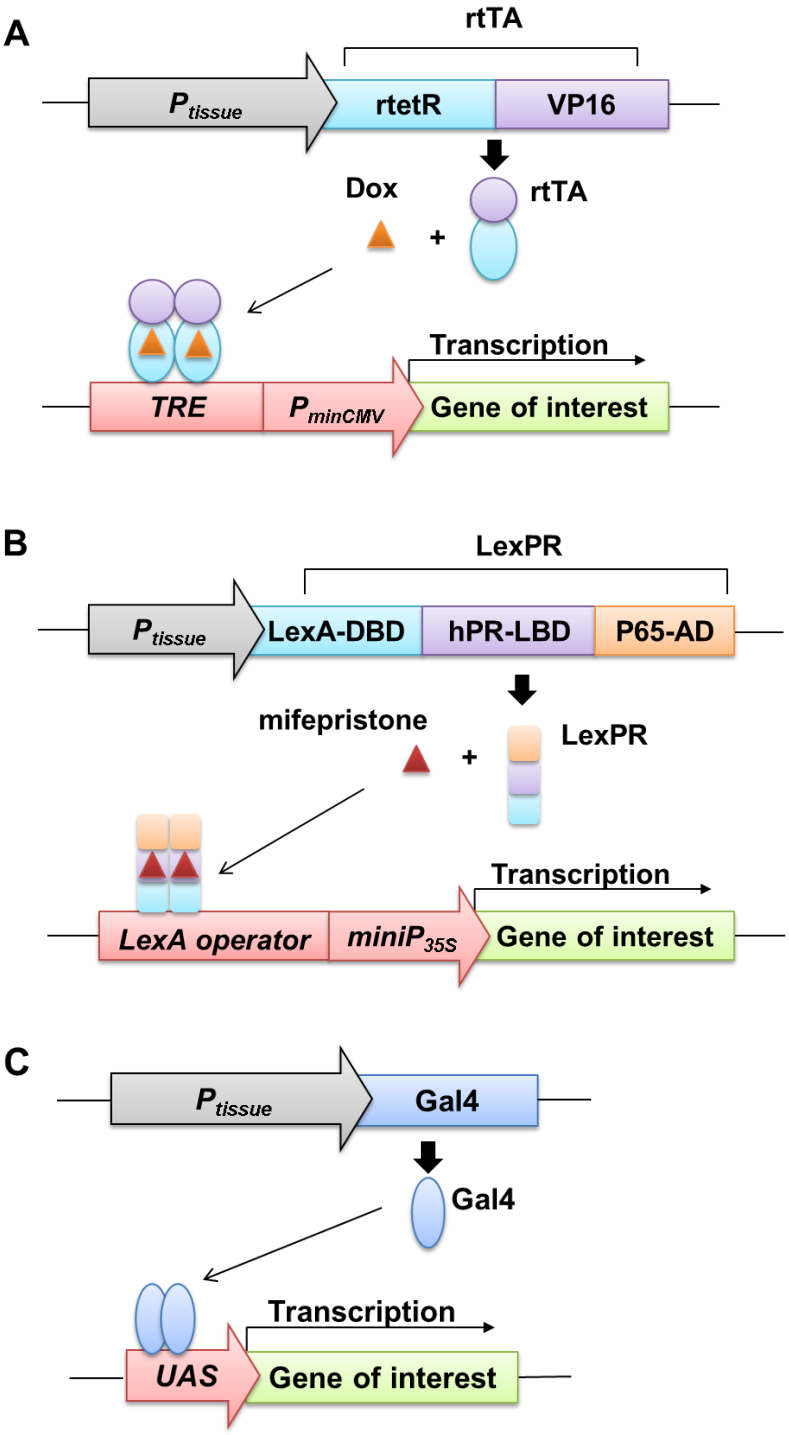
A
rtTA
P tissue
rtetR
VP16
Dox
+
rtTA
Transcription
TRE
P minCMV
Gene of interest
B
LexPR
P tissue
LexA-DBD
hPR-LBD
P65-AD
mifepristone
+
LexPR
Transcription
LexA operator
miniP 35S
Gene of interest
C
P tissue
Gal4
Gal4
Transcription
UAS
Gene of interest

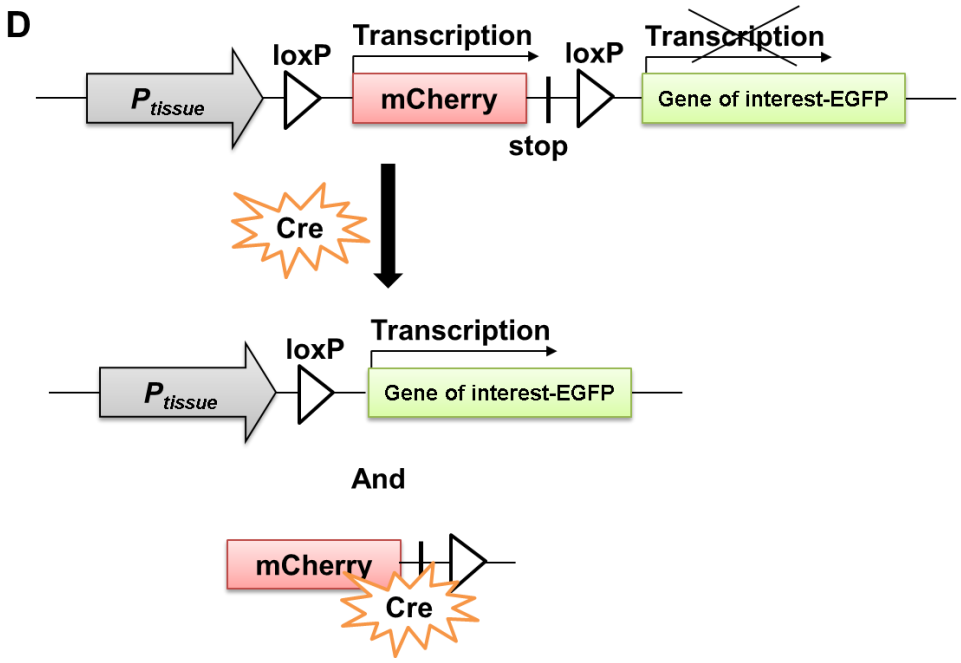

Fig. 1.11 Conditional gene expression systems used in zebrafish.
A, Tet-on system; B, mifepristone-inducible LexPR system; C, Gal4/UAS system; D, Cre-loxP system.

1.5.2 Transposon-mediated transgene insertion for establishing transgenic zebrafish lines

Transposons, also called transposable elements (TE), are DNA sequences that can move to new locations within the genome. Based on the different mechanisms of transposition, transposons can be classified into two types: class I retrotransposons that use 'copy-and-paste' mechanism and class II DNA transposons that use 'cut-and-paste' mechanism (reviewed by Wicker et al., 2007). Class I retrotransposons use RNA as the intermediate for duplication. They are first transcribed from DNA into RNA and then reverse-transcribed into DNA for integration into a new locus, similar as retrovirus. Class II DNA transposons generally have terminal inverted repeats and are recognized by specific transposase for 'cut-and-paste' transposition. But not all

DNA transposons use ‘cut-and-paste’ mechanism. Transposons that use ‘copy-and-paste’ transposition without the RNA intermediate have been reported recently (e.g. *Helitron*) (Lai et al., 2005; Morgante et al., 2005). Transposons have been found in almost all eukaryotic species investigated so far and have been remodelling the eukaryotic genomes for millions of years. However their ultimate origin remains unknown, although it is hypothesized that retrotransposons might originate from retrovirus. The first transposable element (the Ac/Ds system) was discovered in maize by McClintock around 60 years ago (Mc, 1950). Since then thousands of families of transposons have been discovered. It is estimated that transposable elements occupies 80% of plant genome and 3–45% in metazoans (Wicker et al., 2007). Transposable elements can lead to gene mutation, so cells defend against them in multiple ways such as RNAi.

Transposons have been widely used for transgenic technique, because they can carry transgenes for insertion into the genome. The efficiency of transgene integration mediated by transposon is much higher than spontaneous integration. Transposons can lead to insertional mutation, so they also become a useful tool for large-scale mutagenesis study. Transposon-mediated mutagenesis facilitates easy identification of the mutant allele compared to chemical mutagenesis. Because of those advantages, transposons have been widely used in zebrafish for efficient transgenesis and mutagenesis. So far, several transposable elements originated from heterologous hosts have been successfully adopted in zebrafish, including *Tc3* from *Caenorrhabditis*

elegans, *mariner* from *Drosophila mauritiana*, *Tol2* from medaka, *Sleeping Beauty* (a engineered member of the Tc1/mariner superfamily), *Frog Prince* (also a engineered member of the Tc1/mariner superfamily), and *Ac/Ds* from maize (reviewed by Parinov and Emelyanov, 2007). The target DNA sequences can be inserted between the two end sequences of those elements, and the transpositions of those elements into the host genome are done by corresponding transposase through a 'cut-and-paste' mechanism. In zebrafish, the transposase is usually supplied as synthetic mRNA by microinjection into embryos, which will be degraded soon and leave the inserted DNA immobilized. The maize *Ac/Ds* transposon tool have been utilized in zebrafish with advantages of small transposable element size, large fragment carrying capacity, high transposition frequency, efficient germline transmission (up to 60%), and moderate insertion number (Emelyanov et al., 2006; Emelyanov and Parinov, 2008). In this study, we also adopt this *Ac/Ds* transposon tool for establishing transgenic zebrafish lines.

1.6 Aim of this study

In this work, we aim to determine if *alr* play a role in liver organogenesis using the zebrafish model. Specifically, we will:

1. Determine if *alr* is expressed in liver during hepatogenesis and characterize the function of *alr* in liver organogenesis through loss-of-function (MO-mediated knockdown) and gain-of-function (mRNA overexpression) approaches.

2. Establish a temporally and spatially-controlled stable knockdown tool in zebrafish by combining an inducible gene expression system with an artificial miRNA-based knockdown system for liver-specific knockdown of *alr* gene.

CHAPTER 2. MATERIAL AND METHODS

2.1 Zebrafish (*Danio rerio*) maintenance

Fish maintenance and experimental protocols were approved by Institutional Animal Care and Use Committee (IACUC) of National University of Singapore (Protocol 007/06 and 093/10). The wild-type zebrafish were Singapore local strain. Transgenic fish used were *Tg (lfabp: DsRed; elaA: EGFP)* (expressing DsRed in liver and EGFP in pancreas, obtained from Prof Gong's lab) (Korzh et al., 2008) and *Tg (fli1: EGFP)* (expressing GFP in endothelial cells) (Lawson and Weinstein, 2002). *Tg (lfabp: DsRed; elaA: EGFP; fli1: EGFP)* was generated by crossing *Tg (lfabp: DsRed; elaA: EGFP)* and *Tg (fli1: EGFP)* They were maintained and fed as suggested in The Zebrafish Book (Westerfield, 1995).

Adult zebrafish were bred according to methods described in The Zebrafish Book (Westerfield, 1995). For breeding, single pair or 2-3 pairs of fish were transferred to the breeding tank with fish water (supplemented with 2.5 g/L of sea salt) and left overnight. For synchronized spawning, the males and females were separated using a divider which was removed the next early morning and the fish were allowed to mate and spawn.

Embryos were collected and kept in E3 embryo medium (5 mM NaCl, 170 μM KCl, 330 μM $MgSO_4$, 330 μM $CaCl_2$) in an incubator of 28.5 ℃. Embryos older than 24 hpf were raised in 0.003% 1-phenyl-2-thiourea (PTU, Sigma) in E3 embryo medium to inhibit the pigment formation. Embryos were monitored under stereo microscope

for staging. Time of development at 28.5 ℃ and morphological features (Kimmel et al., 1995) were used to stage the embryos.

2.2 Microinjection of morpholinos, mRNAs and DNAs

2.2.1 General microinjection procedure

To prepare needles for microinjection, glass capillaries were pulled to fine tips on a glass micropipette puller (PC-10, Narishige, Japan). The closed tips were broken off at an angle using a blade to create shape open tips. Samples to be injected (morpholinos, mRNA or DNA) were mixed with phenol red solution at final concentration of 0.05%, to aid the observation of solution injected into embryos. Samples were injected into the yolk of 1-2 cell stage zebrafish embryos (2.3 nl per embryo) using Nanoliter 2000 injector (World Precision Instruments) by placing the embryos on a 1.2% agarose plate under a dissection microscope. The injected embryos were immediately put back to the E3 embryo medium.

2.2.2 Knockdown of *alr* by microinjection of morpholinos

Morpholino antisense oligonucleotides were designed to target zebrafish *alr* for knockdown. One morpholino targets the ATG region of zebrafish *alr* mRNA, to block translation; other two morpholinos target the e1i1 and i1e2 splicing sites of *alr* pre-mRNA respectively, to block splicing. For each morpholino, a control morpholino with 5 bp mismatches was also designed. The sequences of morpholinos were displayed in list of primers and morpholinos. They were purchased from Gene Tools,

dissolved in sterile water at the concentration of 1 mM and stored at -80 ℃ in aliquots. The morpholino solutions were heated at 65 ℃ for 10 min to be completely dissolved before the first use and the working vial was stored at 4 ℃. A total amount of 5-10 ng morpholino per embryos was injected.

2.2.3 Overexpression and rescue of morphants by microinjection of synthesized mRNA

The pCS2+ vector containing the CDS of target genes, pCS2+_zf *alr*, pCS2+_zf alr^{C131S}, pCS2+_EGFP, pCS2+_*alr*-EGFP, pCS2+_*hALR205* and pCS2+_*hALR125* were linearized downstream of the poly(A) tail using NotI restriction endonucleases at 37 ℃ for >3 hours. The reaction was run on agarose gel containing 10μg/ml crystal violet and the digested DNA was using purified using Qiaquick Gel Extraction kit (Qiagen) following the manufacturer's instructions. Linearized plasmids were then used for synthesizing 5'-capped poly(A)-tailed mRNAs using mMessenge mMachine kit from Ambion with Sp6 RNA polymerase. For mRNA synthesis, 1 μg of each of the linearized DNA template was added with 10μl of 2× NTP/CAP (10 mM ATP, 10 mM CTP, 10 mM UTP, 2 mM GTP, 8mM cap analog), 2 μl of 10× reaction buffers, 1 μl of Protector RNase inhibitor (Roche) and 2 μl of Sp6 RNA polymerase. The reaction mixture was incubated at 37 ℃ for 3 hours. Subsequently, 1 μl of TURBO DNase (2 U/μl) was added to digest the template DNA by incubating at 37 ℃ for 15 min. The synthesized mRNA was purified using Lithium Chloride (LiCl) precipitation, to remove unincorporated nucleotides and most proteins. Briefly, 30 μl Nuclease-free

water and 30 µl LiCl precipitation solution (7.5 M lithium chloride, 50 mM EDTA) were added to stop the 20 µl reaction and precipitate the RNA, by chilling for ≥30 min at –20 ℃. The solution was centrifuged at 4 ℃ for 15 min at maximum speed to pellet the RNA. The pellet was washed once with ~1 ml 70% ethanol. Finally, the pellet was dissolved in 20-50 µl Nuclease-free water. Nanodrop spectrophotometer ND-1000 was used to measure the RNA concentration. For quality check a small amount of the mRNA was run on agarose gel.

For overexpression study, the synthesized mRNA was injected into 1-2 cell stage embryos, at the highest tolerable doses: 1.6 ng/embryo for *alr*, alr^{C131S} and *alr*-EGFP mRNA; 0.23 ng/embryo for the *hALR205* mRNA; 0.92 ng/embryo for the *hALR125* mRNA. EGFP mRNA is not toxic to embryos and can be injected at very high dose; as a control it was injected at 0.8 ng per embryo. To rescue the *alr* morphants, 5 ng *alr* E1I1 morpholino was co-injected with each of the mRNAs - *alr*, alr^{C131S}, *hALR205* and *hALR125*, at same dose as the overexpression experiments.

2.2.4 Establishing transgenic zebrafish lines by co-injection of *Ac* transposase mRNA and plasmid DNA

For *Ac* mRNA synthesis, the pAc-SP6 plasmid was linearized downstream of the poly(A) tail with the BamHI restriction enzyme and used for generating 5'-capped poly(A)-tailed mRNA *in vitro* with mMESSAGE mMACHINE SP6 kit (Ambion), as described previously. The transgenic fish were created by co-injection of the *Ac* transposase mRNA (50 pg per embryo) and different *Ds* element containing plasmids

(10 pg per embryo) into the yolk of early one-cell stage wild-type embryos. The *Ac* transposase mRNA will be translated into protein and help integration of the transgene into zebrafish genome. Embryos after late one-cell stage should not be used for injection, as the germline integration rate will decrease. Injection of transposase mRNA and plasmid DNA into the cell of the embryo could increase integration rate and number, but is toxic to embryos.

2.3 Whole-mount in situ hybridization (WISH)

2.3.1 Preparation of DIG-labeled RNA probes

10 μg of plasmid DNA was linearized at the 5' end of the cDNA insert (for antisense probe) or 3' end of the cDNA insert (for sense probe) by a proper restriction enzyme. Completion of linearization was confirmed by running a 1% agarose gel. The digested product will be loaded on an agarose gel containing 10 μg/ml crystal violet dye and purified by Qiaquick gel extraction Kit (Qiagen, USA) according to the manufacturer's instructions.

1 μg of linearized DNA was used to synthesize the DIG-labeled probe by *in vitro* transcription. The reaction was performed at 37℃ for 2 hours to overnight in a total volume of 20 μl containing 2 μl of 10× transcription buffer (Roche), 2 μl of DIG-NTP mix [10 mM ATP, 10 mM CTP, 10 mM GTP, 6.5 mM UTP and 3.5 mM DIG-UTP] (Roche), 0.5 μl of Protector RNase inhibitor (40 U/μl) (Roche) and 2 μl of T7 or SP6 RNA polymerase (50 U/μl) (Roche). At the end of the reaction, 1 μl DNase I (Roche)

was added into the reaction mix and incubated for 30 minutes at 37℃ to digest the DNA template. Unincorporated labeled nucleotides can be removed by Roche quick spin column (size exclusion chromatography on RNase-free Sephadex G-25), for the purification of RNA probe, according to the manufacturer's instructions. Briefly, the column was equilibrated by allowing the buffer to drain by gravity. After that, the column was spun at 1100 g for 2 minutes to ensure complete removal of the buffer. The transcription mix was then applied to the column bed and subsequently spun at 1100 g for 4 minutes. The RNA probe bound to the column was eluted with 50 µl H_2O.

The concentration of purified RNA probe was measured using spectrophotometric analysis at OD260/280 nm by Nanodrop ND-1000. Agarose gel electrophoresis was subsequently carried out to access the quality of the probe. The RNA probe stock was stored at -80 ℃. For the working solution, the probe was diluted in hybridization buffer (hereinafter refered to as HYB+) (50% formamide, 5× SSC, 0.1% Tween20, 1M citric acid, pH 6.0 plus heparin (50 µg/ml) and tRNA (500 µg/ml) at a final concentration of 1-10 ng/µl. The working solution was then heated at 80℃ for 5 minutes to removal the secondary structure before using as probe for WISH.

2.3.2 Fixation and storage of embryos

Zebrafish embryos were maintained in embryo water containing phenylthiourea (PTU) which blocked pigmentation in embryos. Chorions of the embryos were removed manually or subjected to pronase treatment for embryos were older than 18-somites

before fixation. Embryos younger than 18-somites were fixed with chorion. Embryos were then chilled on ice for 5 min to prevent curling of the tail. Subsequently, the embryos of various stages were fixed with 4% paraformaldehyde (PFA) in Phosphate Buffered Saline (PBS) at 4 ℃ overnight. The fixed embryos were washed 3 times 5 min each by PBS. Embryos fixed with chorions were dechorionated with the use of forceps. They were dehydrated gradually by 25% methanol, 50% methanol and 100% methanol for 5 min each. Dehydrated embryos can be stored in methanol at -20 ℃ for a few months.

2.3.3 Proteinase K digestion and prehybridization

The dehydrated embryos were rehydrated gradually by 75% methanol, 50% methanol, 25% methanol and PBS for 5 min each. The embryos were then washed with PBS containing 0.1% Tween20 (PBST) for 4 times 15 min each. Embryos that were older than 24 hours post fertilization (hpf) were then digested with 10 μg/ml proteinase K (Roche). The duration of digestion depends on the batch of proteinase K and stage of the embryos, generally 5 min for 24-36 hpf, 15 min for 48 hpf, 30 min for 3-5 dpf. The embryos were then re-fixed in 4% PFA /PBS at room temperature for 20 min. Subsequently, the embryos were rinsed and washed with PBST for 5 times 20 min each. Embryos were then prehybridized by incubating in prehybridization Buffer (50% formamide, 5× SSC, 0.1% Tween20, 1M citric acid, pH 6.0) in a 68 ℃ water bath for overnight. Prehybridized embryos can be stored at -20 ℃ for about one month.

2.3.4 Hybridization

Embryos of different stages or treatments were selected and placed in one tube or separate tubes depending on the experimental conditions. The prehybridization buffer was replaced with the denatured probe dissolving in hybridization buffer. Hybridization was performed at a 68^{o} C water bath overnight.

2.3.5 Post-hybridization wash

RNA probes were removed and saved for future use. Embryos were rinsed with preheated prehybridizatio buffer (hereinafter referred to as HYB-). The embryos were then subjected to these following washes for 15 min each at 68 ℃: 75% HYB-/25% 2× SSCT, 50% HYB-/50% 2× SSCT, 25% HYB-/75% 2× SSCT and 100% 2× SSCT. After which, the embryos were washed twice in 0.2× SSCT for 30 min at 68 ℃. Subsequently, the embryos were subjected to these following washes for 10 min each at room temperature: 75% 0.2× SSCT/ 25% MAB (Maleic Acid Buffer, composed of 150 mM Maleic acid, 100 mM NaCl and 0.1% Tween20), 50% 0.2× SSCT/ 50% MAB, 25% 0.2× SSCT/ 75% MAB and 100% MAB.

2.3.6 Blocking and anti-DIG antibody incubation

The embryos were then incubated in 1× Roche Blocking reagent in MAB for 3-5 hours at room temperature. The 1× Roche Blocking reagent in MAB was then removed and the embryos were incubated with anti-DIG-AP (AP: alkaline phosphatase; Roche) antibody overnight at 4 ℃.

2.3.7 Washing of excess antibody and color development

The antibody was removed and the embryos were washed with MAB for 6 times at every 15 minutes interval. The embryos were then equilibrated with staining buffer (100 mM Tris pH 9.5, 50 mM $MgCl_2$, 100 mM NaCl, 0.1% Tween20) for 3 times at every 5 minutes interval. Substrates were prepared by mixing 4.5 µl of NBT (Nitroblue tetrazolium, 50mg/ml, Promega) and 3.5 µl of BCIP (5-bromo, 4-chloro, 3-indodyl phosphate salt, 50mg/ml, Promega) into 1 ml of staining buffer. The substrates were added into the embryos and the tubes were kept in the dark. Staining was monitored under the stereo microscope at every 30 minutes interval. Staining was stopped by the removal of the staining solution and washing with 1× PBST 3 times at 5 min interval.

2.3.8 Removal of background staining and post-fixation

Stained embryos were subjected to these following washes for 5 min each: 25% Methanol in PBST, 50% Methanol in PBST, 75% Methanol in PBST, 100% Methanol in PBST. After which, embryos were rehydrated by these following washes for 5 min each: 75% Methanol in PBST, 50% Methanol in PBST, 25% Methanol in PBST and 100% PBST. Embryos were then fixed at room temperature in 4% PFA in PBS for 20minutes and stored at 4 ℃ in the dark.

2.3.9 Mounting and imaging

Selected embryos were washed with PBST twice for 10 min each and transferred to glycerol. For whole-mount imaging, a chamber was made by sticking stacks of 3-5 22×22 mm coverslips on both sides of a 25.4×76.2 mm microscope slide. Stained

embryo was transferred to the chamber in a small drop of glycerol and oriented by a needle. A 22×44 mm coverslip was superimposed onto the embryo. The orientation of the embryo can be adjusted by gently moving the coverslip. For flat specimen, the yolk of selected embryo was removed completely by needles. Images were taken using a Zeiss Axioskop 2 microscope.

2.4 Construction of plasmids by DNA cloning

2.4.1 Plasmids for WISH probe synthesis

Plasmids pGEMT_*alr905* and pGEMT_*foxA3* were created for synthesizing *alr* probe and *forkhead box A3* (*foxA3*) probe respectively.

The cDNA of zebrafish *alr* (NM_001089386.1) (905 bp, containing the 5'UTR and 3'UTR before poly(A) tail) was obtained by one-step RT-PCR (Qiagen) using total RNA from mixed stages of zebrafish embryos and 'alr-5UTR-S' and 'alr-3UTR-AS' primers. The PCR product was cloned into pGEM-T vector (Promega) (Fig. 2.1) to create pGEMT_*alr905* plasmid. The insert was validated by sequencing and was in SP6 direction. For *alr* antisense probe synthesis, NotI was used to linearize the plasmid and T7 RNA polymerase was used for *in vitro* transcription. For sense probe synthesis, NcoI was used to linearize the plasmid and SP6 RNA polymerase was used for *in vitro* transcription.

The cDNA of zebrafish *foxA3* (NM_131299) (1.377 kp of the CDS region) was amplified by Qiagen One-step RT-PCR kit using total RNA from mixed stages of

zebrafish embryos, with ‘foxA3-S’ and ‘foxA3-AS’ primers. The PCR product was cloned into pGEM-T vector (Promega) (Fig. 2.1) to create pGEMT_foxA3 plasmid. The insert was in T7 direction and validated by sequencing. For *foxA3* antisense probe synthesis, SacII was used to linearize the plasmid and SP6 RNA polymerase was used for *in vitro* transcription.

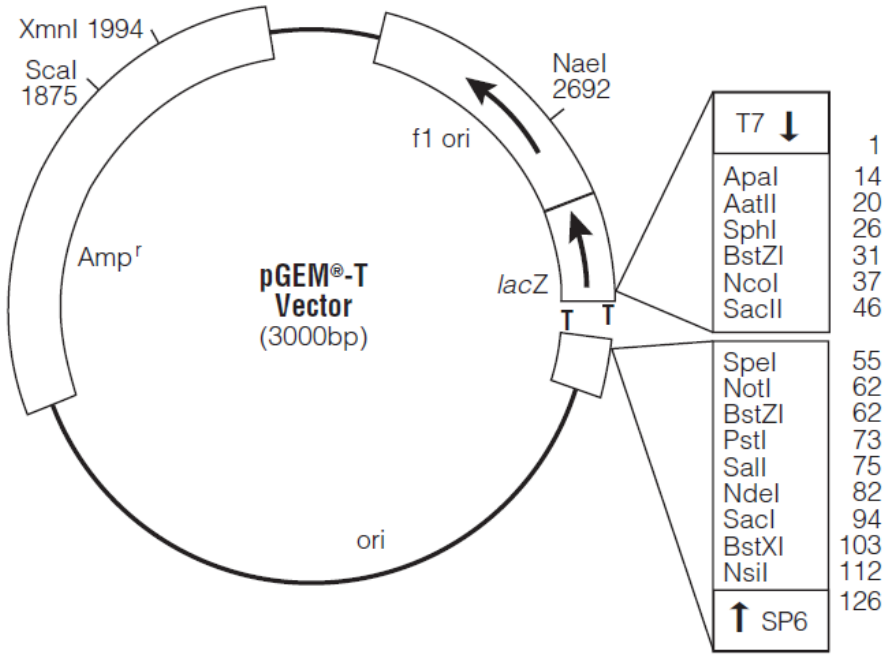

Fig. 2.1 Vector map of pGEM-T. (Adapted from Promega)

2.4.2 Plasmids for 5’-capped poly(A)-tailed mRNA synthesis

The following plasmids (pCS2+ vector containing the CDS of target genes) were used for *in vitro* synthesis of mRNAs: pCS2+_zf*alr*, pCS2+_zf*alr*^{C131S}, pCS2+_EGFP, pCS2+_*alr*-EGFP, pCS2+_h*ALR205* and pCS2+_h*ALR125*. The pCS2+ is a multipurpose expression vector constructed by David Turner and Ralph Rupp (Fred Hutchinson Cancer Center) (Fig. 2.2). It contains a strong enhancer/promoter (simian CMV IE94) followed by a polylinker and the SV40 late polyadenlyation site. An SP6

promoter is present in the 5' untranslated region of the mRNA from the sCMV promoter, allowing in vitro mRNA synthesis of sequences cloned into the polylinker. The pCS2+_EGFP plasmid was obtained from Dr Hong Yunhan. The pAc-SP6 plasmid for Ac mRNA synthesis was obtained from Dr Serguei Parinov (Emelyanov et al., 2006).

The pCS2+_zf*alr* plasmid was created previously in the lab, by cloning the CDS of zebrafish *alr* into pCS2+ between BamH1 and EcoR1 sites. The pCS2+_zfalr^{C131S} plasmid was created using the QuikChange Site-Directed Mutagenesis kit (Stratagene) using pCS2+_zf*alr* as template, following the manufacturer's instruction. The guanine at position 392 of *alr* CDS was mutated to cytosine, as a result cysteine (C) 131 of Alr protein was mutated to serine (S).

The pCS2+_*alr*-EGFP plasmid was created for *in vitro* synthesis of the *alr*-EGFP fusion mRNA. To create this plasmid, the CDS of *alr* and EGFP were fused into pCS2+ vector between the BamHI and EcoRI sites, using Cold Fusion Cloning kit (System Biosciences) following the manufacturer's instructions. Primers 'CF-1-F' and 'CF-1-R' were used for amplifying CDS of *alr* from pGEMT_*alr* plasmid (created previously in the lab), to add vector sequence and BamH1 site at the 5' and some EGFP sequence at the 3'; 'CF-2-F' and 'CF-2-R' primers were used to amplify CDS of EGFP from pEGFP-N1 (Clontech), to add *alr* sequence at the 5' and EcoR1 site plus some vector sequence at the 3'.

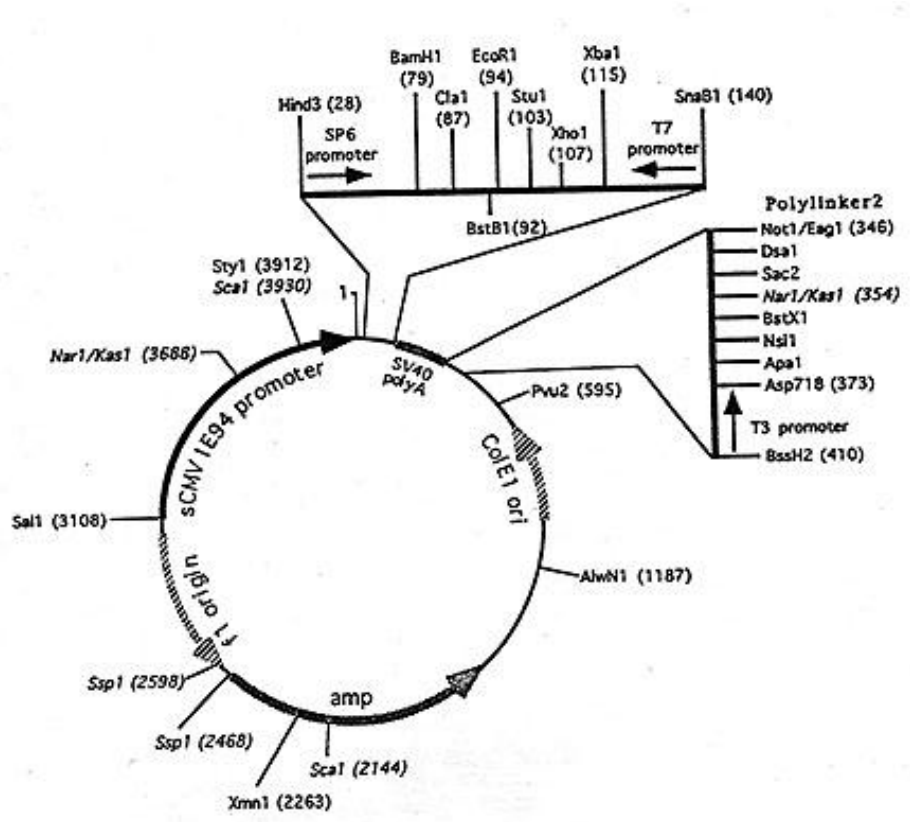

Fig. 2.2 pCS2+ vector map. (Adapted from http://faculty.washington.edu/rtmoon/pcs2+.html)

The CDS of human long form ALR - h*ALR205* was released from pcDNA3.1/myc-HisB_h*ALR205* (obtained from Dr Yang Xiaoming) (Cao et al., 2009) by EcoRI and XhoI digestion, and cloned into pCS2+ between these two restriction enzyme sites to get pCS2+_h*ALR205*. The CDS of human short form ALR – h*ALR125* was released from pcDNA3_h*ALR125* (Yang et al., 1997) by EcoRI and XhoI digestion, and cloned into pCS2+ between these two restriction enzyme sites to get pCS2+_h*ALR125*.

2.4.3 Plasmids for subcellular localization study of Alr

Plasmids pEGFP-N1_*alr* and pEF6/V5-His-TOPO_*alr* were constructed for analyzing the subcellular localization of zebrafish Alr.

Zebrafish *alr* CDS was amplified by PCR from pGEMT_*alr* plasmid using 'alr-S' and 'alr-AS' primers, to add Kozak sequence and restriction enzyme sites. The cDNA was then cloned into pEGFP-N1 vector (Fig. 2.3) (Clontech) within the SacII site before EGFP, to create pEGFP-N1_*alr* plasmid that can express Alr-EGFP fusion protein in eukaryotes.

Zebrafish *alr* CDS was amplified from pGEMT_*alr* plasmid using 'TOPO-F' and 'TOPO-R' primers, and then cloned into pEF6/V5-His-TOPO (Invitrogen) vector (Fig. 2.4) to create pEF6/V5-His-TOPO_*alr* plasmid for transient expression of Alr with a C-terminal V5 epitope and 6×His in cultured cells.

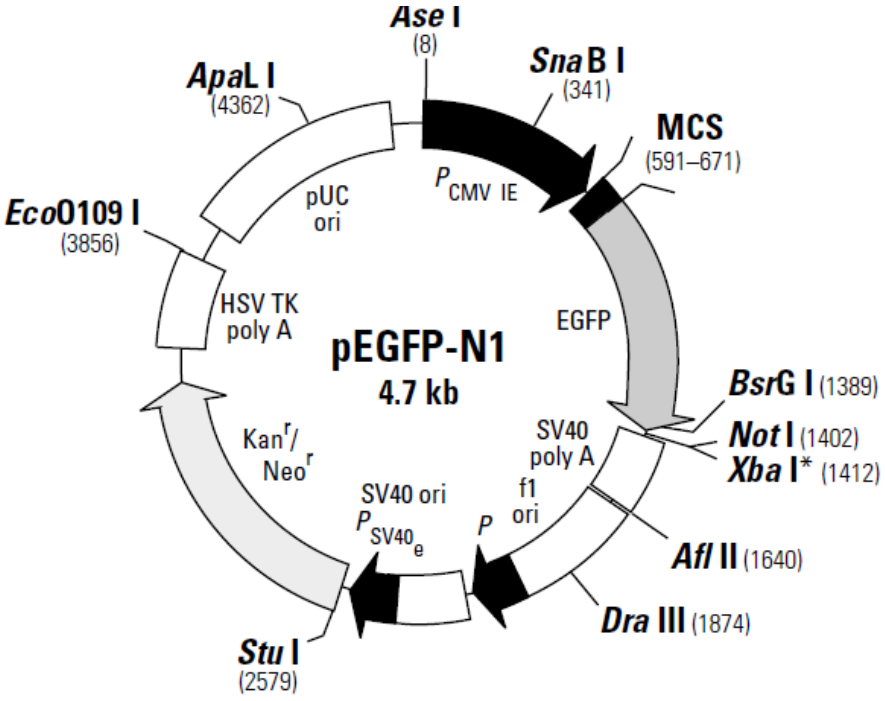

Fig. 2.3 pEGFP-N1 vector map (Adapted from Clontech).

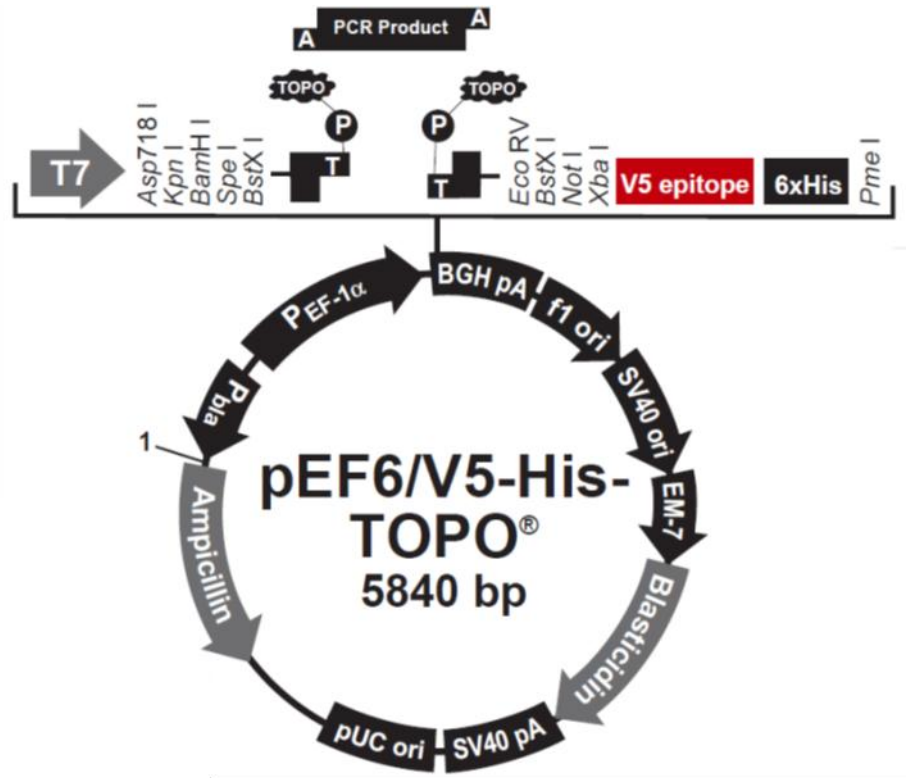

Fig. 2.4 pEF6/V5-His-TOPO vector map. (Adapted from Invitrogen)

2.4.4 Plasmids for recombinant protein expression in *E.coli*

ORF of the wild-type *alr* and mutant *alr*^{C131S} were amplified by PCR from pCS2+_zf*alr* and pCS2+_zf*alr*^{C131S} plasmids respectively using 'P-S' and 'P-AS' primers, and then cloned into pET28b vector (Novagen) (Fig. 2.5) between NdeI and EcoR1 sites to create pET28b_*alr* and pET28b_*alr*^{C131S} plasmids. These two plasmids were used to express and purify recombinant Alr and Alr^{C131S} proteins with N-terminal 6×His from *E.coli*.

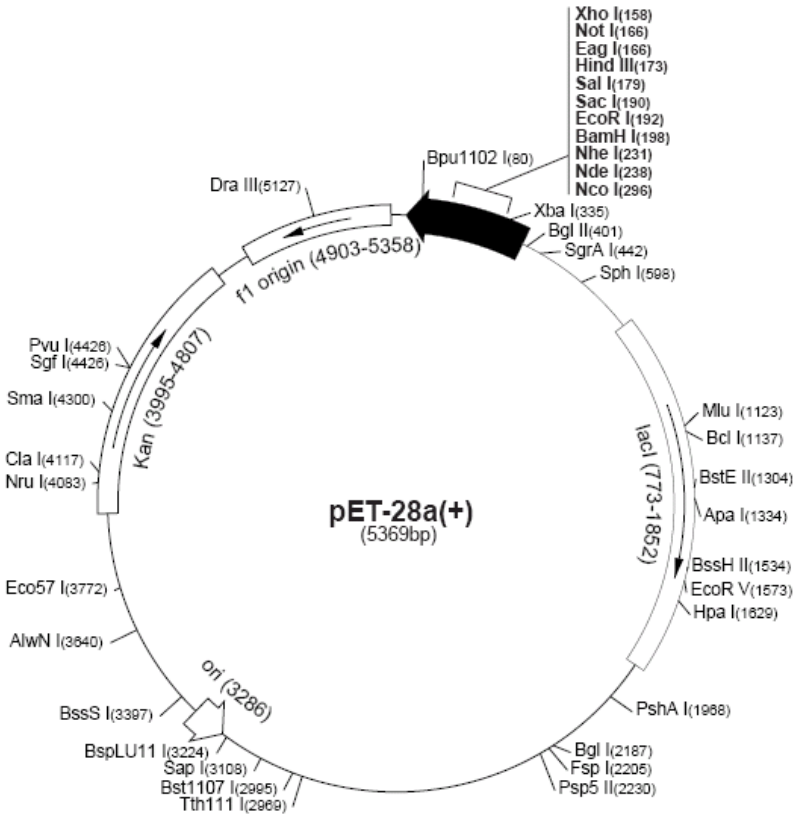

Fig. 2.5 pET-28 vector map. (Adapted from Novagen)

2.4.5 Plasmids constructed for establishing knockdown transgenic fish lines

The sense and antisense strand of designed 68-nt mir-alr/mir-alr^{mis} stem-loop sequence were synthesized as single-stranded DNA oligonucleotides (1st BASE), named '286-307_F' and '286-307_R' for mir-alr, '286-307_mis_F' and '286-307_mis_R' for mir-alr^{mis} in the primer list. They were annealed to form double-stranded DNA oligonucleotides. The annealing reaction was set up by mixing 1 μl of sense oligo (100 μM), 1 μl of antisense oligo (100 μM), 5 μl of 10× annealing buffer (containing 0.4 M Tris-HCl pH 8, 0.2 M $MgCl_2$, 0.5 M NaCl and 10 mM EDTA) and 43 μl of Nuclease-free water, then incubated at 95 ℃ for 2 min and slowly cooled to 35 ℃. The double-stranded 68 bp mir-alr/mir-alr^{mis} stem-loop region

with 4 nt of 5' overhanging at both ends was ligated into BbsI digested pCS2+_mir-linker plasmid (obtained from Dr Ting Xi Liu) (Dong et al., 2009), to get the pCS2+_mir-alr and pCS2_mir-alr^{mis} plasmids. The pCS2+_mir-linker plasmid contains the precursor sequence of zebrafish mir-30e (409 bp), with the 68-bp mir-30e stem-loop region replaced by a linker sequence containing two BbsI sites. Thus the pCS2+_mir-alr/pCS2_mir-alr^{mis} plasmids will have the designed stem-loop region of mir-alr/mir-alr^{mis} embedded in the mir-30e precursor, to express the miR-alr/miR-alr^{mis} using mir-30e backbone. The pCS2+_mir-alr and pCS2_mir-alr^{mis} plasmids was also used for *in vitro* synthesis of poly(A)-tailed mir-alr/ mir-alr^{mis} pri-miRNA using similar methods as described in section 2.2.3, to test the knockdown efficiency of miR-alr.

The mir-alr/mir-alr^{mis} precursor (~400 bp) was amplified from pCS2+_mir-alr/pCS2_mir-alr^{mis} using 'Mir30F-BamHI' and 'Mir30R-BglII' primers to add BamH1 and BglII sites, and cloned into BglII site in intron 2 of zebrafish actin (partial sequence containing an intact exon 2 and intron 2, and the first 21-bp of exon 3) in pCS2+ (obtained from Dr Ting Xi Liu) (Dong et al., 2009). The mir-alr/mir-alr^{mis} precursor containing actin or the actin only was amplified by 'Mir30-Sac2-F' and 'Mir30-Sac2-R' primers, and cloned in-frame to N-terminal of EGFP in the SacII site in pDS(lfabp:LPR-LOP:G4) plasmid (obtained from Dr Serguei Parinov) (Nguyen et al., 2012), to create pDS(lfabp:LPR-LOP:mir-alr-Δactin-EGFP),

pDS(lfabp:LPR-LOP:mir-alr^{mis}-Δactin-EGFP) and pDS(lfabp:LPR-LOP: Δactin-EGFP) plasmids (the construct map was displayed in Fig. 3.44). The three constructs were sequenced using 'p35s-S' and 'EGFP-AS' primers to confirm the correct insert sequence.

2.5 RNA isolation and PCR

2.5.1 Isolation of total RNA

Total RNA from zebrafish embryos and adult tissues was extracted using TRIzol reagent (Invitrogen) following manufacturer's instruction. Zebrafish embryos or tissues were homogenized in 500 µl of TRIzol. After complete dissociation of samples, another 500 µl of TRIzol was added. The homogenate was incubated at room temperature for 5 minutes to dissociate the nucleoproteins from the nucleic acids and centrifuged at 12,000 g for 10 min to remove any tissue cluster. Following this, 200 µl of chloroform was added and thoroughly mixed; the sample was incubated at room temperature for 10 minutes. After that, the sample was centrifuged at 12,000 g for 15 minutes at 4 ℃. Three different phases separated out after the centrifugation and the upper aqueous phase containing the RNA was transferred to another 1.5 ml tube. 500 µl of isopropanol was then added to precipitate the RNA and mixed by vortexing, and the mixture was incubated for 10 minutes at room temperature followed by centrifugation at 12,000 g at 4 ℃ for 8 minutes. The supernatant was then discarded and the pellet was washed with 1 ml 75 % ethanol and

centrifuged at 7500 g for 5 minutes. The pellet was allowed to air dry after the removal of ethanol. RNase-free water was then added to dissolve the pellet. Optical Density (OD) measurement (by Nanodrop ND-1000) and agarose gel electrophoresis were subsequently carried out to access the concentration and the quality of the extracted RNA. The total RNA was then stored at -80 ℃ till further use.

Total RNA was isolation from 30-50 embryos. Adult zebrafish tissues total RNA samples were extracted from a pool of 3-10 fish, depending on the size of the tissue. The livers were dissected from 100 five-days old fish, 50 two-week old fish, 30 three-week old fish, 20 four-week old fish, 10 six-week old fish and 3 adult fish (three-month and nine-month old fish) respectively, for total RNA isolation.

2.5.2 Reverse transcription-PCR (RT-PCR)

RT-PCR was performed in either two-step reaction or one-step reaction. In two step reaction, for the first step first strand cDNA was synthesized using oligo dT primer and the second step involved amplification of fragments of interest with two gene specific primers. The first strand cDNA was synthesized in 20 μl reaction volume using SuperScript III reverse transcriptase (Invitrogen) following the manufacturer's instructions. Briefly, 1 μg of total RNA, 1 μl of 50 μM oligo$(dT)_{20}$ and 1 μl 10 mM dNTP mix was added to nuclease-free water to 13 μl. The mixture was then heated to 65 ℃ for 5 minutes and incubated on ice for 5 min. After that, 4 μl 5 × First-Strand Buffer, 1 μl 0.1 M DTT, 1 μl Protector RNase Inhibitor (40 units/μl) (Roche) and 1 μl of SuperScript III RT (200 units/μl) were added. The reaction was incubated at 50 ℃

for 60 min and heated at 70℃ for 15 min to inactivate the reaction. The first strand cDNA can be stored at -20℃ and used as template for PCR using gene-specific primers.

One-step RT-PCR was performed using One-step RT-PCR kit (Qiagen) and 0.5 μg total RNA in 25μl reaction, following the manufacturer's instructions. The one-step RT-PCR conditions were: 50°C 30 min for reverse transcription; 95°C 15 min to denature the reverse transcriptase and activate the hot-start DNA polymerase; 95°C 30 sec, 55°C 30 sec, 72°C 30 sec, for 25-40 cycles; 72°C 5 min. For expressional analysis of *alr*, 'lfalr-s' and 'alr-Ex3-AS' primers were used (PCR product size is ~200 bp). For the morpholino-mediated gene knockdown efficiency test, primers 'alr-E1-S' and 'alr-Ex3-AS' were used to enable the amplification of alternative spliced products. The zebrafish *ribosomal protein S18* (*rps18*) or *β-actin* were used as internal control. The relative signal intensity of *alr* bands were determined using the ImageJ software by normalizing to the respective *rps18* band.

2.5.3 Isolation of miRNAs

The miRNA was isolated using mirVana miRNA Isolation Kit (Ambion). Around 30-50 embryos or livers from 3 fish were collected; 600 μL Lysis/Binding Solution was added to the samples, followed by immediate homogenization using a plastic pestle to lysis cells. 1/10 volume of miRNA Homogenate Additive (60 μl) was then added to the homogenate, mixed by vortexing, and the mixture was left on ice for 10 min. Organic extraction was performed by adding 600 μl Acid-Phenol:Chloroform,

vortexing mix for 60 sec and centrifuging for 5 min at 10,000 g at room temperature to separate the aqueous and organic phases. The aqueous (upper) phase was transferred to a fresh tube. 1/3 volume of 100% ethanol was added to the aqueous phase and mixed thoroughly by vortexing. The lysate/ethanol mixture was transferred onto the filter cartridge with a 2 ml collection tube and centrifuged at 10,000 g for 15 sec to pass the mixture through the filter. The filtrate contains the miRNAs, while the filter contains an RNA fraction that is depleted of small RNAs and could be recovered from the filter. 2/3 volume 100% ethanol was added to the filtrate; the mixture was passed through a second Filter Cartridge, to bind the small RNA. The filter was washed once with 700 μL miRNA Wash Solution 1, and twice with 500 μL Wash Solution 2/3. Finally, the small RNA was eluted with 50-100 μl 95℃ nuclease-free water.

The RNA was quantified by measuring the absorbance at 260 nm (A260) in a spectrophotometer (Nanodrop ND100). The quality of the small RNA isolated was tested by denaturing acrylamide gel (15% polyacrylamide gel with 8 M urea) using a Mini-PROTEAN 3 Electrophoresis System (Bio-Rad). The denaturing acrylamide gel was prepared as follows: 7.2 g urea, 0.3 ml 50 × TAE (Tris-acetate-EDTA), 5.6 ml 40% acrylamide (acrylamide: bisacrylamide 19:1), 10% APS (ammonium persulfate), 15 μl TEMED (tetramethylethylenediamine) and water up to 15 ml.

2.5.4 Stem-loop reverse transcription of miRNA

The miRNA was quantified using stem-loop reverse transcription (Chen et al., 2005a) followed by SYBR Green real-time PCR analysis. To quantify the miR-alr artificial miRNA and the reference miRNA let-7a, the stem-loop RT primers 'mir-alr_stem loop' and 'let7a_stem loop' were designed, with 8 nt at the 3' end that was complementary to the 3' end of target miRNA and 44 nt stem-loop forming region. The stability of the stem-loop structure of the RT primer precludes its annealing to the pri- or pre-miRNA, due to steric hindrance. The stem-loop RT primers were re-folded in a thermal cycler as follows (Kramer, 2011): heat to 95°C for 10 min; reduce heat slowly to 75°C; hold temperature at 75°C, 68°C, 65°C, and 62°C for 1 hour each; hold at 60°C for several additional hours; stored at -20 °C. The folding procedure need not to be repeated if the primer is never heated above room temperature. The 10 µl stem-loop RT reaction was set as follows: small RNA 250 ng, 2 µM folded stem-loop RT primer 0.5 µl, 5× first strand buffer 2 µl, 0.1 M DTT 0.5 µl, 10 mM dNTP 0.5 µl, Protector RNase Inhibitor (40 units/µl) (Roche) 0.5 µl and of SuperScript III RT (200 units/µl) (Roche) 0.5 µl. The stem-loop RT reaction was performed in a thermal cycler as: 16°C 30 min, 42°C 30 min and 85°C 5 min.

2.5.5 Real-time PCR

QuantiTect SYBR Green PCR Kit (Qiagen) was used for the real-time PCR quantification of miR-alr and let-7a, *alr* and *rps18,* using first-strand cDNA synthesized previously. For miR-alr and let-7a, the 'Universal R' primer and a miRNA specific forward primer ('miR-let-7a-F' and 'miR-alr_F' respectively) were

used. Primers ‘lfalr-s’ and ‘alr-Ex3-AS’ were used for *alr*; primers ‘rps18-F’ and ‘rps18-R’ were used for *rps18.* The real-time PCR was run on LightCycler 480 Real-Time PCR System (Roche). Relative gene quantification was analyzed using delta-delta Ct method where let-7a and *rps18* serve as reference gene for miR-alr and *alr* respectively.

The reaction components for each 10 µl reaction were as follow: 2× Quantitect SYBR Green PCR Master Mix 5 µl, 10 µM forward primer 0.2 µl, 10 µM reverse primer 0.2 µl, cDNA 1 µl, nuclease-free water 3.6 µl. For each gene, three technical replicates were carried out. The cycling parameters were set as such: pre-incubation 95 °C for 15 min; 94 °C 15 sec, 55 °C 15 sec and 72 °C 30 sec, for 40 cycles, plate read after every cycle; melting curve analysis from 60°C to 95 ℃, plate read twice every ℃.

2.6 Proliferation and apoptosis assay

2.6.1 Cryosection of embryos

Embryos were fixed in 4% paraformaldehyde/PBS at 4 °C for overnight. The fixed embryos were transferred into a detached cap of eppendorf tube and immersed in the warm liquid embedding medium constituted of 5% sucrose and 1.5% agarose in PBS. The embryos were adjusted to the required orientation with needles before the agarose solidified. Subsequently, the solidified agarose block was removed from the plastic cap and cut with blade into desired shape. The block was then transferred to 30%

sucrose/PBS solution and incubated at 4 ℃ overnight for equilibration. The block was then placed on the nearly frozen surface of a layer of tissue freezing medium (Tissue-Tek OCT Compound, Sakura) on the pre-chilled tissue holder. The block was then coated with the tissue freezing medium and the holder was immersed in liquid nitrogen until the block had solidified completely. The sample was allowed for equilibration in the Cryostat Sectioning Machine (Leica) pre-adjusted to -30 ℃. Sections of 10 μm thick were cut and placed on superfrost plus slides (Fisher, USA). The slides were dried on a 42 ℃ hot plate for about 1 hour. The dried sections can be stored at -80 ℃ until ready for staining.

2.6.2 Immunofluorescent staining of p-H3 and PCNA

The cryosections were briefly dried; the desired area was circled by hydrophobic PAP pen (DAKO) and the ink was let dry for 10 min. The sections were washed by PBS twice for 5 min each and permeabilized by washing twice for 5 min each, using PBS with 0.1% Triton X-100. Then, the sections were blocked with blocking solution (PBS with 3% BSA, 0.1% Trtion) for 2 hours at room temperature. Subsequently, the sections were incubated with rabbit anti-proliferating cell nuclear antigen (PCNA) (1:250 dilution, Santa Cruz) or rabbit anti-phospho histone H3 (p-H3) antibody (1:100 dilution, Millipore) at 4°C overnight. Then, the sections were washed with washing buffer (PBS containing 0.1% Triton X-100), 6 times for 5 min each. Secondary antibody of Alexa Fluor 568 conjugated anti-rabbit IgG (1:1000 dilution, Invitrogen) was then incubated for 1 h at room temperature. The sections were washed again with

washing buffer for 6 times 5 min each. The sections were then stained with 1 μg/ml 4,6-diamidino-2-phenylindole (DAPI) in PBS for 5 min, to label the nucleus. Finally the sections were mounted in 50% glycerol in PBS and cover with coverslip for confocal microscope imaging.

To calculate the percentage of PCNA/p-H3 positive hepatocytes per embryo, number of stained hepatocytes and total hepatocytes were counted on each section. For PCNA staining of 4 dpf embryos, 3 livers, 7 sections per liver were counted. For p-H3 staining of 4 dpf embryos, 4 livers, 7 sections per liver were counted. For p-H3 staining of 42 hpf and 48 hpf embryos, 5 livers, 7 sections per liver were counted. Data was presented as bar graph of mean ± standard deviation (SD) and $p < 0.05$ was considered significant as analyzed by student's t-test.

2.6.3 TUNEL assay

Hepatocytes apoptosis was analyzed using Roche *In Situ* Cell Death Detection Kit (POD), which was based on the widely used terminal deoxynucleotidyl transferase (TgT)-mediated dUTP nick-end labelling (TUNEL). Following the manufacturer's instruction, the cryosections were briefly dried; the desired area was circled by hydrophobic PAP pen (DAKO) and the ink was let dry for 10 min. The sections were washed by PBS twice for 5 min each. Following that, the sections were incubated with blocking solution (3% H_2O_2 in methanol) for 10 min, to kill the endogenous peroxidase activity. Then the slides were rinsed twice with PBS and incubated in permeabilisation solution (0.1% Triton X-100, 0.1% sodium citrate, freshly prepared)

for 2 min on ice. After rinsing twice with PBS, 50 µl TUNEL reaction mixture (containing Terminal deoxynucleotidyl transferase TdT and fluorescein labeled nucleotides) was added on the section and incubated for 60 min at 37 °C in the dark covered with parafilm. The slides were then washed 3 times with PBS, and the fluorescent signal was observed at this stage. To enhance the signal, the fluorescent signal was converted to colored signal. The slides was incubated with 50 µl converter-POD (anti-fluorescein antibody conjugated with horse-radish peroxidase POD) for 30 min at 37 °C covered with parafilm; washed 3 times with PBS; incubated with 100 µl DAB substrate until proper yellow color was observed. The slides were rinsed 3 times with PBS and mounted with 50% glycerol/PBS under glass coverslip for microscopic imaging. The staining was quantified similarly as the proliferation assay. DNase I-digested samples were used as positive control following the manufacture's instruction.

2.7 Sub-cellular localization analysis of Alr

2.7.1 Culture of HepG2, HEK293T and ZFL cells

Hepatocellular carcinoma cells (HepG2) and human embryonic kidney cells (HEK293T) were obtained from the American Type Cell Culture Collection (ATCC). They were cultured in Dulbecco's Modified Eagle Medium (DMEM) (Sigma) supplemented with 10% heat-inactivated Fetal Bovine Serum (FBS) (Sigma) and 1% Penicillin-Streptomycin (Invitrogen), in 37 °C CO_2 incubator. Zebrafish liver cells

(ZFL) (Ghosh et al., 1994) were obtained from Dr Sinnakaruppan Mathavan (Singapore, GIS). ZFL was grown in LDF medium (made up of 50 % Leibovitz's L-15, 35 % DMEM HG and 15 % Ham's F12, all without sodium bicarbonate, from Gibco), supplemented with 0.15 g/L sodium bicarbonate, 15 mM HEPES pH7.2, 5% heat-inactivated FBS, 0.5% fish serum (from Biodesign) and 1% Penicillin-Streptomycin. The ZFL cells were kept in 28.0 ℃ incubator in air.

All cells were preserved in liquid nitrogen. To cryo-preserve cells, confluent cells were trypsinized, pelleted and resuspended in complete medium, followed by aliquoting into 2 ml plastic cryogenic vial. Dimethyl sulphoxide (DMSO) (Sigma) was added to a final concentration of 10%. The cryovials were left in a Cryo 1 ℃ Freezing Container (Nalgene labware) for overnight at -80 ℃ and transferred to liquid nitrogen tank for storage the next day.

2.7.2 Transfection of cells

The plasmids pEGFP-N1_*alr* and pEF6/V5-His-TOPO_*alr* for expressing Alr-EGFP and Alr-V5 respectively were transfected into HepG2 and HEK293T cells using branched polyethylenimine (bPEI) reagent (Sigma). The cells were passaged one day before transfection and should reach 70% confluence on the day of transfection. The DNA/bPEI complex was formed by adding 15 μg DNA, 20 μl 1 mg/ml bPEI into 1 ml PBS and incubating at RT for 15 min. The DNA/bPEI transfection complex was then added into a 10-cm petri dish of cell dropwise while shaking the dish. The two plasmids were also transfected into ZFL cells using FuGENE HD transfection reagent

(Roche) following the manufacturer's instruction, at the transfection reagent: DNA ratio of 8 μl: 2μg for a well of 6-well plate. For cells grown in other containers, the transfection reagents were adjusted proportionally to the surface area. At 48 hours after transfection, the cells were used for subsequent analysis.

2.7.3 Immunofluorescent staining and confocal microscope imaging

For immunofluorescent staining and confocal imaging, the cells were grown on 0.2% gelatin coated round coverslip placed in 24-well plates. The pEF6/V5-His-TOPO_*alr* transfected cells were first labeled with MitoTracker Red (Invitrogen) before being fixed in 4% PFA. Briefly, the mitochondria staining solution was prepared by diluting 1 mM MitoTracker stock solution to the final working concentration of 100 nM in serum-free medium. The original culture media was replaced by pre-warmed staining solution, followed by incubation for 30 min. The cells were then rinsed twice with PBS and fixed in 4% PFA/PBS for 20 min at RT. After fixation, the cells were washes with PBS/0.1% Triton X-100 for 4 times 5 min each and blocked for 1 hour in blocking solution (PBS with 3% BSA, 0.1% Trion). After blocking, cells were incubated with mouse anti-V5 primary antibody (1:500 dilution, Invitrogen). Then, cells were washed with PBS/0.1% Triton X-100 for 6 times 5 min each and incubated with secondary antibody Alexa Fluo 488 anti-mouse IgG (1:1000 dilution, Invitrogen). After washing for 3 times 5 min each, the cells were stained with DAPI to label the nucleus. The stained cells on coverslip were then mounted to a glass slide, for imaging using the Zeiss LSM 510 Meta confocal microscope. The pEGFP-N1_*alr*

plasmid transfected cells were fixed in 4% PFA, stained with DAPI and directly used for confocal imaging after mounting.

2.7.4 Cell lysis and medium collection

For Western blot analysis, cells were lysed using RIPA lysis buffer (containing 50 mM Tris-HCl pH 7.4, 150 mM NaCl, 1% Triton X-100, 0.5% sodium deoxycholate, 0.1% sodium dodecyl sulfate, 5 mM EDTA) at 48 hour post transfection. The monolayer cells were first rinsed twice with PBS; 1 ml of RIPA lysis buffer with Protease inhibitor cocktail (Roche) was added to one 10-cm petri dish, followed by harvesting the cells by scrappers. Cells were transferred to 1.5 ml tube, incubated on ice for 30 min and vortexed in between. The supernatant was transferred to a clean tube after centrifugation at 13,000 g for 10 min at 4 ℃ and stored at -80 ℃.

The culture medium was collected by Centricon centrifuge filter. One day after transfection, HepG2 and HEK293T cells were changed to condition medium without serum or containing 1% FBS and let grow for another 24-48 hours before collection of medium. For transfected ZFL cells, no change of medium was performed because they are sensitive to no serum condition. So the culture medium was collected 48 hours after transfection. The collected medium was centrifuged to remove floating cells and further concentrated with Centricon centrifuge filter (Millipore) following the manufacturer's recommendation. Briefly, culture medium was transferred into the sample filter cup and the filter unit was centrifuged for 30 min at 3000 g at 4 ℃ in a

swinging-bucket rotor (Beckman) to concentrate to <200 µl. The concentrated sample was transferred to a 1.5 ml tube and stored at -80 ℃.

2.7.5 Isolation of mitochondria

Mitochondria isolation from the cultured cells was carried out using Mitochondria Isolation Kit for Cultured Cells (Pierce). One 10-cm dish of cells was washed with PBS, treated with trypsin and harvested by centrifugation in a 2 ml tube. 800 µl of Mitochondria Isolation Reagent A was added; the cells were vortex at medium speed for 5 sec and incubate tube on ice for exactly 2 min. Next, 10 µl of Mitochondria Isolation Reagent B was added and mixed by vortexing at maximum speed for 5 sec. The tube was incubated on ice for 5 min, vortexed at maximum speed every minute. After that, 800 µl of Mitochondria Isolation Reagent C was added and mixed by inverting. The lysate were then centrifuge tube at 700 g for 10 min at 4 ℃, to pellet the nucleus and cell debris. The supernatant was transferred to a new 2 ml tube and centrifuge at 3000 g for 15 min at 4 ℃ to pellet the mitochondria. The supernatant (cytosol fraction) was transferred to a new tube. The pellet contains the isolated mitochondria. 500 µl Mitochondria Isolation Reagent C was used to wash the pellet, followed by spinning at 12,000 g for 5 min. The mitochondrial pellet was lysed in 100 µl RIPA lysis buffer and stored at -80 ℃.

2.8 Western blot

Western blot was performed using standard method and probed with mouse anti-V5 antibody (Invitrogen), mouse anti-GFP antibody (Millipore), rabbit anti-VDAC/porin antibody (Santa Cruz), mouse anti-α Tubulin (Sigma) and mouse anti-β Actin (Santa Cruz) and mouse anti-His antibody (Invitrogen) respectively.

2.8.1 Preparation of protein samples

Crude total protein samples from cultured cells were prepared by the methods described previously. For the embryo samples, they were prepared by: homogenizing 50 embryos in 100 μl RIPA lysis buffer with proteinase inhibitor cocktail (Roche); brief sonication of the lysate to disrupt the sticky genomic DNA; lysis for 15 min on ice; centrifugation at 14000 rpm for 10 min to remove the debris.

Protein concentration was measured using Bradford assay, using the Bio-Rad Protein Assay Dye Reagent Concentrate, following the manufacturer's instruction. Briefly, 1 ml dye reagent concentrate was diluted with 4ml of distilled water. Bovine serum albumin (BSA) was added to 200 μl dye reagent in 96-well plate to generate the linear range concentration from 10-60 μg/ml. 2 μl protein samples were added to 198 μl dye reagent and incubated at RT for 5 min. Protein concentrations were measured using microplate absorbance spectrophotometer (Bio-Rad) at 595 nm absorbance.

Before loading, the protein samples were mixed with loading buffer (to a final concentration of 62.5 mM Tris-HCl pH 6.8, 10% glycerol, 2% SDS, 0.05% bromophenol blue). 100 mM dithiothreitol (DTT) was also added before boiling in 95 ℃ heating block for 5 min.

2.8.2 SDS-PAGE and protein transfer

For comparison, equal amount of protein lysates (50 μg) was loaded into each well. For pure Alr protein, 0.5μg was loaded. The 10% SDS-PAGE gel was run using a Mini-PROTEAN 3 Electrophoresis System (Bio-Rad) until the dye front reached the edge of resolving gel, to separate the proteins by size. Precision plus protein dual color standards (Bio-Rad) was used as the molecular weight marker.

The proteins on the gel were electrophorectically transferred onto nitrocellulose membrane (Bio-Rad) as follows: the polyacrylamide gel was rinsed in water, placed between layers of Whatman paper and nitrocellulose membrane (facing the anode), covered with sponges on both sides and sandwiched into the plastic holder, soaked into the transfer tank filled with transfer buffer (0.3% Tris, 1.45% glycine and 20% methanol). The transfer was performed at 100 V for 1 hour at 4 ℃.

2.8.3 Immunoblotting and detection

The blotted membrane was washed with 1 × Tris-buffered saline (TBS) buffer (20mM Tris-Cl pH 7.4, 150 mM NaCl). The membrane was blocked with 3% BSA in TBST buffer (0.1% Tween-20 in TBS) for 2 hours at RT. After blocking, membrane was incubated with primary antibody - mouse anti-V5 antibody (Invitrogen) 1:5000, mouse anti-GFP antibody (Millipore) 1:2500, rabbit anti-VDAC/porin antibody (Santa Cruz) 1:1000, mouse anti-α tubulin (Sigma) 1:2500, mouse anti-β actin (Santa Cruz) 1:2500 and mouse anti-His antibody (Invitrogen) 1:2500 respectively, which were diluted in 3% BSA in TBST, for overnight at 4 ℃. The next day, after washing

with TBST for three times 10 min each, the membrane was incubated with corresponding anti-mouse or anti-rabbit IgG HRP-conjugated secondary antibody (Santa Cruz) 1:5000 diluted in TBST for 1 hour at RT. The membrane was then washed for three times 10 min each with TBST. The signal was detected using chemilluminance substrate (SuperSignal West Pico from Pierce) followed by exposure to X-ray films (Kodak).

2.9 Expression and purification of recombinant zebrafish Alr protein from *E.coli*

Wild-type zebrafish Alr and its mutant Alr^{C13S} protein with N-terminal 6×His were expressed in *E. coli* BL21-DE3 strain, from the expression vectors pET28b-alr and mutant pET28b-alr^{C131S}. Bacterial pellet were collected, lysed in lysis buffer, and soluble proteins were subjected to Ni-NTA resin purification under native condition (Promega). The protein was further purified by Fast Performance Liquid Chromatography (FPLC), using size-exclusion column to separate non-specific proteins by size.

2.9.1 Ni-NTA beads purification of zebrafish Alr and Alr^{C131S} from *E.coli*

A single colony from the LB-agar plate was chosen and grown into 1L lactose broth (LB) containing 50 μg/ml kanamycin. The OD600 of culture was monitored using a spectrophotometer. When OD600 reached 0.5, the media was supplemented with 0.5 mM isopropyl-L-thio-β-Dgalactopyranoside (IPTG) and 10 μM flavin adenine dinucleotide (FAD) (Sigma). The cells were incubated at room temperature for 12

hours, shaking at 250 rpm, to induce the expression of target protein as soluble protein. To collect the bacteria pellet, the culture was centrifuged at 5000 g for 10 min at 4 ℃. 20 ml of lysis buffer (100 mM EDTA, 2 mM 2-mecaptoethanol, 100 μg/ml lysozyme, 20 μg/ml of DNase and RNase, 100 mM Tris-HCl pH 7.5) was added to the bacteria pellet, and the suspension was mixed throughly for homogenous re-suspension. Next, the bacteria suspension was lysed by sonication on ice at 20% amplitude, with 50% interval for 30 min. The lysed sample was centrifuged at 5000 g for 10 min at 4 ℃ and the supernatant was collected and bound to Ni-NTA resin, because of the presence of 6×His tag at the amino-terminus of the proteins. The Ni-NTA resin was washed with 10 columns of wash buffer (100 mM Tris-HCl, 10 mM Imidazole, 300 mM NaCl, pH 7.5). Proteins bound to Ni-NTA beads were eluted with elution buffer (100 mM Tris-HCl pH 7.5, 250 mM Imidazole).

2.9.2 Further purification by Fast Performance Liquid Chromatography (FPLC)

Ni-NTA beads purified recombinant Alr or Alr^{C13S} protein of ~20 mg were concentrated to 5 mL using Centricon centrifuge filter (Millipore) by centrifugation at 5000 g for 30 min. Size-exclusion SuperdexTM 75 column was equilibrated with 20 mM Tris-HCl pH 7.5 buffer containing 50 mM NaCl. Samples were injected into the column to be separated by size at a flow rate of 0.8 ml/min. 1 ml elution fractions were collected and analyzed by SDS polyacrylamide gel. Fractions corresponding Alr were collected and pooled together. The pooled protein solution was concentrated to a

higher concentration. The concentration of the purified protein was determined by Bradford assay.

2.9.3 Spectroscopy of zebrafish Alr and Alr^{C13S}

To determine whether zebrafish Alr and Alr^{C13S} bind FAD moiety, the spectroscopy of purified recombinant zebrafish Alr and Alr^{C13S} protein was analyzed. Aliquots of 66.4 μg of purified Alr or Alr^{C13S} proteins was dissolved in 200 μl of 100 mM Phosphate buffer pH 8.0 corresponding to a final concentration of 15 μM. The visible spectrum (300-550 nm) of the protein solution was recorded with a Microplate Spectrometer (Bio-Rad X Mark). Under identical conditions 15 μM FAD (Sigma) was measured as reference.

2.10 Sulfhydryl oxidase enzymatic assay

Lysozyme (Sigma) was reduced and used as substrate as described before (Lisowsky et al., 2001). Reduced glutathione and DTT were also used as substrates. The ability of Alr to introduce disulfide bonds into the substrates were measured by Ellman's reagent (Sigma) which can quantify the number of free thiol groups as described by Lisowsky et al.(Lisowsky et al., 2001). The enzymatic reactions were carried out at room temperature.

2.10.1 Preparation of reduced lysozyme and as the substrate for Alr

The reduction of lysozyme was done by dissolving 20 mg lysozyme in 1mL of deoxygenated (by nitrogen gas flow) 100 mM Tris-HCl buffer containing 6 M

guanidine hydrochloride (Sigma) and 0.3 mM EDTA, followed by addition of DTT to a final concentration of 6 mM. The solution was incubated at 37 ℃ for overnight and then adjusted to pH 3.5 with glacial acetic acid. DTT was removed by passing the solution through Sephadex G25 column (GE Health) equilibrated with deoxygenated 8 M urea containing 0.1% acetic acid and 0.3 mM EDTA.

2.10.2 Enzymatic assay for sulfhydryl oxidase

ALR and ALR^{C131S} protein corresponding to 200 pmol were diluted in 1.2 ml measurement buffer (100 mM Phosphate buffer pH 8.0 and 1 mM EDTA) together with reduced lysozyme that corresponds to 75 nmol reduced thiol groups. The initial content of thiol groups was determined from a sample withdrawn before addition of Alr protein. Aliquots of 200 µl were withdrawn at different time intervals and determined for their thiol content. For this purpose, samples were diluted with 780 µl of measurement buffer and then 20 µl DTNB (Ellman's reagent) (Thermo) was added to a final concentration of 10 µM. After 15 mins, the extinction at 412 nm was measured in a 1-cm cuvette using a spectrophotometer and the thiol content was calculated using an extinction coefficient of 14,150 $M^{-1}cm^{-1}$. Other substrates 1 mM Dithiothreitol (DTT) (Sigma) and 20 mM reduced glutathione (GSH) (Sigma) were investigated similarly.

2.11 Pull-down and mass spectrometry

The proteins in zebrafish mitochondria that bound to recombinant Alr protein with 6×His was pulled down by anti-His magnetic microbeads using the μMACS Epitope Tag Protein Isolation kit from Miltenyi Biotec. For this purpose, ZFL mitochondria isolated from two 10-cm dish was lysed in 200 μl lysis buffer (50 mM Tris-HCl pH 8.0, 150 mM NaCl, 1% Triton X-100). 20 μg of recombinant Alr protein was added to the mitochondria lysate and incubated at 4 ℃ for 1 hour with shaking. No Alr protein added mitochondria lysate was used as the control. The mixture was then bound with 50 μl anti-His magnetic microbeads for 2 hours at 4 ℃ with shaking, for magnetic labeling of His-tagged Alr. Then the mixture was loaded on to the pre-equilibrated column in the magnetic field of the μMACS separator, so that magnetically labeled Alr and proteins bound to Alr will bind to the column. The column was washes for four times with 200 μl of washing buffer 1 (50 mM Tris-HCl pH 8.0, 150 mM NaCl, 1% NP40, 0.5% sodium deoxycholate, 0.1% SDS) and one time with 100 μl of wash buffer 2 (20 mM Tris-HCl pH 8.0). The proteins bound to the column were then eluted with 50 μl pre-heated 95℃ elution buffer (50 mM Tris-HCl pH 6.8, 50 mM DTT, 1% SDS, 1 mM EDTA, 0.005% bromphenol blue and 10% glycerol). The eluted proteins were separated by 10% SDS-PAGE gel and stained with commassie blue. The proteins bands, which were specific to Alr protein added sample and not present in control group (without Alr), were sent for MADLI-TOF-TOF for protein identification.

2.12 Genomic Southern blot

Southern blot using DIG-labeled EGFP DNA probe were carried out to investigate the number of transgene insertion sites in *Tg(lfabp:LPR-LOP:mir-alr-Δactin-EGFP)* F1 generation. Seven F1 fish (named B, C, D, E, F, G, H) were crossed with wild-type fish. Embryos were collected and treated with RU-486 at 3 dpf for 24 hours to screen for green fluorescence signals in the liver. Embryos showing green fluorescence signals were pooled for genomic DNA extraction. Genomic DNA from a mixed pool of embryos that exhibit no green fluorescence (wild-type siblings) was extracted to serve as a negative control for Southern blot.

2.12.1 Genomic DNA extraction

Around 50 embryos were collected in each 1.5 ml tube and the embryos were anesthetized by keeping the tubes on ice for 5 min. The embryos were digested in 600 µl digestion buffer which consisted of 10 mM Tris-HCl pH 8.0, 5 mM EDTA, 1% SDS and 100 µg/ml of proteinase K. The digestion reaction was incubated at 50 ℃ for 3 hours with occasional shaking. 600 µl of phenol was added to each digested mixtures and mixed thoroughly on a shaker. The digested mixture was then centrifuged at 14000 rpm for 10 min. The mixture would separate into two phases. The upper DNA-containing aqueous phase was transferred to a new tube and 600 µl of phenol:chloroform:isoamyl alcohol (25:24:1) was added. The mixture was mixed thoroughly and centrifuged at 14000 rpm for 10 min. The seperated aqueous phase was extracted again with an equal amount of phenol:chloroform:isoamyl alcohol. The

aqueous phase was then transferred to a new tube and mixed with 60 µl of 3 M sodium acetate (pH 5.5) and 1.2 ml of 100% ethanol. The mixture was incubated at room temperature for 15 min, followed by centrifugation at 14000 rpm for 5 min. The supernatant was discarded, leaving the white precipitated DNA pellet. DNA pellet was washed by adding 1 ml of 70% ethanol and centrifugation at 14000 rpm for 5 min. The ethanol was removed and the DNA pellet was air-dried for 5 min. The DNA pellet was then dissolved in 100 µl of TE buffer.

2.12.2 DIG-labeled DNA probe synthesis by PCR

The EGFP in the transgene construct was selected as the probe for Southern blot. DNA probe labeled with DIG-dUTP was synthesized using PCR DIG Probe Synthesis Kit (Roche) following the manufacturer's instruction, using 'GFP_probe_F' and 'GFP_probe_R' as primers and pEGFP-N1 vector as template. A 50 µl PCR reaction was set up containing 5 µl of 10× PCR buffer, 5 µl of 10× PCR DIG probe synthesis mix, 0.5 µl of enzyme mix, 3 µl of 'GFP_probe_F' primer (10µM), 3 µl of 'GFP_probe_R' primer (10µM), 10 ng of pEGFP-N1 vector and 32 µl of water. Cycling conditions were: 95℃ 2 min; 95℃ 30 sec, 60℃ 30 sec, 72℃ for 40 sec, for 30 cycles; 72℃ for 10 min.

2.12.3 Digestion of genomic DNA, agarose gel electrophoresis and transfer of DNA to nylon membrane

12 µg of each of the genomic DNA samples was digested in 120 µl reaction volume by EcoRI and HindIII restriction endonucleases, to produce small-sized DNA

fragments. The digested DNA was then purified and concentrated by ethanol precipitation.

Agarose gel electrophoresis was used for the separation of DNA fragments. 10 µg of each DNA samples was run in 1% agarose gel at 80V for 2 hours. DIG-labeled DNA Molecular Marker II (Roche) was used for the estimation of fragment sizes. After the run, the gel was visualized under UV light. Upon confirmation of complete separation, the gel was submerged in 250 mM HCl for 10 min with shaking to depurinate DNA. Next, the gel was rinsed with water and submerged in denaturation solution (0.5 M NaOH, 1.5 M NaCl) under shaking. Denaturation solution was changed every 15 min for twice. The gel was then rinsed with water and submerged in neutralization solution (0.5 M Tris-HCl pH7.5, 1.5 M NaCl) under constant shaking. Fresh neutralization solution was changed every 15 min for twice. The gel was equilibrated for 10 min in 20× SSC.

The capillary transfer of DNA to positively charged nylon membrane (Roche) was set up following the manufacture's instruction and allowed to transfer at RT overnight. After transfer, the nylon membrane with DNA side facing up was placed on Whatman 3 MM paper that has been soaked in 2× SSC and then it was exposed to 254 nm UV for 1 min. Next, the membrane was rinsed with water and allowed to air dry.

2.12.4 Pre-hybridization and hybridization

Pre-hybridization and hybridization were performed using Easy Hyb Granule (Roche) according to the manufacturer's instructions. Both processes were done in petri dish and tightly sealed with plastic paraffin film to prevent evaporation. Pre-hybridization was done by soaking membrane in 10 ml DIG Easy Hyb buffer at 52 ℃ for 30 min. 8 µl of DIG-labeled DNA probe were diluted in 50 µl of MiliQ water, denatured at 98 ℃ for 5 min and incubated on ice for 2 min. The denatured probe was then diluted in 8 ml pre-heated DIG Easy Hyb buffer, and used for hybridization at 52^{o}C with gentle agitation for overnight.

After hybridization, the membrane was subjected to stringency wash to remove unspecific probe hybridization. The membrane was incubated with 200 ml Low Stringency Buffer (2 × SSC and 0.1% SDS) for 5 min twice. Next, the membrane was incubated with High Stringency Buffer (0.1 × SSC and 0.1% SDS) for 15 min twice. Incubation was done with constant shaking.

2.12.5 Blocking, antibody incubation and detection

The following steps were done using DIG Wash and Block Buffer Set (Roche). Membrane was rinsed with washing buffer for 5 min, followed by incubation in 100 ml blocking solution for 30 min. Next, the membrane was incubated in 20 ml Antibody solution containing 7.5 mU/ml anti-DIG antibody (coupled with alkaline phosphatase) for 30 min. This was then followed by 4 washes of 100 ml washing buffer for 15 min each. Prior to chemiluminescence detection, the membrane was equilibrated for 3 min in 20 ml Detection buffer. The membrane was placed on a

developing cassette and CDP-Star (Roche) substrate was added onto the membrane. X-ray film was used for the detection of chemiluminescence.

2.13 List of morpholino oligos and primers

The morpholino oligos and primers used in this study were listed in Table 1 and Table 2 respectively. The sequences are from 5' to 3' end. A brief description was included for each oligo.

Table 1. List of morpholino oligos used.

Name	Sequence	Description
alr-MO-ATG	cgtgtgcagctgccatgttgttatg	Targeting the ATG region of zebrafish *alr* mRNA, to block translation.
alr-MO-ATGmis	cctgtggagctcccatcttcttatg	5 bp mismatch control of *alr*-MO-ATG morpholino.
alr-MO-E1I1	tcattcataattgttcacctgcacc	Targeting the exon1 and intron 1 boundary of zebrafish *alr* pre-mRNA, to block splicing.
alr-MO-E1I1mis	tgattgataattcttcagctccacc	5 bp mismatch control of *alr*-MO-E1I1 morpholino.
alr-MO-I1E2	ctctcctgtacaacatatcacgttg	Targeting the intron 1 and exon 2 boundary of zebrafish *alr* pre-mRNA, to block splicing.
alr-MO-I1E2mis	ctctcgtctacaagatatgaccttg	5 bp mismatch control of *alr*-MO-I1E2 morpholino.

Table 2. List of primers used.

Name	Sequence	Purpose
SP6	catacgatttaggtgacactatag	DNA Sequencing.
T7	taatacgactcactataggg	DNA Sequencing.
alr-5UTR-S	ctcctacataacaacatggcag	Cloning of zebrafish *alr* cDNA for *in situ* probe.
alr-3UTR-AS	tagaccatctttatttccttctg	
foxA3-S	ccgtttctacgagtacaact	Cloning of zebrafish *foxA3* cDNA for *in situ* probe.
foxA3-AS	ttcaactggctggtaaacac	
ALR-SM-S	ctcccatgtgatgaatccgcagaagacctga	Site-directed mutation of

	g	zebrafish *alr*, to get *alr*^{C131S} mutant
ALR-SM-AS	ctcaggtcttctgcggattcatcacatgggag	
CF-1-F	ctttttgcaggatccatggcagctgcacacgg	Cloning of zebrafish *alr* CDS and EGFP CDS into pCS2+ vector, for *in vitro* synthesis of *alr*-EGFP fusion mRNA.
CF-1-R	gcccttgctcaccattgagtcacaagatccgtc	
CF-2-F	ggatcttgtgactcaatggtgagcaagggcgagga	
CF-2-R	agaggccttgaattcttacttgtacagctcgtc	
alr-S	ctcgaggccgccaccatggcagctgcacac	Cloning of zebrafish *alr* CDS into pEGFP-N1 vector, to express Alr-EGFP fusion protein in cultured cells.
alr-AS	cccgcggtgagtcacaagatccgt	
TOPO-F	gccgccaccatggcagctgcacac	Cloning of zebrafish *alr* CDS into pEF6/V5-His-TOPO, to express Alr with N-terminus 6×His tag in cultured cells.
TOPO-R	tgagtcacaagatccgtccttcca	
P-S	cagatccatatggcagctgcacacgggtc	Cloning of zebrafish *alr* CDS into pET28b vector, to produce recombinant 6×His-Alr protein in *E.coli*.
P-AS	cagctcgaattctcagtcacaagatccgtcct	
286-307_F	ggctatcccacagaaggttaaatagagactggtgcacatgatggagtctttatttccttctgtgggac	Cloning of the 68 bp precursor sequence of the mir-alr artificial miRNA, to target zebrafish *alr* for knockdown.
286-307_R	ggctgtcccacagaaggaaataaagactccatcatgtgcaccagtctctatttaaccttctgtgggat	
286-307_mis_F	ggctatcgcagagaacgttaattagacactggtgcacatgatggagtgtttaattcgttctctgcgac	Cloning of the 68 bp precursor sequence of the mir-alr^{mis} artificial miRNA, as a mismatch control.
286-307_mis_R	ggctgtcgcagagaacgaattaaacactccatcatgtgcaccagtgtctaattaacgttctctgcgat	
Mir30F-BamHI	ataggatccacagccatgccatagttttagg	Cloning of mir-30e backbone containing the mir-alr or mir-alr^{mis} shRNA into intron 2 of Δactin.
Mir30R-BglII	agcagatctagttcatcatatgaccagtgac	
Mir30-Sac2-F	attactccgcgggccaccatggatgaggaaatcgct	Cloning of Δactin (containing mir-alr or mir-alr^{mis} precursor) into pDS(lfabp:LPR-LOP:G4) plasmid, before EGFP.
Mir30-Sac2-R	atagtaccgcggagctcccatgccaaccatca	
p35s-S	cttcgcaagacccttcctctat	DNA sequencing.

EGFP-AS	cgtcgccgtccagctcgaccag	DNA sequencing.
oligodT	ttttttttttttttttttt	First strand cDNA synthesis from total RNA.
rps18-F	atacagccaggtccttgctaatg	RT-PCR of zebrafish *rps18*.
rps18-R	gtgacggagaccacggtgag	
b-actin-F	gatgggaaccgctgcctctt	RT-PCR of zebrafish β-actin
b-actin-R	acggatgtccacgtcgcact	
lfalr-s	gcagctcgagatgacgcagttc	RT-PCR of zebrafish *alr*.
alr-Ex3-AS	ctctccatcgctcatccaccct	
alr-E1-S	gggtcgtctccacatagc	
mir-alr_stemloop	gtcgtatccagtgcagggtccgaggtattcg cactggatacgacgtcccaca	Stem-loop reverse transcription of miR-alr.
let7a_stemloop	gtcgtatccagtgcagggtccgaggtattcg cactggatacgacaactatac	Stem-loop reverse transcription of zebrafish let-7a.
Universal R	ccagtgcagggtccgaggta	Universal reverse primer for qPCR analysis of miRNA after stem-loop RT.
miR-let-7a-F	cgccgctgaggtagtaggttg	qPCR of let-7a
miR-alr_F	cgccgtctttatttccttctg	qPCR of miR-alr
GFP_probe_F	aagggcgaggagctgttcac	PCR synthesis of DIG-labeled DNA probe for Southern blot.
GFP_probe_R	cttctcgttggggtctttgc	
Ds-F	gcgtcccattcgccattcagg	Excision PCR to check Ac transposase activity.
Ds-R	gctgataccgctcgccgcag	
actin-e2-F	atggatgaggaaatcgctgccc	RT-PCR of Δactin-EGFP.

CHAPTER 3. RESULTS

3.1 Cloning and expression analysis of zebrafish *alr*

3.1.1 Cloning of zebrafish *alr* cDNA

3.1.1.1 Isolation of zebrafish full-length *alr* cDNA and sequence analysis

The zebrafish *alr* cDNA was cloned previously in the lab by 5'RACE from total RNA from wild-type embryos. Shortly after that, NCBI database also updated the annotation of zebrafish *alr* full cDNA (GenBank accession number: NM_001089386). Fig. 3.1A shows the cDNA sequence of zebrafish *alr* cloned in our lab and the translated amino acid sequence. It is different from the *alr* sequence in NCBI database by a few nucleotides in the ORF region (Fig. 3.1B). However, the translated polypeptide sequences of 191 amino acids are the same.

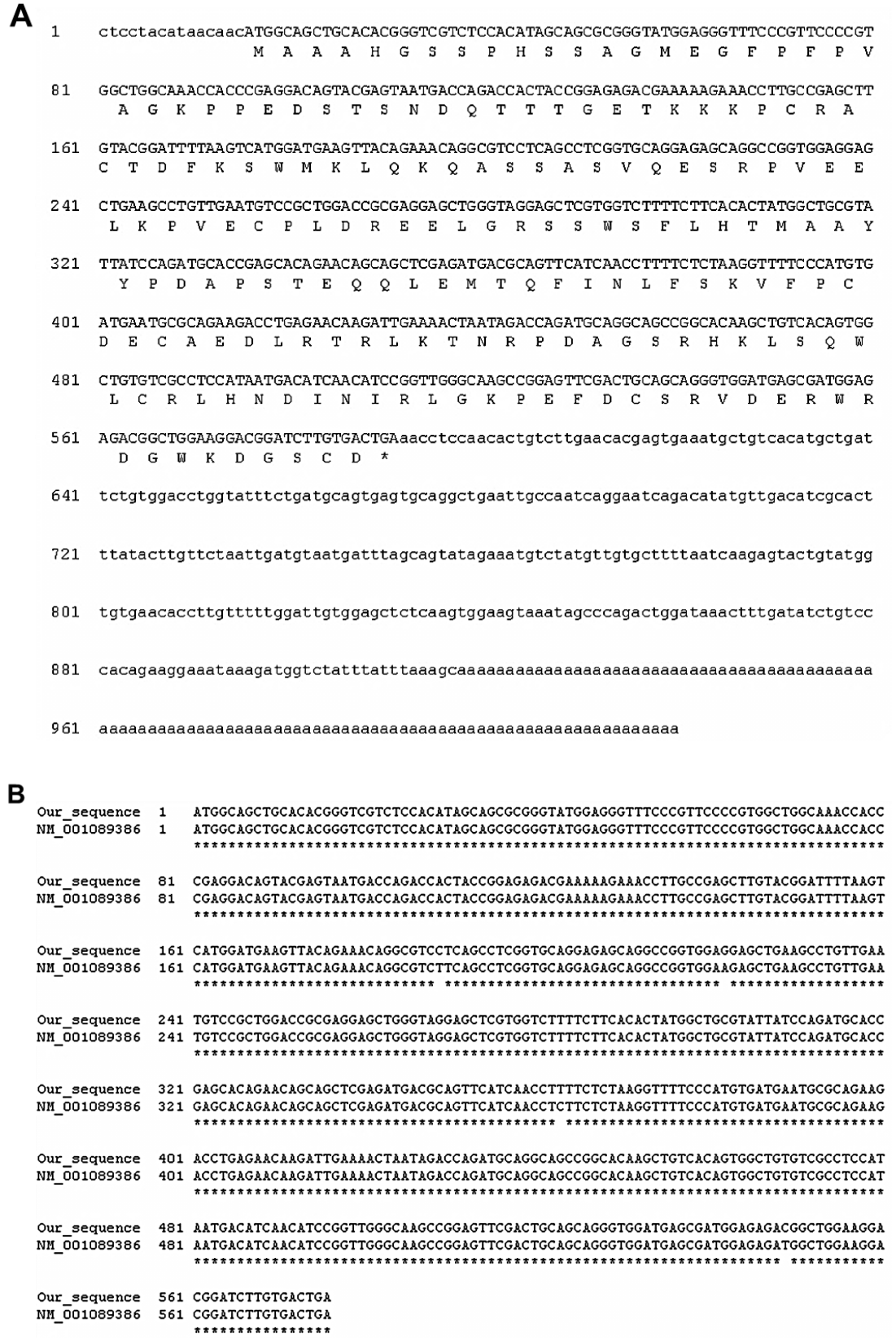

Fig. 3.1 The cDNA sequence of zebrafish *alr*.

A, the *alr* cDNA sequence obtained in our lab and its amino acid sequence. B, sequence alignment of *alr* coding region between our sequence and the NCBI

database sequence (GenBank accession number: NM_001089386). The nucleotide positions without * indicates different nucleotides, probably single-nucleotide polymorphism (SNP) sites.

The zebrafish Alr was compared with the mammalian ALRs and yeast Erv1 (Fig. 3.2). In mammals, ALR have two isoforms (long form and short form), possibly generated from different translation starting sites. The short form lacks 80 amino acids at the N terminus. Sequence alignment showed that zebrafish Alr protein has 62% sequence identity to human and mouse short form ALR, 48% to their long forms. The alignment result shows that Alr has a divergent N-terminal region and a conserved C-terminal region. Within the Erv1/Alr domain, the zebrafish Alr also has a characteristic CxxC motif. Similar to its mammalian orthologs, the zebrafish Alr also have 6 conserved cysteines in the C-terminal Erv1/Alr domain (Fig. 3.2). Structural study of mammalian short form ALRs shows that the six cysteines form two pairs of intramolecular disulfide bonds and one pairs of intermolecular disulfide bonds (Wu et al., 2003). It is highly possible that the zebrafish Alr forms similar structure.

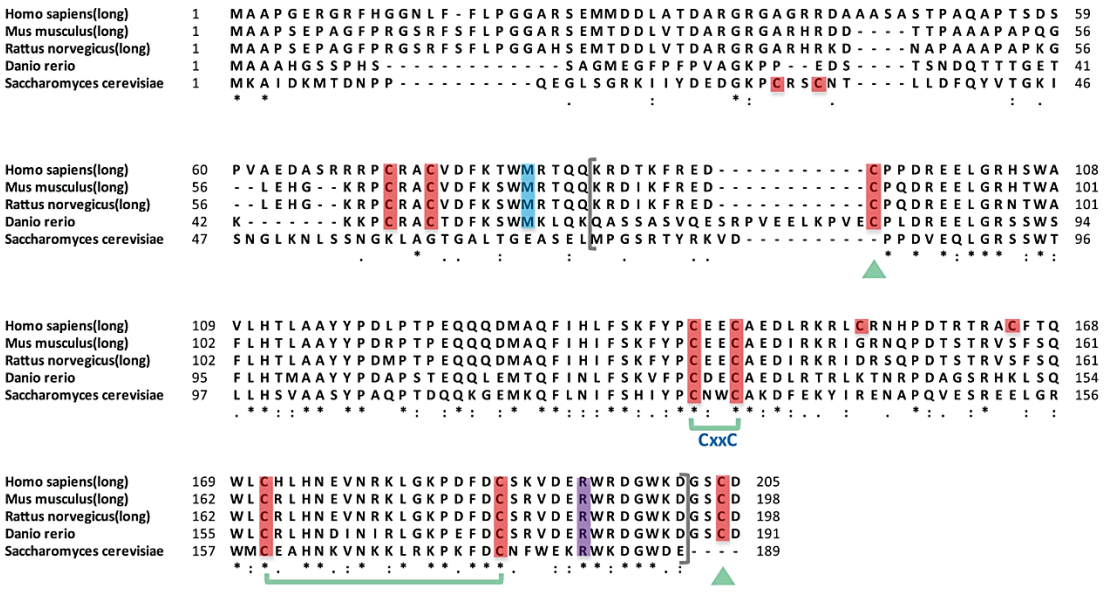

Fig. 3.2 Comparison of ALR protein sequences.
Sequence alignment of ALR proteins were performed using ClustalW program. ALR protein sequences used are: NP_005253 (*Homo sapiens*) (long), NP_075527 (*Mus musculus*) (long), EDM03859 (*Rattus norvegicus*) (long), NP_001082855 (*Danio rerio*), NP_011543 (*Saccharomyces cerevisiae*). All the cysteines are highlighted in red. In human, mouse and rat, methionines labeled by blue are the starting amino acids of the short form ALR proteins; in zebrafish, the conserved methionine at same position is also highlighted by blue. Grey brackets mark the Erv1/Alr domain. Green brackets indicate the known intramolecular disulfide bonds while green arrows indicate the cysteines residues that form the intermolecular disulfide bonds. The conserved Arginines, which correspond to the position of the R194 mutation in human ALR, are highlighted in purple.

3.1.1.2 Phylogenetic analysis of zebrafish *alr*

Phylogenetic analysis of Erv1/Alr proteins in several model species from yeast to human was performed (Fig. 3.3). In mammals, ALR have two isoforms (long form and short form). The long forms were used for the phylogenetic analysis. The zebrafish Alr is clustered in the same big branch with other vertebrate ALRs in the phylogenetic tree (Fig. 3.3), with high level of bootstrap support. This result suggests that zebrafish Alr is an ortholog of human ALR. No paralog was found by sequence blast searching.

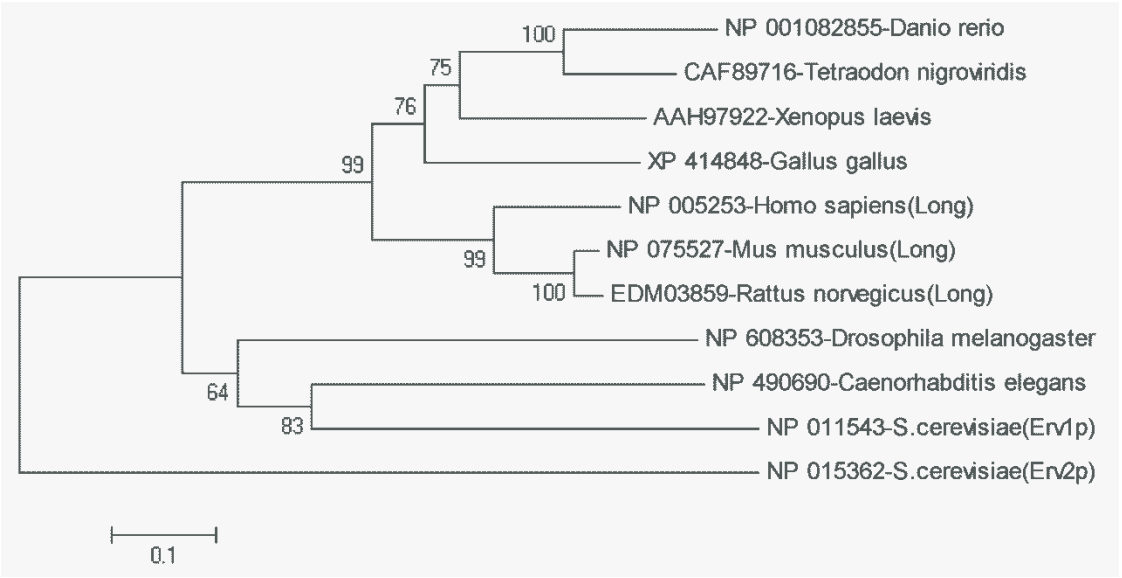

Fig. 3.3 Phylogenetic tree of Erv1/Alr proteins.
Phylogenetic tree was constructed using MEGA version 4 (Tamura et al., 2007). The branches were validated by bootstrap analysis from 1000 replications, which were represented by percentage in branch nodes. The scale bar under the tree indicates the p-distance. The p-distance is the proportion (p) of different nucleotide sites between two sequences compared. ALR protein sequences used in this analysis are: NP_005253 (*Homo sapiens*) (long), NP_075527 (*Mus musculus*) (long), EDM03859 (*Rattus norvegicus*) (long), XP_414848 (*Gallus gallus*), AAH97922 (*Xenopus laevis*), CAF89716 (*Tetraodon nigroviridis*), NP_001082855 (*Danio rerio*), NP_608353 (*Drosophila melanogaster*), NP_490690 (*Caenorhabditis elegans*), NP_011543 (*Saccharomyces cerevisiae*) (Erv1p), NP_015362 (*Saccharomyces cerevisiae*) (Erv2p).

3.1.1.3 Genomic localization and synteny analysis of *alr*

According the annotation information from zebrafish genome database (Ensembl version: Zv9), Zebrafish *alr* locates at Chromosome 3 from 40157181 to 40163264. Similar to the human *ALR*, Zebrafish *alr* also contains 3 exons, with a very short 5' UTR and a relatively long 3' UTR.

Conserved synteny is the phenomenon that gene loci physically co-localize on the chromosome between different species. It is a reliable criterion for predicting orthologous gene relationship in different species, in addition to sequence-based analysis (Barbazuk et al., 2000). Extensive conserved synteny has been reported between human and zebrafish genomes, establishing the usefulness of synteny in predicting orthologous gene relationships (Barbazuk et al., 2000). To further confirm that zebrafish *alr* is the ortholog of human *ALR*, synteny relationship with neighbor genes on the genome was analyzed. Neighbor genes of *alr* (*gfer*) were examined in zebrafish, chicken, mouse and human genomes (Fig. 3.4). In all the four species analyzed, *alr*, *syngr3* (synaptogyrin 3) and *znf598* (zinc finger protein 598) are

arranged in the same order from 5' to 3'. The shared synteny further proves that zebrafish *alr* is the ortholog of mammalian *ALR*, confirming our previous sequence analysis.

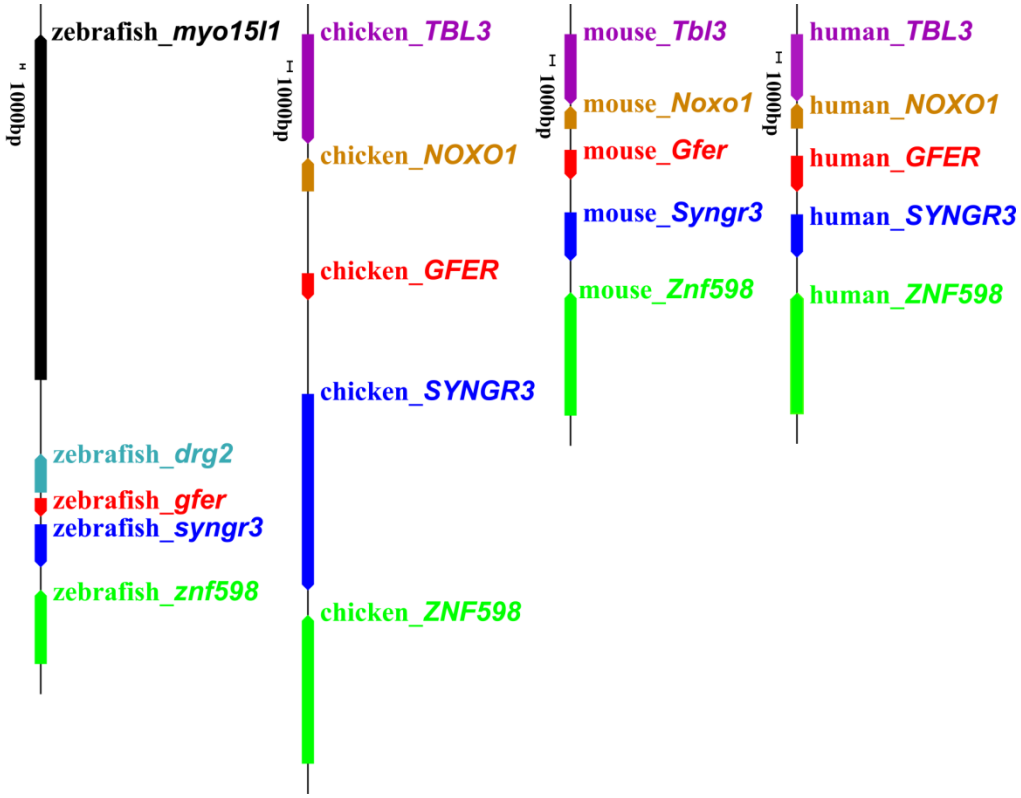

Fig. 3.4 Synteny analysis of *alr* (*gfer*) with neighbor genes in zebrafish, chicken, mouse and human genomes.
Only one copy of *alr* gene was found in the genomes of the four species. Homologous genes are labeled by the same color. Arrow head shows the direction of that gene.

3.1.2 Expression analysis of zebrafish *alr*

3.1.2.1 Expression of *alr* during embryonic development

The dynamic expression level of *alr* at different embryonic stages was examined by RT-PCR, using ribosomal protein S18 (*rps18*) as internal control (Huggett et al., 2005; McCurley and Callard, 2008). The *alr* mRNA could be detected during all the embryonic stages till 5 dpf. Relatively higher expression was found between 26 hpf

and 3 dpf, a period important for liver organogenesis.

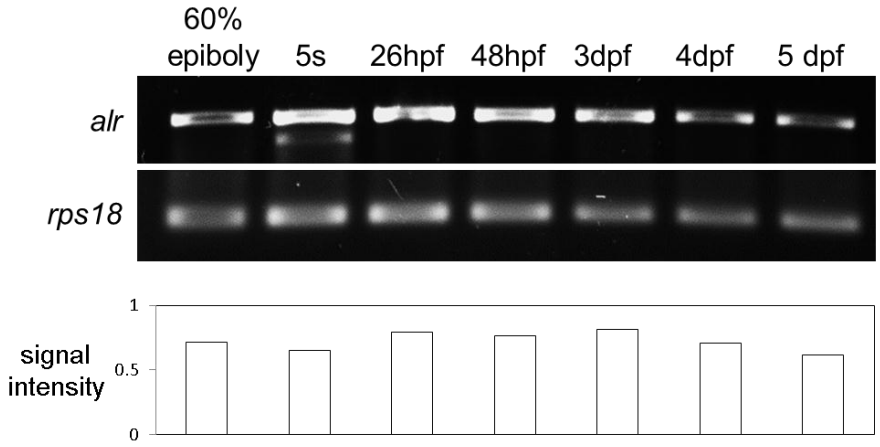

Fig. 3.5 Expression level of zebrafish *alr* at different embryonic stages by RT-PCR.
The embryonic stages used were: 60% epiboly, 5 somites, 26 hpf, 48 hpf, 3 dpf, 4 dpf and 5 dpf. The *rps18* was used as internal control. The intensities of gel bands were quantified by ImageJ software; the relative signal intensity of the respective *alr* bands was shown below gel photos.

To understand the function of *alr* in zebrafish embryonic development, the temporal and spatial expression of *alr* at different embryonic stages was examined by whole-mount in situ hybridization (WISH) using digoxigenin labeled *alr* probe. Embryos from one-cell stage to 5 dpf were examined. The cDNA of *alr*, excluding the poly(A) tail, was used for the antisense probe synthesis. Sense probe was used as the negative control (Fig. 3.6A). The zebrafish *alr* is found to be a maternally expressed gene, with its mRNA detected from one-cell stage (Fig. 3.6B). During early stages (from gastrula period till somitogenesis stages), expression of *alr* in the embryo was ubiquitous. From 28 hpf onwards, the expression of *alr* was detected in liver (Fig. 3.6B, white arrow head) throughout liver organogenesis, suggesting its potential role in liver development. Expression in the brain, pharyngeal arches and intestine were

also observed (Fig. 3.6B).

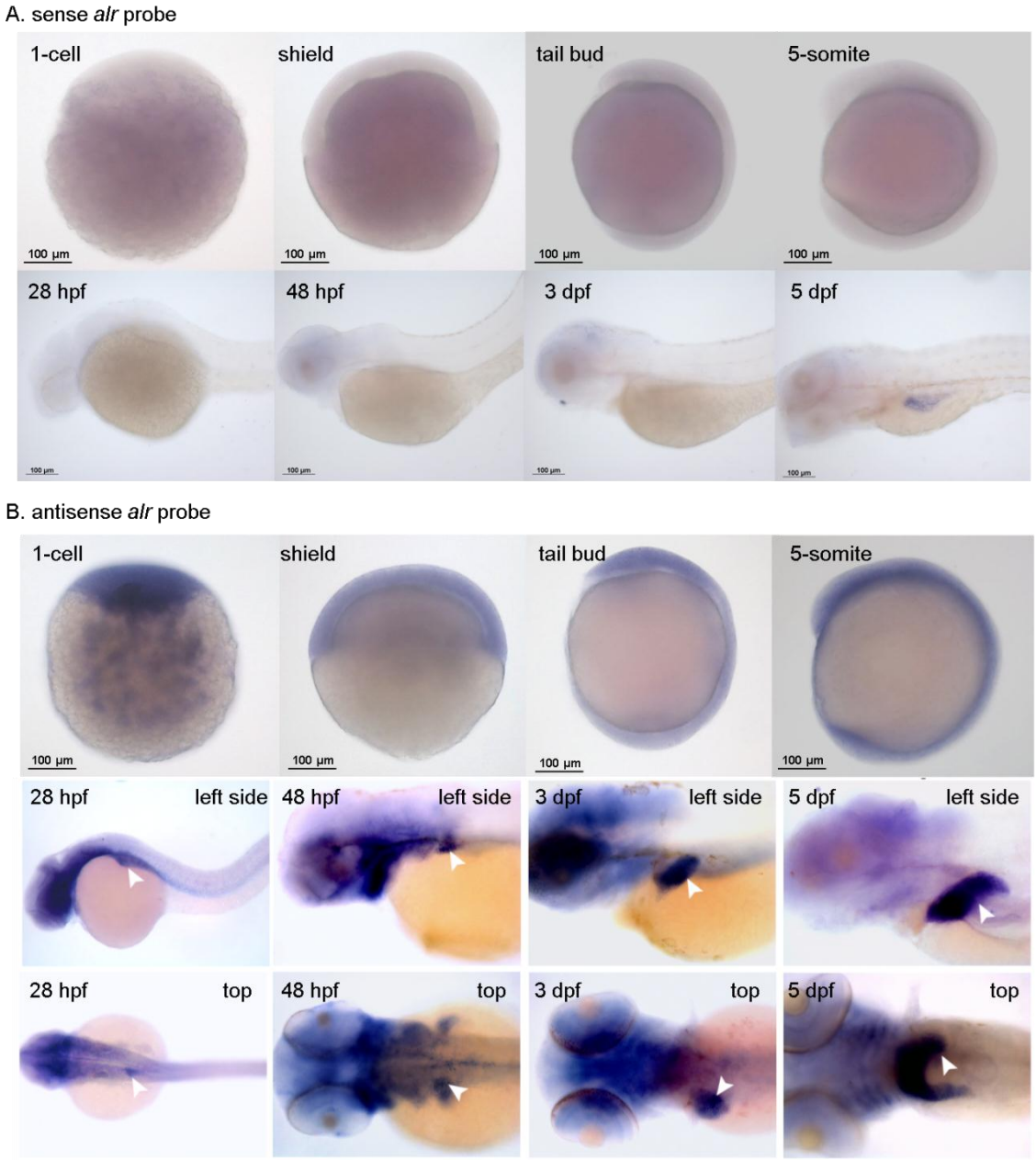

Fig. 3.6 Expression pattern of *alr* during zebrafish embryonic development by WISH.
A, WISH using sense *alr* probe as negative control. B, WISH using antisense *alr* probe, white arrow head indicates liver.

3.1.2.2 Expression of *alr* in different adult tissues and liver of various ages

To understand the function of *alr* in zebrafish adults, its spatial expression pattern in

adult zebrafish tissues was determined. Semi-quantitative RT-PCR revealed that *alr* was expressed at different levels in various adult tissues, with the highest expression in kidney and unfertilized egg (Fig. 3.7A). The high abundance of *alr* mRNA in eggs indicates that *alr* is present as maternal mRNA and may play important roles in early embryonic development. Intermediate level expression of *alr* can be detected in brain and intestine. A low level *alr* expression can be detected in adult liver, spleen, gill, eye and fin, while muscle showed almost no detectable *alr* mRNA.

While previous WISH results from our lab (Fig. 3.6B) showed that *alr* is expressed at very high level in the embryonic liver, subsequent analysis (Fig. 3.7A) showed that *alr* expression in adult livers is at very low level. To understand how *alr* level changes in the liver from embryo stage to adult, the livers were isolated from fish of various ages and subjected to total RNA extraction and RT-PCR. The *alr* is expressed at high levels in 2-4 weeks old fish, but reduces significantly in 6 weeks old fish. The expression level is further reduced in adult fish (3-9 months old). The expression of *alr* in 5 dpf whole embryo is used as a comparison. This result suggests that liver *alr* expression is highest in young fish and gradually declines to a moderate level in adults (Fig. 3.7B).

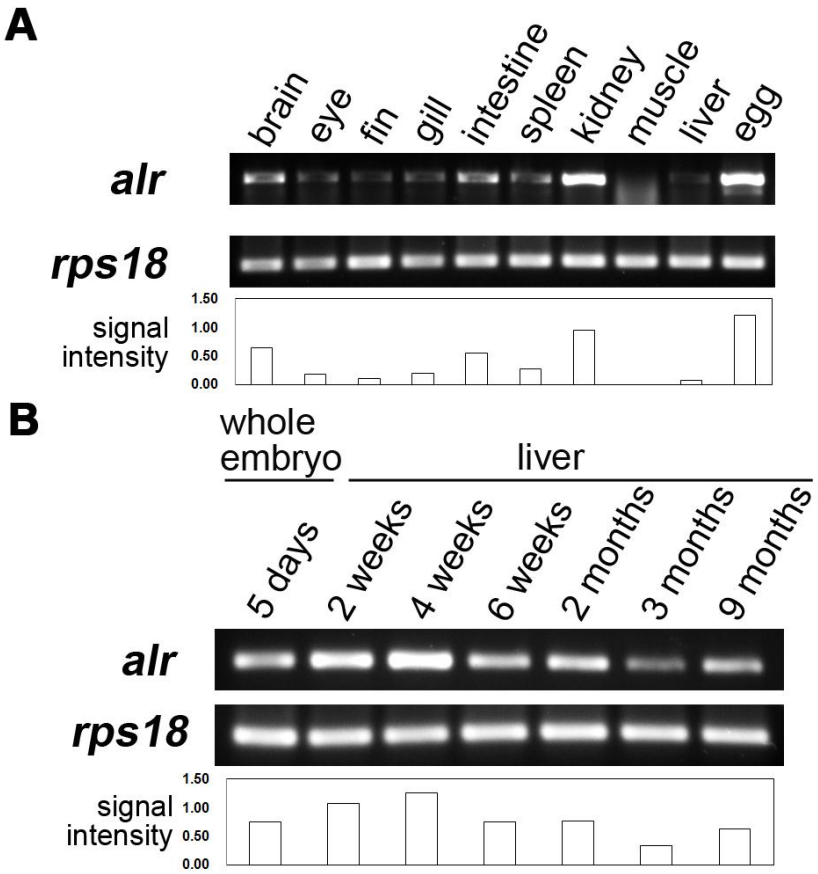

Fig. 3.7 Expression of zebrafish *alr* in adult tissues, livers of various ages by RT-PCR.

A. *alr* expression in zebrafish adult tissues. B. *alr* expression in liver of various ages. The expression of *alr* in 5 dpf whole embryo is used as a comparison. The *rps18* was used as the internal control. The intensity of gel bands were quantified by ImageJ software, and the relative signal intensity of all the *alr* bands were shown below the gel photos.

3.1.2.3 Response of *alr* to liver damage

It is known that expression of ALR will increase in acute or chronic human liver diseases such as fibrosis and cirrhosis, as well as in liver carcinoma (Cao et al., 2009; Tanigawa et al., 2000; Thasler et al., 2005), suggesting liver protective functions of ALR in liver diseases. Acute liver damage induced by toxins, such as ethanol, is also known to stimulate hepatic stimulatory substance (HSS) (a crude extract from which

ALR was purified) activity in the injured livers, and exogenous HSS administration increased the injured liver hepatic proliferation post toxin treatment (Kondili et al., 2005; Liatsos et al., 2003). This suggests that ALR has liver protective function in both liver disease and liver damage process.

Therefore we investigated the response of Alr during liver damage in zebrafish model. When zebrafish embryos at 5 dpf and larvae of three-weeks old were treated with 2% ethanol, a condition previously shown to induce hepatic steatosis (fatty liver) in zebrafish (Passeri et al., 2009). The liver was dissected from 5 days and 3 weeks old fish, for RNA isolation and RT-PCR. The *alr* expression was significantly up-regulated in the liver (Fig. 3.8). This result indicates that liver injury can lead to increased *alr* expression in the liver of zebrafish larvae, similar to the behavior of mammalian ALR after liver injury. However, the role of Alr in zebrafish liver steatosis is unclear at this stage.

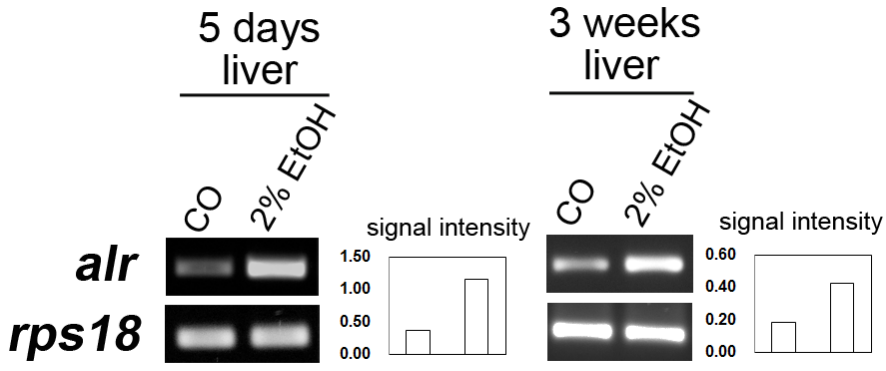

Fig. 3.8 Response of *alr* to alcohol-induced liver damage by RT-PCR.
Fish were treated with 2% ethanol for 32 hours, to induce hepatic steatosis. Liver RNA was used for RT-PCR. The *rps18* was used as the internal control. The intensity of gel bands were quantified by ImageJ software, and the relative signal intensity of all the *alr* bands were shown beside the gel photos.

3.2 Functional study of zebrafish *alr*

3.2.1 Loss-of-function analysis

3.2.1.1 Knockdown of *alr* by morpholino antisense oligonucleotides

To investigate the developmental functions of *alr* in zebrafish, morpholino antisense oligonucleotide (morpholino or MO)-mediated gene knockdown was performed. As illustrated in Fig. 3.9A, zebrafish *alr* gene has three exons separated by two introns. Two types of morpholinos were designed: the translation-blocking morpholino which targets the translation starting site, named as the ATG MO; the splicing-inhibiting morpholinos targeting the exon1-intron1 boundary (the E1I1 MO) and intron1-exon2 boundary (the I1E2 MO) respectively (Fig. 3.9A). Morpholinos were injected into one-cell stage embryos, using 5 bp mismatch morpholinos as controls.

The potency of knockdown can be verified at protein level through Western blot for the translation-blocking morpholino or at mRNA level through RT-PCR for the splicing-inhibiting morpholino. As anti-zebrafish Alr antibody was not available, the knockdown of endogenous Alr by ATG MO could not be verified through Western blot. We could, however, verify the knockdown of *alr* by the E1I1 MO and I1E2 MO through RT-PCR. Both splicing-inhibiting morpholinos E1I1 MO and I1E2 MO could potently knockdown the endogenous *alr* mRNA. Significant reductions of endogenous *alr* mRNA were demonstrated in embryos injected with either E1I1 MO or I1E2 MO at 5 ng per embryo, while same amount of the their 5 bp mismatch control morpholinos did not affect *alr* mRNA level (Fig. 3.9B).

Unique alternative splicing products could be detected, resulting from blocking the splice sites by E1I1 MO and I1E2 MO (Fig. 3.9B, bands a, b and c). To validate these new splicing products and examining their functional potential, the DNA bands were cloned and sequenced. As illustrated in Fig. 3.9A, the E1I1 MO blocked the exon 1 intron 1 splice donor site and resulted in two alternative splicing products: product a included 229 nt of the first intron by using an alternative splice donor site further downstream in the first intron; product b lost 59 nt in the 3' end of the first exon by using an alternative splice donor site within the first exon. The I1E2 MO blocked the intron 1 exon 3 splice acceptor site and generated an aberrant RNA product lacking the second exon. All three aberrant RNA products carry premature stop codons, will probably encode proteins containing only part of the N-terminus of Alr, and are thus predicted to be non-functional.

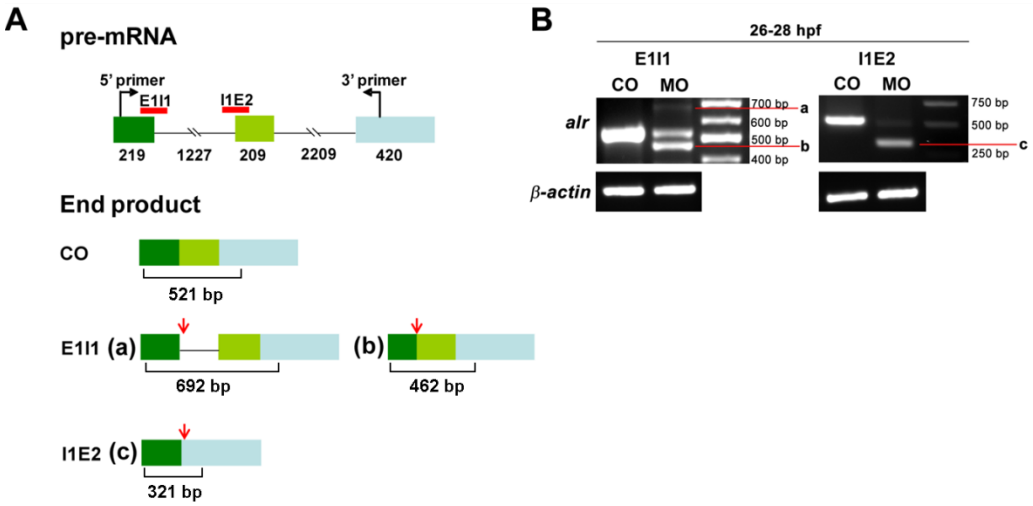

Fig. 3.9 Knockdown of *alr* by morpholino antisense oligonucleotides.
A, Schematic presentation of *alr* pre-mRNA and morpholino design. *alr* pre-mRNA consists of 3 exons (shown by squares) and 2 introns (shown by lines). The number of nucleotides in each region is labeled. The targeting sites of the two splicing-inhibiting morpholinos, E1I1 MO and I1E2 MO, were labeled (red lines). The red arrows show the stop codons present in these alternatively spliced mRNAs.

B. RT-PCR results demonstrate the potent knockdown of endogenous *alr* mRNA by the splicing-inhibiting morpholinos. Bands a, b and c are described in Fig. 3.9A, with their sizes indicated. CO, 5-bp mismatch morpholino injected embryos; MO, morpholino injected embryos. *β-actin* was used as internal control for RT-PCR.

3.2.1.2 Knockdown of *alr* inhibits hepatocytes differentiation without affecting hepatoblasts specification

The amount of MO injected per embryo was carefully titrated. When injected at ≥ 10 ng morpholino per embryo, embryos showed severe morphological defects including curved bodies, small heads with high level of apoptosis seen in brain, no circulation, and cardiac edema. In comparison, embryos injected with the same amount of 5 bp mismatch control morpholino did not produce such morphological defects. This was more obvious with the translation-blocking morpholino. It therefore seems that the maternally supplied *alr* mRNA and *alr* expressed in early stage embryos plays some fundamental roles in early zebrafish embryonic development. High amount of morpholino (10 ng/embryo) leads to death of embryos within 24 hpf. When injected at 5 ng morpholino per embryo, embryos are morphologically normal, except for a mild developmental delay. Thus all functional studies presented below were carried out with this morpholino dose.

Zebrafish liver development can be divided into two stages: budding stage and growth stage. During liver budding stage (24 hpf-48 hpf), competent endoderm cells become specified into bi-potential hepatoblasts upon induction and later differentiate into hepatocytes or cholangiocytes (Field et al., 2003). During growth stage (48 hpf-5dpf), proliferation of hepatocytes underscores the rapid increase of the liver volume. In

order to determine at which stage of liver development *alr* functions, WISH with hepatoblast/hepatocyte markers were performed in *alr* morphants.

Localized expression of *prox1* in the liver region at 22-26 hpf indicates the specification of hepatoblasts from endoderm cells (Field et al., 2003). As shown in Fig. 3.10 A and B, *prox1* expression in the liver primordial region was detected at 26 hpf in *alr* morphants, suggesting that the specification of liver progenitor cell hepatoblasts was not affected by *alr* knockdown. Differentiation of hepatoblasts into hepatocytes could be identified by hepatocyte marker *cp* from 32 hpf (Korzh et al., 2001). The hepatocyte marker *cp* was absent in liver bud in 47% of the embryos injected with *alr* morpholino at 34 hpf (Fig. 3.10 C and D), while the expression of *cp* in yolk syncytial layer was normal, showing that hepatocyte differentiation was affected by *alr* knockdown. The hepatocyte differentiation was delay for a few hours by *alr* knockdown, as *cp* could be detected in the liver after 48 hpf in all the *alr* morpholino injected embryos.

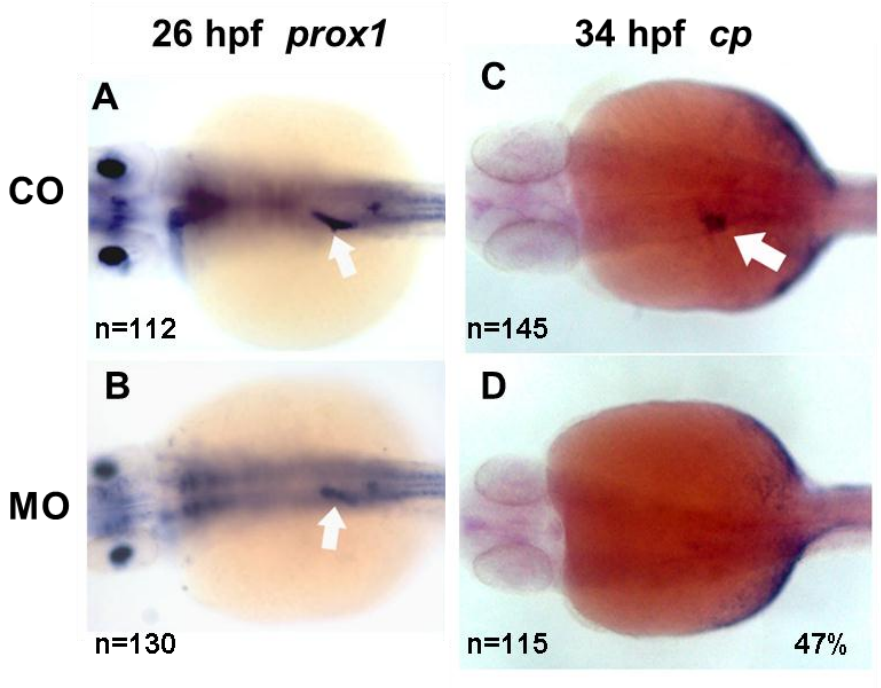

Fig. 3.10 Liver formation in *alr* morphants.
Hepatoblast specification was monitored by *prox1* (A and B) and hepatocyte differentiation was identified by *cp* (C and D). CO, 5 bp mismatch morpholino injected; MO, *alr* morpholino injected. The number of embryos analyzed was shown on the bottom left of each panel while the percentage of embryos with liver defects was labeled on the bottom right corner. White arrow points to liver bud. All images are dorsal view, anterior to the left.

3.2.1.3 Knockdown of *alr* inhibits liver outgrowth

The effect of *alr* knockdown on liver outgrowth was monitored using the transgenic line *Tg(lfabp:DsRed; elaA:EGFP).* In this transgenic line, liver-specific expression of DsRed (red fluorescence) under liver fatty acid-binding protein (*lfabp*) promoter is easily visible after 60 hpf while the exocrine pancreas is labeled green with EGFP from 4 dpf onwards (Farooq et al., 2008). Knockdown of *alr* lead to an obvious reduction in liver size in morphants from 3-5 dpf compared to control morpholino injected embryos at the same stage (Fig. 3.11A). Cryostat sections of the liver were obtained from morpholino injected 5 dpf *Tg(lfabp:DsRed; elaA:EGFP)* embryos (Fig.

3.12). Sections from anterior to posterior liver showed that knockdown of *alr* indeed significantly inhibited the overall liver growth while did not disturb the organization of liver cells.

Consistently, liver size marked by *prox1* expression is also obviously smaller in the morphants at 48 hpf (55% of embryos) and 3 dpf (51% of embryos) (Fig. 3.11B). An obvious reduction of liver size was also observed in *alr* morphants using *cp* as a marker from 48 hpf till 5 dpf, while the expression of *cp* in the yolk syncytial layer is not affected (Fig. 3.11C).

Knockdown of *alr* using three different morpholinos showed similar small liver phenotype, and the photos shown in Fig. 3.10-3.12 were from ATG MO injected embryos. In summary, the above results suggest that zebrafish *alr* is required for liver outgrowth and knockdown of *alr* inhibits liver growth without affecting hepatoblast specification.

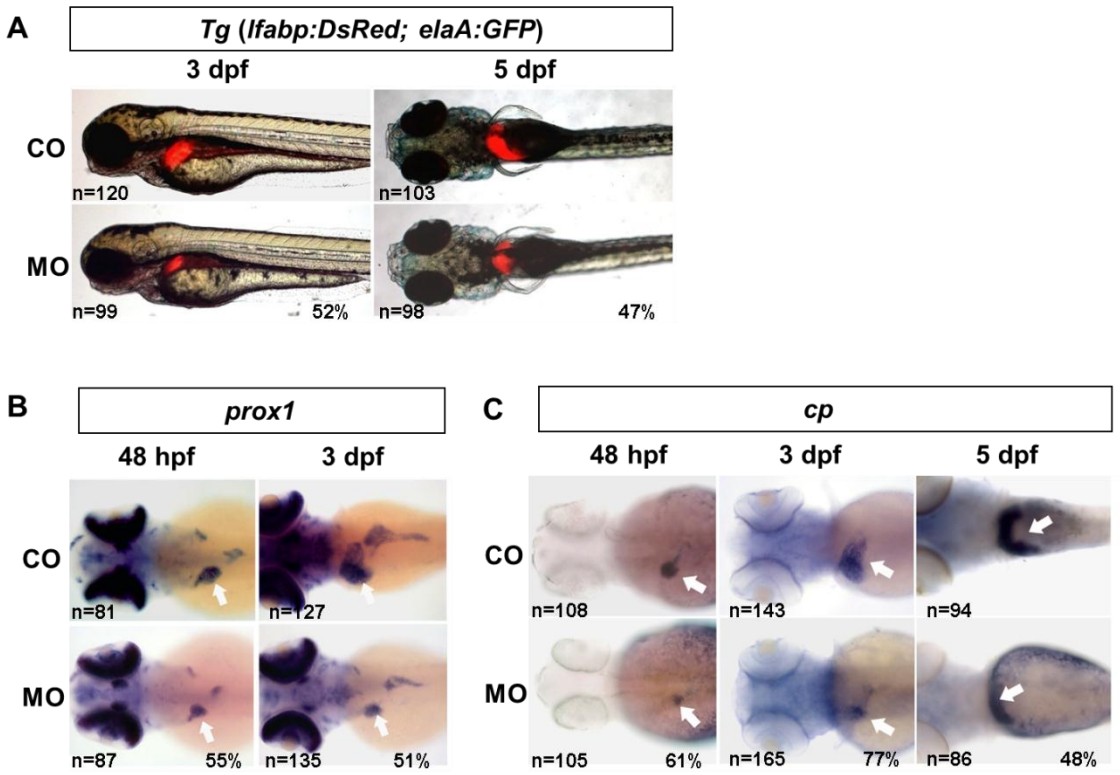

Fig. 3.11 Liver ourgrowth in *alr* morphants.

Liver outgrowth was monitored in *Tg(lfabp:DsRed;elaA:EGFP)* (A), by hepatoblasts/hepatocyte marker *prox1* (B) and hepatocyte marker *cp* (C). CO, 5 bp mismatch morpholino injected; MO, *alr* morpholino injected. The number of embryos analyzed was shown on the bottom left of each panel while the percentage of embryos with liver defects was labeled on the bottom right corner. White arrow points to liver bud. All images are dorsal view, anterior to the left.

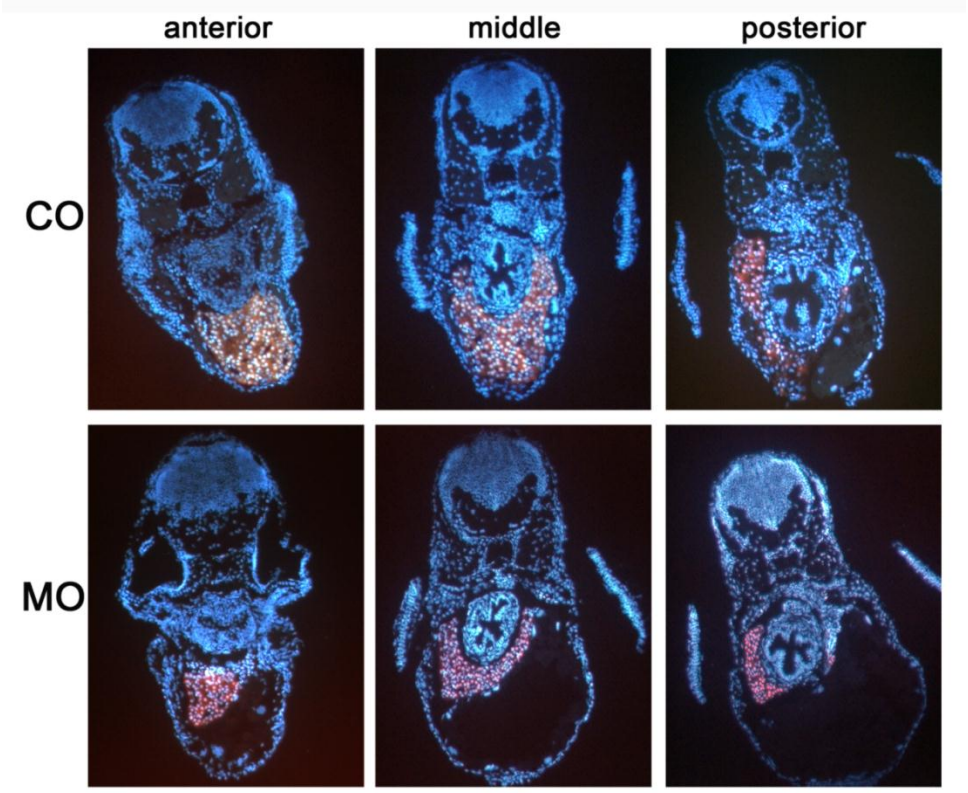

Fig. 3.12 Liver size reduction in *alr* morphants on sections.
Cryostat sections were obtained from 5 dpf *Tg(lfabp:DsRed; elaA:EGFP)* embryos. CO, 5 bp mismatch morpholino injected; MO, *alr* morpholino injected. Red color is from the DsRed expressed under *lfabp* promoter, indicating the liver. Blue color is the nucleus staining by DAPI. Images in the same column are sections from similar anterior-posterior position of liver.

3.2.1.4 Knockdown of *alr* does not affect liver sinusoids network

The requirement of endothelial cells and blood circulation during liver development has been proved in both mice. In mouse embryos lacking endothelial cells, the liver could undergo the initial step of hepatic specification, but further liver morphogenesis fails prior to mesenchyme invasion (Matsumoto et al., 2001). However, in zebrafish mutant embryos lacking endothelial cells, liver budding occurred normally (Field et al., 2003), suggesting that endothelial cells are not required for zebrafish early liver development. During liver budding stage (24-48 hpf) no blood circulation exists;

during the subsequent liver outgrowth stage (48 hpf - 5 dpf) blood circulation starts. But whether endothelial cells and blood circulation is required for zebrafish liver outgrowth is still controversial. Farooq et al. (2008) reported that liver outgrowth does not require vascularization, while Korzh et al. (2008) showed that during the growth phase there are avascular growth at 50–55 hpf, endothelium-dependent growth at 55–72 hpf and circulation-dependent growth after 72 hpf.

To investigate whether knockdown of *alr* inhibits liver growth through affecting the sinusoids network formation in liver, the transgenic fish *Tg(lfabp:DsRed; elaA:EGFP; fli1:EGFP)* was generated by crossing *Tg(lfabp:DsRed; elaA:EGFP)* with *Tg(fli1:EGFP)*. In *Tg(lfabp:DsRed; elaA:EGFP; fli1:EGFP)* fish, the hepatocytes are dsRed labeled and blood vessels are EGFP labeled, allowing for the observation of sinusoids in liver.

As shown in Fig. 3.13, knockdown of *alr* significantly inhibited liver growth, but did not affect sinusoids network formation in liver. The *alr* morphants had large sinusoids that were connected, which was similar as CO. Blood circulation could be observed by eye under bright field stereomicroscope. The organization of liver cells was also not disturbed – the hepatocytes formed a distinctive daisy pattern and almost every hepatocyte was connected to the sinusoids.

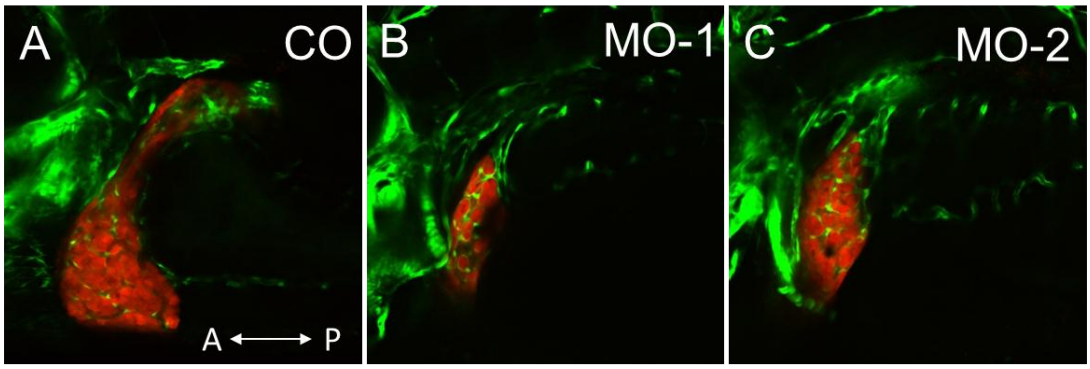

Fig. 3.13 Liver sinusoids in *alr* morphants.
Confocal projections of livers from 4 dpf transgenic fish *Tg(lfabp:DsRed; elaA:EGFP; fli1:EGFP)*, showing the sinusoids network (green) in liver (red). CO, 5 bp mismatch control morpholino injected embryo; MO-1 and MO-2, *alr* morpholino injected embryos. All images were from left lateral view, with anterior of the embryos to the left.

3.2.1.5 Knockdown of *alr* inhibits liver outgrowth by reducing hepatocyte proliferation

As hepatocytes are the parenchymal cells in liver which constitute more than 80% of the liver, the small liver phenotype in *alr* morphants could result from reduced hepatocyte proliferation and/or increased apoptosis. To determine the mechanism, hepatocyte proliferation was analyzed by cell proliferation markers phosphor-histone 3 (p-H3), which is a marker of cells in late G2 and M phase (Hendzel et al., 1997). To determine at which stage of liver development the proliferation was affected, embryos injected with ATG-region morpholino were collected at liver budding phase (42 hpf) and liver growth phase (4 dpf), and processed for cryostat section and immunofluorescent staining with anti-p-H3 antibody. Fig. 3.14 and Fig. 3.15 showed that the hepatocyte proliferation rate (percentage of cells in late G2 and M phase) in the liver of 42 hpf and 4 dpf embryo was reduced more than 60% in *alr* morphants

compared to control embryos (injected with same amount of 5 bp mismatch control morpholino). Thus, we concluded that knockdown of *alr* inhibits liver development by inhibiting liver hepatocyte proliferation. Inhibition of hepatocyte proliferation starts from liver budding phase and persists throughout liver outgrowth phase, indicating that *alr* is required for hepatocyte proliferation throughout liver organogenesis.

To further confirm the proliferation assay accuracy, another proliferation marker proliferating cell nuclear antigen (PCNA) was used to investigate the liver cell proliferation rate in *alr* morphants. PCNA is a proliferation marker that labels cells at late G1 to S phase (Connolly and Bogdanffy, 1993), and will label a broader group of cells than the p-H3 marker. Consistent with p-H3 cell proliferation assay results, the proliferation rate of hepatocytes was reduced for 50% in *alr* morphants compared to the control group (Fig. 3.16). Together, these results demonstrate that *alr* functions as a hepatocyte mitogen and promotes liver growth by stimulating hepatocyte proliferation during zebrafish liver organogenesis.

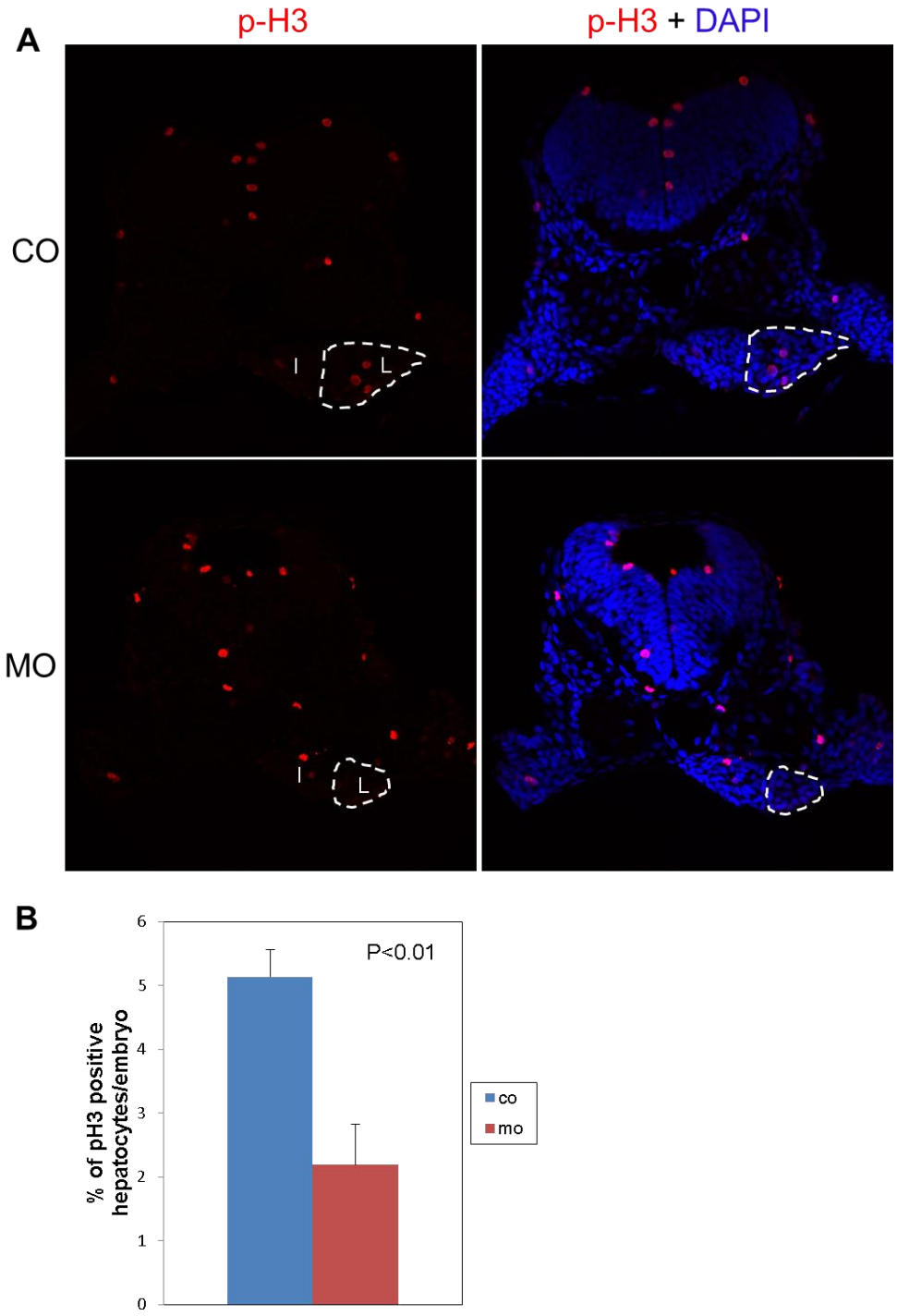

Fig. 3.14 Inhibition of liver proliferation during liver budding phase by knockdown of *alr*.

A, hepatocyte proliferation demonstrated by immunofluorescent staining of proliferation markers p-H3 in 42 hpf embryos. The sections were counterstained with DAPI to label nucleus, to facilitate tissue recognition and quantification in panel B. The p-H3 staining is co-localized with DAPI, indicative of nucleus staining. The p-H3 staining showed a significantly reduced hepatocyte proliferation in morphants, without affecting proliferation in other tissues such as intestine and brain. I, intestine;

L, liver. Dash line circles the boundary of liver.

B, quantification of hepatocyte proliferation. Percentage of p-H3 positive hepatocytes was counted from 5 embryos, 5 sections per embryo. Values are means ± standard deviation (SD). Hepatocytes were counted based on cell morphology.

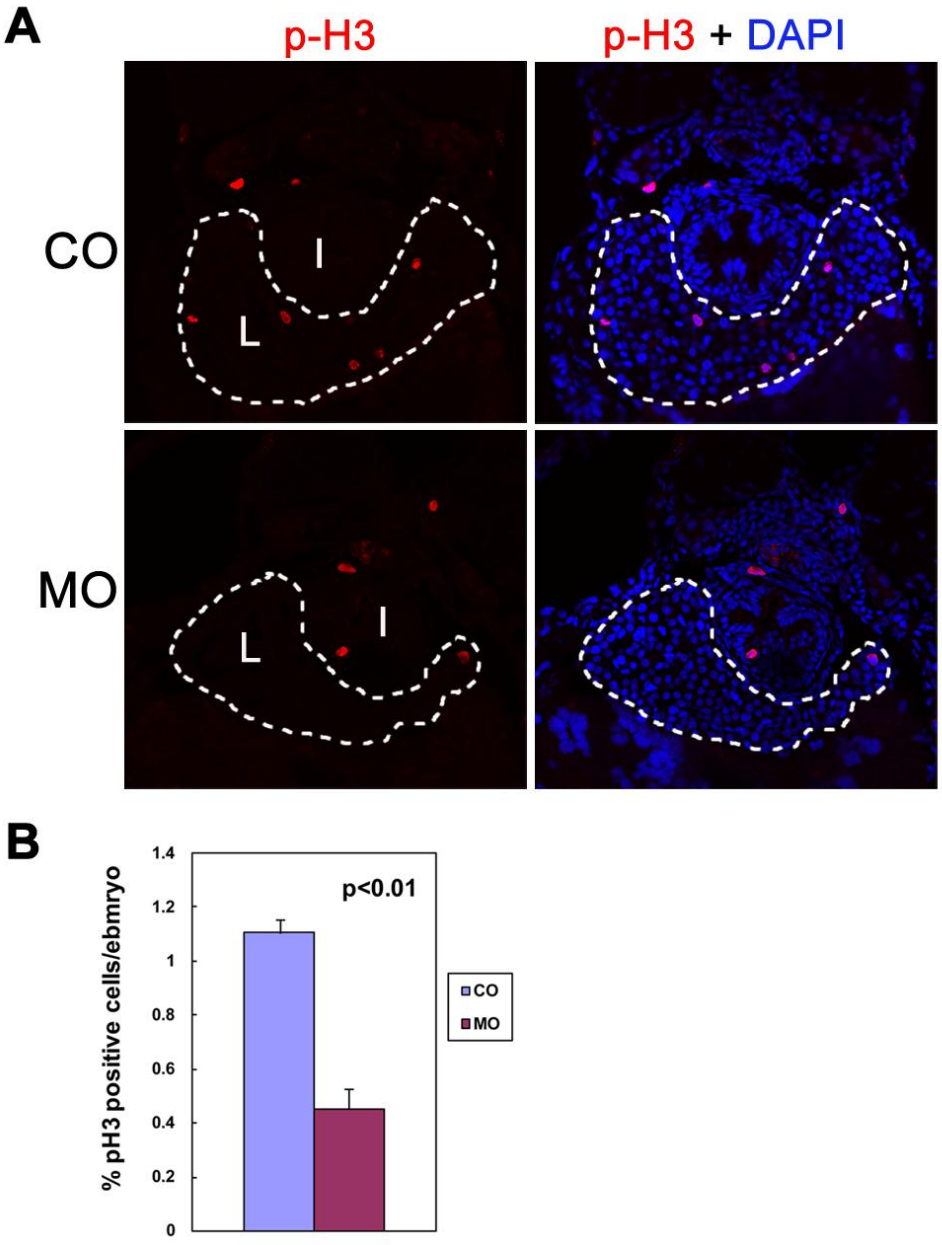

Fig. 3.15 Inhibition of liver proliferation (p-H3 marker) during liver growth phase by knockdown of *alr*.

A, hepatocyte proliferation demonstrated by immunofluorescent staining of proliferation markers p-H3 in 4 dpf embryos. The sections were counterstained with DAPI to label nucleus. The p-H3 staining showed a significantly reduced hepatocyte proliferation in *alr* morphants without affecting proliferation in other tissues such as intestine. I, intestine; L, liver. Dash line circles the boundary of liver.

B, quantification of hepatocyte proliferation. Percentage of p-H3 positive hepatocytes was counted from 4 embryos, 7 sections per embryo. Values are means ± standard deviation (SD). Hepatocytes were counted based on cell morphology.

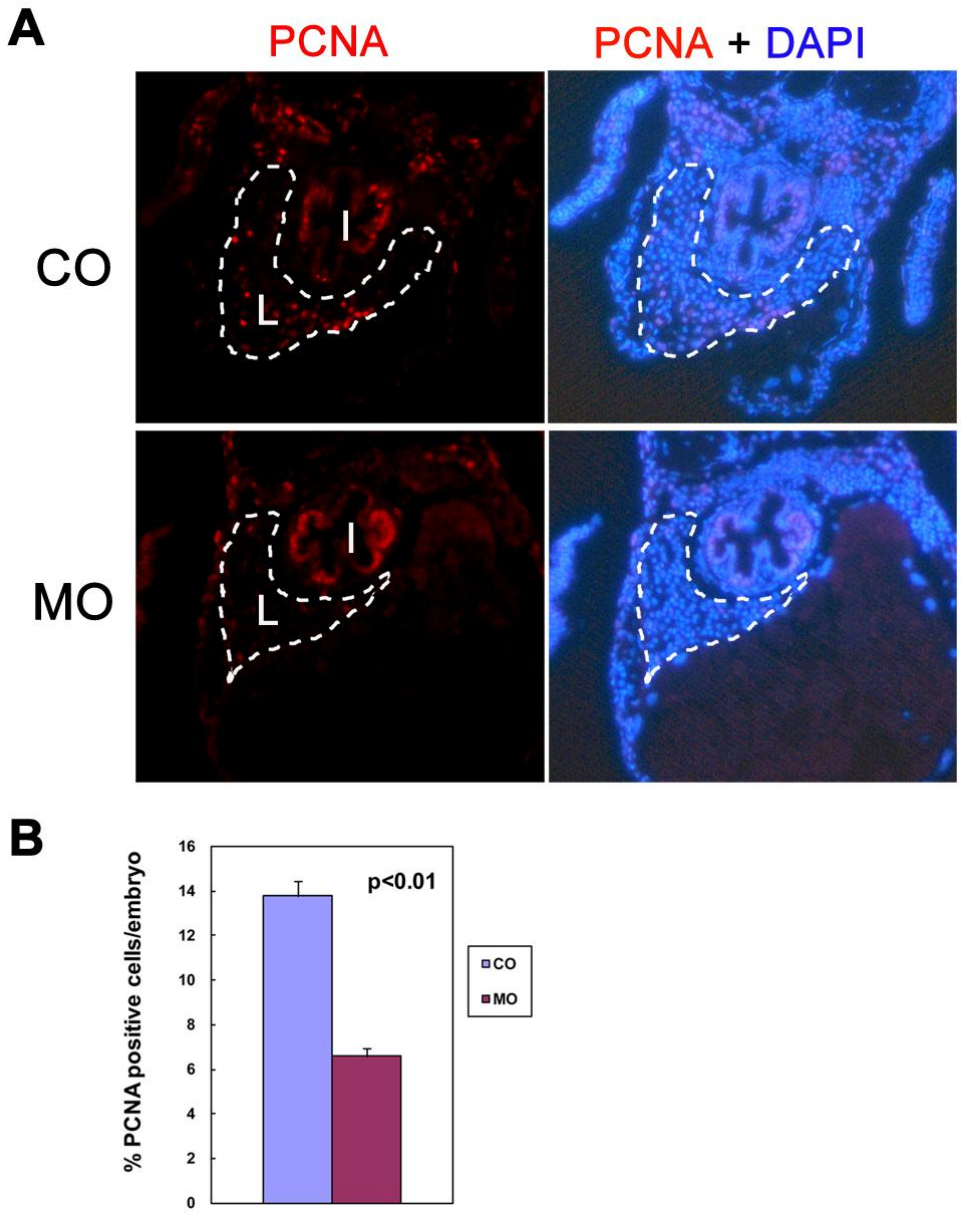

Fig. 3.16 Inhibition of liver proliferation (PCNA marker) during liver growth phase in *alr* morphants

A, hepatocyte proliferation demonstrated by immunofluorescent staining of proliferation markers PCNA in 4 dpf embryos. The sections were counterstained with DAPI to label nucleus. The PCNA staining is co-localized with DAPI, indicative of nucleus staining. The PCNA staining showed a significantly reduced hepatocyte proliferation in *alr* morphants without affecting proliferation in other tissues such as intestine. I, intestine; L, liver. Dash line circles the boundary of liver.

B, quantification of hepatocyte proliferation. Percentage of p-H3 positive hepatocytes

was counted from 3 embryos, 7 sections per embryo. Values are means ± standard deviation (SD). Hepatocytes were counted based on cell morphology.

3.2.1.6 Knockdown of *alr* does not affect hepatocyte apoptosis

To investigate whether knockdown of *alr* affects hepatocyte apoptosis to inhibit liver growth, liver cell apoptosis in *alr* morphants was determined by TUNEL assays. No difference in hepatocyte apoptosis level was detected. A similar low level hepatocyte apoptosis was observed in 4 dpf *alr* morphants and control embryos, with only a couple of cells stained positive on each section (Fig. 3.17A-F). The low level of apoptosis in the developing liver is consistent with previous report (Chen et al., 2005b).

To prove that it was not because of any technical problem during the TUNEL assay that resulted in only a few cells stained in Fig. 3.17A-F, positive control experiments were carried out at the same stage using DNase I treated cryo-sections. TUNEL assay detects DNA strand breaks during cell apoptosis. DNase I-treatment causes DNA strand breaks and is the suggested positive control according to the manufacturer's instruction. Large amount of apoptotic cells were stained positive by TUNEL assay in the DNase I treated control embryos (Fig. 3.17G). In addition, high level of apoptosis was also detected in embryos after heat-shock (Fig. 3.17H), a treatment known to induce apoptosis (Yabu et al., 2001).

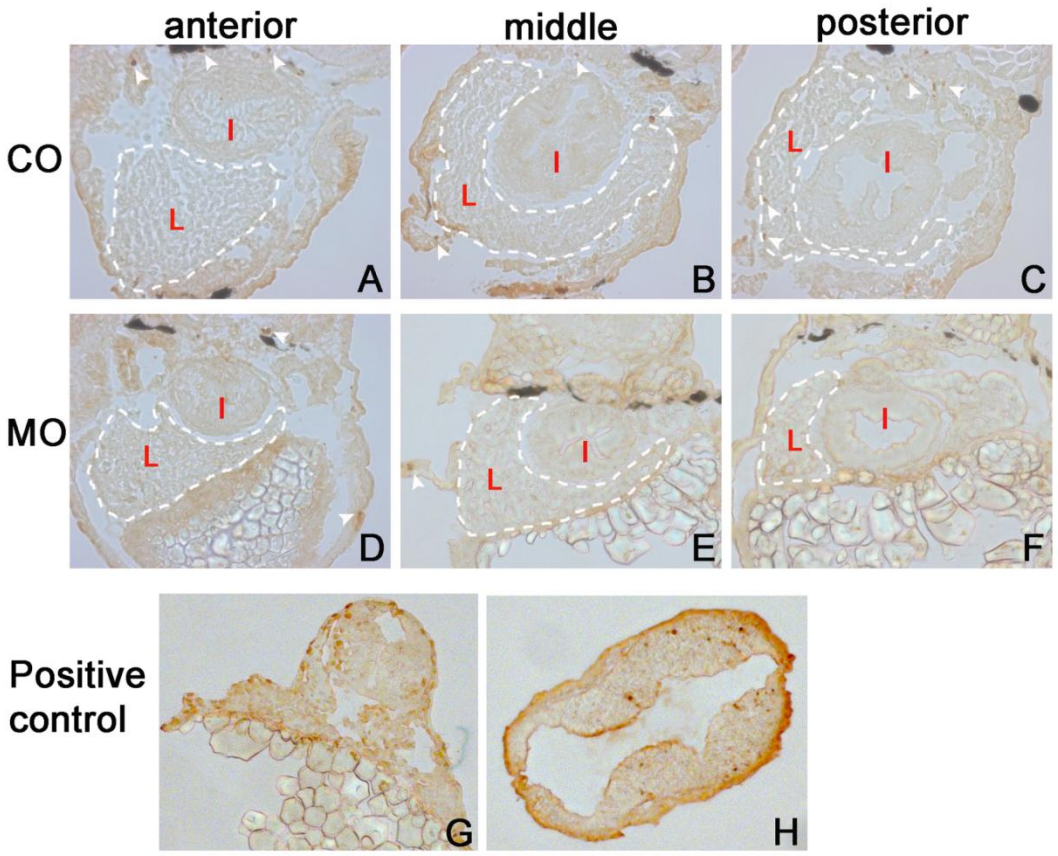

Fig. 3.17 Hepatocyte apoptosis is not elevated in *alr* morphants.
A-F, TUNEL assay performed on 4 dpf embryo liver sections. White dashed lines outline the liver. White arrowheads indicate some of the positively stained cells, which were undergoing apoptosis. Very low level of apoptosis was found in the developing livers of control embryos and *alr* morphants. G, DNase treated sample from 30 hpf embryos, as a positive control. H, brain section from 30 hpf embryos, treated by heat shock (39 degree, 1 hour) to induce apoptosis, also as a positive control. L: liver; I: intestine.

3.2.1.7 Effect of *alr* knockdown on other endoderm organs

As discussed previously, the function of *alr* in zebrafish embryonic development is not restricted to liver organogenesis. When higher dose of morpholinos were injected, defects in multiple organs were observed, including curved bodies, small heads, no circulation, and cardiac edema. This phenotype is consistent with the maternal expression of *alr* and its ubiquitous expression in early stage embryos. As the

expression of *alr* was also detected in endoderm region from 28 hpf to 4 dpf by WISH (Fig. 3.6), the effect of *alr* knockdown on other endodermal organs was investigated.

WISH was performed using the pan-endoderm marker *foxa3* to label all the endodermal organs, including the intestine rod, liver, pancreas and swim bladder (Fig. 3.18A). By 26 hpf, the flattened endoderm precursor cells have converged into a ribbon of tissue at the midline, forming the intestinal rod. The presence of a sickening of the anterior intestinal rod at 30 hpf indicates liver budding, and sickening of the posterior intestinal rod on the right side indicates pancreas budding. Fig. 3.18A (left panels) showed that the intestine rod and the pancreas budding were not affected in *alr* morphants compared to the control morpholino injected embryos at 30 hpf, although the sickening of the liver bud seemed affected in *alr* morphants. At 48 hpf (Fig. 3.18A, right panels), while liver is the mainly affected organ, mild inhibitions of the swim bladder and pancreas were observed in *alr* morphants.

Growth of the pancreas was further analyzed by endocrine pancreas marker *pro-insulin*, exocrine pancreas marker *elaA* and *elaB*. Endocrine pancreas was not affected by knockdown of *alr* in any of the stages analyzed (Fig. 3.18B). Growth of the exocrine pancreas was inhibited in *alr* morphants (Fig. 3.18C). At 5 dpf, both liver and exocrine pancreas was much smaller in *alr* morphants comparing with the control (Fig. 3.18C, right panels). The smaller exocrine phenotype was also observed using exocrine pancreas marker *elaB* in WISH (Fig. 3.18C, left panels).

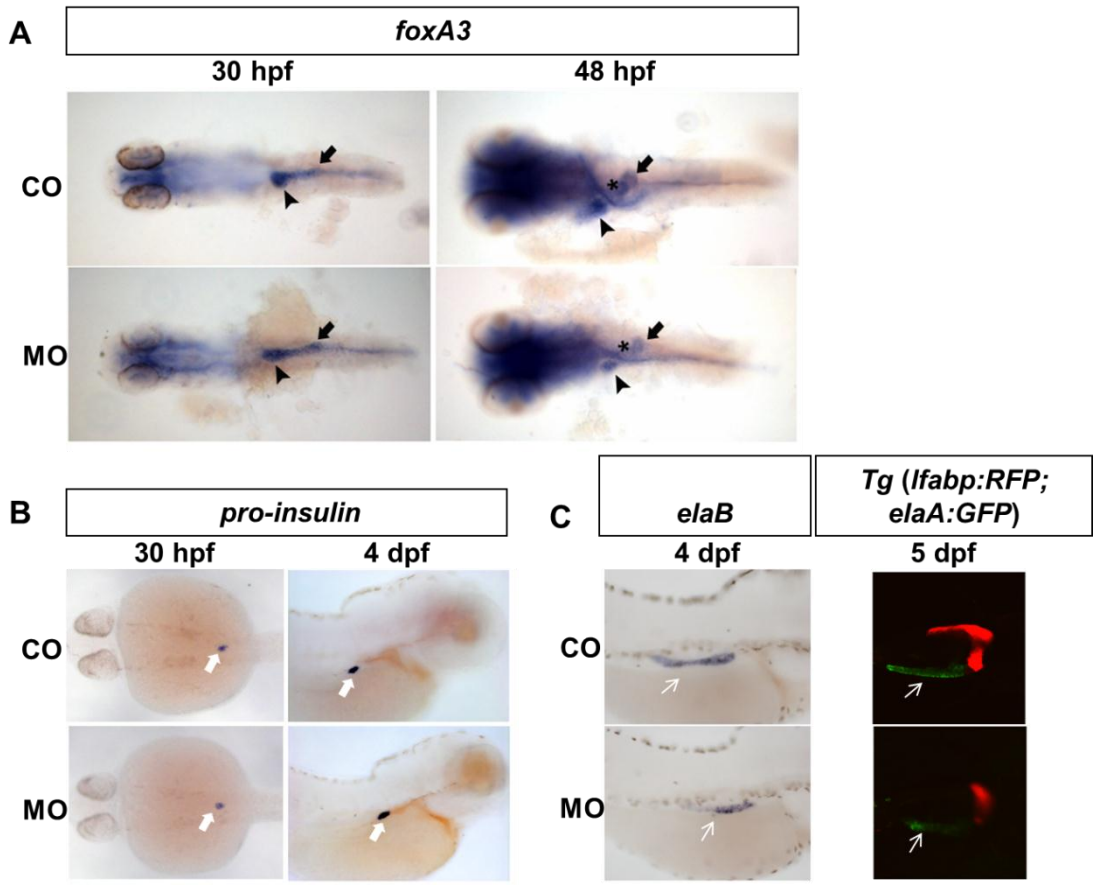

Fig. 3.18 Effect of *alr* knockdown on other endoderm organs.
A, WISH using pan-endoderm maker *foxA3* as probe. Black arrow head indicates liver (or liver bud); black arrow indicates pancreas (or pancreas bud); black star indicates swim bladder. B, WISH using endocrine pancreas marker *pro-insulin* as probe. White arrow points to endocrine pancreas. C, exocrine pancreas development analyzed by WISH using exocrine pancreas marker *elaB* as probe (left panel) and in *Tg(lfabp: DsRed; elaA: EGFP)* (right panel, exocrine pancreas in green color). White thin arrow points to exocrine pancreas.

3.2.2 Gain-of-function analysis

3.2.2.1 Determining the stability of microinjected *alr* mRNA and its protein product in embryos

In conjunction with the MO-mediated knockdown of *alr* described above, gain-of-function analysis was also performed to study the developmental function of zebrafish *alr*. Overexpression of *alr* was carried out by microinjection of *in vitro*

synthesized mRNA rather than DNA constructs into one-cell stage embryos, because synthetic mRNA injection will lead to a rapid and uniform expression whereas DNA constructs usually result in a mosaic expression pattern. However, the stability of microinjected synthetic mRNAs may vary a lot for different genes. There have been some studies showing that some microinjected mRNAs have short lifespan of less than one day (Cheung et al., 2006; Yin et al., 2011). In this case, liver organogenesis will be a relatively late developmental event for mRNA overexpression study.

Previous experience of using synthetic EGFP mRNA suggests that EGFP mRNA/protein have long lifespan, as the green fluorescence could even be observed up to 5 days after microinjection. The *alr*-EGFP fusion mRNA was thus synthesized and tested for its lifespan. The maturation time of the Alr-EGFP fusion protein is as fast as EGFP alone (Wiedenmann et al., 2009), with green fluorescence become visible 2-4 h after mRNA injection (Fig. 3.19). However, the green fluorescence signal from Alr-EGFP fusion protein is no longer visible after 48hpf, while EGFP is still easily visible in 3 dpf embyos.

The stability of *alr* mRNA was also analyzed, as shown in Fig. 3.20. The protein product of synthetic *alr* mRNA was still in high abundance at 24 hpf, but by 48 hpf most of the protein had been degraded. It seems that the lifespan of *alr*-EGFP and *alr* are similar. To avoid the possible effect of EGFP on the function of Alr, *alr* alone rather than *alr*-EGFP was used for the subsequent gain-of-function analysis.

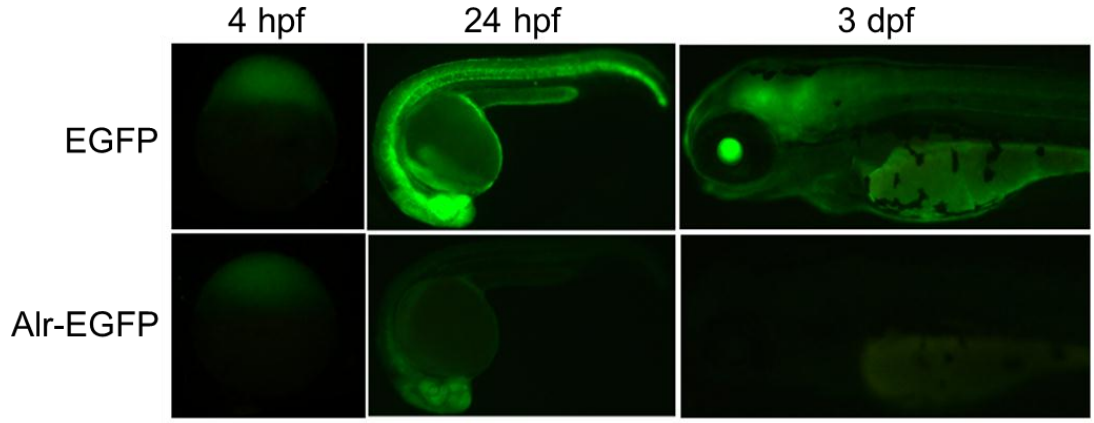

Fig. 3.19 Lifespan of synthetic EGFP/*alr*-EGFP mRNA and the protein product
Equal molar amount of EGFP (0.8 ng per embryo) and *alr*-EGFP (1.6 ng per embryo) mRNA were injected into one-cell stage embryos. Green fluorescent signal was analyzed at different stages. Same exposure time was used for imaging, to facilitate signal intensity comparison.

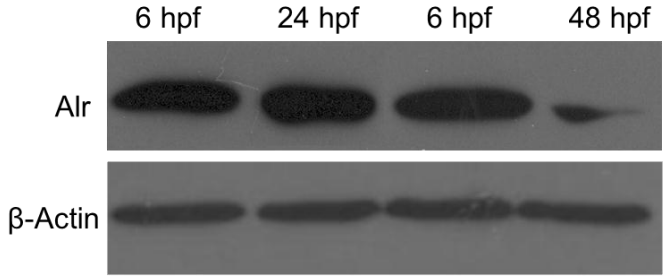

Fig. 3.20 Lifespan of synthetic *alr* mRNA and its protein product.
The synthetic *alr* mRNA was injected at the highest dose that embryos can tolerate, at 1.6 ng per embryo. The Alr protein with N-terminal 6×His was analyzed by Western blot using anti-His antibody. β-Actin was used as loading control. The first two lanes (6 hpf and 24 hpf) are from same batch of microinjected embryos, the following two lanes (6 hpf and 48 hpf) are from another batch.

3.2.2.2 Overexpression of zebrafish *alr* promotes liver growth in wild-type embryos and could rescue the liver growth defect in *alr* morphants

The *in vitro* transcribed *alr* mRNA was injected into zebrafish embryos, at the highest tolerable dose of 1.6 ng per embryo. Embryos injected with *alr* mRNA at ≤ 1.6 ng per embryo developed normally with no gross morphological abnormalities. Based on the

alr mRNA/protein lifespan determined previously, embryos at 48 hpf were used for liver organogenesis analysis by *prox1* WISH. At this stage, a clear small-liver phenotype can be observed in *alr* morphants and Alr produced from the microinjected mRNA are still present. To quantify the liver size, *prox1* WISH was done to label the livers, photo were taken from the dorsal view under the same magnification and resolution, and then Photoshop software was used to measure the relative liver size in 2-D dimension.

Notably, overexpression of Alr significantly enhanced liver growth, with embryos in the overexpression group showing a 37% increase in average liver size comparing to WT embryos at 48 hpf (Fig. 3.21A). The small-liver phenotype resulted from E1I1 morpholino injection (the splicing interference morpholino) was effectively rescued by co-injection of *alr* mRNA (Fig. 3.21B). In *alr* morphants, the relative liver sizes were mainly within the region of 0.6-0.8. Overexpression of Alr completely restored the liver size in morphants. Moreover, liver sizes in the *alr* mRNA rescued morphants were about 30% larger than WT embryos, and similar to liver sizes in *alr* overexpressed wild-type (WT) embryos (Fig. 3.21 A and B). These results together with morpholino knockdown results establish that Alr is a stimulator of liver growth in zebrafish hepatogenesis.

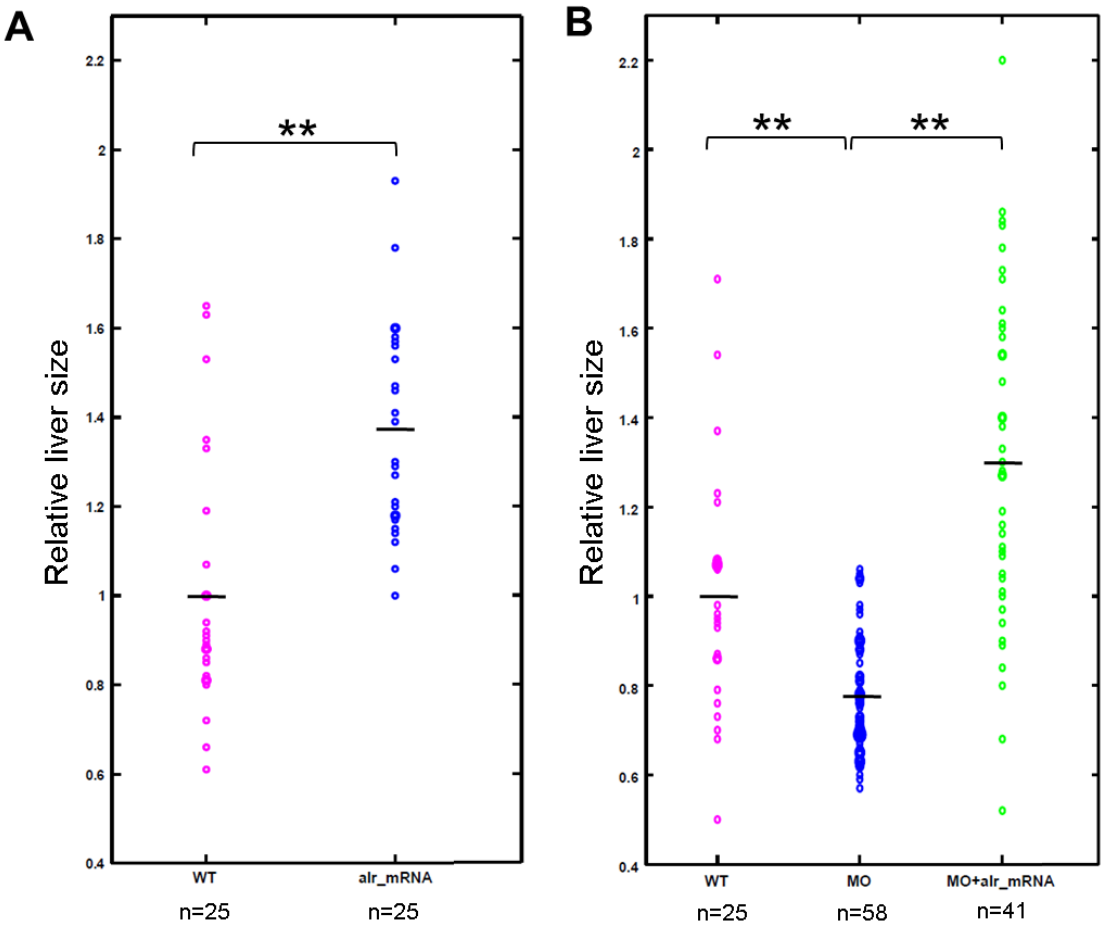

Fig. 3.21 Overexpression of *alr* promotes liver growth and rescues *alr* morphants.

A. Overexpression of *alr* can promote liver growth. The mean liver sizes (means ± SD) are: WT (1.00 ± 0.28), *alr* mRNA (1.37 ± 0.23). B. The *alr* overexpression can rescue *alr* morphant and restore liver size. The mean liver sizes (means ± SD) are: WT (1.00 ± 0.25), MO (0.78 ± 0.13) and MO + *alr* mRNA (1.30 ± 0.37). Each circle represents one embryo. The black line in the middle of scattered dots indicates the mean liver size in that group. The brackets on top indicate the respective two samples compared by student's t-test. n, number of embryo analyzed. **, $p<0.01$.

3.2.2.3 Overexpression of zebrafish *alr* promotes liver growth by enhancing hepatocyte proliferation

As shown above, knockdown of *alr* inhibits liver growth by reducing hepatocyte proliferation, suggesting that *alr* is involved promoting cell proliferation during liver organogenesis. Whether the liver growth enhancing effect of overexpressing *alr* is

also through promoting hepatocyte proliferation was therefore examined. Embryos were injected with 1.6 ng synthetic *alr* mRNA per embryos to overexpress *alr*, and then collected at 48 hpf. The hepatocytes proliferation rate was analyzing using p-H3 as proliferation marker (Fig. 3.22). Overexpression of *alr* indeed promoted hepatocytes proliferation by 22%.

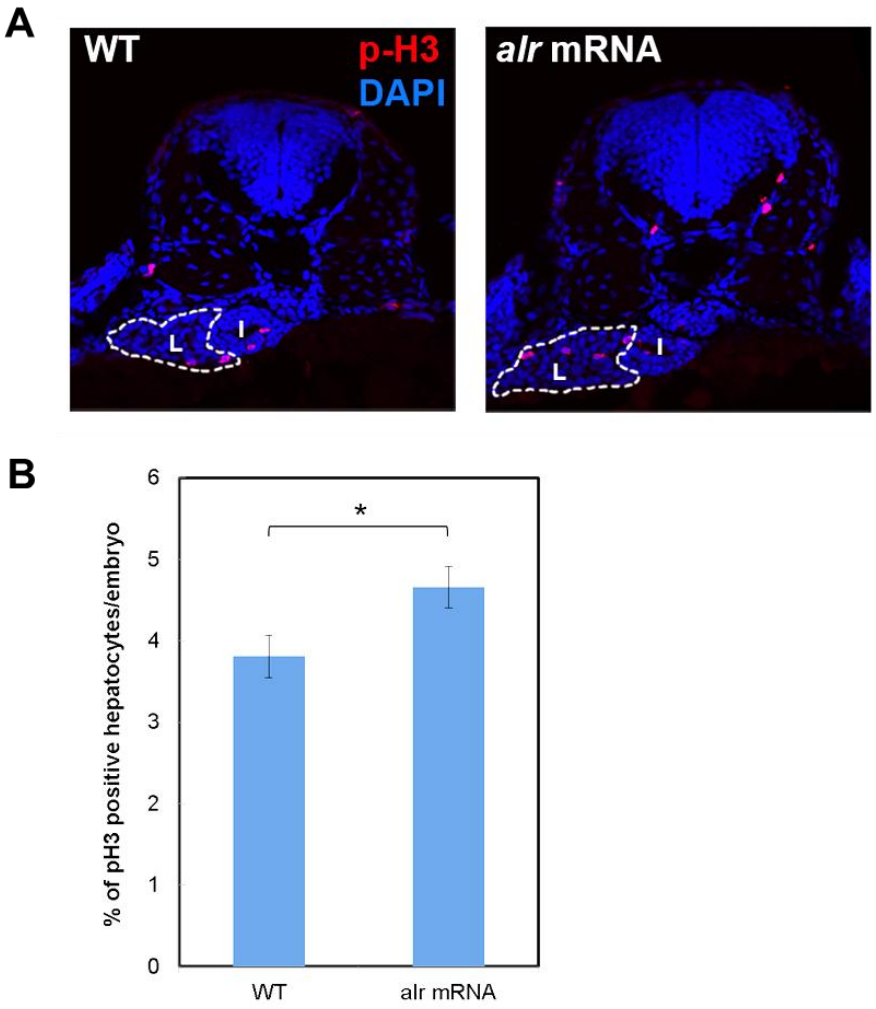

Fig. 3.22 Overexpression of zebrafish *alr* promotes liver growth by enhancing hepatocyte proliferation.

A, hepatocyte proliferation analyzed by immunofluorescent staining of proliferation marker p-H3 (red color) in 48 hpf embryos. The tissue sections were counterstained with DAPI (blue) to label nucleus. I: intestine; L: liver. Dash line circles the boundary of liver. B, quantification of hepatocyte proliferation rate. 5 livers, 7 sections per liver were counted. The percentage of p-H3 positive hepatocytes per embryos was 3.81% in WT and 4.66% in *alr* mRNA injected embryos respectively, a

22% increase in alr mRNA injected embryos. Data was presented as bar graph of mean ± standard deviation (SD). ∗, $p<0.05$.

3.2.2.4 Neither long form nor short form human *ALR* could rescue the liver defect in *alr* morphants

Heterologous functional complementation is an important approach to demonstrate the conserved function within the same cellular process across species. The function of human ALR in mitochondria as a yeast Erv1 homolog was recognized after the C-terminal region of human ALR functionally rescued yeast Erv1 mutants (Lisowsky et al., 1995). While no liver developmental function of the human ALR has been reported, we demonstrated that the zebrafish Alr was required for liver organogenesis by promoting hepatocyte proliferation. It would be interesting to study whether the human ALR is a functional homolog of the zebrafish Alr in liver organogenesis, thus providing evidence for the possible conserved function of ALR protein in vertebrate liver development.

Two isoforms of human ALR has been identified - hALR125 (short form, 125 amino acids) and hALR205 (long form, 205 amino acids) as illustrated in Fig. 3.2 (Lu et al., 2002b). The short form hALR125 differs from the long form hALR205 by lacking 80 amino acids at the N-terminus, probably due to different translation starting sites. The zebrafish Alr is similar in size to the long form human. However, it is not known which isoform is functionally closer to the zebrafish Alr. The 5'-capped poly(A)-tailed hALR205 and hAlr125 mRNAs were synthesized by *in vitro* transcription and microinjected into zebrafish embryos together with E1I1 MO to check their ability of

rescuing *alr* morphants. The maximum dose that embryos can tolerate (embryos develop normally with no gross morphological abnormalities) has been determined to be 0.23 ng per embryo for the hALR205 and 0.92 ng per embryo for the hALR125. To make the rescue effect comparable between hALR205 and hALR125, equal molar amount of either mRNA (equalling to 0.23 ng hALR205 per embryo) was injected together with 5 ng E1I1 MO into one-cell stage embryos.

As shown in Fig. 3.23A, overexpression of hALR205 could not restore the liver size of *alr* morphants, with the mean liver size similar as that of MO group. Overexpression of hALR125 also failed to rescue the small liver size of *alr* morphants (Fig. 3.23B). For hALR205, the highest tolerable dose has been used, while for hALR125 a higher dose of 0.92 ng per embryos could be further tested. However, hALR125 at the highest tolerable dose still failed to show any liver growth promoting effect (Fig. 3.24A) or rescuing effect of *alr* morphants (Fig. 3.24B).

Together, the results showed that zebrafish Alr and human ALRs were not functional interchangeable. Failing to demonstrate a cross species functional complementation might be attributed to the highly divergent N-terminus of Erv1/Alr family. It is possible that the divergent N-terminus of Alr is important for the subcellular localization and different substrate/interacting protein reorganization in different species. In support of this, it has been shown that the complete human ALR protein with its own amino terminus is not able to substitute the yeast Erv1 protein, unless the human ALR was fused to the N-terminus of yeast Erv1 (Hofhaus et al., 1999).

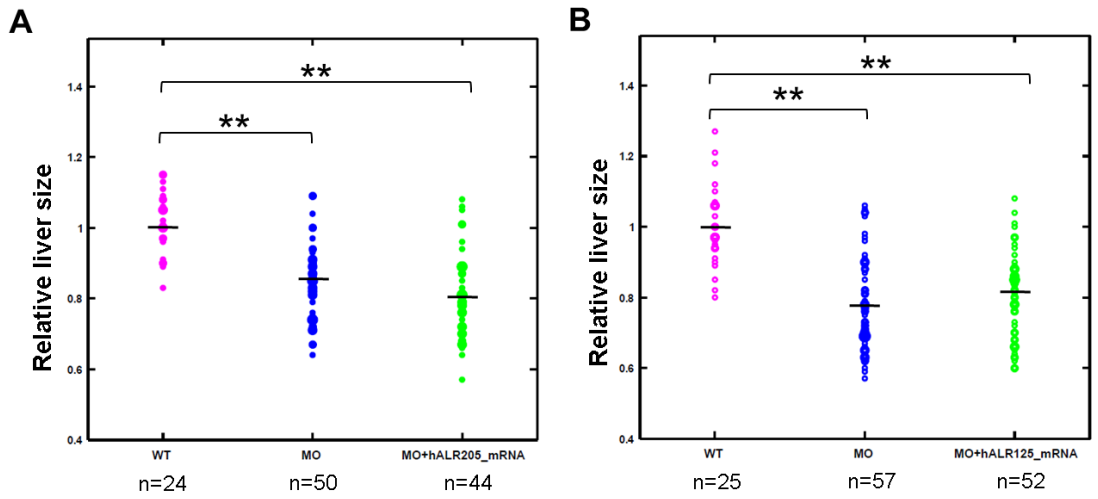

Fig. 3.23 Overexpression of the two isoforms of human *ALR* could not rescue *alr* morphants.

A. Overexpression of human long form *ALR* (hALR205) failed to rescue *alr* morphants. The mean liver sizes (means ± SD) are: WT (1.00 ± 0.09), MO (0.84 ± 0.10) and MO+hALR205 mRNA (0.80 ± 0.12). B. Overexpression of human short form *ALR* (hALR125) could not rescue *alr* morphants. The mean liver sizes (means ± SD) are: WT (1.00 ± 0.11), MO (0.78 ± 0.11), MO + hALR125 mRNA (0.80 ± 0.12). The black line in the middle of scattered dots indicates the mean liver size in that group. The brackets on top indicate the respective two samples compared by student's t-test. n, number of embryo analyzed. **, $p<0.01$.

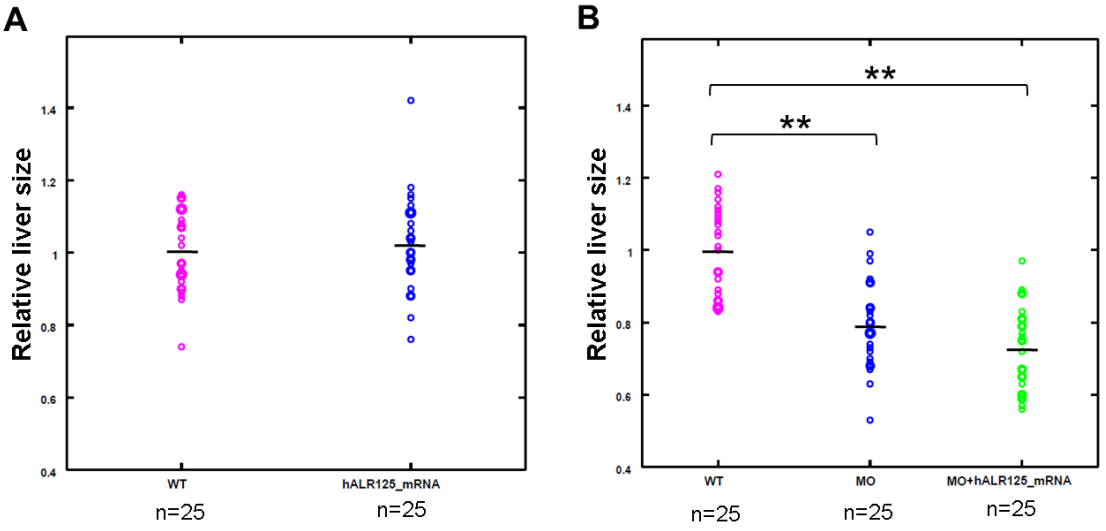

Fig. 3.24 Overexpression of human short form *ALR* is not able to promote liver growth and fails to rescue *alr* morphants at the highest tolerable dose.

A. Overexpression of human short form *ALR* (hALR125) could not promote liver growth. The mean liver sizes (means ± SD) are: WT (1.00 ± 0.11), hALR125 mRNA

(1.03 ± 0.13). B. The human short form *ALR* (hALR125) overexpression failed to rescue *alr* morphants. The mean liver sizes (means ± SD) are: WT (1.00 ± 0.12), MO (0.79 ± 0.12), and MO + hALR125 mRNA (0.73 ± 0.12). The black line in the middle of scattered dots indicates the mean liver size in that group. The brackets on top indicate the respective two samples compared by student's t-test. n, number of embryo analyzed. **, $p<0.01$.

3.3 Molecular characterization of zebrafish Alr

3.3.1 Subcellular localization of zebrafish Alr protein

Subcellular localization is important for protein function. In mammals, two protein isoforms of ALR exist: the long form and the short form. While the short from have been shown to be localized in the nucleus, the long form is localized in the intermembrane space of mitochondria and the cytosol (Gatzidou et al., 2006; Hofhaus et al., 1999; Lange et al., 2001; Li et al., 2002b). The identity of the secreted Alr isoform is still unclear up to now. *In vitro*, both human ALR125 (short form) and ALR205 (long form) can stimulate hepatoma cell proliferation as an extracellular growth factor (Lu et al., 2002b; Yang et al., 1997). The zebrafish Alr is similar in size to the long form of mammalian ALR as well as the yeast Erv1. No equivalent short form zebrafish Alr has been detected in both embryos and adult zebrafish. Sequence analysis of zebrafish Alr showed that similar to ALRs in other species, zebrafish Alr does not contain any identifiable signal peptide or typical mitochondria import sequence. So the subcellular localization of zebrafish Alr has to be determined experimentally.

3.3.1.1 Zebrafish Alr is not a secreted protein

To determine the subcellular localization of zebrafish Alr, plasmid expressing Alr-EGFP fusion protein was generated. The Alr-EGFP fusion protein was transiently expressed in HepG2 (human hepatocellular carcinoma cell), HEK293T (human embryonic kidney cell). Both the cell lysate and conditioned medium were collected

for Western blot using anti-GFP antibody. Compared to the high expression level in the cell lysates, no Alr-EGFP protein could be detected in the conditioned medium of transfected HEK293T and HepG2 cells (Fig. 3.25).

Considering that EGFP as a huge protein tag might interfere the subcellular localization of the Alr protein, Alr-V5 (zebrafish Alr with C-terminal V5 tag) was later generated. Alr-V5 was transfected into human cells and the presence of Alr-V5 was examined by Western blot using anti-V5 antibody. Similar as Alr-EGFP, Alr-V5 was also not detectable in the conditioned medium of transfected HEK293T and HepG2 cells (Fig. 3.26 A and B). To test whether the zebrafish Alr is only secreted under species- and tissue-specific conditions, zebrafish liver cell line (ZFL) was used to examine whether Alr-V5 could be secreted in zebrafish liver cells. Fig. 3.26C showed that Alr-V5 could not be detected in the conditioned medium of transfected ZFL cells.

These results indicates that zebrafish Alr, which does not have any signal peptide, is most likely not secreted outside of the cell under normal cell culture conditions. Whether zebrafish Alr could be secreted into blood circulation during liver regeneration similar as the mammalian ALR is not known.

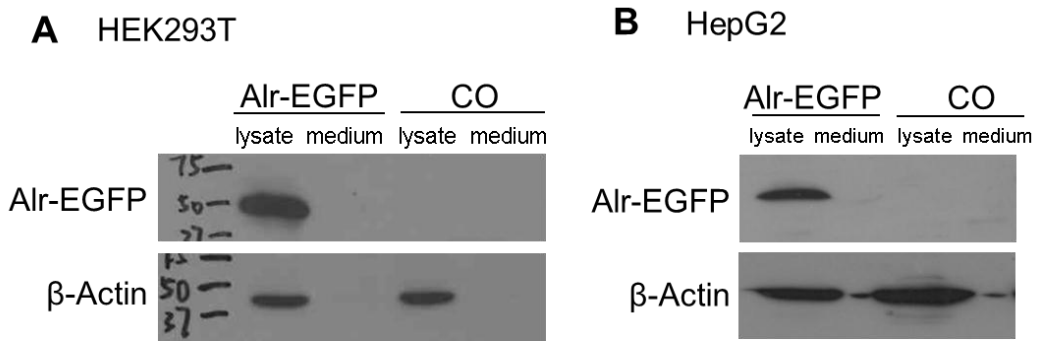

Fig. 3.25 Alr-EGFP is not secreted into the cell culture medium.
A, detection of Alr-EGFP protein in the cell lysate and conditioned medium of transfected HEK293T cells. B, detection of Alr-EGFP protein in the cell lysate and conditioned medium of transfected HepG2 cells. CO was mock transfected. The size of Alr-EGFP fusion protein is around 50 kD. The β-Actin was used as quality control, which should be present in the cell lysate only.

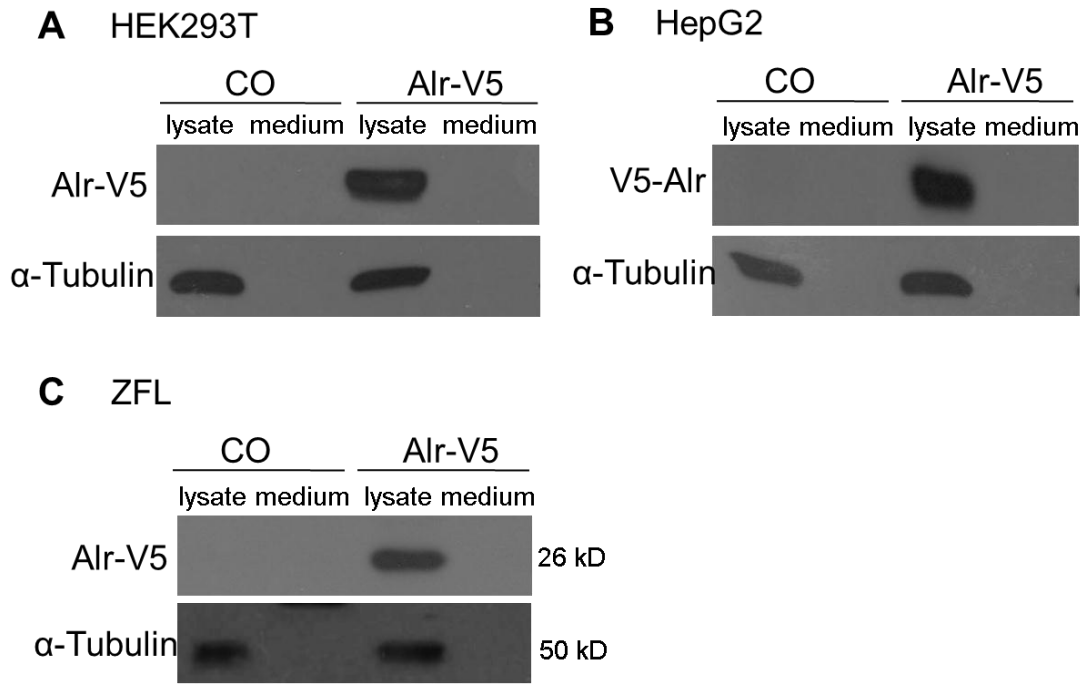

Fig. 3.26 Alr-V5 is not secreted into the cell culture medium.
A, detection of Alr-EGFP protein in the cell lysate and conditioned medium of transfected HEK293T cells. B, detection of Alr-EGFP protein in the cell lysate and conditioned medium of transfected HepG2 cells. C, detection of Alr-EGFP protein in the cell lysate and medium of transfected ZFL cells. CO was mock transfected. The size of Alr-V5 is around 26 kD. The α-Tubulin was used as quality control, which should be present in the cell lysate only.

3.3.1.2 Zebrafish Alr is localized in the cytosol and mitochondria, but not the nucleus

The intracellular localization of zebrafish Alr was investigated by transfecting Alr-EGFP expressing plasmid into cultured human cells. Live cell imaging showed that Alr-EGFP is mainly localized in the cytoplasm, but not in the nucleus (Fig. 3.27). Furthermore, when Alr-EGFP expressing plasmid was injected into 1-2 cell stage zebrafish embryos, Alr-EGFP fusion protein is predominantly cytoplasmic when stained with anti-EGFP antibody in 6 hpf embryos (Fig. 3.28).

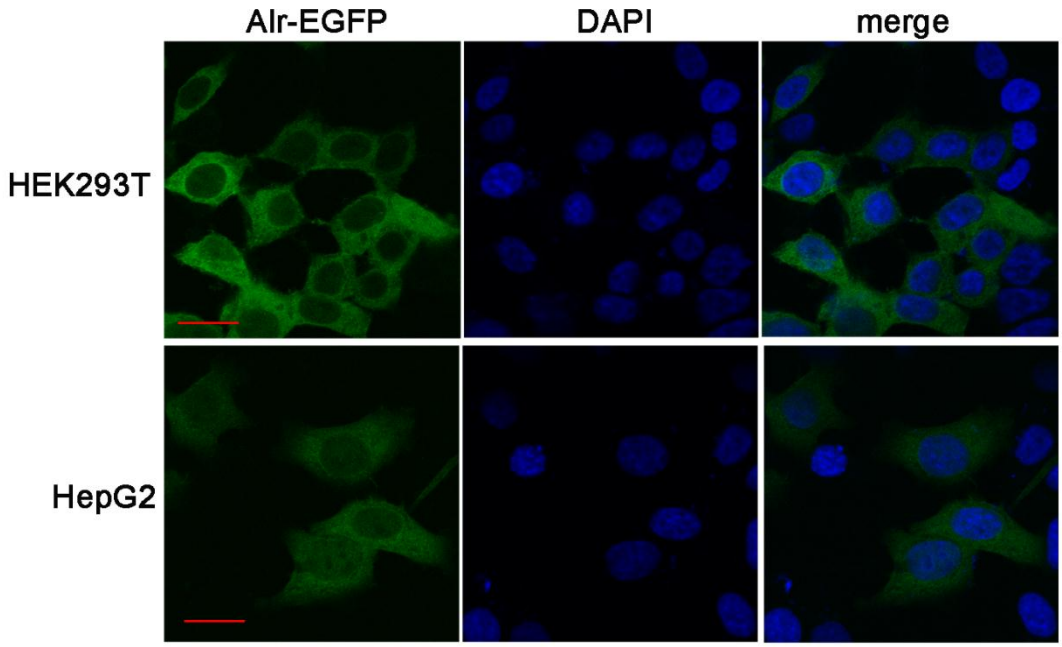

Fig. 3.27 Subcellular localization of Alr-EGFP in cultured human cells
HepG2 and HEK293T cells were transfected with Alr-EGFP expressing plasmid. The cells were counterstained with DAPI to mark the nucleus. The Alr-EGFP fusion protein is localized in the cytoplasm but not in nucleus. Scale bar is 20 μm.

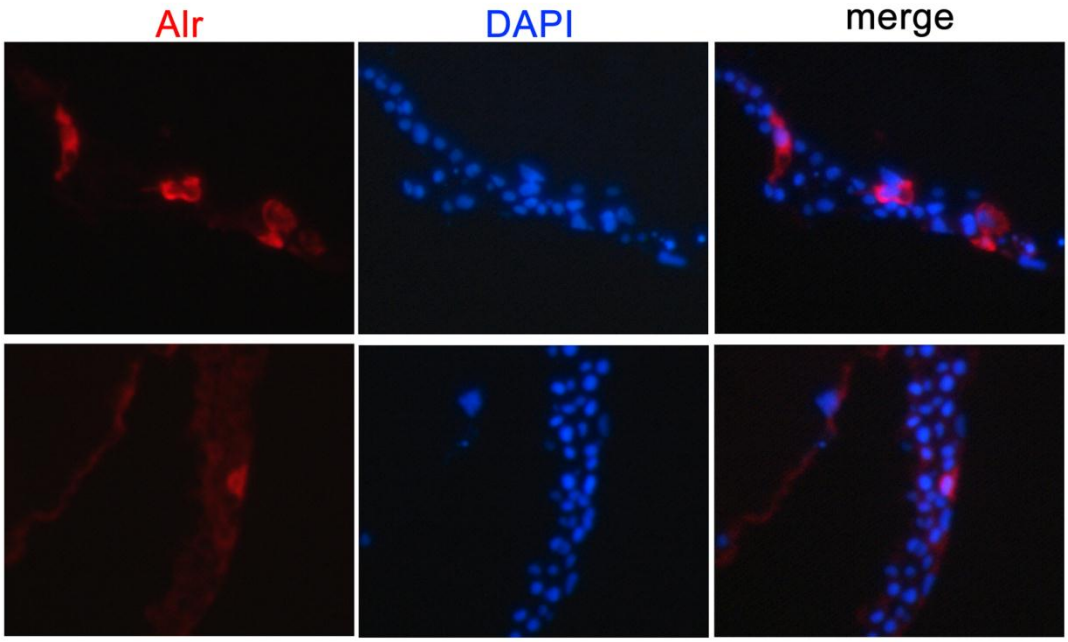

Fig. 3.28 Subcellular localization of Alr-EGFP in zebrafish embryo.
Alr-EGFP is mainly localized in the cytoplasm in zebrafish embryo. The plasmid expressing Alr-EGFP fusion protein under the CMV promoter was injected into zebrafish one-cell stage embryos. These embryos were fixed at shield stages (6 hpf) and processed for sectioning. The cryosections were stained with mouse anti-GFP primary antibody and Alexa Fluor 568-conjugated anti-mouse IgG secondary antibody. DAPI was used to stain the nucleus. Red color shows the predominant presence of Alr-EGFP fusion protein in the cytoplasm, but not the nucleus.

To determine whether Alr-EGFP is localized in the mitochondria similar to the human ALR and yeast Erv1, mitochondria of the transfected human cells were isolated. Cell fractionation and Western blot revealed that Alr-EGFP was localized in the cytoplasm as well as mitochondria in both transfected HEK293T and HepG2 cells (Fig. 3.29). In the same cell fractionation experiment, the mitochondrial protein voltage dependent anion channel protein (VDAC) was present in the mitochondrial fraction only while α-Tubulin was presented in the cytosolic fraction only, demonstrating the purity of cell fractions isolated.

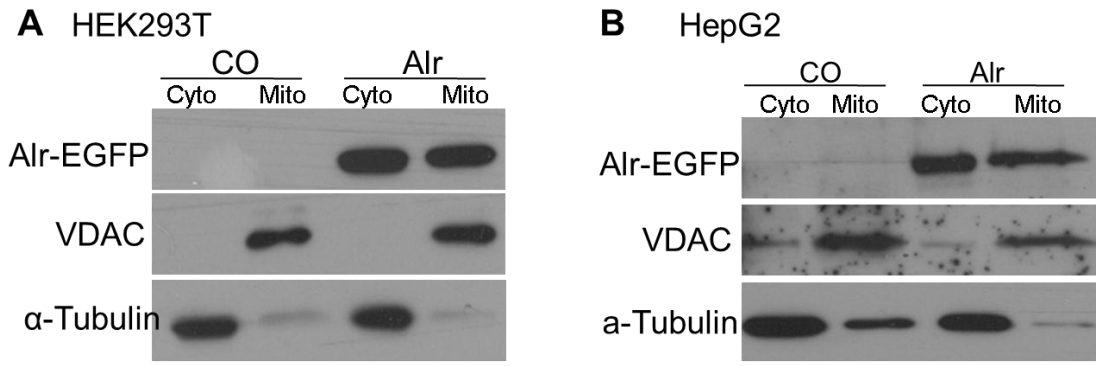

Fig. 3.29 Subcellular localization of Alr-EGFP determined by cell fraction.
Cell fractionation revealed that Alr-EGFP was localized in both the cytosol and mitochondria in transfected HEK293T and HepG2 cells. Alr-EGFP was detected by Western blot using anti-GFP antibody. The mitochondrial voltage-dependent anion channel (VDAC) was used as the mitochondria marker while α-Tubulin was used as the cytosolic marker. CO, mock transfection; Alr, Alr-EGFP plasmid transfection.

The subcellular localization of Alr-V5 was also determined in HepG2, HEK293T and zebrafish liver cells. Live cell imaging demonstrated that Alr-V5 protein was mainly localized in the cytosol but not in the nucleus (Fig. 3.30). The Alr-V5 in the cytosol showed a distinctive pattern of localization, resembled the mitochondria morphology. Double-staining with the mitochondria-specific dye MitoTracker demonstrated that Alr-V5 was co-localized with MitoTracker in mitochondria in all three cell types. Cell fractionation and Western blot revealed that Alr-V5 was localized in the cytoplasm as well as mitochondria (Fig. 3.31).

Although cell fraction followed by Western blot showed similar results of subcellular localization between Alr-EGFP and Alr-V5, fluorescent images of the cells presented different patterns (Fig. 3.27 and 3.30). The Alr-V5 showed perfect co-localization with mitochondria marker, while Alr-EGFP in the cytoplasm did not show such obvious pattern of localization. The present of EGFP tag at C-terminus of Alr might

have affected its localization to mitochondria to some extent.

Taken together, the results above demonstrated that zebrafish Alr is a cytoplasmic protein rather than a nuclear protein. It is localized in both cytosol and mitochondria. The zebrafish Alr may have functions in both the mitochondria as well as the cytosol. Although no predicted mitochondrial localization signal is found in Alr protein sequence, localization of Alr into mitochondria is neither species specific nor cell type specific, indicating the existence of a common pathway to import Alr into mitochondria.

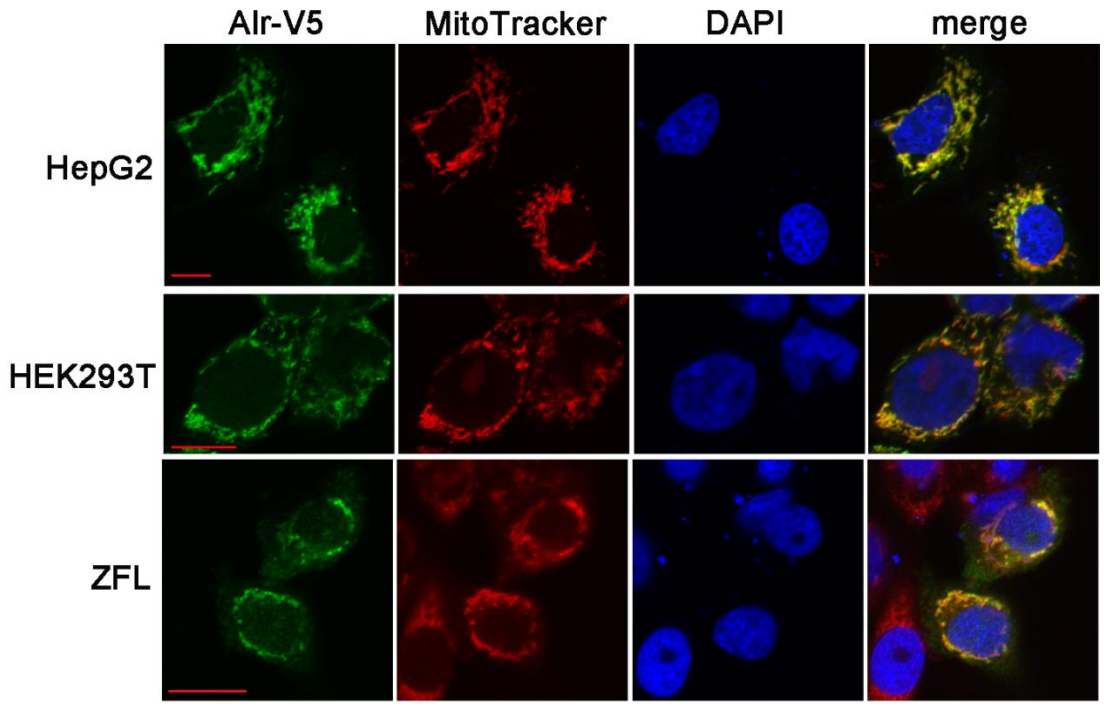

Fig. 3.30 Alr subcellular localization by immunofluorescent staining.
Human cells HepG2 and HEK293T, zebrafish liver cells ZFL were transfected with pEF6/V5-His-TOPO plasmid expressing Alr-V5. MitoTracker was used to label the mitochondria and the cells were counterstained with DAPI to mark the nucleus. The Alr protein is co-localized with MitoTracker in the mitochondria, but not present in the nucleus. Scale bar is 10 μm.

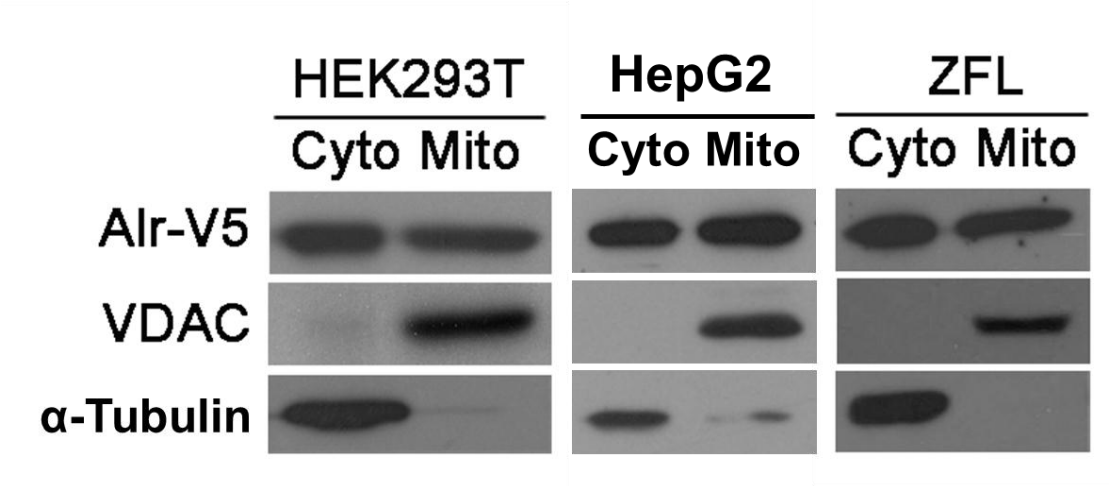

Fig. 3.31 Subcellular localization of Alr-V5 determined by cell fraction and Western blot.
Cell fractionation revealed that Alr-V5 was localized in both the cytosol and mitochondria in transfected HEK293T and HepG2 cells. Alr-V5 was detected by anti-V5 antibody. The mitochondrial porin voltage-dependent anion channel (VDAC) was used as the mitochondrial marker while α-Tubulin was used as the cytosolic marker.

3.3.2 Zebrafish Alr is a FAD-linked sulfhydryl oxidase

Several members of the Erv1/Alr protein family has been shown to have sulfhydryl oxidase enzymatic activity, including those from human, rat, *Arabidopsis*, and yeast (Lee et al., 2000; Levitan et al., 2004; Lisowsky et al., 2001). The importance of sulfhydryl oxidase enzymatic property of Erv1 has been well studied in yeast (Bihlmaier et al., 2007; Tokatlidis, 2005). The yeast Erv1, localized in the intermembrane space of mitochondria, forms a disulfide relay system with Mia40. Erv1 oxidizes Mia40 to recycle it for oxidative folding of proteins imported to mitochondria. The electron of Erv1 is then transferred to cytochrome C and finally to oxygen. The mammalian ALR is known as a “cytozyme”, bearing both cytokine and enzymatic activity. Intracellular human short form ALR (sfALR) binds to Jun

Activation domain-Binding protein 1 (JAB-1) and potentiates Activator Protein-1 (AP-1) signalling pathway in a sulfhydryl oxidase dependent manner (Chen et al., 2003). Thus, whether the zebrafish Alr is also a sulfhydryl oxidase and if yes, whether the enzymatic activity is involved in liver organogenesis and hepatocyte proliferation was investigated.

3.3.2.1 Purification of recombinant Alr and Alr^{C131S} from *E.coli*

Study of yeast Erv1 and mammalian ALR has revealed that there is a conserved CxxC motif in the Erv1/Alr domain and this motif is essential for the sulfhydryl oxidase enzymatic activity of ALR (Lee et al., 2000; Lisowsky et al., 2001). Mutation of either cysteine of the CxxC motif will abolish the enzymatic activity. Sequence alignment of zebrafish Alr with yeast Erv1 and mammalian ALR shows that zebrafish Alr also has a CxxC motif in the Erv1/Alr domain (Fig. 3.32A). It is most likely that the CxxC motif is also needed for the enzymatic activity of zebrafish Alr, if it is also a sulfhydryl oxidase. Thus the CxxC motif mutant - Alr^{C131S} was created by site-directed mutagenesis, by mutating the second cysteine of the CxxC into serine (Fig. 3.32B).

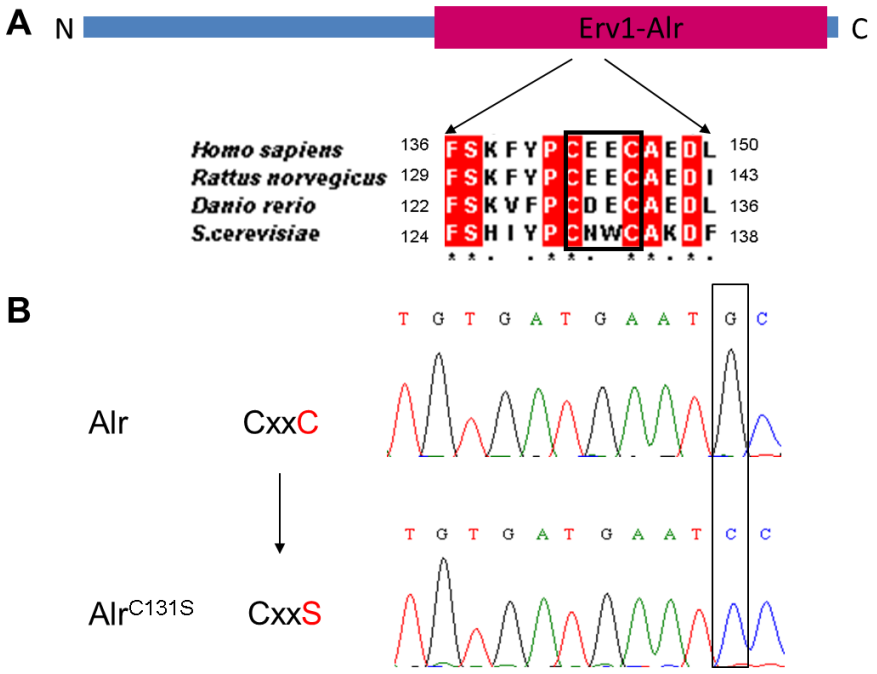

Fig. 3.32 Mutation of the CxxC motif by site-directed mutagenesis.
A. The diagram illustrates the domain organization of Alr protein, with the conserved Erv1/Alr domain at the C-terminus. Sequence alignment shows the amino acids around the CxxC motif (highlighted in the black box) within the Erv1/Alr domain.
B. The mutant Alr^{C131S} was generated by site-directed mutagenesis. The sequencing results showed the nucleotides that codes the amino acids CDEC of the CxxC motif. The cysteine 131 was mutated into serine in Alr^{C131S}, because of a G to C mutation of the DNA. The CDEC motif was thus mutated into CDES.

The wild-type zebrafish Alr and the CxxC motif mutant Alr^{C131S} was cloned into bacterial expression vector and transformed into *E. coli* BL21(λDE3) to produce the recombinant Alr protein with 6×His at the N-terminus. Both proteins could be successfully produced by *E.coli* (Fig. 3.33A) as soluble proteins. Thus the recombinant proteins were purified by Ni-NTA beads under native conditions, without using the denaturant urea.

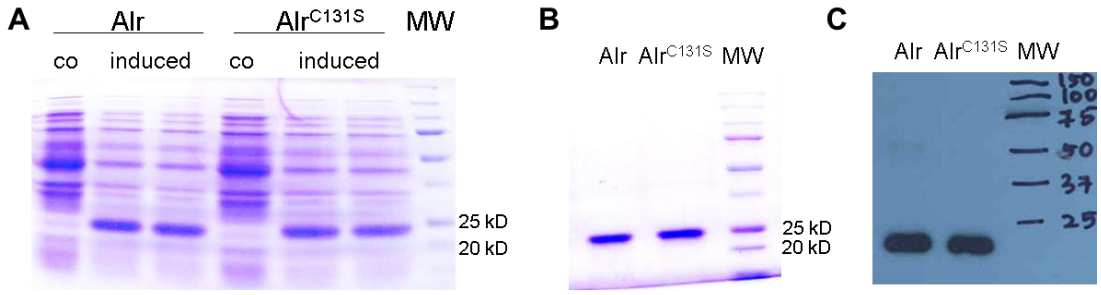

Fig. 3.33 Purification of recombinant Alr and Alr^{C131S} in *E.coli.*

A. Alr and Alr^{C131S} proteins with 6×His at the N-terminus were successfully produced in *E.coli*. After induction with IPTG, the bacteria lysates were run on SDS-PAGE gel and stained with commassie blue. Co was from un-induced bacteria lysate. The thick protein bands around 24 kD were the recombinant Alr and Alr^{C131S} protein.

B. After Ni-NTA beads purification and FPLC, the purity of Alr and Alr^{C131S} protein was tested by SDS-PAGE and commassie blue staining. The size of purified protein matches the predicted molecular weight of 23.6 kD.

C. The identity of the purified protein was confirmed by Western blot using anti-His antibody.

3.3.2.2 Zebrafish Alr exists as homodimer and binds FAD moiety

In the presence of the reducing agent DTT, a single band around 24 kDa was observed in both Alr and Alr^{C131S}, consistent to the predicted monomer size (Fig. 3.34A). In the absence of DTT, the monomer band disappeared; instead, multiple dimeric bands were detected between the 40-46 kD range. This result indicates that zebrafish Alr also exists as dimer, similar to its human and yeast counterparts (Lee et al., 2000; Li et al., 2002b). Mutation of cysteine in the C-terminal CxxC motif does not disrupt dimerization.

A common characteristic of sulfhydryl oxidase is the presence of a flavin adenine dinucleotide (FAD) containing redox center adjacent to the conserved CxxC motif in the Erv1/Alr domain. Zebrafish Alr also binds the FAD moiety as determined by

spectroscopic absorption, showing two distinct peaks at 360 nm and 450 nm characteristic of FAD (Fig. 3.34B). Binding to FAD makes the Alr protein solution yellow color. Mutation of the CxxC motif does not affect the FAD binding ability of Alr, as the mutant Alr^{C131S} showed equal FAD loading efficiency as the wild-type Alr. Based on the structural studies (Daithankar et al., 2010; Wu et al., 2003), each ALR monomer should bind one FAD molecule. However, the loading of FAD to the recombinant zebrafish Alr/ Alr^{C131S} is around 0.5 FAD molecule per Alr momoner (Fig. 3.34B), which is lower than the expected ratio of 1:1. This is possibly due to the improper folding of the bacteria produced protein or the protein preparation condition.

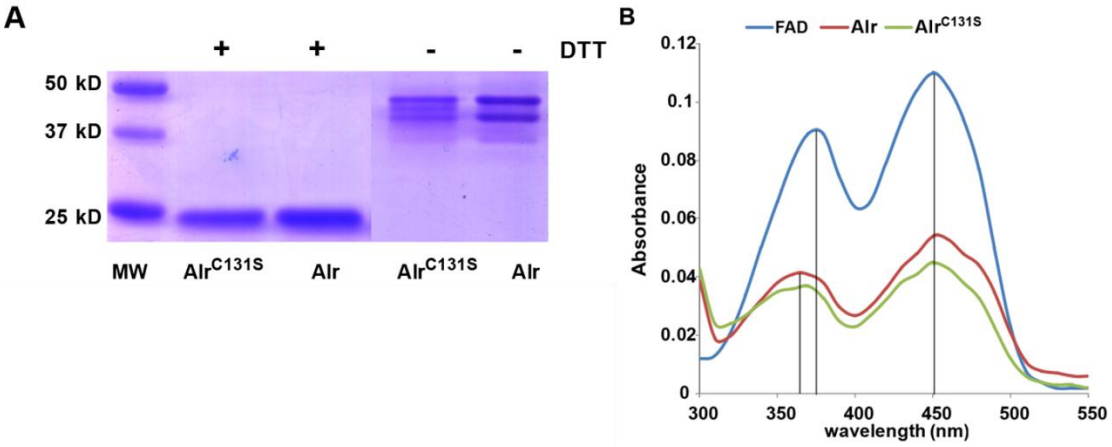

Fig. 3.34 Zebrafish Alr exists as homodimers and binds FAD moiety

A. Alr forms homodimers. Recombinant zebrafish Alr purified from *E.coli* was examined by SDS-PAGE and stained by commassie blue. In the presence of the reducing reagent DTT, Alr protein is in the monomer form, with a size of around 23.6 kD. In the absence of DTT, both Alr and the mutant Alr^{C131S} are present as dimers with sizes in the 40~46 kD region.

B. Absorption spectra of recombinant zebrafish Alr and Alr^{C131S} protein at 15 μM. Free FAD at 15 μM was used as reference and its spectra show the typical riboflavin spectrum, with two absorbance peaks at around 375 nm and 450 nm. The absorption spectra of both the wild-type Alr protein and mutant Alr^{C131S} protein are characteristic of the FAD moiety, with a minor shift of the first peak to 365 nm compared to the free FAD. Under equal molar concentration, the amount of Alr-bound FAD is only half of

the free FAD, indicating a loading efficiency of ~0.5 FAD molecule per Alr monomer.

3.3.2.3 Zebrafish Alr is a sulfhydryl oxidase and the CxxC motif is essential for the enzymatic activity of Alr

Sulfhydryl oxidases are protein enzymes that can introduce disulfide bonds into proteins by oxidizing their free thiol groups. For *in vitro* sulfhydryl oxidase enzymatic assay, different types of substrates have been used previously (reviewed by Thorpe et al., 2002a). The established substrates include reduced proteins such as lysozyme and RNaseA, monothiol substrates such as reduced glutathione (GSH), dithiol substrates such as dithiothreitol (DTT). The activity of Alr towards different substrates was tested. The recombinant Alr/Alr^{C131S} protein was incubated with GSH, reduced lysozyme or DTT respectively; the free thiol groups were measured at different time points of assay by Ellman's reagent to test the ability of Alr to oxidize the thiol groups.

Neither Alr nor Alr^{C131S} protein showed any activity towards GSH and reduced lysozyme, as the free thiol groups remained unchanged compared to the substrate alone (Fig. 3-35 A and B). This result suggests that GSH and reduced lysozyme are not the preferred substrates of zebrafish Alr *in vitro*. This is consistent with the reports of human ALR and yeast Erv2, which also showed very weak or almost no activity towards GSH and reduced lysozyme substrates (Daithankar et al., 2009; Wang et al., 2007).

However, zebrafish Alr showed strong activity towards DTT (Fig. 3.35C), within 40

minutes all the free thiols of DTT was oxidized. Indeed, DTT has been shown to be a very good model substrate for flavin-dependent sulfhydryl oxidases, especially the Erv1/Alr protein family members. Zebrafish Alr oxidized DTT efficiently, while Alr^{C131S} completely lost this activity (Fig. 3.35C). Thus, zebrafish Alr is a sulfhydryl oxidase that relies on the proximal CxxC motif for its enzymatic activity.

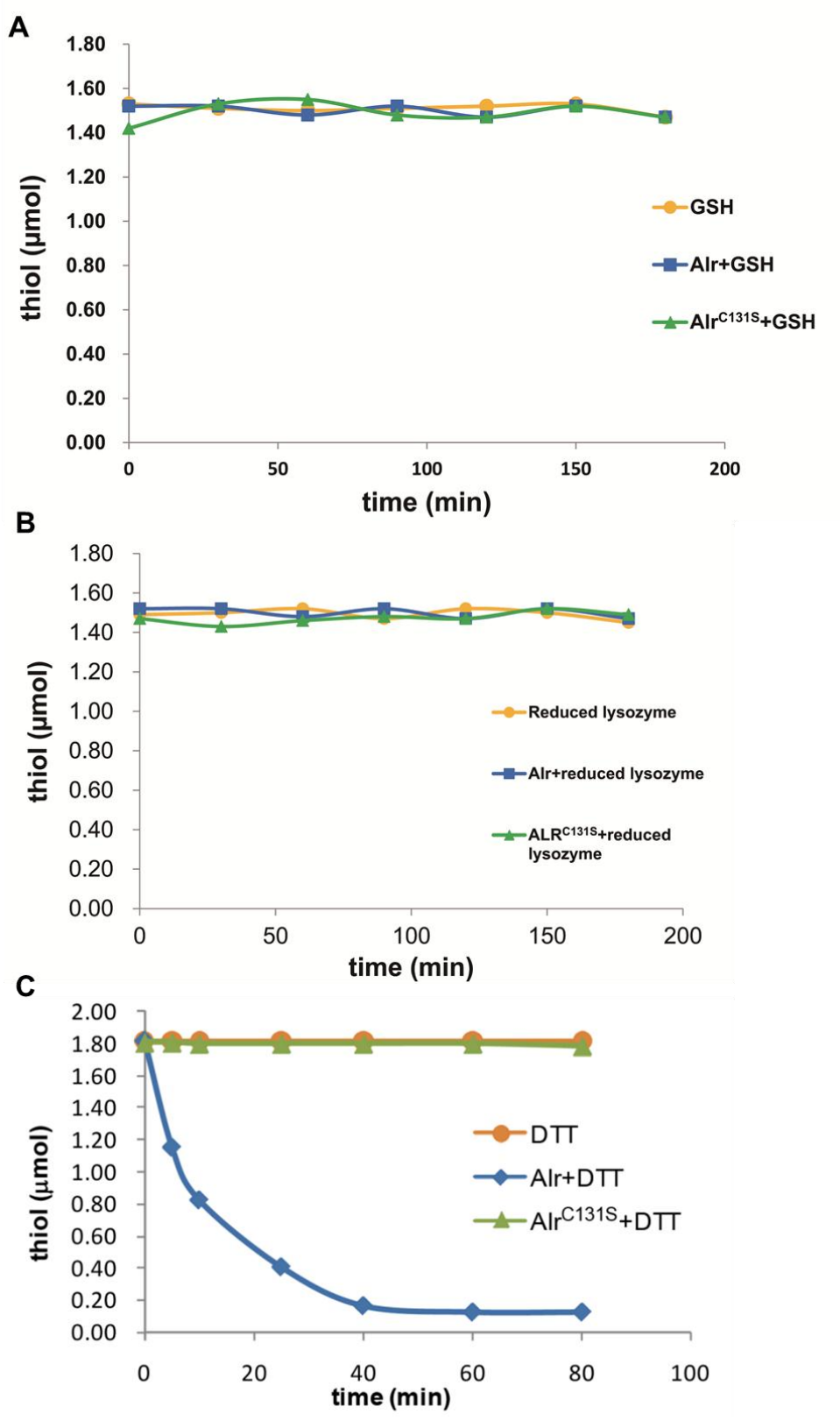

Fig. 3.35 Enzymatic assay of zebrafish recombinant Alr and Alr^{C131S}.

A, sulfhydryl oxidase enzymatic assay using monothiol GSH as the substrate. B, sulfhydryl oxidase enzymatic assay using reduced lysozyme as the substrate. In both A and B, no reduction of thiol groups could be detected, suggesting that GSH and

reduced lysozyme were not optimal substrates of zebrafish Alr. C. Enzymatic assay using DTT as the substrate, showing the reduction of free thiol groups overtime. The blue line represents DTT alone. Wild-type Alr protein oxidized thiol groups over time while the CxxC motif mutant, Alr^{C131S}, completely lost the sulfhydryl oxidase activity.

3.3.2.4 The enzymatically-inactive mutant Alr^{C131S} is able to promote liver outgrowth by enhancing hepatocyte proliferation

Whether the sulfhydryl oxidase enzymatic activity of Alr is related to its function in regulating zebrafish liver development was investigated. The wild-type *alr* as well as the enzymatic-inactive mutant alr^{C131S} mRNAs were generated by *in vitro* transcription and injected into one-cell stage embryos to check their effect on liver growth. They were also injected together with *alr* splicing-inhibiting morpholino E1I1 MO to examine their ability to rescue the morphants. The wild-type *alr* mRNA has previously been shown to be able to promote liver growth and rescue the morphants' small liver phenotype. Here the effect of the mutant alr^{C131S} was compared with that of the wild-type *alr*.

Overexpression of Alr (at 1.6 ng mRNA/embryo) significantly enhanced liver growth, comparing to uninjected wild-type embryos at 48 hpf as determined by *prox1* WISH (Fig. 3.36A). Interestingly, overexpression of the enzymatically inactive mutant Alr^{C131S} also mildly but significantly promoted liver growth. Comparing to WT Alr, the effect of Alr^{C131S} is noticeably weaker (about 15% increase in average liver size) (Fig. 3.36A). Nevertheless, the liver growth promoting effect is a consistent phenotype.

The small-liver phenotype resulted from E1I1 morpholino injection was effectively

rescued by co-injection of either *alr* or *alr*^{C131S} mRNA (Fig. 3.36B). Overexpression of either WT or mutant Alr completely restored the liver size in morphants. Overexpression of the enzyme-inactive Alr^{C131S} promoted liver growth less efficiently comparing to the WT Alr (Fig. 3.36B). Although Alr^{C131S} effectively rescued the *alr* morphants and restored the small liver to sizes slightly larger than the WT liver (about 15% larger), the average liver size of Alr^{C131S} rescued embryos is obviously smaller than that of the WT Alr rescued embryos. It therefore seems that the sulfhydryl oxidase activity of Alr also contributes to liver outgrowth. We further showed that the enhanced liver growth is through stimulating hepatocyte proliferation as demonstrated by p-H3 staining (Fig. 3.37). Those results suggest that zebrafish *alr* may use both enzyme-dependent as well as enzyme-independent pathways to promote liver growth.

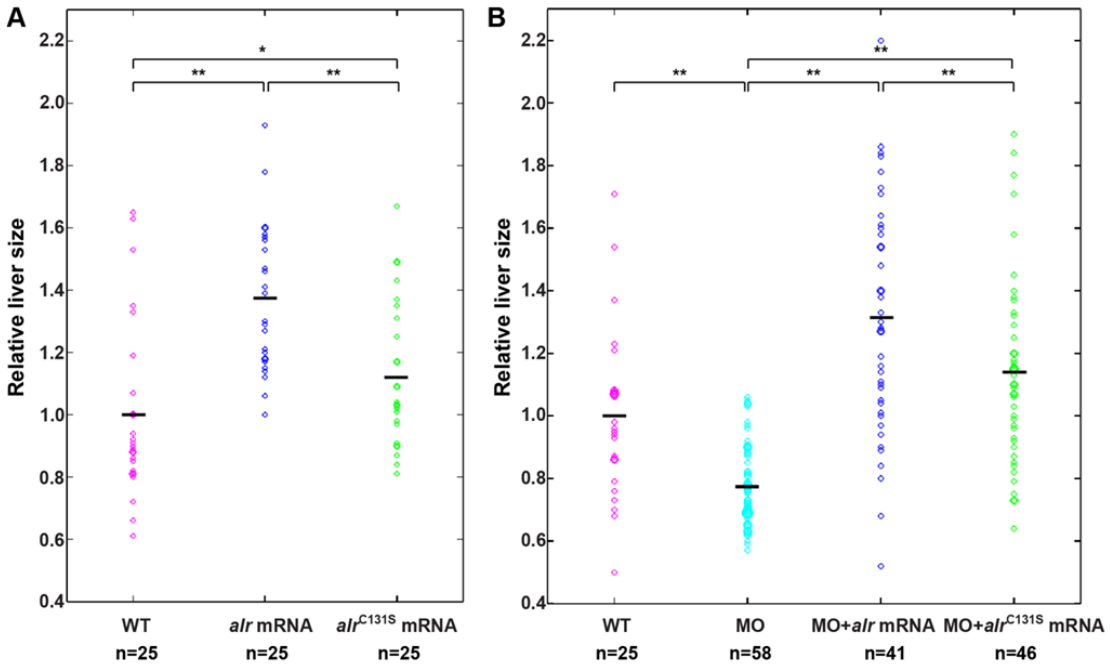

Fig. 3.36 Effect on liver growth of *alr* and *alr*^{C131S} by overexpression and morphants rescue analysis.

A. Overexpression of both wild-type *alr* and enzyme-inactive mutant *alr*^{C131S} can promote liver growth. But the wild-type *alr* is more efficient than *alr*^{C131S} mutant. The mean liver sizes (means ± SD) are: WT (1.00 ± 0.28), *alr* mRNA (1.37 ± 0.23) and *alr*^{C131S} mRNA (1.13 ± 0.23).
B. Both *alr* and *alr*^{C131S} overexpression can rescue *alr* morphant and restore liver size. The mean liver sizes (means ± SD) are: WT (1.00 ± 0.25), MO (0.78 ± 0.13), MO + *alr* mRNA (1.30 ± 0.37) and MO + *alr*^{C131S} mRNA (1.14 ± 0.30). The black line in the middle of scattered dots indicates the mean liver size in that group. The brackets on top indicate the respective two samples compared by student's t-test. n, number of embryo analyzed. ∗, p<0.05; ∗∗, p<0.01.

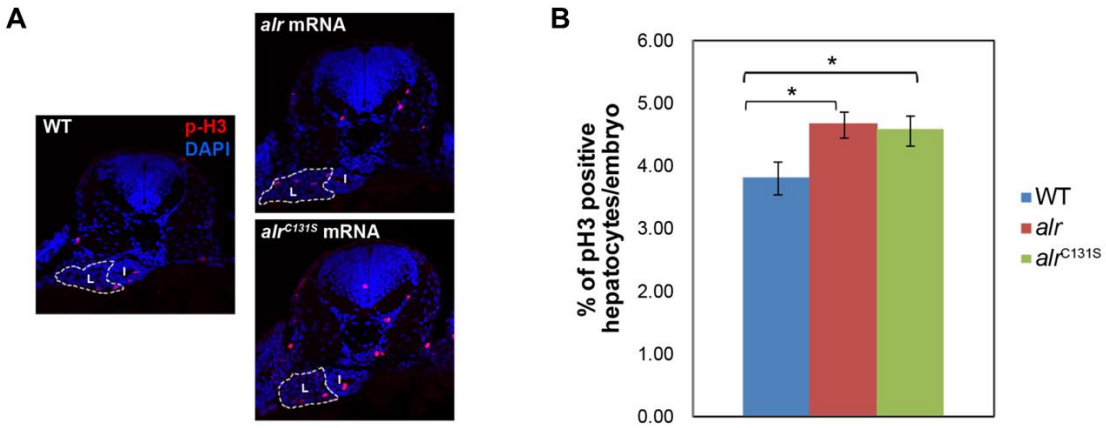

Fig. 3.37 Both *alr* and *alr*^{C131S} could promote hepatocytes proliferation.
Overexpression of *alr* and *alr*^{C131S} promote liver growth by promoting hepatocyte proliferation. Hepatocyte proliferation was demonstrated by immunofluorescent staining of proliferation marker p-H3 in 48 hpf embryos (red color). The tissue sections were counterstained with DAPI (blue) to label nucleus. I: intestine; L: liver. Dash line circles the boundary of liver. ∗, p<0.05.

3.3.3 Identifying the interacting proteins of zebrafish Alr by pull-down and MALDI-TOF-TOF mass spectrometry

Previous subcellular localization analysis demonstrates that Alr is a cytosolic and mitochondrial protein. Immunofluorescent staining showed that mitochondrion was the dominant subcellular location of zebrafish Alr. To understand the mechanism of Alr promoting hepatocyte proliferation and liver growth, the interacting proteins of

Alr within mitochondria was investigated using pull-down assay. Recombinant Alr protein with N-terminal 6×His was incubated with zebrafish liver cell mitochondrial lysate; Alr and its interacting proteins were pulled down by anti-His magnetic beads. Control pull-down group using anti-His magnetic beads incubated with mitochondria lysate without Alr protein was used to control for the background binding of mitochondria lysate to anti-His beads. As shown in the commassie blue stained SDS-PAGE gel in Fig. 3.38, while control group showed some background binding, a few unique protein bands that were specifically pulled down by Alr were identified. Those proteins bands were analyzed by MALDI-TOF-TOF mass spectrometry to reveal the protein identity. Three of the bands were successfully identified by MS to be G elongation factor mitochondrial 2 (Gfm2) (75 kD), Aspartyl-tRNA synthetase (Dars) (60 kD) and Eukaryotic translation elongation factor 1 alpha 1 like 1 (Eefla1l1) (50 kD) respectively. Fig. 3.39 showed the regions of the three proteins matched with the mass spectrometry peptides. The sequence coverage of Gfm2, Dars and Eefla1l1 were 13%, 15% and 16% respectively.

There are two protein translational systems in eukaryotes, the cytoplasmic and the mitochondrial translational system. Mitochondrial translation is crucial for maintaining mitochondrial function by producing proteins from mitochondrial DNA, *e.g.* the respiratory chain-oxidative phosphorylation system. Gfm1 and Gfm2 are proteins involved in mitochondrial protein synthesis. Gfm1 catalyzes translocation during peptide elongation, while Gfm2 mediates ribosomal disassembly. No

expressional or functional study of Gfm2 has been reported in zebrafish.

It is surprising that Dars and Eefla1l1 have been identified by mass spectrometry with high scores, as the mitochondrial lysate was used for the pull-down assay and Dars and Eefla1l1 are known as the cytoplasmic proteins involved in cytoplasmic translation. There are two aspartyl-tRNA synthetases in eukaryotes: aspartyl-tRNA synthetase cytoplasmic (*dars*) and aspartyl-tRNA synthetase 2 mitochondria (*dars2*) respectively. The Dars identified by MS was the cytoplasmic aspartyl-tRNA synthetase. No expressional or functional studies of zebrafish Dars have been reported.

Identification of Eefla1l1 as the interacting protein of zebrafish Alr is consistent with the study of human ALR which also identified Elongation factor 1α (human ortholog of zebrafish Eefla1l1) as interacting protein of human ALR by yeast two-hybrid screening (Cheng et al., 2003). Expression of *eefla1l1* was found in zebrafish embryonic livers (by WISH) and adult livers by RT-PCR (Rauch, 2003). Zebrafish *eefla1l1* mutant line is available but not characterized, except for the small head/eyes phenotype visibly observed (Amsterdam et al., 2004). Mammalian Eef1a has been found responsible for enzymatic delivery of aminoacyl tRNAs to the ribosome and nuclear export of proteins, with variable subcellular localizations. Thus, existence of Eef la1l1 in mitochondria is also possible.

The identity of the thick protein band at around 25 kD, which should be the bait protein (recombinant zebrafish Alr), was also confirmed by MS to be the zebrafish Alr.

Furthermore, identification of Gfm2, Dars and Eef1a1l1 as interacting proteins of zebrafish Alr by MS can be readily reproduced. Nevertheless, the binding of Gfm2, Dars and Eef1a1l1 to zebrafish Alr protein needs to be further validated by other methods such as co-immunoprecipitation experiment.

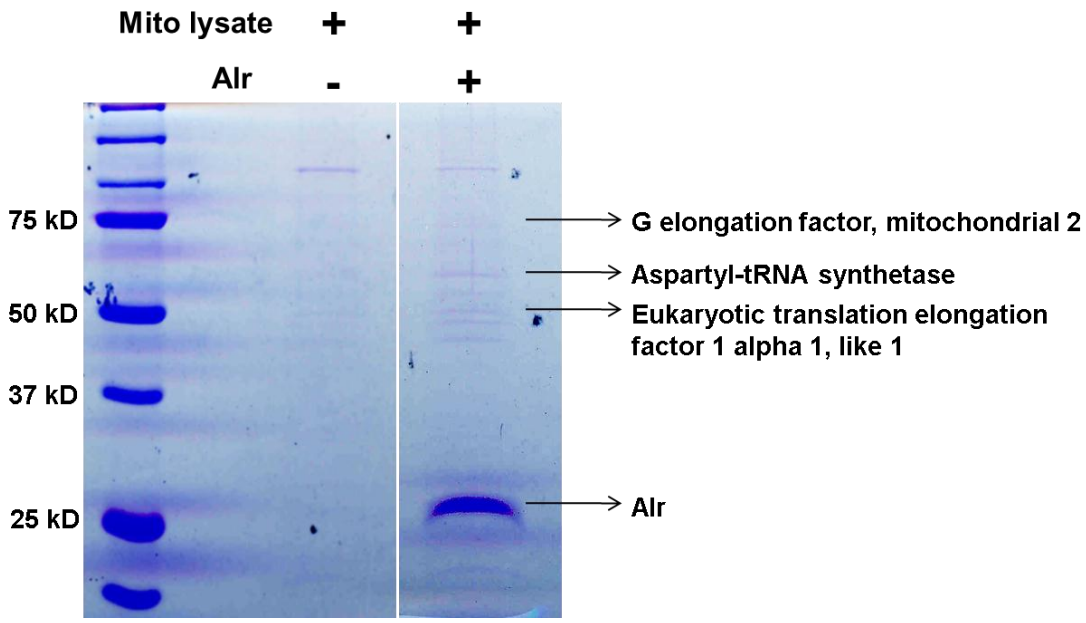

Fig. 3.38 Identification of the interacting proteins of Alr.
Alr was incubated with the mitochondria lysate of zebrafish liver cells; anti-His magnetic beads was used to pull down Alr and its interacting proteins. SDS-PAGE stained by commassie blue showed the protein bands that were pulled down by Alr. No Alr protein group was the control. The protein bands pulled down by Alr were identified by mass spectrometry.

A G elongation factor, mitochondrial 2 (Gfm2)

1 MLLSLTFPVL RGCTGHLVNR SLQAPRWRVT WKRSYSLLQD EVKSLRTVVN
51 PDISKIRNIG IMAHIDAGKT TTTERMLYYS GYTRALGDVD DGDTVTDYMA
101 QERERGITIQ SAAVTFDWKD YRINLIDTPG HVDFTLEVER ALRVLDGAVA
151 VFDASAGVEA QTMTVWRQAE KHQIPCVCFL NKMDKPAASL RYSLDSIKAK
201 LKANPVLLQI PIGSGKSFTG LVDLITRQKM MWQGNALTND GRSFEINSLQ
251 PSDDPNVLLA VSEARAALIE QVADLDDEFA ELLLGEYGEN FDAVPAVKLQ
301 EAVRRVTLAR KGVPVLCGSS LKNKGVQPLL DAITAYLPAP NERNHDLVRW
351 YKNDLCALAF KVVHDKQRGP LVFVRIYSGS MKAQSSVHNI NRNETEKMSR
401 LLLPFADQQI EIPSLSAGNI ALTVGLKQTV TGDTIVSSKA SAAAAIRRAQ
451 AEAESMSNSH SAALAGVEVP EPVFFCSIEP PTMAKQADLE HALNCLQRED
501 PSLKVRIDPD SGQTVLCGMG ELHIEIIHDR IKREYKIETH LGPLQVAYRE
551 TILQSVTAKD LLDRILGEKR HVVSVELTVH PLKENSSASC DITFEEDVKA
601 MLPADVREAV ENGVQSAYLQ GPVLGFPVQG VQTVIQDVRL ESGTSAAMVS
651 ACVSRCMLKA LKQAGGQVLE PVMALEVTVG EEHLSSVLAD LSQRRGTICD
701 IQSRQDNKIL LADVPLAEMM GYSTVLRTLT SGNATFSLEL SSYEPMNSQD
751 QNILLNKMAG LT

B Aspartyl-tRNA synthetase (Dars)

1 MTKENVQGGG EEEQQAQSKK ALKKQQKEAE KAAKKAEKQA KLASEQQETE
51 EDDFAKDRYG ICPMVQSQQK LDRALVRVQD LTLEKAEQQI WVRARIHTSR
101 AKGKQCFLVL RHQQFTVQAL LAVGDRASKQ MVKFAANITK ESIIDVEAVV
151 KKVEQKIESC SQQDVELHVE RIFVISQSEA RLPLQLEDAV RPEGEGDEEG
201 RATVNQDTRL DNRVIDLRTT TSQAIFRLQS GVCQLFRDTL INKGFVEIQT
251 PKIISAASEG GANVFTVSYF KTSAYLAQSP QLYKQMCICA DFDKVFCVGP
301 VFRAEDSNTH RHLTEFVGLD IEMAFSYHYH EVIDSITDTM VQIFKGLRDR
351 FQTEIQTVNK QYPSEPFKFL EPTLRLEYKE GLAMLRAAGV EMGDEEDLST
401 PNEKLLGRLV KEKYDTDFYV LDKYPLAVRP FYTMPDPNNP KYSNSYDMFM
451 RGEEILSGAQ RIHDAQLLTE RAMHHNIDLE KIKAYIDSFR YGAPPHAGGG
501 IGLERVTMLY LGLHNVRQTS MFPRDPKRLT P

C Eukaryotic translation elongation factor 1 alpha 1, like 1 (Eef1a1l1)

1 MGKEKTHINI VVIGHVDSGK STTTGHLIYK CGGIDKRTIE KFEKEAAEMG
51 KGSFKYAWVL DKLKAERERG ITIDIALWKF ETSKYYVTII DAPGHRDFIK
101 NMITGTSQAD CAVLIVAGGV GEFEAGISKN GQTREHALLA FTLGVKQLIV
151 GVNKMDSTEP PYSQARFEEI TKEVSAYIKK IGYNPASVAF VPISGWHGDN
201 MLEASSNMGW FKGWKIERKE GNASGTTLLD ALDAILPPSR PTDKPLRLPL
251 QDVYKIGGIG TVPVGRVETG VLKPGMVVTF APANVTTEVK SVEMHHESLT
301 EATPGDNVGF NVKNVSVKDI RRGNVAGDSK NDPPMEAANF NAQVIILNHP
351 GQISQGYAPV LDCHTAHIAC KFAELKEKID RRSGKKLEDN PKALKSGDAA
401 IVEMVPGKPM CVESFSTYPP LGRFAVRDMR QTVAVGVIKS VEKKIGGAGK
451 VTKSAQKAAK TK

Fig. 3.39 Sequence coverage of Gfm2, Dars and Eeflα1l1by MALDI-TOF-TOF mass spectrometry.

The regions in the three proteins that matched with mass spectrometry results were colored red. The scores of Gfm2, Dars and Eeflα1l1 were 42, 86 and 216 respectively. The sequence coverages of Gfm2, Dars and Eeflα1l1 were 13%, 15% and 16% respectively.

3.4 Inducible, liver-specific knockdown of *alr* by artificial miRNA

3.4.1 System design and establishment of the transgenic line

3.4.1.1 Design of the knockdown system

To establish a novel system for gene knockdown in late developmental stages and in adult fish in a spatially-temporally controllable manner, we adopted a transgenic approach by combining the chemically-inducible gene expression systems (Emelyanov and Parinov, 2008) and the artificial miRNA knockdown system (Dong et al., 2009). The design of the transgene cassette for inducible, liver specific knockdown of *alr* by artificial miRNA is illustrated in Fig. 3.40.

To facilitate transgene integration into the zebrafish genome, maize Dissociation (*Ds*) transposable elements of 600 bp in length are placed at both terminus of the transgene cassette, in inverted directions (Fig. 3.40, blank arrow heads) (Emelyanov et al., 2006). The Ac transposase can induce excision at the 5' end of the *Ds* element and carry the whole transgene cassette (including the terminal *Ds* elements) into a new genomic location, using the 'cut-and-paste' mechanism. Between the *Ds* elements, the following basic elements are arranged in a 5' to 3' direction: (1) the liver specific promoter *liver fatty acid-binding protein* (*lfabp*); (2) the mifepristone-inducible LexPR-LexOP system; (3) the artificial miRNA embedded in the intron 2 of truncated *β–actin* gene; (4) the EGFP gene fused in frame to the 3' end of truncated *β–actin* gene.

Controlled by the upstream *lfabp* promoter, the LexPR transactivator will be

expressed only in liver. The transactivator LexPR is engineered by fusion of the DNA binding domain of the bacterial LexA repressor, the truncated ligand binding domain of human progesterone receptor and the activation domain of human p65 protein (Reviewed previously in Section 1.5.1, Fig. 1.11) (Emelyanov and Parinov, 2008). The operator-promoter sequence LexOP consists of a synthetic LexA operator and a minimal 35S promoter from Cauliflower Mosaic Virus. The synthetic steroid mifepristone (also known as RU486) can bind to the ligand binding domain of LexPR. Upon binding of miferpristone, the transactivator LexPR will become activated. The activated LexPR will then bind to the LexA operator and activate the minimal 35S promoter, to turn on the transcription of downstream gene (Fig. 3.40).

The backbone of miRNA precursor is important for miRNA processing and maturation. Making use of the backbone of natural miRNA precursor, artificial miRNAs can be expressed for targeted gene knockdown (Chung et al., 2006; Zeng et al., 2002). This concept was first demonstrated by Dong et al. (2009) for its use in zebrafish. In their design, the artificial miRNA in zebrafish *mir-30e* backbone was placed into the intron 2 of truncated *β–actin* gene, to facilitate the expression of the artificial miRNA under the control of tissue-specific pol II promoters in transgenic fish. This study provides a valuable tool for stable and tissue-specific knockdown in zebrafish embryos. But this system does not allow temporal control of knockdown. Thus, it could not be used for study of genes that have dynamic functions in the same tissue in different embryo stages and in adults. This intronic artificial miRNA

expression system was adapted in our study, to achieve temporal and spatial control of knockdown.

As shown in Fig. 3.40, the truncated β-actin (Δactin) and EGFP will be expressed as a single transcript generating the ΔActin-EGFP fusion protein. The intronic artificial miRNA will be generated as a byproduct during the splicing of Δ*actin*-EGFP pre-mRNA, allowing for simultaneous expression of the Δ*actin*-EGFP reporter gene and the artificial miRNA. The expression of the Δ*actin*-EGFP reporter gene and the artificial miRNA are simultaneously controlled by the upstream LexOP operator-promoter sequence.

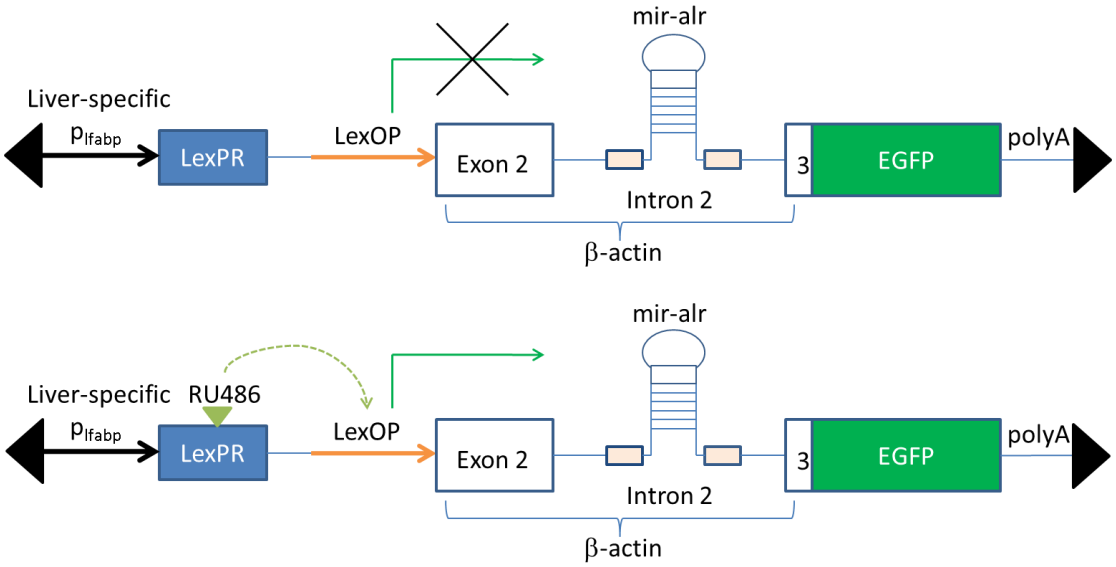

Fig. 3.40 Design of the knockdown system for the inducible, liver-specific knockdown of *alr* by artificial miRNA.
The transgene cassette is flanked by the *Ds* transposable elements in reverse directions (black arrowheads). The liver specific promoter controls the expression of LexPR in liver only. In the absence of mifepristone (RU486), the LexOP operator-promoter could not turn on the expression of downstream gene (upper panel). In the presence of RU486, it binds to and activates LexPR. The activated LexPR could then activate LexOP and thus turn on the expression of downstream gene (bottom panel). The artificial miRNA mir-alr uses the *mir-30e* backbone and could co-express with the Δactin-EGFP fusion transcript.

3.4.1.2 Knockdown of *alr* by artificial miRNA (miR-alr)

The artificial miRNA that was designed to target zebrafish *alr* for knockdown was named miR-alr; the corresponding mismatch control miRNA was named miR-alr^{mis}. It is known that accessibility by miRNA could be affected by the local secondary structure and local free energy of the target region (Kertesz et al., 2007; Shao et al., 2007). So the secondary structure of alr 3'UTR was predicted by mFold web server (Zuker, 2003); the loop regions with low local free energy were used for selection of target sequence and design the miR-alr (Dong et al., 2009). Two miR-alr were designed initially, targeting the 135-156 nt and 286-307 nt regions of *alr* 3' UTR respectively. The efficacy of the two designed miR-alr to knockdown endogenous *alr* was tested by injecting the *in vitro* synthesized pri-mir-alr mRNA into one-cell stage embryos at equal amount, followed by RT-PCR to test *alr* mRNA level change. The miR-alr (targeting 286-307 nt) showed much higher potency of knockdown of *alr* and was thus selected.

In animals, miRNAs normally pair to the 3'UTR of their mRNA targets with only limited complementarity. Recent publications support the view that base-pairing to the seed region (between miRNA position 2 and 8) is critical and in some cases sufficient for target recognition. Animal microRNAs can therefore have many targets. Whether the selected artificial miRNA have other potential targets was predicted by blast search against zebrafish Reference RNA Sequence database. Among the 132 hits, only 9 hits (GenBank accession numbers: XM_001344781, XM_003201426,

NM_001201420, NM_001201419, NM_001201418, NM_001201417, NM_198911, XM_003199229, XM_682861) show high complementary to the artificial miRNA seed region at their 3'UTR. But those 9 possible targets are most probably not expressed in zebrafish embryonic liver (ZFIN Directly Submitted Expression Data, http://zfin.org/). Since the artificial miRNA is specifically expressed in liver in the transgenic fish, any liver phenotype should be specific to knockdown of *alr*.

Fig.3.41A showed the selected *mir-alr* and *mir-alr*^{mis} precursor sequences. The control miRNA miR-alr^{mis} has two nucleotides mismatches in the seed region and three nucleotides mismatches in other places (Fig. 3.41A). The *mir-alr* and *mir-alr*^{mis} precursor was constructed by replacing the hairpin region of the mir-30e stem-loop with the shRNA sequences shown in Fig. 3.41A. The target region of miR-alr on the secondary structure of *alr* 3'UTR predicted by mFold web server was shown in Fig. 3.41B (in the red bracket). RT-PCR results showed (Fig. 3.42) that microinjection of mir-alr precursor resulted in significant knockdown of *alr* mRNA compared to uninjected control, while the mismatch mir-alr^{mis} precursor did not disturb the expression of *alr* as expected.

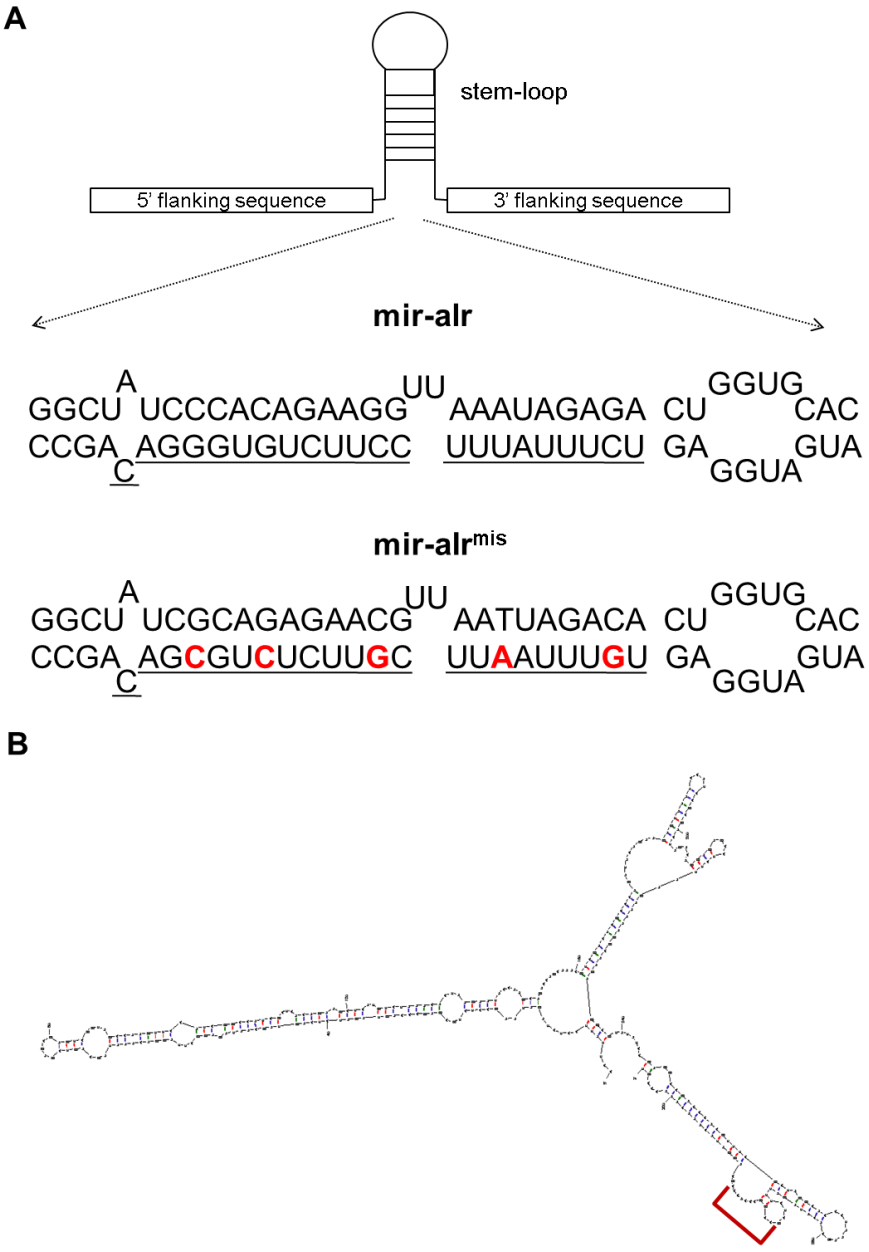

Fig. 3.41 Diagram of mir-alr and mir-alr^{mis} against the 3'UTR of of *alr* mRNA
A, diagram showing the stem-loop sequences of mir-alr and mir-alr^{mis} precursor. The underlined regions will give rise to the mature miRNAs. The mismatched nucleotides were colored red in mir-alr^{mis}. B, the target region of miR-alr was shown (within red bracket) on the predicted secondary structure of the 3'UTR of zebrafish *alr*.

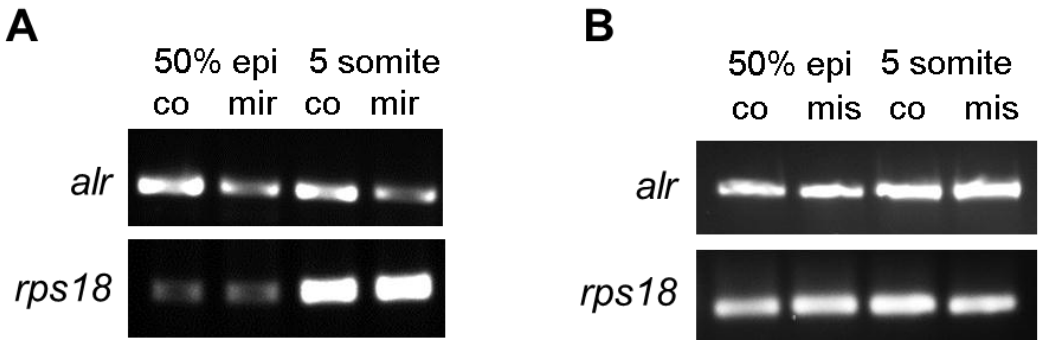

Fig. 3.42 Knockdown of *alr* by microinjection of *in vitro* synthesized pri-mir-alr and pri-mir-alr^{mis} mRNA.
Embryos were collected at 50% epiboly and 5-somites stages to examine the *alr* mRNA level. RT-PCR results showed that the selected mir-alr could knockdown *alr* significantly (A), while the mismatch mir-alr^{mis} did not affect the expression of *alr* (B). Co, uninjected embryos; mir, mir-alr precursor injected embryos; mis, mir-alr^{mis} precursor injected embryos. The *rps18* was used as the loading control.

3.4.1.3 Establishment of the transgenic zebrafish lines

The *in vitro* synthesized 5'-capped and poly(A)-tailed *Ac* transposase mRNA (50 pg per embryo) and the transgene DNA construct (10 pg per embryo) (illustrated in Fig. 3.40) was co-injected into the yolk of the one-cell stage wild-type embryos, to establish the transgenic lines. The injected *Ac* transposase mRNA will be translated into Ac transposase protein, which can induce excision at the 5' end of the *Ds* elements and transposition of the Ds elements together with the transgene inside into the zebrafish genome (the 'cut-and-paste' way). The activity of *Ac* mRNA injected was tested for its ability to induce excisions in the circular transgene plasmid injected. The embryos injected were collected at 24 hpf for total DNA extraction and PCR using 'Ds-F' and 'Ds-R' primers flanking the *Ds* sequence (denoted as red arrows below the transgene construct in Fig. 3.43A), to check for the excision product

(Emelyanov et al., 2006). As shown in Fig. 3.43B, the excision products (PCR products around 600 bp) was only detected in embryos injected with both the *Ac* transposase mRNA and the transgene vector, while not in the embryos injected with transgene vector only.

As 400 bp mir-alr precursor gene has been inserted into the intron 2 of *actin* gene, it is important to determine whether this insertion affect the correct splicing of *actin* mRNA. The *Ac* mRNA and transgene plasmid injected embryos was induced with mifepristone; GFP positive embryos were collected at 3 dpf for total RNA extraction. RT-PCR was performed using 'actin-e2-F' and 'EGFP-AS' primers flanking the intron 2 of *actin* (black arrows indicates the positions of primers), to check whether the intron of *actin* could be correctly spliced out. As expected, a 240 bp product was detected (Fig. 3.43C), matching the size of correct splicing. This RT-PCR product was further sequenced to confirm the correct junction of exon 2 and 3 of *actin*.

The injected embryos were grown to 3 dpf and treated with 100 nM mifepristone for 12 hours to induce the transgene expression. Embryos with GFP specifically in the liver (Fig. 3.43D) were raised to adulthood as F_0 fish. Generally 20-50% of the injected embryos will be positive for liver GFP after induction. Ectopic expression of GFP in other tissues were observed in 20-40% of the embryos (Fig. 3.43 E and F), probably due to promoter/enhancer trapping.

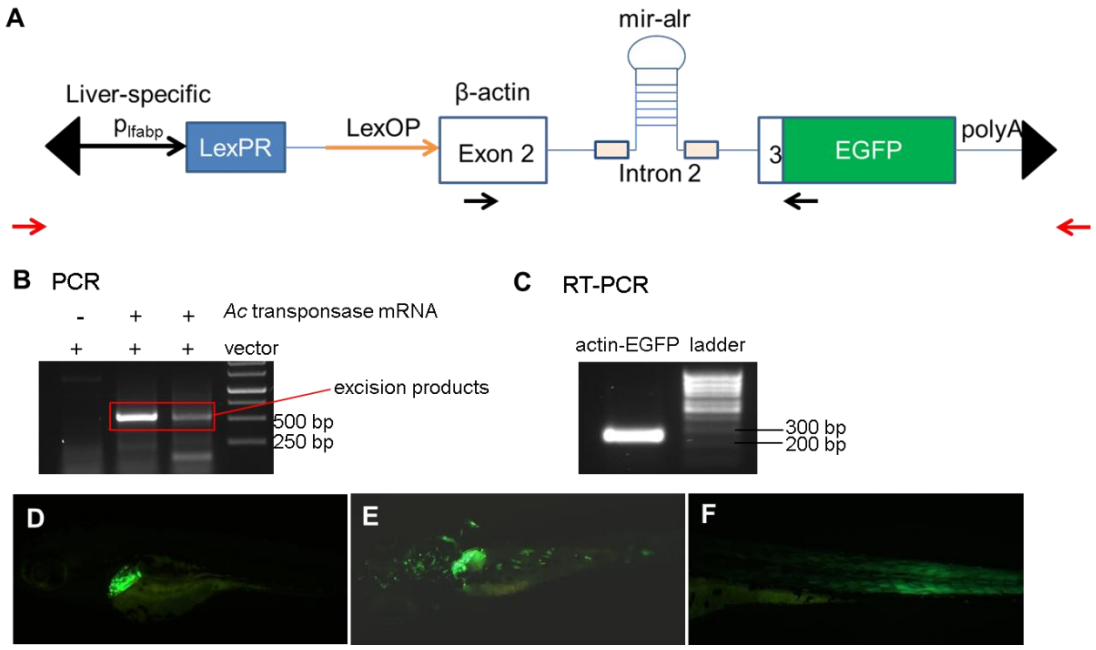

Fig. 3.43 Characterization of the *Ac* mRNA and transgene plasmids injected embryos.

A, position of primers (by red arrows) for detecting the excision product in B and checking the splicing of *actin* in C (by black arrows). B, excision products (around 600 bp) were detected in *Ac* mRNA and plasmid co-injected embryos only, showing the functionality of *Ac* mRNA injected. C, detection of the correctly spliced Δ*actin*-EGFP transcript by RT-PCR. D, embryos with specific liver GFP was grown up as F0 fish. E and F, ectopic expression of GFP in tissues such as skin and muscle were observed in 20-40% of the injected embryos.

The F_0 fish were screened by pairwise outcrossing with wild-types fish and the offsprings were examined for inducible liver GFP expression. The F_0 fish that can transmit the transgene to the next generation are called founder fish, indicating that they have germline integration of the transgene. Around 80% of the F0 fish were identified to be founder fish, showing that the Ac/Ds transposon system can integrate the transgene into fish genome effectively and provide high germline transmission rate.

After crossing F0 transgenic fish and wild-type fish, the percentage of GFP-positive

embryos could differ from as low as 10% to 50%. The low percentage (<50%) of GFP-positive progeny suggests late integration of the transgene in F_0 fish and as a result the mosaic germline integration of the transgene. This is probably because of injection of the plasmid DNA into the yolk not the cell, which takes time for the plasmid DNA to diffuse into the nucleus and get integrated into the genome by transposase.

The F_1 fish were grown up by outcrossing the F_0 founder fish with wild-type fish and screening for GFP-positive embryos. Three transgenic fish lines were created, being the knockdown line *Tg(lfabp:LPR-LOP:mir-alr-Δactin-EGFP)* and two control lines *Tg(lfabp:LPR-LOP:mir-alr^{mis}-Δactin-EGFP)* and *Tg(lfabp:LPR-LOP:Δactin-EGFP).* The diagrams of transgene cassette in the three lines were illustrated in Fig. 3.44. The line *Tg(lfabp:LPR-LOP:mir-alr^{mis}-Δactin-EGFP)* express a mismatch miRNA miR-alr^{mis}, to control for the non-specific side effects resulting from expressing an artificial miRNA at high level in liver. The line *Tg(lfabp:LPR-LO:Δactin-EGFP)* do not express any artificial miRNA, but controls for the non-specific side effects of expressing ΔActin-EGFP fusion protein at high level in the liver.

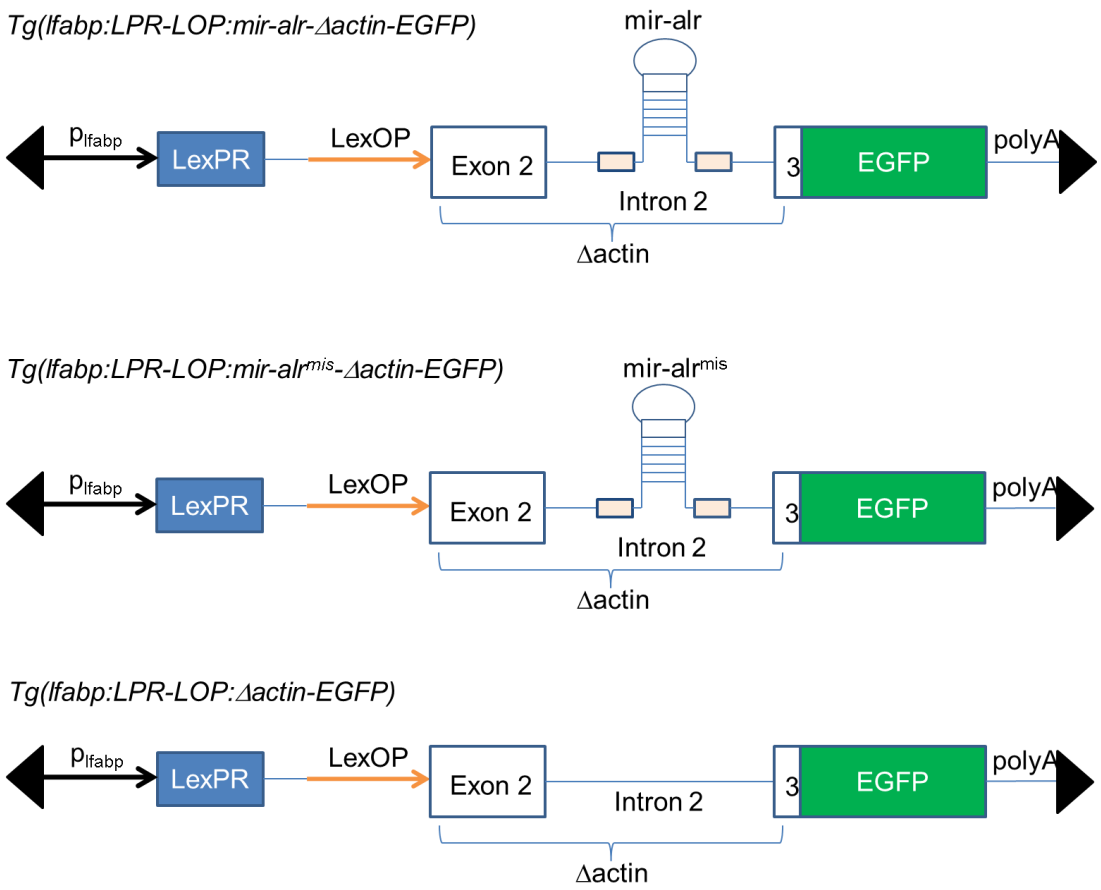

Fig. 3.44 Diagrams of transgene cassette in the three transgenic lines created. The *Tg(lfabp:LPR-LOP:mir-alr-Δactin-EGFP)* is the knockdown transgenic line. The *Tg(lfabp:LPR-LOP:mir-alr^{mis}-Δactin-EGFP)* and *Tg(lfabp:LPR-LO:Δactin-EGFP)* are the two control transgenic lines, to control for the non-specific effects resulting from expressing an artificial miRNA and ΔActin-EGFP fusion protein at high level in the liver respectively.

3.4.2 Characterization of the knockdown transgenic line *Tg(lfabp:LPR-LOP:mir-alr-Δactin-EGFP)*

3.4.2.1 Number of transgene insertion sites in F_1 generation

When crossing the F_1 transgenic fish with wild-type fish, the rate of liver GFP positive embryos could be as high as 90%, suggesting multiple transgene integration sites within the genome of F_1 fish. The number of transgene insertion sites in different F_1 fish was characterized by genomic southern blot. To avoid sacrificing transgenic F_1

fish, genomic DNA was extracted from pooled F_2 embryos by outcrossing each F_1 fish with a wild-type fish; pooled randomly selected liver EGFP positive F_2 embryos was used for Southern blot analysis. Genomic DNA was digested with restriction endonucleases EcoRI and HindIII to produce small-sized DNA fragments and hybridized with DIG-labeled EGFP probe. Seven different F_1 fish (named B-H) that originated from the same founder (F_0) was analyzed for the number of transgene insertion sites. Southern blot results (Fig. 3.45) revealed predominantly multiple insertion sites in the genome of different F_1 fish, ranging from one to five insertion sites. Different F_1 fish from the same F_0 founder fish harbored distinct insertions.

Transposon-mediated transgene insertion is usually single copy in each insertion site. It is not possible to maintain the transgene copy number in the multiple insertion fish, as they will give rise to a diverse pool of progeny with different transgene copy numbers. But the single insertion fish can be stably maintained. So the single insertion fish numbered G was maintained and its F_2 progeny was used for validating miR-alr miRNA expression and determining the efficiency of *alr* knockdown.

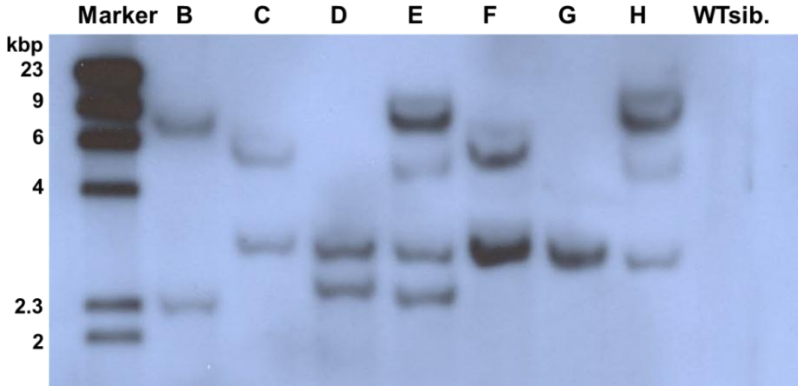

Fig. 3.45 Evaluation of the number of transgene insertion sites in F_1 fish.
DIG-labeled EGFP was used as the probe for genomic southern blot. First lane,

DIG-labeled DNA marker. Lane B-H, progeny of seven different F_1 fish that originated from the same founder (F_0). Last lane, wild-type embryos, as negative control.

3.4.2.2 Detection of miR-alr expression and knockdown of endogenous *alr* mRNA

Adult F_2-G fish (progeny of F_1-G which has single insertion of the transgene) were treated with 1μM mifepristone for 4 days, to induce the expression of miR-alr in liver. The livers were then dissected for total RNA extraction and small RNA isolation. The total RNA was used to examine the *alr* level to check knockdown efficiency. The small RNA was isolated to detect the expression of miR-alr.

Traditional method to detect miRNA expression is through Northern blot, which is complicated and time-consuming. The expression level of miRNA could not be accurately quantified by Northern blot. PCR based quantification of miRNA has been developed in recent years. One of the widely used methods is stem-loop RT-PCR (Chen et al., 2005a). The stem-loop real-time quantification of miRNAs involves two steps, stem-loop RT and real-time PCR. As illustrated in Fig. 3.46A, stem-loop RT primer which has 8 nt complementary to the 3' portion of miRNA will be used for reverse transcription, to get an extended first-strand cDNA of the miRNA. This cDNA is around 66 nt in length and is long enough for real time PCR quantification using miRNA specific forward primers and common reverse primer from the stem-loop region. The stem-loop RT primer specifically amplified the mature miRNA, not the precursor.

Expression of miR-alr and let-7a was quantified by stem-loop RT-qPCR in

mifepristone untreated (UT) and treated (T) F_2-G fish livers. The let-7a was the internal control, which showed equal expression level in untreated and treated fish (Fig. 3.46B). Expression of miR-alr was detected in the mifepristone treated fish. Untreated transgenic fish show low level of amplification signal. But similar amplification signal could also be detected in wild type fish, which do not express the artificial microRNA miR-alr. So this level of amplification signal in the untreated transgenic fish is likely from non-specific amplification. Gel electrophoresis (Fig. 3.46C) showed that stem-loop RT-PCR of let-7a and miR-alr yield one single product at around 70 bp, matching the expected size.

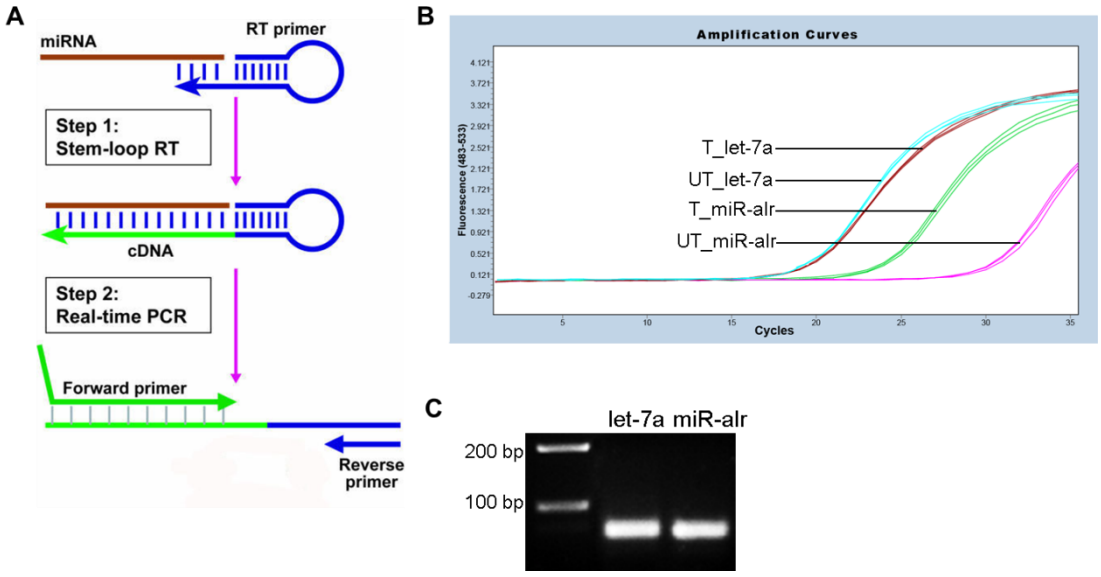

Fig. 3.46 Detection of miR-alr expression by stem-loop RT-PCR.
A, schematic illustration of the stem-loop RT-qPCR. Stem-loop RT primer which bind the 3' portion of miRNA was used for reverse transcripton; miRNA specific forward primer and universal reverse primer from the stem-loop region was used for real-time PCR (modified from Chen et al., 2005a).
B, real-time amplification of miR-alr and let7a by stem-loop RT-PCR, in mifepristone untreated (UT) and treated (T) F_2-G fish livers. Let-7a was used as internal control.
C, gel electrophoresis of the stem-loop RT-PCR product. One single band at around 70 bp was detected for both let-7a and miR-alr from the treated fish, matching the expected size.

The level of *alr* was quantified by real-time RT-PCR using rps18 as the reference gene, and compared to the wild-type fish under the same treatment condition. The untreated F_2-G fish was not used as control, because we have observed that mifepristone (dissolved in ethanol solvent) treatment condition will induce increased expression of *alr*. For each batch of treatment, the total RNA sample was extracted from a pool of three livers. Level of *alr* mRNA was reduced by 54% and 32% respectively in the two batches of treatment (Fig. 3.47), demonstrating that the induced expression of artificial miR-alr could mediate effective *alr* knockdown.

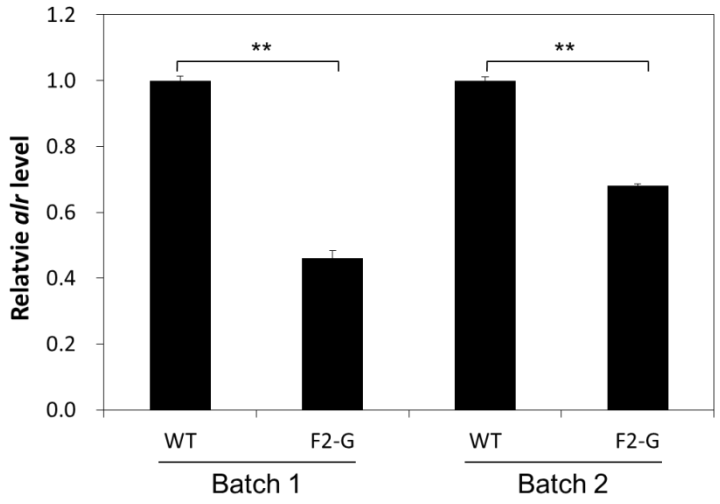

Fig. 3.47 Knockdown of endogenous *alr* by induced expression of miR-alr.
The level of *alr* was quantified by real-time PCR, using *rps18* as reference gene. Relative *alr* level was calculated by comparing to wild-type fish under the same treatment condition.

3.4.3 Effect of *alr* knockdown on liver growth in larval fish by induced expression of the miR-alr

Previous morpholino based knockdown has demonstrated that *alr* is involved in

hepatocyte differentiation and embryonic liver outgrowth. An advantage of this knockdown transgenic line is that it enables gene knockdown tissue-specifically and at late growth stages. Using this transgenic line, the effect of liver-specific knockdown of *alr* was observed from early larva (3-7 dpf) to late larva (7-14 dpf), by continual treatment of 1 μM mifepristone.

Embryos from four transgenic lines, *Tg(lfabp:DsRed; elaA:EGFP), Tg(lfabp:LPR-LOP:mir-alr-Δactin-EGFP), Tg(lfabp:LPR-LOP:mir-alr^{mis}-Δactin-EGFP)* and *Tg(lfabp:LPR-LOP:Δactin-EGFP)* were collected and continuously treated with 1 μM mifepristone from 36 hpf onwards. The liver marker line *Tg(lfabp:DsRed; elaA:EGFP)* was used as the control. Continual treatment of 1μM mifepristone had no effect on embryo gross morphology and liver growth, as shown in *Tg(lfabp:DsRed; elaA:EGFP)* (Fig. 3.48). In mifepristone treated *Tg(lfabp:LPR-LOP:mir-alr-Δactin-EGFP)* fish which express miR-alr, liver growth is significantly inhibited (Fig. 3.48 A and B). But overexpression of a mismatch miRNA miR-alr^{mis} in *Tg(lfabp:LPR-LOP:mir-alr^{mis}-Δactin-EGFP)* did not affect the liver size. Overexpression of Δ*actin*-EGFP in *Tg(lfabp:LPR-LOP:Δactin-EGFP)* also did not affect liver growth.

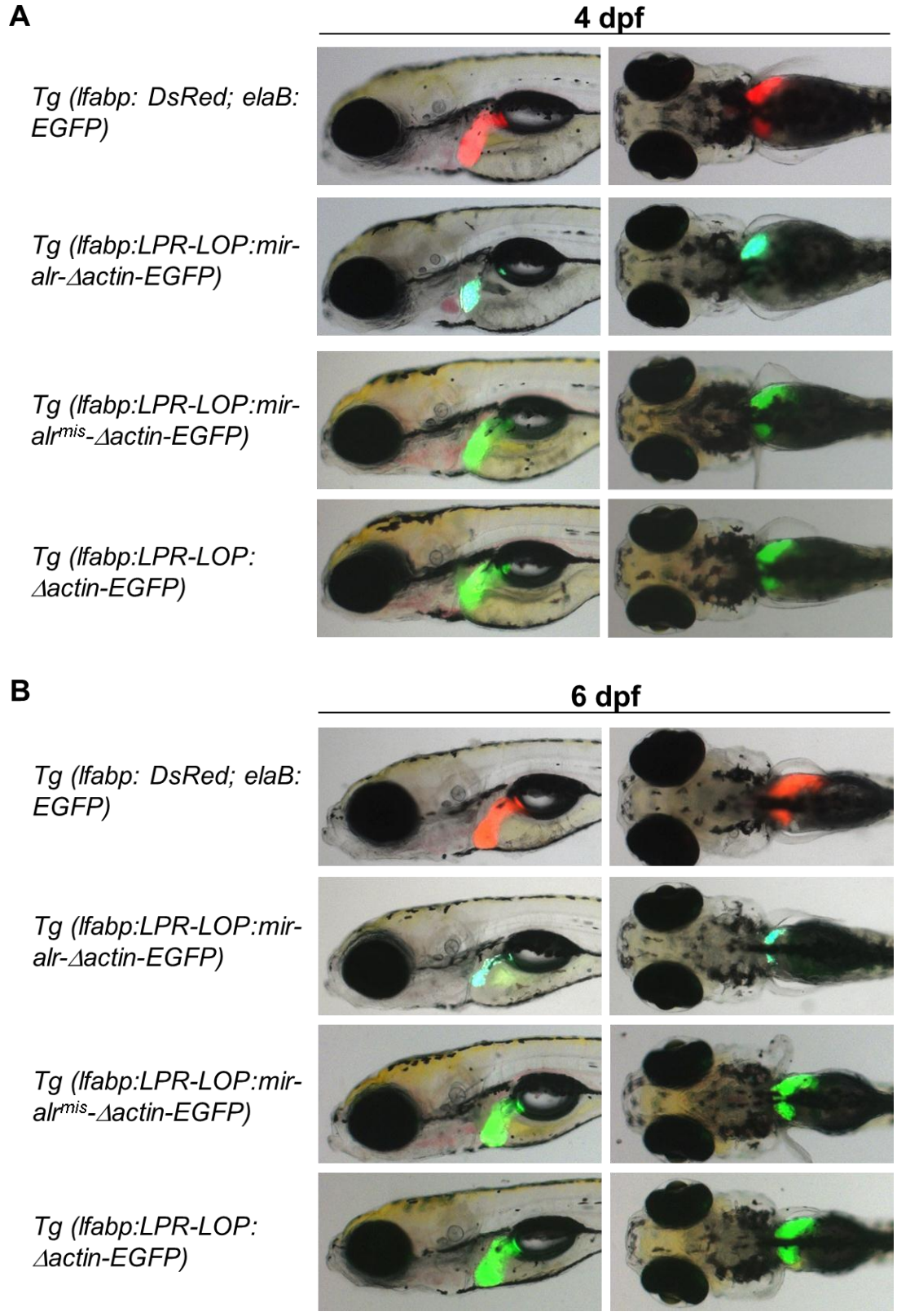

Fig. 3.48 Effect of *alr* knockdown on the liver growth of early stage larva

A, 4 dpf larva. B, 6 dpf larva. Left panels, left lateral view; right panels, ventral view. All four transgenic fish lines were continuously treated with 1 μM mifepristone from 36 hpf onwards. Compared to the liver marker line *Tg(lfabp:DsRed; elaA:EGFP)*, the

liver size is significantly small in *Tg(lfabp:LPR-LOP:mir-alr-Δactin-EGFP)*. While in *Tg(lfabp:LPR-LOP:mir-alr^{mis}-Δactin-EGFP) and Tg(lfabp:LPR-LOP: Δactin-EGFP)* treated, the liver growth was normal.

It is believed that by 5 dpf the zebrafish liver has become functional (Korzh et al., 2008). Since proper liver size and function is critical for fish survival, liver growth perturbation at larva stage might lead to severe phenotype or even death. The effect of miR-alr continual expression on late stage larva liver growth and survival was investigated. In the two control lines *Tg(lfabp:LPR-LOP:mir-alr^{mis}-Δactin-EGFP) and Tg(lfabp:LPR-LOP: Δactin-EGFP),* continually induced expression of the miR-alr^{mis} or Δ*actin*-EGFP only lead minimum (less than 10%) decrease of survival rate compared to the untreated transgenic fish and treated wild-type siblings (Fig. 3.49 B and C). While in *Tg(lfabp:LPR-LOP:mir-alr-Δactin-EGFP)* fish, induced expression of miR-alr reduced the survival rate by more than 60% compared to the untreated transgenic fish and treated wild-type siblings. Fluorescent images showed that at 14 dpf, the liver size is much smaller in the *Tg(lfabp:LPR-LOP:mir-alr-Δactin-EGFP)* larva that is still surviving. Only a ventral lobe was observed, the left lobe is not developed.

As a summary, these results demonstrated that *alr* is essential for liver growth and survival. Knockdown of *alr* inhibits not only embryonic liver growth but also larval stage liver growth; loss-of-function of *alr* will lead to death of fish at larval stage.

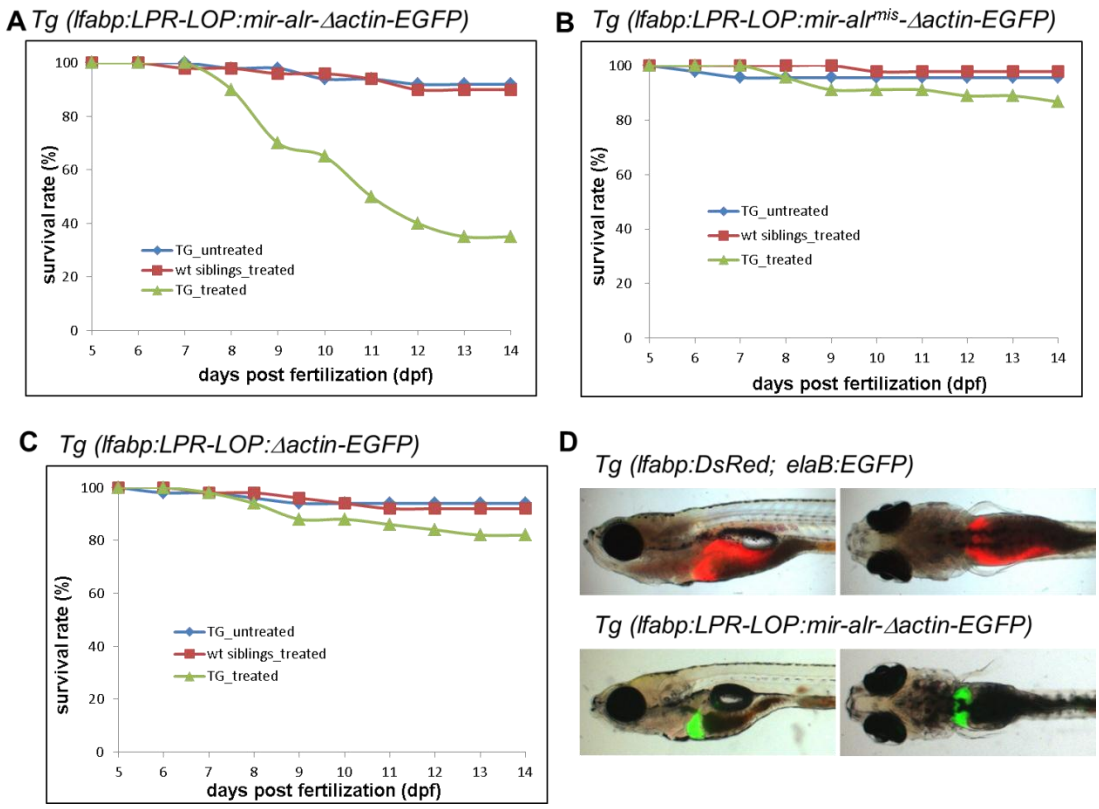

Fig. 3.49 Effect of continual knockdown of *alr* on liver growth and survival rate of late stage larva.

A, B and C, death curve of different transgenic lines with continual mifepristone treatment (TG_treated) were recorded. The untreated transgenic fish (TG_untreated) and treated wild-type siblings (wt siblings_treated) are the control groups. D, fluorescent images showing the liver size at 14 dpf with continual mifepristone treatment from 36 hpf onwards. Left panels, left lateral view; right panels, ventral view.

CHAPTER 4. DISCUSSION

4.1 Developmental functions of Alr in zebrafish

In this study, we investigated the developmental functions of *alr* in zebrafish model system. In particular, we focused on the role of *alr* in zebrafish embryonic liver development and found that *alr* promotes liver growth by promoting hepatocyte proliferation in both liver budding and outgrowth phases. The embryonic liver growth is coordinated by multiple signal pathways acting during different phases in processes of transcriptional regulation, cell proliferation and apoptosis, cell-cell interactions and morphogenesis (reviewed by Chu and Sadler, 2009). This study placed *alr* in the class of cell proliferation regulators that function in liver budding and growth phases.

It is clear that the function of *alr* in zebrafish development may not be restricted to liver organogenesis. Zebrafish *alr* is stored at high level in one-cell stage embryos as a maternal gene, as shown by the WISH staining (Fig. 3.6). Interestingly, *ALR* was identified to be one of the 216 genes enriched in mouse embryonic, neural, and hematopoietic stem cells in a study trying to define the genetic program for stem cells (Ramalho-Santos et al., 2002). The function of *ALR* in mouse embryonic stem cells (ESC) was later investigated by knockdown of *ALR* in ESC. It functions by preserving ESC mitochondrial morphology and function, to maintain ESC pluripotency and survival (Todd et al., 2010a). The evidence above suggests that *alr* might have conserve roles for very early embryonic growth before gastrulation.

WISH result (Fig. 3.6) showed that *alr* is ubiquitously expressed at high levels in

early embryos before segmentation and later in the developing brain and pharyngeal arches in addition to the expression in liver. Consistently, when high doses of morpholino were injected, severe developmental defects and early embryonic death was observed, while no obvious defect was seen in same amount of control morpholino injected embryos. Therefore, it seems that Alr has fundamental roles for cell survival in different tissues, possibly through acting on mitochondria involving its sulfhydryl oxidase activity. Hence the partial and dose-dependent suppression of *alr* function through morpholino-mediated knockdown presented a clear advantage over the gene knockout approach, allowing the identification of a late developmental role of *alr* in vertebrate liver organogenesis. No *ALR* knockout mouse has been reported so far, possibly because of embryonic lethality caused by complete loss-of-function of *ALR*. Incidentally, *alr* mutant in Drosophila is recessive lethal and homozygous *alr* mutation leads to developmental arrest in flies (McClure et al., 2008).

We noted that knockdown of *alr* also resulted in a smaller exocrine pancreas phenotype (Fig. 3.18). It seems that *alr* could be playing a role in the development of exocrine pancreas. Excess blood vessel using the *Tg(fli1:EGFP)* fish (all the blood vessel were marked with EGFP) and less hematopoietic cells by *gata1* WISH in *alr* morphants was observed (unpublished data in the lab), suggesting the potential role of alr in the differentiation of hemangioblasts into hematopoietic cells and endothelial cells (Xiong, 2008). Future investigations are required to elucidate the role of *alr* in exocrine pancreas development and hemangioblasts differentiation.

4.2 Human ALRs and zebrafish liver development

All our gain-of-function analysis was performed by injection *in vitro* synthesized mRNA into one-cell stage embryos, which is a very convenient method. However, the challenge of using synthesized mRNA for liver growth study is the short lifespan of the mRNA injected; generally the mRNA and its protein product only survive for less than one day before the liver outgrowth stage. We have investigated the life span of the zebrafish *alr* mRNA injected by testing its protein product. We found that the protein product will start to degrade fast after 24 hpf, and by 48 hpf very little protein is left (Fig. 3.20) although a very high dose of mRNA was injected. Thus we always inject the maximum tolerable dose of mRNA into embryos for functional analysis.

With the zebrafish *alr* being a liver growth promoting factor, whether the human ortholog also functions in the same developmental process is unknown. Thus, a cross-species functional test was performed in an attempt to establish the human ALR as functional homologs of zebrafish Alr, by injecting the *in vitro* synthesized human *ALR* mRNA for overexpression and morphants rescue analysis. However, both the human long form and short form *ALR* mRNA failed to demonstrate a cross-species activity. Both isoforms of human *ALR* could not rescue small liver phenotype of the morphants and they did not show any liver growth promoting effect when overexpressed (Fig. 3.23 and Fig. 3.24). The life span of the injected mRNA and the ALR protein product level at the stage of phenotype analysis was in doubt, which

might be a possible reason for failing to rescue the morphants and promote liver growth. It is also possible that the human ALR and zebrafish Alr have diverged during evolution and could not functional complement each other. Surprisingly, the human short form ALR is able to partially rescue yeast Erv1 mutant which is not viable, although the yeast Erv1 mutant expressing human ALR grew slower (Hofhaus et al., 1999; Lisowsky et al., 1995). But the complete human ALR with its own amino terminus is not able to complement the yeast Erv1, unless its N-terminus was replaced with the yeast Erv1 N-terminal 21 amino acids (Hofhaus et al., 1999; Lisowsky et al., 1995), suggesting the highly divergent N-terminus is important for its proper function in different species. Similarly, the highly divergent N-terminus could be possible reasons for explaining why the human ALRs could not functional replace the zebrafish Alr in our results. Future investigations could be performed by replacing the human N-terminus with the zebrafish Alr and test for the cross-species activity of the chimeric protein.

4.3 Isoforms of Alr in different organisms

Two isoforms of ALR protein have been identified in mammals, possibly due to different translation starting sites (Gatzidou et al., 2006; Lu et al., 2002b). As shown in Fig. 3.2, the show form ALR uses a downstream methionine as the start; as a result it lacks the N-terminal non-conserved region which contains two conserved cysteine and retains the conserved Erv1/Alr domain. The zebrafish Alr (191 amino acids) is

more similar to the long form mammalian ALR (205 amino acids) in length, as both have comparable N-terminal region with two conserved cycteines and the Erv1/Alr domain in the C-terminus. The starting amino acid methionine of mammalian short form ALRs is conserved in zebrafish amino acid sequence, so it is possible that the zebrafish Alr also use this methionine as start to translate a short isoform. However, whether this endogenous short isoform is also present in zebrafish is unknown at this moment, because proper anti-zebrafish Alr antibody is not available.

But we indeed isolated different transcripts of *alr*. When amplifying *alr* cDNA, an extra DNA bands which is 150 bp smaller than the main DNA product was usually observed (Fig. 3.5 and Fig. 3.7A). The smaller band, which was much weaker compared to the main band, has been detected in different tissues and embryonic stages, with different sets of primers. It was thus cloned into pGEM-T easy vector (Promega) and sequenced. Sequencing results revealed that the smaller *alr* transcript was generated by alternative splicing, with 148 bp of the exon two spliced into intron and deleted (Fig. 4.1 A and B). No comparable alternative splicing forms has been found in other species. Whether this short form alr has any functional significance or encodes any protein product is unknown. Future investigations are required to investigate whether this short form *alr* transcript encodes any protein and elucidate the role of the protein product if any. For this purpose, the full length cDNA of the short form alr need to be obtained by Rapid Amplification of cDNA Ends (RACE) first. Whether this transcript has protein coding ability depends on whether it can bind

ribosome which can be analyzed through RNA co-immunoprecipitation. If the short transcript can bind ribosome, *in vitro* transcription can then be performed to synthesize the protein product and the ORF can be estimated by sequencing its C-terminus.

If this short form *alr* is translated in to protein using the same start codon as the long form *alr*, an early stop codon will be found at the 5' end of exon 3. As a result, the short form alr will only encode the N-terminal 89 amino acids of long form Alr, lacking most of the Erv1/Alr domain (Fig. 4.1C).

A

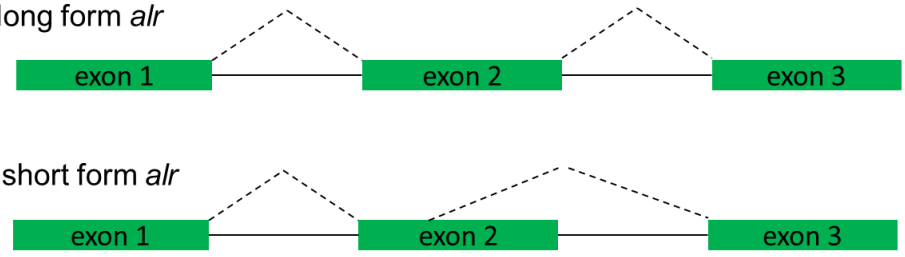

B

ctcctacataacaacATGGCAGCTGCACACGGGTCGTCTCCACATAGCAGCGCGGGTATGGAGG
GTTTCCCGTTCCCCGTGGCTGGCAAACCACCCGAGGACAGTACGAGTAATGACCAGACCAC
TACCGGAGAGACGAAAAAGAAACCTTGCCGAGCTTGTACGGATTTTAAGTCATGGATGAAG
TTACAGAAACAGGCGTCCTCAGCCTCGGTGCAGgt.....(intron1).....agGAGAGCAGGC
CGGTGGAGGAGCTGAAGCCTGTTGAATGTCCGCTGGACCGCGAGGAGCTGGGTAGGAGC
TCGTGGTCTTTTCTTCACACTATGGCTGCGTATTATCCAGATGCACCGAGCACAGAACAGCA
GCTCGAGATGACGCAGTTCATCAACCTTTTCTCTAAGGTTTTCCCATGTGATGAATGCGCAG
AAGACCTGAGAACAAGgt.....(intron2).....agATTGAAAACTAATAGACCAGATGCAGG
CAGCCGGCACAAGCTGTCACAGTGGCTGTGTCGCCTCCATAATGACATCAACATCCGGTTG
GGCAAGCCGGAGTTCGACTGCAGCAGGGTGGATGAGCGATGGAGAGACGGCTGGAAGG
ACGGATCTTGTGACTGAaacctccgacactgtcatgaacacgagtgaaatgctttcacatgctgattctgtggac
ctggtatttctgatgcagtgagtgcaggctgaattgccaatcaggaatcagacatatgttgacatcgcactttatacttgtt
ctaattgatgtaatgatttagcagtatagaaatgtctatgttgtgcttttaatcaagagtacggtatggtgtgaacaccttg
tttttggattgtggagctctcaagtggaagtaaat

C

Existing long form Alr protein (191 a.a)

MAAAHGSSPHSSAGMEGFPFPVAGKPPEDSTSNDQTTTGETKKKPCRACTDFKSWMKLQK
QASSASVQESRPVEELKPVECPLDREELGRSSWSFLHTMAAYYPDAPSTEQQLEMTQFINLFSK
VFPCDECAEDLRTRLKTNRPDAGSRHKLSQWLCRLHNDINIRLGKPEFDCSRVDERWRDGWK
DGSCD

Putative short form Alr (translation starting from the first ATG) 89 a.a

MAAAHGSSPHSSAGMEGFPFPVAGKPPEDSTSNDQTTTGETKKKPCRACTDFKSWMKLQK
QASSASVQESRPVEELKPVECPLDREELD

Fig. 4.1 Alternative splicing of zebrafish *alr* pre-mRNA

A. Schematic illustration of alternative splicing of *alr* pre-mRNA, which generates the long form *alr* and short form *alr* respectively. Dash lines show the regions to be spliced. B. Genomic sequence of zebrafish *alr* was shown. Capital letters are the coding sequence in long form *alr*. Blue region is spliced into intron and is deleted in the short form *alr* transcript. The underlined ATG represents the start of the conventional short form Alr in mammals. C. Protein sequence of existing long form Alr and the putative short form Alr from the alternatively-transcripted *alr* if the first ATG is the start.

4.4 Alr and hepatocyte apoptosis regulation

Knockdown of ALR in rat primary hepatocytes leads to cell apoptosis through Cytochrome c release and Caspase 3 activation (Thirunavukkarasu et al., 2008), suggesting that ALR is an intracellular survival factor for hepatocytes. Contrary to this, our results demonstrated that knockdown of *alr* inhibited hepatocyte proliferation but did not increase apoptosis (Fig. 3.17). The different effect of *alr* knockdown on apoptosis might be attributed to the very low level of apoptosis and the presence of many proliferation promoters during embryonic liver formation, while the adult hepatocytes are more susceptible to apoptosis. The minimum apoptosis level during zebrafish liver development was also shown by others (Chen et al., 2005b).

What is worth noting is that the anti-apoptotic function of ALR was mainly reported during pathological rather than physiological conditions of mammalian liver. Those pathological conditions include exposing to apoptosis inducers (Ilowski et al., 2011), liver regeneration after partial hepatectomy (Polimeno et al., 2011), cancer (hepatoma) (Cao et al., 2009), etc. So it is highly possible that zebrafish Alr has no effect on hepatocyte survival in normal liver, instead protects liver from stress and disease. An

indirect evidence for this is that expression of zebrafish *alr* increased in response to ethanol treatment (Fig. 3.8). Ethanol is a hepatocyte apoptosis inducer, and it has been shown that human ALR can significantly decrease apoptosis of primary hepatocytes treated with ethanol (Ilowski et al., 2011).

Whether the cell survival function is tissue-specific is in doubt. Ilowski et al. (2011) claimed that the anti-apoptotic effect of ALR was in a liver specific manner. There are reports showing that the anti-apoptosis function of ALR is not restricted to hepatocytes. Studies have demonstrated its protective effect on kidney after liver transplantation (Chen et al., 2011) and neuroblastoma cells which were subjected to hydrogen peroxide induced apoptosis (Polimeno et al., 2009), when both cell types were under stress conditions. On one hand, the protective effect on liver and kidney suggests that ALR could be a promising hepatoprotective factor and co-treatment factor candidate in clinics; on the other hand, the protective role of ALR on hepatoma cells from irradiation and oxidative stress renders it a possible target of cancer therapy.

4.5 Subcellular localization of Alr

Expression of Alr-V5 and Alr-EGFP fusion proteins in cultured human cells and zebrafish liver cells shows that Alr is localized in both the cytosol and mitochondria, but not in the nucleus or the culture medium (Fig. 3.25-3.31). Mitochondrial proteins that are encoded by the nucleus DNA are usually synthesized as cytosolic precursors

with either N-terminal or internal mitochondrial targeting sequence and get imported into mitochondria through Translocase of the Outer Membrane (TOM) after recognized by channel-linked receptors on mitochondrial outer membrane (reviewed by Schmidt et al., 2010). While sequence analysis using tools from ExPASy proteomics server could not found any mitochondrial localization signal on any of the Erv1/Alr protein family members including yeast Erv1, human and zebrafish Alr, how Alr localizes into mitochondria is unknown. Moreover, the localization of Alr into mitochondria is neither species specific nor cell type specific as shown in human HepG2 and HEK293T cells as well as ZFL cells (Fig. 3.30 and Fig. 3.31). This implicates that a common and non-typical way of entering mitochondria was utilized by Alr.

The two isoforms of human ALR have been reported to be localized differently. While the short from ALR (125 amino acids) is mainly localized in the nucleus, the long form ALR (205 amino acids) is localized in the intermembrane space of mitochondria and the cytosol (Gatzidou et al., 2006; Hofhaus et al., 1999; Lange et al., 2001; Li et al., 2002b). The intracellular localization of zebrafish Alr is similar to the long form of human ALR. It is believed that the intracellular ALR is present in many cell types and carries out fundamental cellular functions such as promoting disulfide bond formation in proteins, Fe-S cluster formation and cellular Fe homeostasis (Gatzidou et al., 2006; Lange et al., 2001). Functional important of ALR localizing in the mitochondria has be extensively studied in yeast. The yeast Erv1 forms a disulfide relay system with

Mia40 in the intermembrane space of mitochondria, thus catalyse the import of cysteine-rich proteins into mitochondria by oxidative folding of those proteins (Mesecke et al., 2005; Tokatlidis, 2005). Mia40 oxidize the imported protein to facilitate their proper folding; Erv1 then oxidize Mia40 to recycle it using its sulfhydryl oxidase activity. Mia40 is also proved a substrate of human long form ALR (Banci et al., 2011; Daithankar et al., 2009). The disulfide relay system is connected to the respiratory chain. The electron of Erv1 will be passed to cytochrome c, which will then be oxidized by cytochrome c oxidase; the electron will finally be passed to oxygen (Allen et al., 2005; Bihlmaier et al., 2007). Cytochrome c is also demonstrated to be the electron receptor of human ALR (Farrell and Thorpe, 2005). Whether the zebrafish Alr can also oxidize Mia40 in mitochondria and whether it will be oxidized by cytochrome c to pass the electrons to respiratory chain need to be further investigated.

Although we did not detect any secreted zebrafish Alr-V5 or Alr-EGFP fusion protein in the media of cultured cells, it is probable that Alr can be released by hepatocyte under specific environmental conditions such as after liver injury. Notably, the secretion of the mammalian ALR into blood circulation is only sharply up-regulated during liver regeneration after partial hepatectomy with concomitant decrease in hepatic ALR protein (Gandhi et al., 1999). How ALR was secreted into blood circulation is unknown, because both long and short forms ALR contain no signal peptide at the N-terminal. Moreover, the composition of the secreted ALR that

stimulate hepatocyte proliferation is still not very clear up to now (Gandhi et al., 1999). Incidentally, although low level ALR was detected in medium of primary rat hepatocytes by ELISA (Gandhi et al., 1999), no secreted ALR could be detected when a rat ALR cDNA expression plasmid was transfected into cultured COS cells by an *in vivo* functional assay (Hagiya et al., 1994). Hence, different detection methods, different cell types used and different environmental conditions may generate varied results in terms of ALR secretion. Therefore, it is still highly probable that zebrafish Alr can be secreted during hepatogenesis.

4.6 Zebrafish Alr as a sulfhydryl oxidase in liver development

What is unique about ALR is that this protein is a "cytozyme" (cytokine and enzyme), not only a hepatic cytokine but also a sulfhydryl oxidase carrying out fundamental redox reactions in cells. The sulfhydryl oxidase activity of the yeast ALR ortholog, ERV1, is essential for the survival of this single cell organism (Lee et al., 2000; Lisowsky, 1992). Recombinant zebrafish Alr protein expressed from *E.coli* also binds FAD and has sulfhydryl oxidase activity (Fig. 3.34 and Fig. 3.35), presenting similar enzymatic characteristics as mammalian ALRs/yeast ERV1.

Through overexpression and morphant-rescue experiments, we demonstrated that the sulfhydryl oxidase activity may not be essential for Alr's function in promoting liver outgrowth during embryonic development. Overexpression of the enzymatically-inactive mutant Alr^{C131S} also promoted liver growth and rescued the

small-liver phenotype in *alr* morphants (Fig. 3.36 and Fig. 3.37). Nevertheless, overexpression of Alr^{C131S} promoted liver growth less efficiently comparing to the wild-type Alr (Fig. 3.36 and Fig. 3.37). Furthermore, although Alr^{C131S} effectively rescued the *alr* morphants, the average liver size of Alr^{C131S} rescued embryos is smaller than that of the wild-type Alr rescued embryos. This suggests that zebrafish *alr* most likely promotes liver growth through both enzyme-dependent as well as enzyme-independent signaling pathways.

Both enzyme-dependent and -independent signaling pathways of ALR have been illustrated in cultured human hepatoma cells. Extracellular ALR can activate the mitogen-activated protein kinase (MAPK) cascade through its cell surface receptor independent of its sulfhydryl oxidase activity (Chen et al., 2003; Li et al., 2000). On the other hand, the ability of intracellular ALR to potentiate the activator protein-1 (AP-1) pathway through JAB1 is dependent on its enzymatic function (Chen et al., 2003). Alr may use both the enzyme-dependent (through AP-1 pathway) and enzyme-independent signaling pathways (through MAPK pathway) to promote liver growth during hepatogenesis.

4.7 The artificial miRNA-mediated, inducible and tissue-specific knockdown system

The attempt to use authentic miRNA backbone expressing artificial miRNA was pioneered by Zeng and Cullen. They found several features about the human miR-30

that is basic to develop miR-30 based artificial miRNA: the 80 nt stem-loop structure of the pre-mir-30 can be inserted at the intron of another transcript controlled by different Pol II promoters, to produce mature miR-30; the stem region of the pre-mir-30 can be replaced by any double-stranded sequence of similar length and express a 22 nt artificial miRNA; tandem repeats of the miR-30 expressing cassette can be expressed from the polycistronic transcipt (Zeng et al., 2005; Zeng and Cullen, 2003; Zeng et al., 2002). Chung et al. (2006) showed that the mammalian miR-155 can also be engineered similarly as miR-30. At the same time, there are many other studies reporting the using of vectors for RNAi in mammals (reviewed by Lan et al., 2011). Vectors with pol II or pol III driven shRNA or artificial miRNAs have become commercially available for mammals.

Compared to the great advance made in mammals, development of vector based RNAi in zebrafish is left behind. Dong et al. (2009) first reported the use of intronic artificial miRNA for tissues specific knockdown of gene expression in transgenic zebrafish. Their system is a very useful tool for controlled knockdown in zebrafish. However there is no spatial regulation in this system. In our study, we improved this system by placing the intronic artificial miRNA and the Δactin-EGFP reporter under the control of mifepristone-inducible operator/promoter. Our artificial miRNA based, inducible and tissue-specific knockdown system enables the precise regulation of knockdown.

We showed that the designed miR-alr can decrease alr expression by 40%-60%, which

is not very potent. The efficiency of knockdown could be increased by placing multiple tandem copies of the shRNA structure in the pri-mir-30 flanking sequence, to increase the expression level of artificial miRNA (Dong et al., 2009). However, expressing too much artificial miRNA might also cause problem. The animal miRNAs are known to bind to their targets with minimal complementary sequence and are predicted to have large number of targets (Bartel, 2004). The artificial miRNA might also have multiple off-targets and trigger non-specific phenotype when expressed at very high level. Moreover, it is difficult to prove the off-target effect. So the critical step of this knockdown system is to select an effective artificial miRNA that targets the region that is sequence specific.

The transgenic fish were established by *Ac/Ds* transposon-mediated gene insertion. The use of *Ac/Ds* transposable element indeed yields very high germline integration rate, up to 80% of the F0 fish were able to transmit the transgene into the progeny. But, the number of transgene insertions is highly variable even in the F1 fish from a single F0 fish, ranging from 1 to 5 insertion sites (Fig. 3.45). Consequently, the expression level of the transgene (evaluated by the green fluorescence intensity) is highly variable and the knockdown efficiency will vary among different fish. Thus we choose to maintain the F1 fish with single insertion of the transgene, to get a pool of offsprings with same level of knockdown efficiency when induced. However, a problem of using the single-insertion fish is that the transgene expression level is low, as the EGFP fluorescent signal is weak. For multiple-insertion fish, the transgene

expression is much stronger. However, problems with using the multiple-insertion fish are their genetic variation and difficulty to maintain the high insertion numbers because of segregation of the transgenes during meiosis.

CHAPTER 5. CONCLUSIONS AND FUTURE WORKS

5.1 Conclusions

In the first part of this study, we demonstrated for the first time that *alr* plays a critical role in liver growth during zebrafish hepatogenesis, using several experimental evidences. We showed that *alr* is expressed in the developing liver at a high level throughout zebrafish liver organogenesis, and the high expression of *alr* will gradually decrease to a very low level in adult liver. Knockdown of *alr* by morpholino antisense oligonucleotide does not affect hepatoblast determination from the anterior endoderm, but inhibits hepatocyte differentiation and suppresses liver outgrowth, generating a small-liver phenotype. We further demonstrated that *alr* promotes liver growth by stimulating hepatocyte proliferation in both liver budding stage and liver outgrowth stage, rather than inhibiting apoptosis. Biochemical study showed that zebrafish Alr naturally exist in dimer form and is also a flavin-linked sulfhydryl oxidase. The conserved CxxC motif in the Erv1/Alr domain is essential for its sulfhydryl oxidase and mutation of the cysteines will abolish it enzymatic activity. By combining biochemistry study with developmental biology study, we show that zebrafish *alr* may use both enzyme-dependent and enzyme-independent signaling pathways to promote liver growth during hepatogenesis. We also showed that neither the long form nor short form human ALR can functional complement zebrafish Alr, possibly due to the highly divergent N-terminus of Alr proteins in different species. Several potential interacting protein of zebrafish Alr was identified in the

mitochondria, including the G elongation factor mitochondrial 2 (Gfm2), Aspartyl-tRNA synthetase (Dars) and Eukaryotic translation elongation factor 1 alpha 1 like 1 (Eeflα1l1), suggesting that zebrafish Alr might have basic function for protein synthesis.

In the second part of this study, we developed an artificial miRNA based, inducible tissue-specific knockdown system in zebrafish, using *alr* as the proof-of-concept target. We successfully expressed the intronic artificial miRNAs together with the Δactin-EGFP reporter, under the control of mifepristone-inducible LexPR system. The artificial miRNA miR-alr targets the 3'UTR of zebrafish *alr* and mediates potent knockdown of *alr* at mRNA level in the liver after mifepristone induction, while the mismatch control miR-alr^{mis} does not affect *alr* level. Liver specific knockdown of *alr* by artificial miRNA results in liver growth defects in both larval and juvenile stages, suggesting that *alr* is required for liver growth of all stages which is consistent with its expression at those stages. We also showed that expression of *alr* in late larval and juvenile liver is essential for fish survival.

5.2 Future perspectives

5.2.1 Investigation of downstream pathways of Alr in embryonic liver growth

The zebrafish Alr, a flavoprotein with sulfhydryl oxidase activity in the cytosol and mitochondria but not the nucleus, is more likely function in embryonic development through protein-protein interactions rather than as a gene expression regulator.

Although there are studies reported that extracellular ALR induced c-myc expression in primary human hepatocytes (Dayoub et al., 2006) and intracellular ALR downregulated Dynamic-related protein 1 (Drp-1) when overexpressed (Todd et al., 2010a; Todd et al., 2010b), these regulations of gene expression were most likely indirect regulations. ALR needs to interact with other proteins to eventually affect gene expression. Thus, knowing the interacting partners and protein substrates of Alr is crucial for uncovering its mechanism of liver growth promotion.

We have performed some preliminary experiments searching for the interacting proteins of zebrafish Alr in liver cells. Pull-down assay identified G elongation factor mitochondrial 2 (Gfm2), Aspartyl-tRNA synthetase (Dars) and Eukaryotic translation elongation factor 1 alpha 1 like 1 (Eefla1l1) as the possible interacting proteins of Alr in zebrafish liver cell mitochondria lysate. Incidentally, elongation factor 1 alpha (the human ortholog of zebrafish Eefla1l1) was also found interacting with human ALR in a yeast-two hybrid assay (Cheng et al., 2003).

But Mia40 was not identified in our pull-down assay, which is a conserved substrate of Erv1/ALR in mitochondria in both yeast and human (Farrell and Thorpe, 2005; Mesecke et al., 2005). Nor is cytochrome c, although both yeast Erv1 and human ALR use Cytochrome c as the electron receptor via direct interaction (Bihlmaier et al., 2007; Farrell and Thorpe, 2005). It is possible that we have missed Mia40 and Cytochrome c in the above assays, as they are proteins of very small size (15 kD for Mia40, 10 kD for Cytochrome c). A more probable reason is that the interactions between enzyme

and substrate are usually transient and unstable, so they were dissociated from Alr after stringent washing conditions. Future investigations could be carried out using chemical cross-linkers to capture the transient interacting proteins and substrates of Alr, to check whether Mia40 and cytochrome c are also conserved substrates of zebrafish Alr and whether there are additional interacting protein or substrates.

Of the interacting proteins identified, we hypothesize that Gfm1 is more possibly related to the function of Alr in liver development. Studies have shown that patients with mutations in the GFM1 showed fatal hepatopathy (Antonicka et al., 2006). Liver was the most severely affected tissue compared to other tissue phenotypes, with significant decrease of respiratory chain complex I and IV. It is possible that loss-of-function of Gfm2 will have the similar phenotype, as Gfm1 and Gfm2 are both involved in mitochondrial translation. The spatial and temporal expression of Gfm2 needs to be examined, to see whether it is expressed in liver. The hypothesized significance of Alr interacting with Gfm2 is that: Alr might be involved in the proper folding of Gfm2 imported into mitochondria; knockdown of Alr affects the proper folding and importing of Gfm2, thus leads to mitochondria translation defect and liver growth defect. To test the hypothesis, the interaction of Alr and Gfm2 needs to be confirmed by co-immunoprecipitation (co-IP). *In vitro* assay can be performed to determine whether Alr can oxidize Gfm2 and is involved in its oxidative folding. The mitochondrial proteins translation defects need to be examined after knockdown of *alr*.

5.2.2 Using of the stable knockdown transgenic fish to study the function of Alr in zebrafish liver regeneration and liver diseases

Zebrafish has become an important vertebrate model for both liver development and liver diseases (Matthews, 2009). With the artificial miRNA based, inducible and tissue-specific knockdown system we established, lose-of-function study in adult zebrafish has been made easier. For example, by inducing the liver-specific expression of artificial miRNA to knockdown candidate genes in adult zebrafish liver, the function of those candidate genes during liver disease and liver regeneration can be examined.

The mammalian ALR has been shown to have important function during liver regeneration by stimulating hepatocyte proliferation (reviewed by Gatzidou et al., 2006). Beyond its well-established function in liver regeneration, there are evidences showing that expression level of mammalian ALR is increased during liver cirrhosis and in liver carcinoma, suggesting its possible involvement in liver diseases and cancer (Thasler et al., 2005; Yu et al., 2010). ALR also protects liver from different kinds of injury induced by ethanol, hydrogen peroxide etc. (Ilowski et al., 2011; Polimeno et al., 2009). ALR is found to be involved in maintaining hepatoma cell viability and resistance to radiation-induced oxidative stress (Cao et al., 2009), suggesting that it can be a potential target for liver cancer therapy.

Whether the zebrafish Alr also have any function during liver regeneration, chemical induced liver injury, liver disease (such as hepatic steatosis, cirrhosis) or liver cancer

is unknown and can be investigated by making use of the stable miR-alr transgenic fish. Partial hepatectomy is a method frequently used in mice/rat to study liver regeneration. This technique has been adopted for use in adult zebrafish (Sadler et al., 2007). To characterize the effect of *alr* knockdown on liver regeneration, adult *Tg(lfabp:LPR-LOP:mir-alr-Δactin-EGFP)* fish can be pre-treated with mifepristone to induce miR-alr expression and *alr* knockdown. Subsequently, partial hepatectomy can be performed by removing the ventral lobe of liver. The role of Alr in adult liver regeneration can then be examined. Acute injury of liver, hepatic steatosis and cirrhosis can be induced by chemical treatment in *Tg(lfabp:LPR-LOP:mir-alr-Δactin-EGFP)* and the role of Alr in these diseases can be evaluated.

REFERENCES

Allen, S., Balabanidou, V., Sideris, D.P., Lisowsky, T., Tokatlidis, K., 2005. Erv1 mediates the Mia40-dependent protein import pathway and provides a functional link to the respiratory chain by shuttling electrons to cytochrome c. J Mol Biol 353, 937-944.

Amiot, C., Musard, J.F., Hadjiyiassemis, M., Jouvenot, M., Fellmann, D., Risold, P.Y., Adami, P., 2004. Expression of the secreted FAD-dependent sulfydryl oxidase (QSOX) in the guinea pig central nervous system. Molecular Brain Research 125, 13-21.

Amsterdam, A., Burgess, S., Golling, G., Chen, W., Sun, Z., Townsend, K., Farrington, S., Haldi, M., Hopkins, N., 1999. A large-scale insertional mutagenesis screen in zebrafish. Genes Dev 13, 2713-2724.

Amsterdam, A., Nissen, R.M., Sun, Z., Swindell, E.C., Farrington, S., Hopkins, N., 2004. Identification of 315 genes essential for early zebrafish development. Proceedings of the National Academy of Sciences of the United States of America 101, 12792-12797.

Ang, S.K., Lu, H., 2009. Deciphering structural and functional roles of individual disulfide bonds of the mitochondrial sulfhydryl oxidase Erv1p. The Journal of biological chemistry 284, 28754-28761.

Antonicka, H., Sasarman, F., Kennaway, N.G., Shoubridge, E.A., 2006. The molecular basis for tissue specificity of the oxidative phosphorylation deficiencies in patients with mutations in the mitochondrial translation factor EFG1. Human molecular genetics 15, 1835-1846.

Argast, G.M., Campbell, J.S., Brooling, J.T., Fausto, N., 2004. Epidermal growth factor receptor transactivation mediates tumor necrosis factor-induced hepatocyte replication. Journal of Biological Chemistry 279, 34530-34536.

Banci, L., Bertini, I., Calderone, V., Cefaro, C., Ciofi-Baffoni, S., Gallo, A., Kallergi, E., Lionaki, E., Pozidis, C., Tokatlidis, K., 2011. Molecular recognition and substrate mimicry drive the electron-transfer process between MIA40 and ALR. Proceedings of the National Academy of Sciences of the United States of America 108, 4811-4816.

Barbazuk, W.B., Korf, I., Kadavi, C., Heyen, J., Tate, S., Wun, E., Bedell, J.A., McPherson, J.D., Johnson, S.L., 2000. The syntenic relationship of the zebrafish and human genomes. Genome Res 10, 1351-1358.

Bartel, D.P., 2004. MicroRNAs: Genomics, Biogenesis, Mechanism, and Function. Cell 116, 281-297.

Baskerville, S., Bartel, D.P., 2005. Microarray profiling of microRNAs reveals frequent coexpression with neighboring miRNAs and host genes. RNA 11, 241-247.

Benayoun, B., Esnard-F ève, A., Castella, S., Courty, Y., Esnard, F., 2001. Rat seminal vesicle FAD-dependent sulfhydryl oxidase. Biochemical characterization and molecular cloning of a member of the new sulfhydryl oxidase/quiescin Q6 gene family. Journal of Biological Chemistry 276, 13830-13837.

Bihlmaier, K., Mesecke, N., Terziyska, N., Bien, M., Hell, K., Herrmann, J.M., 2007. The disulfide relay system of mitochondria is connected to the respiratory chain. J Cell Biol 179, 389-395.

Bort, R., Signore, M., Tremblay, K., Barbera, J.P.M., Zaret, K.S., 2006. Hex homeobox gene controls the transition of the endoderm to a pseudostratified, cell emergent epithelium for liver bud development. Developmental biology 290, 44-56.

Cai, X., Hagedorn, C.H., Cullen, B.R., 2004. Human microRNAs are processed from capped, polyadenylated transcripts that can also function as mRNAs. RNA 10, 1957-1966.

Cao, Y., Fu, Y.L., Yu, M., Yue, P.B., Ge, C.H., Xu, W.X., Zhan, Y.Q., Li, C.Y., Li, W., Wang, X.H., Wang, Z.D., Li, Y.H., Yang, X.M., 2009. Human augmenter of liver regeneration is important for hepatoma cell viability and resistance to radiation-induced oxidative stress. Free Radic Biol Med 47, 1057-1066.

Chang, C., Hu, M., Zhu, Z., Lo, L.J., Chen, J., Peng, J., 2011. liver-enriched gene 1a and 1b Encode Novel Secretory Proteins Essential for Normal Liver Development in Zebrafish. PLoS One 6, e22910.

Chen, C., Ridzon, D.A., Broomer, A.J., Zhou, Z., Lee, D.H., Nguyen, J.T., Barbisin, M., Xu, N.L., Mahuvakar, V.R., Andersen, M.R., Lao, K.Q., Livak, K.J., Guegler, K.J., 2005a. Real-time quantification of microRNAs by stem-loop RT-PCR. Nucleic Acids Research 33, e179.

Chen, J., Ruan, H., Ng, S.M., Gao, C., Soo, H.M., Wu, W., Zhang, Z., Wen, Z., Lane, D.P., Peng, J., 2005b. Loss of function of def selectively up-regulates Delta113p53 expression to arrest expansion growth of digestive organs in zebrafish. Genes Dev 19, 2900-2911.

Chen, X., Li, Y., Wei, K., Li, L., Liu, W., Zhu, Y., Qiu, Z., He, F., 2003. The potentiation role of hepatopoietin on activator protein-1 is dependent on its sulfhydryl oxidase activity. The Journal of biological chemistry 278, 49022-49030.

Chen, Y., Luo, F., Luo, S., Wu, Z., Zhou, J., 2011. The augmenter of liver regeneration protects the kidneys after orthotopic liver transplantation possibly by upregulating HIF-1alpha and O(2)-sensitive K (+) channels. Surg Today 41, 382-389.

Chendrimada, T.P., Gregory, R.I., Kumaraswamy, E., Norman, J., Cooch, N., Nishikura, K., Shiekhattar, R., 2005. TRBP recruits the Dicer complex to Ago2 for microRNA processing and gene silencing. Nature 436, 740-744.

Cheng, J., Wang, L., Li, K., Lu, Y.Y., Wang, G., Liu, Y., Zhong, Y.W., Duan, H.J., Hong, Y., Li, L., Zhang, L.X., Chen, J.M., 2003. Screening of augmenter of liver regeneration-binding proteins by yeast-two hybrid technique. Hepatobiliary Pancreat Dis Int 2, 81-84.

Cheng, W., Guo, L., Zhang, Z., Soo, H.M., Wen, C., Wu, W., Peng, J., 2006. HNF factors form a network to regulate liver-enriched genes in zebrafish. Developmental biology 294, 482-496.

Cheung, C.Y., Webb, S.E., Meng, A., Miller, A.L., 2006. Transient expression of apoaequorin in zebrafish embryos: extending the ability to image calcium transients during later stages of development. The International journal of developmental biology 50, 561-569.

Chu, J., Sadler, K.C., 2009. New school in liver development: lessons from zebrafish. Hepatology (Baltimore, Md 50, 1656-1663.

Chung, K.H., Hart, C.C., Al-Bassam, S., Avery, A., Taylor, J., Patel, P.D., Vojtek, A.B., Turner, D.L., 2006. Polycistronic RNA polymerase II expression vectors for RNA interference based on BIC/miR-155. Nucleic Acids Research 34, e53.

Connolly, K.M., Bogdanffy, M.S., 1993. Evaluation of proliferating cell nuclear antigen (PCNA) as an endogenous marker of cell proliferation in rat liver: a dual-stain comparison with 5-bromo-2'-deoxyuridine. J Histochem Cytochem 41, 1-6.

Coppock, D.L., Cina-Poppe, D., Gilleran, S., 1998. The Quiescin Q6 gene (QSCN6) is a fusion of two ancient gene families: Thioredoxin and ERV1. Genomics 54, 460-468.

Coppock, D.L., Thorpe, C., 2006. Multidomain flavin-dependent sulfhydryl oxidases. Antioxidants and Redox Signaling 8, 300-311.

Curado, S., Ober, E.A., Walsh, S., Cortes-Hernandez, P., Verkade, H., Koehler, C.M., Stainier, D.Y.R., 2010. The mitochondrial import gene tomm22 is specifically required for hepatocyte survival and provides a liver regeneration model. DMM Disease Models and Mechanisms 3, 486-495.

Daithankar, V.N., Farrell, S.R., Thorpe, C., 2009. Augmenter of liver regeneration: substrate specificity of a flavin-dependent oxidoreductase from the mitochondrial intermembrane space. Biochemistry 48, 4828-4837.

Daithankar, V.N., Schaefer, S.A., Dong, M., Bahnson, B.J., Thorpe, C., 2010. Structure of the human sulfhydryl oxidase augmenter of liver regeneration and characterization of a human mutation causing an autosomal recessive myopathy. Biochemistry 49, 6737-6745.

Das, K.C., 2001. c-Jun NH2-terminal kinase-mediated redox-dependent degradation of IkappaB: role of thioredoxin in NF-kappaB activation. The Journal of biological chemistry 276, 4662-4670.

Dayoub, R., Thasler, W.E., Bosserhoff, A.K., Singer, T., Jauch, K.W., Schlitt, H.J., Weiss, T.S., 2006. Regulation of polyamine synthesis in human hepatocytes by hepatotrophic factor augmenter of liver regeneration. Biochem Biophys Res Commun 345, 181-187.

Di Fonzo, A., Ronchi, D., Lodi, T., Fassone, E., Tigano, M., Lamperti, C., Corti, S., Bordoni, A., Fortunato, F., Nizzardo, M., Napoli, L., Donadoni, C., Salani, S., Saladino, F., Moggio, M., Bresolin, N., Ferrero, I., Comi, G.P., 2009. The mitochondrial disulfide relay system protein GFER is mutated in autosomal-recessive myopathy with cataract and combined respiratory-chain deficiency. Am J Hum Genet 84, 594-604.

Diederichs, S., Haber, D.A., 2007. Dual Role for Argonautes in MicroRNA Processing and Posttranscriptional Regulation of MicroRNA Expression. Cell 131, 1097-1108.

Diehl, A.M., Shi Qi, Y., Yin, M., Hui Zhi, L., Nelson, S., Bagby, G., 1995. Tumor necrosis factor-alpha modulates CCAAT/enhancer binding proteins-DNA binding activities and promotes hepatocyte-specific gene expression during liver regeneration. Hepatology (Baltimore, Md 22, 252-261.

Dong, M., Fu, Y.F., Du, T.T., Jing, C.B., Fu, C.T., Chen, Y., Jin, Y., Deng, M., Liu, T.X., 2009. Heritable and lineage-specific gene knockdown in zebrafish embryo. PLoS One 4, e6125.

Dovey, M., Patton, E.E., Bowman, T., North, T., Goessling, W., Zhou, Y., Zon, L.I., 2009. Topoisomerase IIα is required for embryonic development and liver regeneration in zebrafish. Molecular and Cellular Biology 29, 3746-3753.

Doyon, Y., McCammon, J.M., Miller, J.C., Faraji, F., Ngo, C., Katibah, G.E., Amora, R., Hocking, T.D., Zhang, L., Rebar, E.J., Gregory, P.D., Urnov, F.D., Amacher, S.L., 2008. Heritable targeted gene disruption in zebrafish using designed zinc-finger nucleases. Nat Biotechnol 26, 702-708.

Du, T., Zamore, P.D., 2005. microPrimer: The biogenesis and function of microRNA. Development 132, 4645-4652.

Duncan, S.A., 2003. Mechanisms controlling early development of the liver. Mechanisms of development 120, 19-33.

Eisen, J.S., Smith, J.C., 2008. Controlling morpholino experiments: don't stop making antisense. Development 135, 1735-1743.

Elbashir, S.M., Harborth, J., Lendeckel, W., Yalcin, A., Weber, K., Tuschl, T., 2001. Duplexes of 21-nucleotide RNAs mediate RNA interference in cultured mammalian cells. Nature 411, 494-498.

Emelyanov, A., Gao, Y., Naqvi, N.I., Parinov, S., 2006. Trans-kingdom transposition of the maize dissociation element. Genetics 174, 1095-1104.

Emelyanov, A., Parinov, S., 2008. Mifepristone-inducible LexPR system to drive and control gene expression in transgenic zebrafish. Developmental biology 320, 113-121.

Farooq, M., Sulochana, K.N., Pan, X., To, J., Sheng, D., Gong, Z., Ge, R., 2008. Histone deacetylase 3 (hdac3) is specifically required for liver development in zebrafish. Developmental biology 317, 336-353.

Farrell, S.R., Thorpe, C., 2005. Augmenter of liver regeneration: a flavin-dependent sulfhydryl oxidase with cytochrome c reductase activity. Biochemistry 44, 1532-1541.

Farver, O., Vitu, E., Wherland, S., Fass, D., Pecht, I., 2009. Electron transfer reactivity of the Arabidopsis thaliana sulfhydryl oxidase AtErv1. The Journal of biological

chemistry 284, 2098-2105.

Fass, D., 2008. The Erv family of sulfhydryl oxidases. Biochimica et Biophysica Acta - Molecular Cell Research 1783, 557-566.

Field, H.A., Ober, E.A., Roeser, T., Stainier, D.Y., 2003. Formation of the digestive system in zebrafish. I. Liver morphogenesis. Developmental biology 253, 279-290.

Francavilla, A., Hagiya, M., Porter, K.A., Polimeno, L., Ihara, I., Starzl, T.E., 1994. Augmenter of liver regeneration: its place in the universe of hepatic growth factors. Hepatology (Baltimore, Md 20, 747-757.

Gallucci, R.M., Simeonova, P.P., Toriumi, W., Luster, M.I., 2000. TNF-α regulates transforming growth factor-α expression in regenerating murine liver and isolated hepatocytes. Journal of Immunology 164, 872-878.

Gandhi, C.R., Kuddus, R., Subbotin, V.M., Prelich, J., Murase, N., Rao, A.S., Nalesnik, M.A., Watkins, S.C., DeLeo, A., Trucco, M., Starzl, T.E., 1999. A fresh look at augmenter of liver regeneration in rats. Hepatology (Baltimore, Md 29, 1435-1445.

Gatzidou, E., Kouraklis, G., Theocharis, S., 2006. Insights on augmenter of liver regeneration cloning and function. World J Gastroenterol 12, 4951-4958.

Ghosh, C., Zhou, Y.L., Collodi, P., 1994. Derivation and characterization of a zebrafish liver cell line. Cell Biology and Toxicology 10, 167-176.

Gregory, R.I., Yan, K.P., Amuthan, G., Chendrimada, T., Doratotaj, B., Cooch, N., Shiekhattar, R., 2004. The Microprocessor complex mediates the genesis of microRNAs. Nature 432, 235-240.

Gross, E., Sevier, C.S., Vala, A., Kaiser, C.A., Fass, D., 2002. A new FAD-binding fold and intersubunit disulfide shuttle in the thiol oxidase Erv2p. Nat Struct Biol 9, 61-67.

Gualdi, R., Bossard, P., Zheng, M., Hamada, Y., Coleman, J.R., Zaret, K.S., 1996. Hepatic specification of the gut endoderm in vitro: Cell signaling and transcriptional control. Genes and Development 10, 1670-1682.

Hagiya, M., Francavilla, A., Polimeno, L., Ihara, I., Sakai, H., Seki, T., Shimonishi, M., Porter, K.A., Starzl, T.E., 1994. Cloning and sequence analysis of the rat augmenter of liver regeneration (ALR) gene: expression of biologically active

recombinant ALR and demonstration of tissue distribution. Proceedings of the National Academy of Sciences of the United States of America 91, 8142-8146.

Han, J., Lee, Y., Yeom, K.H., Kim, Y.K., Jin, H., Kim, V.N., 2004. The Drosha-DGCR8 complex in primary microRNA processing. Genes and Development 18, 3016-3027.

Hayashi, H., Nagaki, M., Imose, M., Osawa, Y., Kimura, K., Takai, S., Imao, M., Naiki, T., Kato, T., Moriwaki, H., 2005. Normal liver regeneration and liver cell apoptosis after partial hepatectomy in tumor necrosis factor-α-deficient mice. Liver International 25, 162-170.

Hell, K., 2008. The Erv1-Mia40 disulfide relay system in the intermembrane space of mitochondria. Biochim Biophys Acta 1783, 601-609.

Hemmann, U., Gerhartz, C., Heesel, B., Sasse, J., Kurapkat, G., Grötzingerl, J., Wollmert, A., Zhong, Z., Darnell Jr, J.E., Graeve, L., Heinrich, P.C., Horn, F., 1996. Differential activation of acute phase response factor/Stat3 and Stat1 via the cytoplasmic domain of the interleukin 6 signal transducer gp130: II. Src homology SH2 domains define the specificity of stat factor activation. Journal of Biological Chemistry 271, 12999-13007.

Hendzel, M.J., Wei, Y., Mancini, M.A., Van Hooser, A., Ranalli, T., Brinkley, B.R., Bazett-Jones, D.P., Allis, C.D., 1997. Mitosis-specific phosphorylation of histone H3 initiates primarily within pericentromeric heterochromatin during G2 and spreads in an ordered fashion coincident with mitotic chromosome condensation. Chromosoma 106, 348-360.

Hinton, D.E., Couch, J.A., 1998. Architectural pattern, tissue and cellular morphology in livers of fishes: relationship to experimentally-induced neoplastic responses. EXS 86, 141-164.

Hofhaus, G., Stein, G., Polimeno, L., Francavilla, A., Lisowsky, T., 1999. Highly divergent amino termini of the homologous human ALR and yeast scERV1 gene products define species specific differences in cellular localization. Eur J Cell Biol 78, 349-356.

Houssaint, E., 1980. Differentiation of the mouse hepatic primordium. I. An analysis of tissue interactions in hepatocyte differentiation. Cell Differentiation 9, 269-279.

Huang, H., Ruan, H., Aw, M.Y., Hussain, A., Guo, L., Gao, C., Qian, F., Leung, T.,

Song, H., Kimelman, D., Wen, Z., Peng, J., 2008. Mypt1-mediated spatial positioning of Bmp2-producing cells is essential for liver organogenesis. Development 135, 3209-3218.

Huang, X., Nguyen, A.T., Li, Z., Emelyanov, A., Parinov, S., Gong, Z., 2011. One step forward: the use of transgenic zebrafish tumor model in drug screens. Birth defects research. Part C, Embryo today : reviews 93, 173-181.

Huggett, J., Dheda, K., Bustin, S., Zumla, A., 2005. Real-time RT-PCR normalisation; strategies and considerations. Genes and immunity 6, 279-284.

Huh, C.G., Factor, V.M., Sánchez, A., Uchida, K., Conner, E.A., Thorgeirsson, S.S., 2004. Hepatocyte growth factor/c-met signaling pathway is required for efficient liver regeneration and repair. Proceedings of the National Academy of Sciences of the United States of America 101, 4477-4482.

Ilowski, M., Kleespies, A., de Toni, E.N., Donabauer, B., Jauch, K.W., Hengstler, J.G., Thasler, W.E., 2011. Augmenter of liver regeneration (ALR) protects human hepatocytes against apoptosis. Biochem Biophys Res Commun 404, 148-152.

Jung, J., Zheng, M., Goldfarb, M., Zaret, K.S., 1999. Initiation of mammalian liver development from endoderm by fibroblast growth factors. Science 284, 1998-2003.

Köster, R.W., Fraser, S.E., 2001. Tracing transgene expression in living zebrafish embryos. Developmental biology 233, 329-346.

Kertesz, M., Iovino, N., Unnerstall, U., Gaul, U., Segal, E., 2007. The role of site accessibility in microRNA target recognition. Nat Genet 39, 1278-1284.

Ketting, R.F., Fischer, S.E.J., Bernstein, E., Sijen, T., Hannon, G.J., Plasterk, R.H.A., 2001. Dicer functions in RNA interference and in synthesis of small RNA involved in developmental timing in C. elegans. Genes and Development 15, 2654-2659.

Kim, V.N., 2005. MicroRNA biogenesis: Coordinated cropping and dicing. Nature Reviews Molecular Cell Biology 6, 376-385.

Kirillova, I., Chaisson, M., Fausto, N., 1999. Tumor necrosis factor induces DNA replication in hepatic cells through nuclear factor κB activation. Cell Growth and Differentiation 10, 819-828.

Klein, C., Mikutta, J., Krueger, J., Scholz, K., Brinkmann, J., Liu, D., Veerkamp, J.,

Siegel, D., Abdelilah-Seyfried, S., le Noble, F., 2011. Neuron navigator 3a regulates liver organogenesis during zebrafish embryogenesis. Development 138, 1935-1945.

Kondili, V.G., Tzirogiannis, K.N., Androutsos, C.D., Papadimas, G.K., Demonakou, M.D., Hereti, R.I., Manta, G.A., Kourentzi, K.T., Triantaphyllou, M.I., Panoutsopoulos, G.I., 2005. The hepatoprotective effect of hepatic stimulator substance (HSS) against liver regeneration arrest induced by acute ethanol intoxication. Dig Dis Sci 50, 297-307.

Korzh, S., Emelyanov, A., Korzh, V., 2001. Developmental analysis of ceruloplasmin gene and liver formation in zebrafish. Mechanisms of development 103, 137-139.

Korzh, S., Pan, X., Garcia-Lecea, M., Winata, C.L., Wohland, T., Korzh, V., Gong, Z., 2008. Requirement of vasculogenesis and blood circulation in late stages of liver growth in zebrafish. BMC Dev Biol 8, 84.

Kramer, M.F., 2011. Stem-loop RT-qPCR for miRNAs. Current protocols in molecular biology / edited by Frederick M. Ausubel ... [et al.] Chapter 15, Unit 15 10.

Krol, J., Loedige, I., Filipowicz, W., 2010. The widespread regulation of microRNA biogenesis, function and decay. Nature Reviews Genetics 11, 597-610.

LaBrecque, D.R., Pesch, L.A., 1975. Preparation and partial characterization of hepatic regenerative stimulator substance (SS) from rat liver. The Journal of physiology 248, 273-284.

Lai, J., Li, Y., Messing, J., Dooner, H.K., 2005. Gene movement by Helitron transposons contributes to the haplotype variability of maize. Proceedings of the National Academy of Sciences of the United States of America 102, 9068-9073.

Lan, C.C., Leong, I.U., Lai, D., Love, D.R., 2011. Disease modeling by gene targeting using microRNAs. Methods in cell biology 105, 419-436.

Lange, H., Lisowsky, T., Gerber, J., Muhlenhoff, U., Kispal, G., Lill, R., 2001. An essential function of the mitochondrial sulfhydryl oxidase Erv1p/ALR in the maturation of cytosolic Fe/S proteins. EMBO Rep 2, 715-720.

Lawson, N.D., Weinstein, B.M., 2002. In Vivo Imaging of Embryonic Vascular Development Using Transgenic Zebrafish. Developmental biology 248, 307-318.

Lee, C.S., Friedman, J.R., Fulmer, J.T., Kaestner, K.H., 2005. The initiation of liver

development is dependent on Foxa transcription factors. Nature 435, 944-947.

Lee, J., Hofhaus, G., Lisowsky, T., 2000. Erv1p from Saccharomyces cerevisiae is a FAD-linked sulfhydryl oxidase. FEBS Lett 477, 62-66.

Lee, R.C., Feinbaum, R.L., Ambros, V., 1993. The C. elegans heterochronic gene lin-4 encodes small RNAs with antisense complementarity to lin-14. Cell 75, 843-854.

Lee, Y., Kim, M., Han, J., Yeom, K.H., Lee, S., Baek, S.H., Kim, V.N., 2004. MicroRNA genes are transcribed by RNA polymerase II. EMBO Journal 23, 4051-4060.

Leong, I.U.S., Lan, C.C., Skinner, J.R., Shelling, A.N., Love, D.R., 2012. In vivo testing of MicroRNA-mediated gene knockdown in zebrafish. Journal of Biomedicine and Biotechnology 2012.

Levitan, A., Danon, A., Lisowsky, T., 2004. Unique features of plant mitochondrial sulfhydryl oxidase. The Journal of biological chemistry 279, 20002-20008.

Li, W., Liang, X., Kellendonk, C., Poli, V., Taub, R., 2002a. STAT3 contributes to the mitogenic response of hepatocytes during liver regeneration. Journal of Biological Chemistry 277, 28411-28417.

Li, W., Liang, X., Leu, J.I., Kovalovich, K., Ciliberto, G., Taub, R., 2001. Global changes in interleukin-6-dependent gene expression patterns in mouse livers after partial hepatectomy. Hepatology (Baltimore, Md 33, 1377-1386.

Li, Y., Li, M., Xing, G., Hu, Z., Wang, Q., Dong, C., Wei, H., Fan, G., Chen, J., Yang, X., Zhao, S., Chen, H., Guan, K., Wu, C., Zhang, C., He, F., 2000. Stimulation of the mitogen-activated protein kinase cascade and tyrosine phosphorylation of the epidermal growth factor receptor by hepatopoietin. The Journal of biological chemistry 275, 37443-37447.

Li, Y., Liu, W., Xing, G., Tian, C., Zhu, Y., He, F., 2005. Direct association of hepatopoietin with thioredoxin constitutes a redox signal transduction in activation of AP-1/NF-kappaB. Cellular signalling 17, 985-996.

Li, Y., Wei, K., Lu, C., Li, M., Xing, G., Wei, H., Wang, Q., Chen, J., Wu, C., Chen, H., Yang, S., He, F., 2002b. Identification of hepatopoietin dimerization, its interacting regions and alternative splicing of its transcription. Eur J Biochem 269, 3888-3893.

Li, Y.H., Chen, M.H., Gong, H.Y., Hu, S.Y., Li, Y.W., Lin, G.H., Lin, C.C., Liu, W., Wu, J.L., 2010. Progranulin A-mediated MET signaling is essential for liver morphogenesis in zebrafish. The Journal of biological chemistry 285, 41001-41009.

Liatsos, G.D., Mykoniatis, M.G., Margeli, A., Liakos, A.A., Theocharis, S.E., 2003. Effect of acute ethanol exposure on hepatic stimulator substance (HSS) levels during liver regeneration: protective function of HSS. Dig Dis Sci 48, 1929-1938.

Lisowsky, T., 1992. Dual function of a new nuclear gene for oxidative phosphorylation and vegetative growth in yeast. Mol Gen Genet 232, 58-64.

Lisowsky, T., Lee, J.E., Polimeno, L., Francavilla, A., Hofhaus, G., 2001. Mammalian augmenter of liver regeneration protein is a sulfhydryl oxidase. Dig Liver Dis 33, 173-180.

Lisowsky, T., Weinstat-Saslow, D.L., Barton, N., Reeders, S.T., Schneider, M.C., 1995. A new human gene located in the PKD1 region of chromosome 16 is a functional homologue to ERV1 of yeast. Genomics 29, 690-697.

Lorent, K., Yeo, S.Y., Oda, T., Chandrasekharappa, S., Chitnis, A., Matthews, R.P., Pack, M., 2004. Inhibition of Jagged-mediated Notch signaling disrupts zebrafish biliary development and generates multi-organ defects compatible with an Alagille syndrome phenocopy. Development 131, 5753-5766.

Lu, C., Li, Y., Zhao, Y., Xing, G., Tang, F., Wang, Q., Sun, Y., Wei, H., Yang, X., Wu, C., Chen, J., Guan, K.L., Zhang, C., Chen, H., He, F., 2002a. Intracrine hepatopoietin potentiates AP-1 activity through JAB1 independent of MAPK pathway. Faseb J 16, 90-92.

Lu, J., Xu, W.X., Zhan, Y.Q., Cui, X.L., Cai, W.M., He, F.C., Yang, X.M., 2002b. Identification and characterization of a novel isoform of hepatopoietin. World J Gastroenterol 8, 353-356.

Lund, E., Güttinger, S., Calado, A., Dahlberg, J.E., Kutay, U., 2004. Nuclear Export of MicroRNA Precursors. Science 303, 95-98.

Mairet-Coello, G., Tury, A., Esnard-Feve, A., Fellmann, D., Risold, P.Y., Griffond, B., 2004. FAD-Linked Sulfhydryl Oxidase QSOX: Topographic, Cellular, and Subcellular Immunolocalization in Adult Rat Central Nervous System. Journal of Comparative Neurology 473, 334-363.

Matsumoto, K., Yoshitomi, H., Rossant, J., Zaret, K.S., 2001. Liver organogenesis promoted by endothelial cells prior to vascular function. Science 294, 559-563.

Matthews, R.P., 2009. Zebrafish as a Model System for the Study of Liver Development and Disease, The Liver. John Wiley & Sons, Ltd, pp. 1067-1074.

Mayer, A.N., Fishman, M.C., 2003. nil per os encodes a conserved RNA recognition motif protein required for morphogenesis and cytodifferentiation of digestive organs in zebrafish. Development 130, 3917-3928.

Mc, C.B., 1950. The origin and behavior of mutable loci in maize. Proceedings of the National Academy of Sciences of the United States of America 36, 344-355.

McClure, K.D., Sustar, A., Schubiger, G., 2008. Three genes control the timing, the site and the size of blastema formation in Drosophila. Developmental biology 319, 68-77.

McCurley, A.T., Callard, G.V., 2008. Characterization of housekeeping genes in zebrafish: male-female differences and effects of tissue type, developmental stage and chemical treatment. BMC molecular biology 9, 102.

McLin, V.A., Rankin, S.A., Zorn, A.M., 2007. Repression of Wnt/β-catenin signaling in the anterior endoderm is essential for liver and pancreas development. Development 134, 2207-2217.

Meng, X., Noyes, M.B., Zhu, L.J., Lawson, N.D., Wolfe, S.A., 2008. Targeted gene inactivation in zebrafish using engineered zinc-finger nucleases. Nat Biotechnol 26, 695-701.

Mesecke, N., Terziyska, N., Kozany, C., Baumann, F., Neupert, W., Hell, K., Herrmann, J.M., 2005. A disulfide relay system in the intermembrane space of mitochondria that mediates protein import. Cell 121, 1059-1069.

Michalopoulos, G.K., DeFrances, M.C., 1997. Liver regeneration. Science 276, 60-66.

Morgante, M., Brunner, S., Pea, G., Fengler, K., Zuccolo, A., Rafalski, A., 2005. Gene duplication and exon shuffling by helitron-like transposons generate intraspecies diversity in maize. Nat Genet 37, 997-1002.

Mudumana, S.P., Wan, H., Singh, M., Korzh, V., Gong, Z., 2004. Expression analyses

of zebrafish transferrin, ifabp, and elastaseB mRNAs as differentiation markers for the three major endodermal organs: liver, intestine, and exocrine pancreas. Dev Dyn 230, 165-173.

Nasevicius, A., Ekker, S.C., 2000. Effective targeted gene 'knockdown' in zebrafish. Nat Genet 26, 216-220.

Nguyen, A.T., Emelyanov, A., Koh, C.H., Spitsbergen, J.M., Parinov, S., Gong, Z., 2012. An inducible kras(V12) transgenic zebrafish model for liver tumorigenesis and chemical drug screening. Disease models & mechanisms 5, 63-72.

Noël, E.S., Casal-Sueiro, A., Busch-Nentwich, E., Verkade, H., Dong, P.D.S., Stemple, D.L., Ober, E.A., 2008. Organ-specific requirements for Hdac1 in liver and pancreas formation. Developmental biology 322, 237-250.

Noji, S., Tashiro, K., Koyama, E., Nohno, T., Ohyama, K., Taniguchi, S., Nakamura, T., 1990. Expression of hepatocyte growth factor gene in endothelial and Kupffer cells of damaged rat livers, as revealed by in situ hybridization. Biochemical and Biophysical Research Communications 173, 42-47.

Ober, E.A., Field, H.A., Stainier, D.Y., 2003. From endoderm formation to liver and pancreas development in zebrafish. Mechanisms of development 120, 5-18.

Ober, E.A., Verkade, H., Field, H.A., Stainier, D.Y., 2006. Mesodermal Wnt2b signalling positively regulates liver specification. Nature 442, 688-691.

Parinov, S., Emelyanov, A., 2007. Transposable elements in fish functional genomics: technical challenges and perspectives. Genome biology 8 Suppl 1, S6.

Passeri, M.J., Cinaroglu, A., Gao, C., Sadler, K.C., 2009. Hepatic steatosis in response to acute alcohol exposure in zebrafish requires sterol regulatory element binding protein activation. Hepatology (Baltimore, Md 49, 443-452.

Patton, E.E., Zon, L.I., 2001. The art and design of genetic screens: zebrafish. Nature reviews 2, 956-966.

Pawlowski, R., Jura, J., 2006. ALR and liver regeneration. Mol Cell Biochem 288, 159-169.

Polimeno, L., Capuano, F., Marangi, L.C., Margiotta, M., Lisowsky, T., Ierardi, E., Francavilla, R., Francavilla, A., 2000. The augmenter of liver regeneration induces

mitochondrial gene expression in rat liver and enhances oxidative phosphorylation capacity of liver mitochondria. Dig Liver Dis 32, 510-517.

Polimeno, L., Pesetti, B., Annoscia, E., Giorgio, F., Francavilla, R., Lisowsky, T., Gentile, A., Rossi, R., Bucci, A., Francavilla, A., 2011. Alrp, a survival factor that controls the apoptotic process of regenerating liver after partial hepatectomy in rats. Free Radic Res.

Polimeno, L., Pesetti, B., Lisowsky, T., Iannone, F., Resta, L., Giorgio, F., Mallamaci, R., Buttiglione, M., Santovito, D., Vitiello, F., Mancini, M.E., Francavilla, A., 2009. Protective effect of augmenter of liver regeneration on hydrogen peroxide-induced apoptosis in SH-SY5Y human neuroblastoma cells. Free Radic Res 43, 865-875.

Qi, F., Song, J., Yang, H., Gao, W., Liu, N., Zhang, B., Lin, S., 2010. Mmp23b promotes liver development and hepatocyte proliferation through the tumor necrosis factor pathway in zebrafish. Hepatology (Baltimore, Md 52, 2158-2166.

Rai, K., Chidester, S., Zavala, C.V., Manos, E.J., James, S.R., Karpf, A.R., Jones, D.A., Cairns, B.R., 2007. Dnmt2 functions in the cytoplasm to promote liver, brain, and retina development in zebrafish. Genes and Development 21, 261-266.

Ramalho-Santos, M., Yoon, S., Matsuzaki, Y., Mulligan, R.C., Melton, D.A., 2002. "Stemness": transcriptional profiling of embryonic and adult stem cells. Science 298, 597-600.

Rauch, G.J., Lyons, D.A., Middendorf, I., Friedlander, B., Arana, N., Reyes, T., and Talbot, W.S., 2003. Submission and Curation of Gene Expression Data. ZFIN Direct Data Submission (http://zfin.org).

Reinhart, B.J., Slack, F.J., Basson, M., Pasquienelll, A.E., Bettlnger, J.C., Rougvle, A.E., Horvitz, H.R., Ruvkun, G., 2000. The 21-nucleotide let-7 RNA regulates developmental timing in Caenorhabditis elegans. Nature 403, 901-906.

Rhoades, M.W., Reinhart, B.J., Lim, L.P., Burge, C.B., Bartel, B., Bartel, D.P., 2002. Prediction of plant microRNA targets. Cell 110, 513-520.

Rodriguez, A., Griffiths-Jones, S., Ashurst, J.L., Bradley, A., 2004. Identification of mammalian microRNA host genes and transcription units. Genome Research 14, 1902-1910.

Rossi, J.M., Dunn, N.R., Hogan, B.L.M., Zaret, K.S., 2001. Distinct mesodermal

signals, including BMPs from the septum, transversum mesenchyme, are required in combination for hepatogenesis from the endoderm. Genes and Development 15, 1998-2009.

Ruby, J.G., Jan, C.H., Bartel, D.P., 2007. Intronic microRNA precursors that bypass Drosha processing. Nature 448, 83-86.

Sadler, K.C., Krahn, K.N., Gaur, N.A., Ukomadu, C., 2007. Liver growth in the embryo and during liver regeneration in zebrafish requires the cell cycle regulator, uhrf1. Proceedings of the National Academy of Sciences of the United States of America 104, 1570-1575.

Schmidt, O., Pfanner, N., Meisinger, C., 2010. Mitochondrial protein import: from proteomics to functional mechanisms. Nature reviews. Molecular cell biology 11, 655-667.

Senkevich, T.G., White, C.L., Koonin, E.V., Moss, B., 2000. A viral member of the ERV1/ALR protein family participates in a cytoplasmic pathway of disulfide bond formation. Proceedings of the National Academy of Sciences of the United States of America 97, 12068-12073.

Sevier, C.S., Kaiser, C.A., 2008. Ero1 and redox homeostasis in the endoplasmic reticulum. Biochimica et Biophysica Acta - Molecular Cell Research 1783, 549-556.

Shao, Y., Chan, C.Y., Maliyekkel, A., Lawrence, C.E., Roninson, I.B., Ding, Y., 2007. Effect of target secondary structure on RNAi efficiency. RNA 13, 1631-1640.

Shin, D., Shin, C.H., Tucker, J., Ober, E.A., Rentzsch, F., Poss, K.D., Hammerschmidt, M., Mullins, M.C., Stainier, D.Y., 2007. Bmp and Fgf signaling are essential for liver specification in zebrafish. Development 134, 2041-2050.

Si-Tayeb, K., Lemaigre, F.P., Duncan, S.A., 2010. Organogenesis and Development of the Liver. Developmental Cell 18, 175-189.

Silva, J.M., Li, M.Z., Chang, K., Ge, W., Golding, M.C., Rickles, R.J., Siolas, D., Hu, G., Paddison, P.J., Schlabach, M.R., Sheth, N., Bradshaw, J., Burchard, J., Kulkarni, A., Cavet, G., Sachidanandam, R., McCombie, W.R., Cleary, M.A., Elledge, S.J., Hannon, G.J., 2005. Second-generation shRNA libraries covering the mouse and human genomes. Nat Genet 37, 1281-1288.

Skromne, I., Prince, V.E., 2008. Current perspectives in zebrafish reverse genetics:

Moving forward. Developmental Dynamics 237, 861-882.

Sosa-Pineda, B., Wigle, J.T., Oliver, G., 2000. Hepatocyte migration during liver development requires Prox1. Nat Genet 25, 254-255.

Stahl, N., Boulton, T.G., Farruggella, T., Ip, N.Y., Davis, S., Witthuhn, B.A., Quelle, F.W., Silvennoinen, O., Barbieri, G., Pellegrini, S., Ihle, J.N., Yancopoulos, G.D., 1994. Association and activation of Jak-Tyk kinases by CNTF-LIF-OSM-IL-6 β receptor components. Science 263, 92-95.

Stainier, D.Y., 2001. Zebrafish genetics and vertebrate heart formation. Nature reviews 2, 39-48.

Tamura, K., Dudley, J., Nei, M., Kumar, S., 2007. MEGA4: Molecular Evolutionary Genetics Analysis (MEGA) software version 4.0. Molecular biology and evolution 24, 1596-1599.

Tanigawa, K., Sakaida, I., Masuhara, M., Hagiya, M., Okita, K., 2000. Augmenter of liver regeneration (ALR) may promote liver regeneration by reducing natural killer (NK) cell activity in human liver diseases. Journal of gastroenterology 35, 112-119.

Taub, R., 2004. Liver regeneration: from myth to mechanism. Nature reviews. Molecular cell biology 5, 836-847.

Thasler, W.E., Schlott, T., Thelen, P., Hellerbrand, C., Bataille, F., Lichtenauer, M., Schlitt, H.J., Jauch, K.W., Weiss, T.S., 2005. Expression of augmenter of liver regeneration (ALR) in human liver cirrhosis and carcinoma. Histopathology 47, 57-66.

Thirunavukkarasu, C., Wang, L.F., Harvey, S.A., Watkins, S.C., Chaillet, J.R., Prelich, J., Starzl, T.E., Gandhi, C.R., 2008. Augmenter of liver regeneration: an important intracellular survival factor for hepatocytes. J Hepatol 48, 578-588.

Thorpe, C., Hoober, K.L., Raje, S., Glynn, N.M., Burnside, J., Turi, G.K., Coppock, D.L., 2002a. Sulfhydryl oxidases: emerging catalysts of protein disulfide bond formation in eukaryotes. Arch Biochem Biophys 405, 1-12.

Thorpe, C., Hoober, K.L., Raje, S., Glynn, N.M., Burnside, J., Turi, G.K., Coppock, D.L., 2002b. Sulfhydryl oxidases: Emerging catalysts of protein disulfide bond formation in eukaryotes. Archives of Biochemistry and Biophysics 405, 1-12.

Todd, L.R., Damin, M.N., Gomathinayagam, R., Horn, S.R., Means, A.R., Sankar, U., 2010a. Growth Factor erv1-like Modulates Drp1 to Preserve Mitochondrial Dynamics and Function in Mouse Embryonic Stem Cells. Mol. Biol. Cell, E09-11-0937.

Todd, L.R., Gomathinayagam, R., Sankar, U., 2010b. A novel Gfer-Drp1 link in preserving mitochondrial dynamics and function in pluripotent stem cells. Autophagy 6, 821-822.

Tokatlidis, K., 2005. A disulfide relay system in mitochondria. Cell 121, 965-967.

Vitu, E., Bentzur, M., Lisowsky, T., Kaiser, C.A., Fass, D., 2006. Gain of Function in an ERV/ALR Sulfhydryl Oxidase by Molecular Engineering of the Shuttle Disulfide. Journal of Molecular Biology 362, 89-101.

Wandzioch, E., Zaret, K.S., 2009. Dynamic signaling network for the specification of embryonic pancreas and liver progenitors. Science 324, 1707-1710.

Wang, C.P., Zhou, L., Su, S.H., Chen, Y., Lu, Y.Y., Wang, F., Jia, H.J., Feng, Y.Y., Yang, Y.P., 2006. Augmenter of liver regeneration promotes hepatocyte proliferation induced by Kupffer cells. World J Gastroenterol 12, 4859-4865.

Wang, G., Yang, X., Zhang, Y., Wang, Q., Chen, H., Wei, H., Xing, G., Xie, L., Hu, Z., Zhang, C., Fang, D., Wu, C., He, F., 1999. Identification and characterization of receptor for mammalian hepatopoietin that is homologous to yeast ERV1. The Journal of biological chemistry 274, 11469-11472.

Wang, W., Winther, J.R., Thorpe, C., 2007. Erv2p: characterization of the redox behavior of a yeast sulfhydryl oxidase. Biochemistry 46, 3246-3254.

Wang, Y., Lu, C., Wei, H., Wang, N., Chen, X., Zhang, L., Zhai, Y., Zhu, Y., Lu, Y., He, F., 2004. Hepatopoietin interacts directly with COP9 signalosome and regulates AP-1 activity. FEBS Letters 572, 85-91.

Watt, A.J., Zhao, R., Li, J., Duncan, S.A., 2007. Development of the mammalian liver and ventral pancreas is dependent on GATA4. BMC Developmental Biology 7.

Webber, E.M., Bruix, J., Pierce, R.H., Fausto, N., 1998. Tumor necrosis factor primes hepatocytes for DNA replication in the rat. Hepatology (Baltimore, Md 28, 1226-1234.

Westerfield, M., 1995. The Zebrafish Book. University of Oregon Press, Eugene,

USA.

Wicker, T., Sabot, F., Hua-Van, A., Bennetzen, J.L., Capy, P., Chalhoub, B., Flavell, A., Leroy, P., Morgante, M., Panaud, O., Paux, E., SanMiguel, P., Schulman, A.H., 2007. A unified classification system for eukaryotic transposable elements. Nature reviews 8, 973-982.

Wiedenmann, J., Oswald, F., Nienhaus, G.U., 2009. Fluorescent proteins for live cell imaging: opportunities, limitations, and challenges. IUBMB Life 61, 1029-1042.

Wittke, I., Wiedemeyer, R., Pillmann, A., Savelyeva, L., Westermann, F., Schwab, M., 2003. Neuroblastoma-Derived Sulfhydryl Oxidase, a New Member of the Sulfhydryl Oxidase/Quiescin6 Family, Regulates Sensitization to Interferon γ-Induced Cell Death in Human Neuroblastoma Cells. Cancer Research 63, 7742-7752.

Wood, A.J., Lo, T.W., Zeitler, B., Pickle, C.S., Ralston, E.J., Lee, A.H., Amora, R., Miller, J.C., Leung, E., Meng, X., Zhang, L., Rebar, E.J., Gregory, P.D., Urnov, F.D., Meyer, B.J., 2011. Targeted genome editing across species using ZFNs and TALENs. Science 333, 307.

Wu, C.K., Dailey, T.A., Dailey, H.A., Wang, B.C., Rose, J.P., 2003. The crystal structure of augmenter of liver regeneration: A mammalian FAD-dependent sulfhydryl oxidase. Protein Sci 12, 1109-1118.

Xiong, J.W., 2008. Molecular and developmental biology of the hemangioblast. Dev Dyn 237, 1218-1231.

Xu, L., Yin, W., Xia, J., Peng, M., Li, S., Lin, S., Pei, D., Shu, X., 2012. An antiapoptotic role of sorting nexin 7 is required for liver development in zebrafish. Hepatology (Baltimore, Md 55, 1985-1993.

Yabu, T., Todoriki, S., Yamashita, M., 2001. Stress-induced apoptosis by heat shock, UV and γ-ray irradiation in zebrafish embryos detected by increased caspase activity and whole-mount TUNEL staining. Fisheries Science 67, 333-340.

Yamada, Y., Kirillova, I., Peschon, J.J., Fausto, N., 1997. Initiation of liver growth by tumor necrosis factor: Deficient liver regeneration in mice lacking type I tumor necrosis factor receptor. Proceedings of the National Academy of Sciences of the United States of America 94, 1441-1446.

Yang, X., Xie, L., Qiu, Z., Wu, Z., He, F., 1997. Human augmenter of liver

regeneration: Molecular cloning, biological activity and roles in liver regeneration. Science in China 40, 642-647.

Yi, R., Qin, Y., Macara, I.G., Cullen, B.R., 2003. Exportin-5 mediates the nuclear export of pre-microRNAs and short hairpin RNAs. Genes and Development 17, 3011-3016.

Yin, J., Brocher, J., Fischer, U., Winkler, C., 2011. Mutant Prpf31 causes pre-mRNA splicing defects and rod photoreceptor cell degeneration in a zebrafish model for Retinitis pigmentosa. Mol Neurodegener 6, 56.

Ying, S.Y., Lin, S.L., 2006. Current perspectives in intronic micro RNAs (miRNAs). Journal of Biomedical Science 13, 5-15.

Yu, H.Y., Xiang, D.R., Huang, H.J., Li, J., Sheng, J.F., 2010. Expression level of augmenter of liver regeneration in patients with hepatic failure and hepatocellular carcinoma. Hepatobiliary Pancreat Dis Int 9, 492-498.

Zeng, Y., Cai, X., Cullen, B.R., 2005. Use of RNA polymerase II to transcribe artificial microRNAs. Methods Enzymol 392, 371-380.

Zeng, Y., Cullen, B.R., 2003. Sequence requirements for micro RNA processing and function in human cells. RNA 9, 112-123.

Zeng, Y., Wagner, E.J., Cullen, B.R., 2002. Both Natural and Designed Micro RNAs Can Inhibit the Expression of Cognate mRNAs When Expressed in Human Cells. Molecular Cell 9, 1327-1333.

Zhao, X., Monson, C., Gao, C., Gouon-Evans, V., Matsumoto, N., Sadler, K.C., Friedman, S.L., 2010. Klf6/copeb is required for hepatic outgrowth in zebrafish and for hepatocyte specification in mouse ES cells. Developmental biology 344, 79-93.

Zhou, H., Xia, X.G., Xu, Z., 2005. An RNA polymerase II construct synthesizes short-hairpin RNA with a quantitative indicator and mediates highly efficient RNAi. Nucleic Acids Research 33, e62.

Zuker, M., 2003. Mfold web server for nucleic acid folding and hybridization prediction. Nucleic Acids Res 31, 3406-3415.